NUREG/CR-3169
BNL-NUREG-51650
AN

SUPER SYSTEM CODE (SSC, REV. 0) AN ADVANCED THERMOHYDRAULIC SIMULATION CODE FOR TRANSIENTS IN LMFBRs

J.G. Guppy, Principal Investigator

Contributors

A.K. Agrawal
S.F. Carter
E.G. Cazzoli
B.C. Chan
L.G. Epel
W.C. Horak
R.J. Kennett
I.K. Madni
T.C. Nepsee
R. Pyare
E.S. Srinivasan
G.J. Van Tuyle
W.L. Weaver III
J.W. Yang
M. Khatib-Rahbar

Date Published — April 1983

REACTOR SAFETY RESEARCH DIVISION
DEPARTMENT OF NUCLEAR ENERGY
BROOKHAVEN NATIONAL LABORATORY
UPTON, LONG ISLAND, NEW YORK 11973

Prepared for
U.S. NUCLEAR REGULATORY COMMISSION
WASHINGTON, D.C., 20555

TABLE OF CONTENTS

LIST OF TABLES

LIST OF FIGURES

ACKNOWLEDGEMENT

A number of people have been associated with the Super System Code (SSC) development program over the years. A note of appreciation and thanks is particularly due to H. Makowitz, B. A. Martin, and D. R. Stampf, all of the Applied Mathematics Department, BNL, for their assistance in programming; to N. Tanaka, guest engineer from the Power Reactor and Nuclear Fuel Development Corporation (PNC), Japan, and V. Quan, now at Rockwell International, for their contributions on the sodium boiling and fission gas release model; to T. Iwashita, guest engineer, also affiliated with PNC/Japan, for his effort at extending the steam generator representation; to J. E. Meyer, Massachusetts Institute of Technology, for valuable comments and suggestions regarding many modeling areas; to K. B. Cady, Cornell University for his assistance in modeling sodium-to-air heat exchangers; to G. J. Brown, University of Lowell, for his work on the reactivity feedback calculations; and to K. St. John, University of Lowell, for calculations of steady-state coolant flow in different channels.

Preparation and typing of this manuscript were ably done by D. Clay, C. Falkenbach, N. Nagy, P. Siemen, and L. Zaharatos.

Furthermore, this present work is based in part on previous documentation coordinated and directed by the former Principal Investigator of this effort, A. K. Agrawal. These reports, which were the forerunners of this present unified work are the following:

A. K. Agrawal, et al., "An Advanced Thermohydraulic Simulation Code for Transients in LMFBRs (SSC-L Code)," BNL-NUREG-50773, February 1978, and

A. K. Agrawal, et al., "User's Manual for the SSC-L Code," BNL-NUREG-50914, October 1978.

This work was done under the auspices of the U.S. Nuclear Regulatory Commission.

ABSTRACT

The Super System Code (SSC) calculates the response of nuclear reactor systems during operational, incidental and accidental transients, especially natural circulation events. Modules simulated and parameters calculated include: core flow rates and temperatures, loop flow rates and temperatures, pump performance, and heat exchanger operation. Additionally, all plant protection systems and plant control systems are accounted for. All calculations are done in SI units.

SSC is a general system transient code. It is highly flexible, with complete variable dimensioning, allowing any number of user specified loops, pipes and nodes. Single phase and two phase thermal hydraulics are used in a multi-channel core representation. Inter-assembly flow redistribution is accounted for; a detailed fuel pin model is used. The heat transport system geometry is user specified.

The code has both transient and steady state options. Restart capability is provided. Input is free format in a modular structure that makes use of abstract data management techniques.

Plant modules are simulated by individual computer subprograms which are controlled by a master program through the use of a multiple timestep scheme. This approach allows each module to be simulated with an optimum numerical method. Direct integration, finite differences, and weighted residuals are examples of the methods used to solve the governing differential equations which describe the response of the system. Physical properties are represented by polynominal fits and calculated as in-line functions.

SSC was developed using the CDC 7600. It has been successfully implemented on IBM compatible systems with only minor modification. The code is designed to yield real time or better simulation on a CDC 7600. Actual running time varies depending on the detail specified and transient simulated.

SSC is available in either a CDC UPDATE format or as FORTRAN source. The customary transmittal package also includes the input files for the three standard benchmark problems, as well as 48x microfiche which contain the SSC support documentation and sample output for each of the benchmark problems. SSC is currently available as a draft release from Brookhaven National Laboratory with NRC consent.

For further information regarding the evolution of SSC, the reader is referred to two additional reports, which were the forerunners of this present unified work: i.e., 1) A. K. Agrawal, et al., "An Advanced Thermohydraulic Simulation Code for Transients in LMFBRs (SSC-L Code)," BNL-NUREG-50773, February 1978, and 2) A. K. Agrawal, et al., "User's Manual for the SSC-L Code," BNL-NUREG-50914, October 1978.

2. INTRODUCTION

2.1 BACKGROUND

The simulation of a liquid metal cooled fast breeder reactor (LMFBR) plant for a variety of off-normal or accident conditions ('Anticipated', 'Unlikely', and 'Extremely Unlikely') is an important part of the overall safety evaluation. Examples of different off-normal or accident conditions include (a) the withdrawal of a control rod, (b) pump seizure in one of the loops, (c) after-heat removal in the absence of any forced pumping power and (d) a major pipe break in the primary heat transport system (PHTS) or intermediate heat transport system (IHTS). In all of these events, the plant protection system (PPS) is assumed operative per design. The safety implication here is to assure that in any of these events the plant coolability is not endangered.

In some of the off-normal conditions, a proper design of the PPS prevents any loss of fuel pin integrity. For some other conditions, such as a massive pipe rupture in the primary heat transport system, one needs to assure that the coolable geometry is maintained. In this case, the PPS is expected to initiate reactor scram, and, if possible, the affected loop is isolated. The decay heat will then have to be removed, for both short-term and long-term, in an acceptable manner through the remaining unaffected loops or via alternate emergency heat removal paths. Depending on the nature and location of a pipe rupture and the state of the plant prior to the rupture, coolant flow reversal or coolant stagnation could occur in the reactor core. Even if this condition were to persist for only a few seconds, a significant fraction of the total fuel pins could fail and release fission gases either prior to or subsequent to sodium boiling. Any system analysis code, therefore, must provide a

capability to analyze such an accident.

Another important area for the system response evaluation is the plant's capability to dissipate after-heat from an intact system in the absence of any forced pumping power. The natural convection that may be established in the plant needs to be evaluated from the point of view of assuring the long-term cooling capability of the plant. The entire plant, with all of the essential components, needs to be modeled in sufficient detail to predict, in particular, the thermohydraulic behavior of the reactor core.

For some of the problems, the plant simulation may be required only for several tens of seconds. On the other hand, the long-term after-heat dissipation capability may require simulation for up to an hour or more of transient time. The computational time should, therefore, not be excessive, in order to permit execution of a sufficient number of parametric studies.

Restricted analytical models and associated computer codes such as IANUS, [2-1] DEMO, [2-2] and NATRANS [2-3] have been developed by other organizations to simulate the overall response of a fast reactor plant. The first two codes were specifically designed for the Fast Flux Test Facility (FFTF) and the Clinch River Breeder Reactor Plant (CRBRP) respectively. The IANUS code models the PHTS, the IHTS, and the dump heat exchanger. The DEMO code is for CRBRP, with the exception that the dump heat exchanger is replaced by a steam generator and other components of the tertiary water loop.

Another code, called NALAP, [2-4] for the transient simulation of an LMFBR system is also available. This code was obtained by adopting RELAP 3B [2-5] (BNL version of RELAP 3) by substituting sodium properties in place of those of water. Although this code is capable of providing a rudimentary flow decay

for a pipe rupture accident, a number of modeling as well as operating limitations exist.

A number of simplifying assumptions and approximations are made in these codes, which may be acceptable from the design point of view, but are unacceptable for safety analyses. For example, the modeling of the entire reactor core by a single average channel is highly questionable. The thermohydraulic or neutronic couplings between 'hot', 'peak', 'average', and 'cold' channels must be included to account for the fact that up to 20 to 25 percent of the reactor core could be operating at peak channel conditions. An adequate representation for mixing of coolant coming out of different channels (or assemblies) having different temperatures in the outlet plenum is critical in determining sodium conditions at the vessel outlet. The coolant temperature here influences the natural convection capability in the plant.

There are processes that may be peculiar to safety analyses. For example, sodium boiling and fission gas release are two important phenomena that could be encountered in both of the safety problems discussed earlier. It should, however, be noted that these phenomena may not occur in all of the channels but only in part of the core.

2.2 OBJECTIVES

To provide for a general system code, a work plan was written in fiscal year 1976 to develop the Super System Code (SSC). The prime objective of this program is to develop an advanced system transient code for LMFBRs which will be capable of predicting the plant response when subjected to various off-normal and accident conditions. Two major accidents that this code will be

designed to simulate are: (1) pipe breaks up to and including a double-ended rupture anywhere in the PHTS, or IHTS (2) the long-term after-heat removal in the absence of any forced pumping power. In both of these events, the plant protection system (PPS) will be assumed to be functioning. In addition, SSC will be able to simulate many of the 'level-2' transients such as withdrawal of a control rod followed by reactor scram through PPS action.

Another key objective of the code is to provide a capability within the code for doing steady-state or preaccident initialization. The initialized conditions will be calculated from the user-specified design parameters and operating conditions. A restart capability is provided so that a series of transient analyses can be made from a single steady-state computation. A restart option during transient analyses is also available.

The first in the series of codes in the SSC program is designed to simulate thermohydraulic transients in loop-type LMFBRs. Subsequent versions include a similar capability for the 'pool' - or 'pot'-type designs of LMFBRs.

2.3 SUMMARY

The SSC Program consists of developing system transient codes for both loop- and pool-type designs of LMFBRs. These series of codes are labeled SSC-L and SSC-P, respectively. The work reported here is on the SSC-L code. The essential components and their arrangements in a loop system, such as the Clinch River Breeder Reactor Plant (CRBRP), [2-6] are shown schematically in Figure 2-1. Under normal operation, liquid sodium flows in both primary and intermediate heat transport systems. The steam generating loop or tertiary

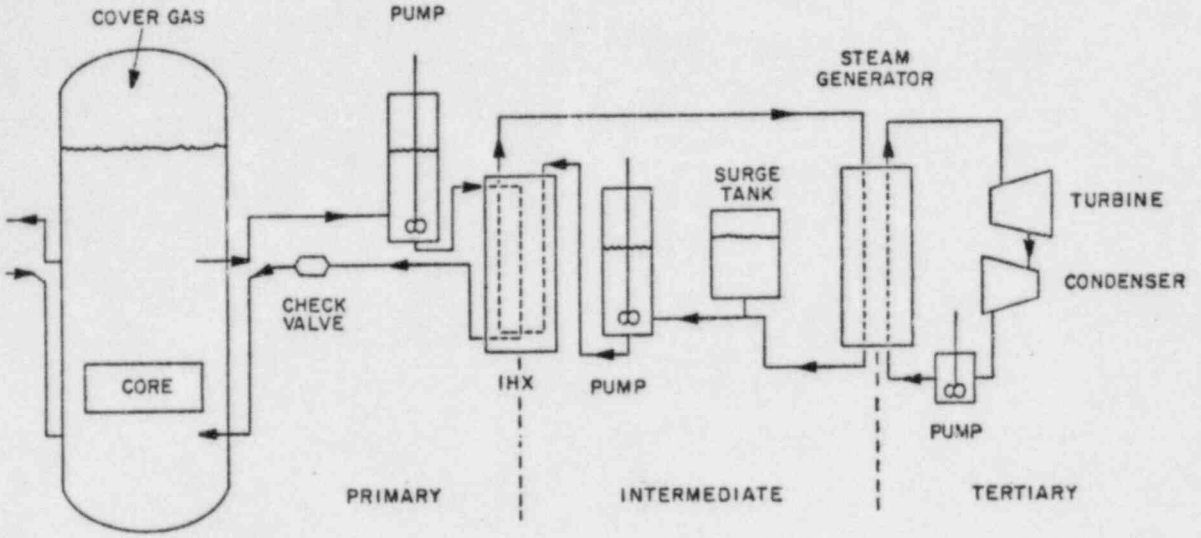

Figure 2-1 Sketch of One Set of Loops in an LMFBR

loop is also shown in this figure.

A comprehensive description of all of the models that were either developed or adapted to simulate processes of interest is given in Chapter 3. In this chapter, descriptions of models for the steady-state plant characterization, prior to the initiation of transients, are noted before going into their transient counterparts.

Numerical methodology, that was developed for the SSC-L code, is discussed in Chapter 4. As a starting point for any transient calculation, a stable and unique steady-state or pretransient solution for the entire plant is obtained. In doing so, the time-independent form for continuity, energy, and momentum conservation equations are reduced to a set of nonlinear algebraic equations. These equations are solved in two steps: first, the global parameters are obtained; then, more detailed characterization is done by using the global conditions, obtained in the first step, as boundary conditions.

The energy and momentum conservation equations which describe water/steam flow in the tertiary loop are coupled since the constitutive laws depend explicitly on fluid pressure. These equations are represented in the form of a set of algebraic equations for each control volume. These equations are then solved iteratively for the steam generating system.

For sodium loops, the energy and momentum conservation equations may be decoupled when the effect of pressure on subcooled liquid sodium properties is neglected. This is a valid assumption. Therefore, the energy equations for both primary and intermediate heat transport systems are solved in conjunction with the detailed solution for the steam generator. The head requirement for sodium pumps is then determined by computing the entire pressure drop in the

loop. The actual pressure at any location in either the primary or secondary system is then related directly to the cover gas pressure.

The numerical integration of the transient form of the governing equations is done using a multiple timestep scheme (MTS) [2-7]. In this method, different processes are integrated by using different timestep sizes. This is achieved by dividing the entire system into a number of subsystems. Each of these subsystems uses a different timestep in time advancement. In order to keep the logic required for integrating the different subsystems manageable, a total of four different timestep sizes are used. These are for (1) hydraulic response of both the primary and intermediate heat transport systems, (2) thermal response of both the primary and intermediate heat transport systems, (3) fuel rod heat conduction and power generation computations and coolant dynamics in the reactor core, and (4) computations in the steam generating system.

Individual processes are solved by the numerical algorithm that is most suitable for the process under consideration. For example, the heat conduction equations for a fuel rod are solved by a first-order fully implicit finite differencing scheme. The fission heating computations, on the other hand, can be computer by a modified Kaganove method which uses a polynomial method or by the prompt jump approximation. The overall interfacing of all processes is achieved by matching boundary conditions at the respective interfaces. The overall timestep is controlled by requiring solutions to be numerically stable as well as by user-specified accuracy criteria. A feature that is built into the code allows the timestep sizes to be automatically reduced or increased.

A large number of modeling options are built into the code. These are discussed in detail in Chapter 3. A user can select options through various flags or switches that are required as a part of the input.

A number of constitutive relations and correlations are required. These can be input either in a tabular form or in an analytic form. For the sake of computing efficiency, analytic forms are preferred and, hence, used in the SSC-L code. Chapter 5 gives a list of all constitutive relations and correlations that are needed by the code. A set of appropriate values for coefficients in these analytic equations is also noted, although no claim for their suitability for any analysis is made (i.e., whether they are best values, conservative values, or desirable values). These coefficients are made available, as default, in the code. They can be overridden through input.

The SSC-L code is deliberately structured in a modular fashion. The data transfer between various modules is accomplished by COMMON blocks. The entire code is written in a variably dimensioned format, which allows for the most effective usage of computer core space. Standard coding practices were followed so that exportability of the code to other institutions can be achieved. Chapter 6 discusses various guidelines that were used in development of the SSC-L code. A naming convection for all global variables, as well as subprograms, was developed and utilized in the code. This considerably simplifies debugging of the code. A simplified flow chart, with brief descriptions of all major subprograms, is also given in Chapter 6.

Chapter 7 gives detailed instructions on how to use this code. Included in this documentation is a detailed data dictionary, sample input deck, and output of the code.

A word on the units is in order. The SSC-L code is written in a consistent set of SI units [2-8].

2.4 APPLICATIONS

The SSC-L code is developed as an advanced thermohydraulic transient code for loop-type designs of LMFBRs. Although the emphasis here is on transients for safety analysis, this code can be utilized for a variety of other objectives, including (a) scoping analysis for design of a plant and (b) specification of various components.

REFERENCES FOR SECTION 2

2-1 S. L. Additon, T. B. McCall and C. F. Wolfe, "IANUS - Outline Description," Westinghouse Advanced Reactors Division, Waltz Mill, Pennsylvania, FPC-939.

2-2 "LMFBR Demonstration Plant Simulation Model, DEMO," Westinghouse Advanced Reactors Division, WARD-D-0005 (Rev 3), February 1975.

2-3 D. Brosche, "NATRANS-Ein Rechenmodel zur Berechnung des Dynamischen Verhaltens von Reaktorkuhlkreislaufen bei Stoerfallen," Laboratorium fuer Reaktorregelung and Anlagensicherung Garching, Report MRR-71, April 1971.

2-4 B. A. Martin, A. K. Agrawal, D. C. Albright, L. G. Epel, and G. Maise, "NALAP: An LMFBR System Transient Code," BNL-50457, July 1975.

2-5 "RELAP3B Manual, A Reactor System Transient Code," Brookhaven National Laboratory, RP 1035, December 1974.

2-6 Clinch River Breeder Reactor Project, Preliminary Safety Analysis Report, Vol. 4, Project Management Corporation, 1975.

2-7 J. G. Guppy, "Application of Multiple Timestep Integration Method in SSc", Trans. Am. Nucl. Soc. 33, 340, 1979.

2-8 "The International System of Units (SI)," C. H. Page and P. Vigoureux Editors, National Bureau of Standards Special Publication 330, 1972 Edition.

3.1 IN VESSEL HEAT TRANSFER

The reactor vessel is modeled by four regions (see Fig. 3.1-1).

1) Lower (inlet) plenum
2) "Extended" core
3) Upper (outlet) plenum
4) Bypass channel.

The five elevations (a-e) indicated in Fig. 3.1-1 are the sodium level, outlet nozzle, inlet nozzle, extended core top, and extended core bottom, respectively. These elevations are the reference locations for pressure calculations in the core. The mass flow rate, fluid pressure, and fluid temperature at the inlet and outlet nozzle connect the flow dynamics in the vessel to those in the primary loops.

3.1.1 LOWER (INLET) PLENUM

Fig. 3.1-2 shows a schematic of the inlet plenum of a reactor vessel. At steady-state the fluid and the metal in the lower plenum are assumed to be in thermal equilibrium. These temperatures are then equal to the fluid temperature at the inlet nozzle, i.e.,

$$T_{FLP} = T_{MLP} = T_{IZ} \tag{3.1-1}$$

where,

T_{FLP} = temperature of the fluid in the lower plenum,

T_{MLP} = temperature of the metal (structure) in the lower plenum,

T_{IZ} = fluid temperature at the inlet nozzle.

During transients, the coolant enthalpy is computed assuming complete mixing of various flows entering the region. The governing equations (in finite dif-

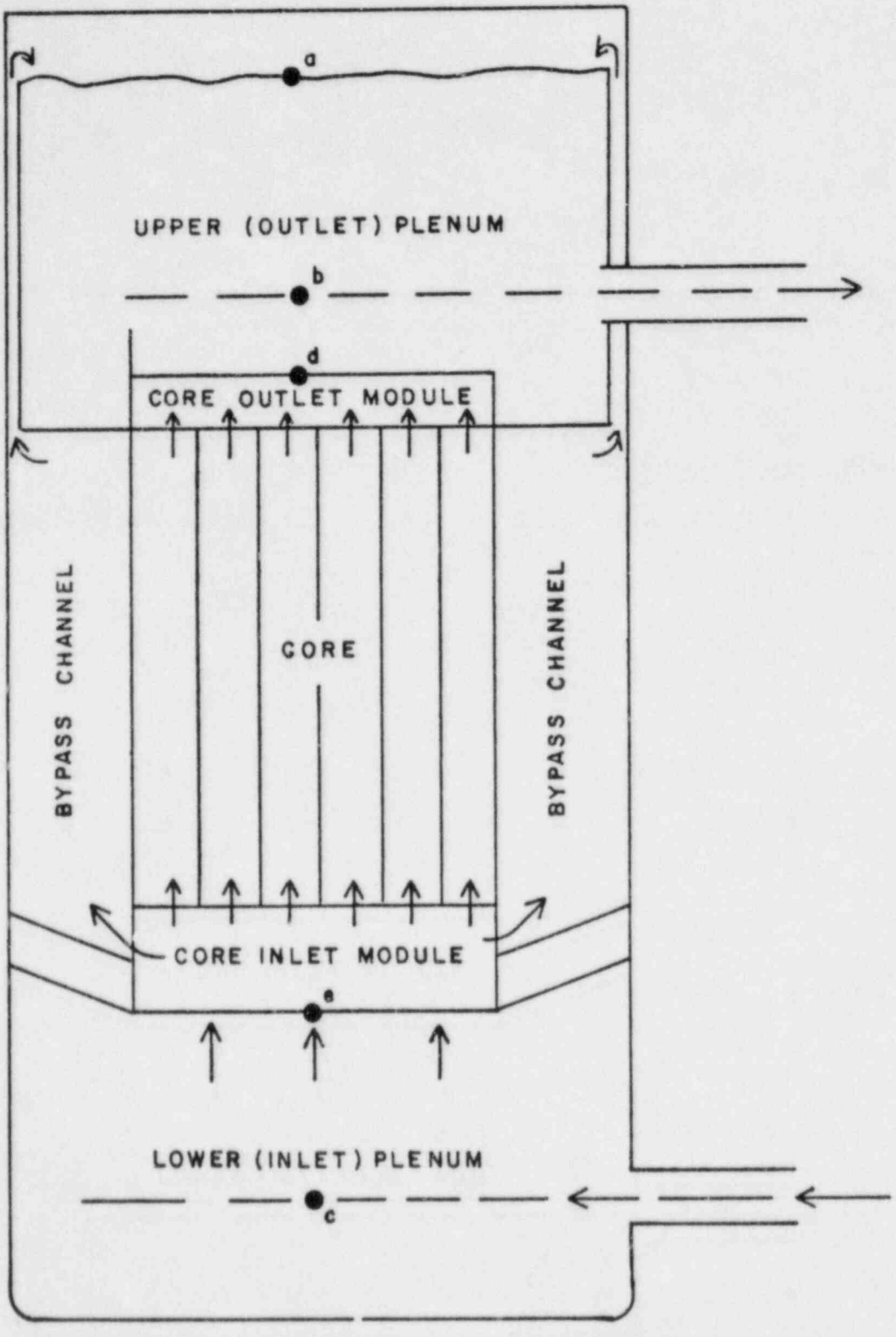

Figure 3.1-1 Schematic of the In-Vessel Model Used in SSC

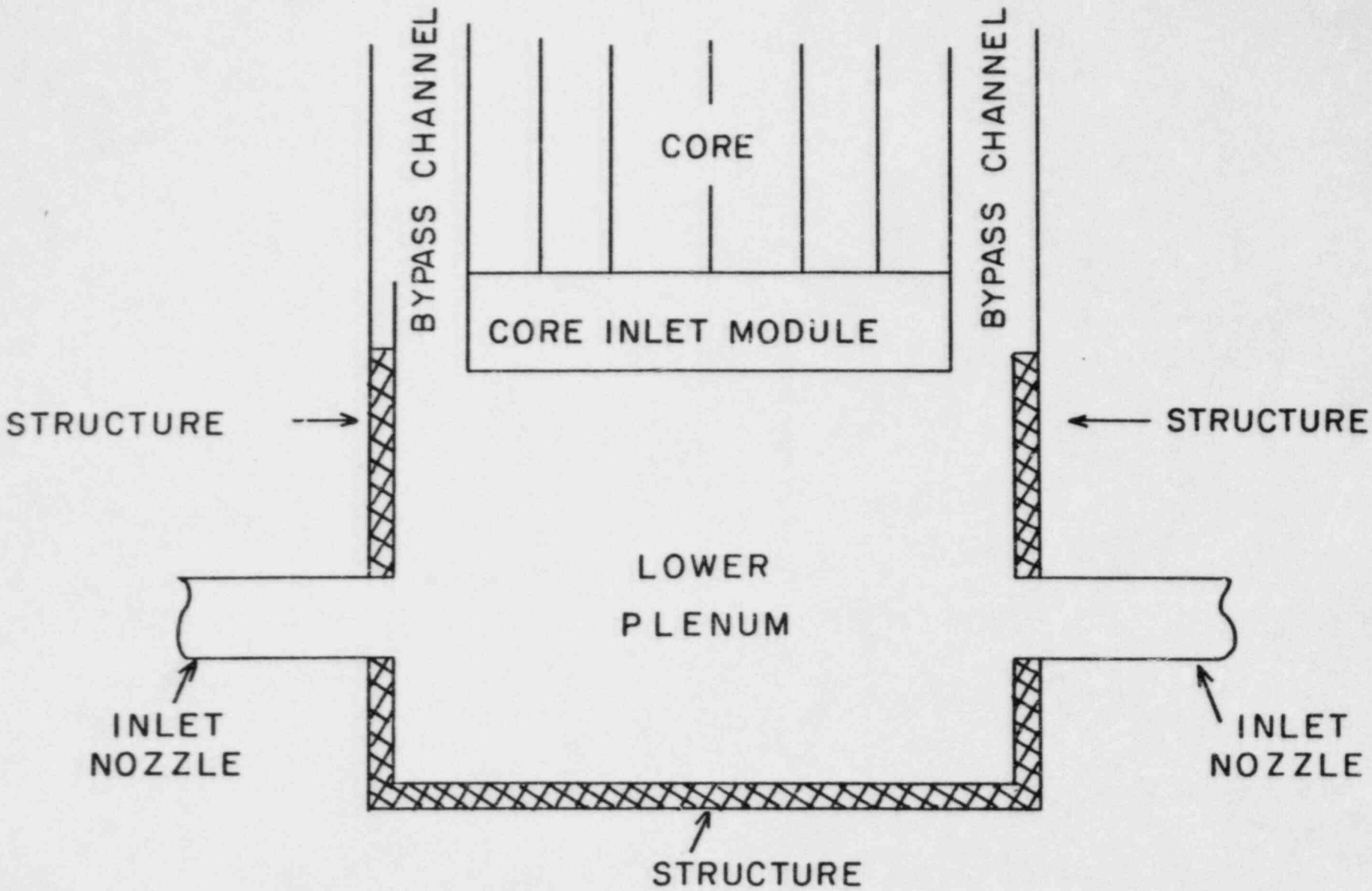

Figure 3.1-2 A Schematic of the Lower (Inlet) Plenum of a Reactor Vessel

ference form) are

$$(\rho V)_{FLP}(h^{k}_{FLP} - h^{k-1}_{FLP})/\Delta t = \sum_{i=1}^{I_{in}} W_i\ (h_i^{k} - h^{k}_{FLP}) -$$

$$\sum_{j=1}^{J_{out}} W_j\ (\ h^{k}_{j} - h^{k}_{FLP}) + Q^{k-1} \qquad (3.1\text{-}2)$$

$$(\rho V c_p)_{MLP}(T^{k}_{MLP} - T^{k-1}_{MLP})/\Delta t = - Q^{k-1} \qquad (3.1\text{-}3)$$

$$Q^{k-1} = UA(T^{k-1}_{MLP} - T^{k-1}_{FLP}) \qquad (3.1\text{-}4)$$

$$T_{FLP}{}^{k} = f(h^{k}_{FLP}) \qquad (3.1\text{-}5)$$

where,

$(\rho V)_{FLP}$ = mass of fluid in the lower plenum

h_{FLP} = enthalpy of fluid in the lower plenum

k = timestep index

Δt = timestep

W_i = mass flow rate into lower plenum

h_i = enthalpy of inlet flow

I_{in} = total number of inlet flows

W_j = outlet mass flow rate

h_j = enthalpy of outlet flow

J_{out} = total number of outlet flows

Q = heat rlow from metal to fluid

$(\rho V c_p)_{MLP}$ = mass and specific heat of metal on lower plenum

UA = overall heat transfer coefficient from metal to fluid in lower plenum.

3.1.2 IN-CORE HEAT TRANSFER

Fig. 3.1-3 shows a general schematic of fuel bundles and their associated coolant channels. In SSC, intra-assembly cross-flow and inter-and intra-assembly heat transfer effects are not modeled at present, decoupling the thermal hydraulics of a single fuel rod, with its associated coolant channel and structure, from the others. A general form of such a fuel channel (divided into N6ASEC axial nodes) is shown in Fig. 3.1-4. The rod is composed of up to five axial regions: lower plenum, lower blanket, active fuel, upper blanket, and upper plenum. One or more of these regimes may be omitted at the user's request, but the sequence will be maintained. Axial heat conduction is also neglected, permitting the analysis to be done on an axial level, channel by channel basis. Other channels (e.g., blanket, contrtol) are analyzed identically to a fuel channel.

3.1.2.1 RADIAL NODING

A typical axial slice of a fuel channel is shown in Fig. 3.1-5. The fuel is divided into NF (user input as N5NFR) nodes; the gap, clad, coolant and structure have one node each. Thermal expansions are accounted for in the fuel and clad in the steady-state and transient. The fuel is allowed to restructure once in the steady-state, the restructuring is then carried over into the transient.

The radial nodes in the fuel are determined by either the equal radial increment method or the equal area method (user input option). For the equal radial increment method, the radii are given by:

$$R_1 = R_{FI}\ (1 + \alpha_1(T_1 - T_{REF})) \qquad (3.1\text{-}6a)$$

$$R_i = R_{i-1} + \Delta R(1 + \alpha_{i-1}(T_{i-1} - T_{REF}),\ i=2\ldots,\ NF + 1. \qquad (3.1\text{-}6b)$$

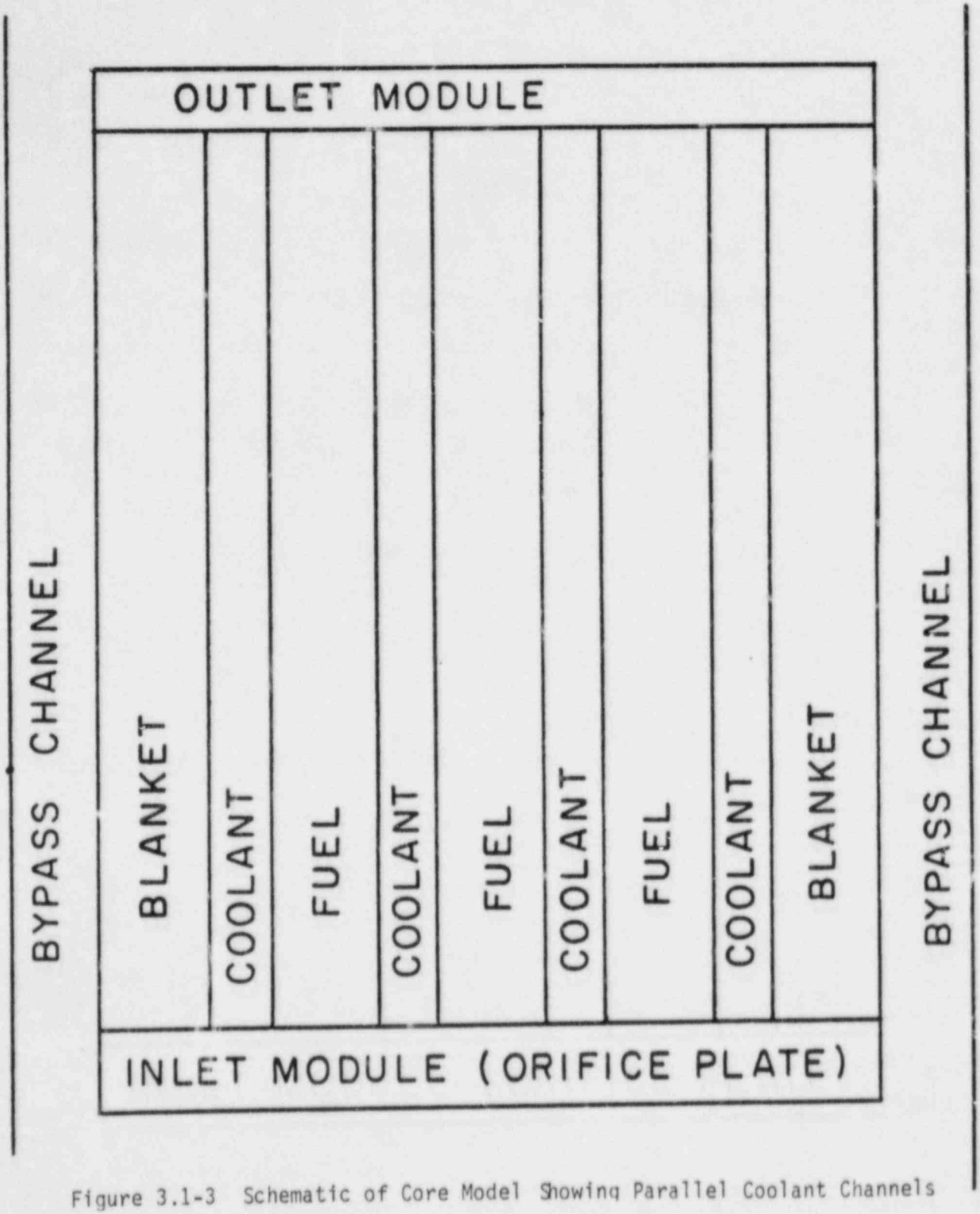

Figure 3.1-3 Schematic of Core Model Showing Parallel Coolant Channels

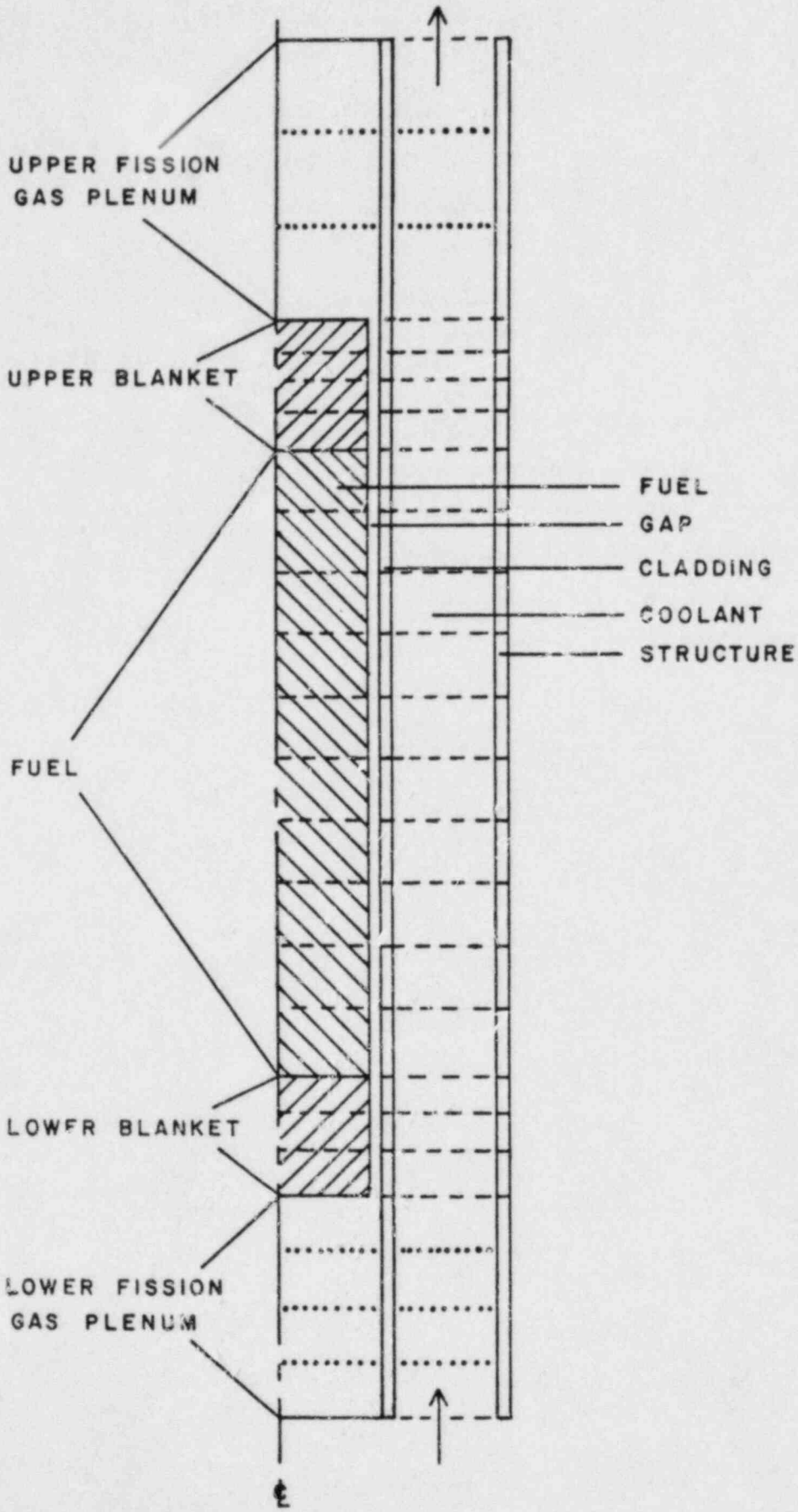

Figure 3.1-4 Axial Noding in a Core (Fuel) Channel

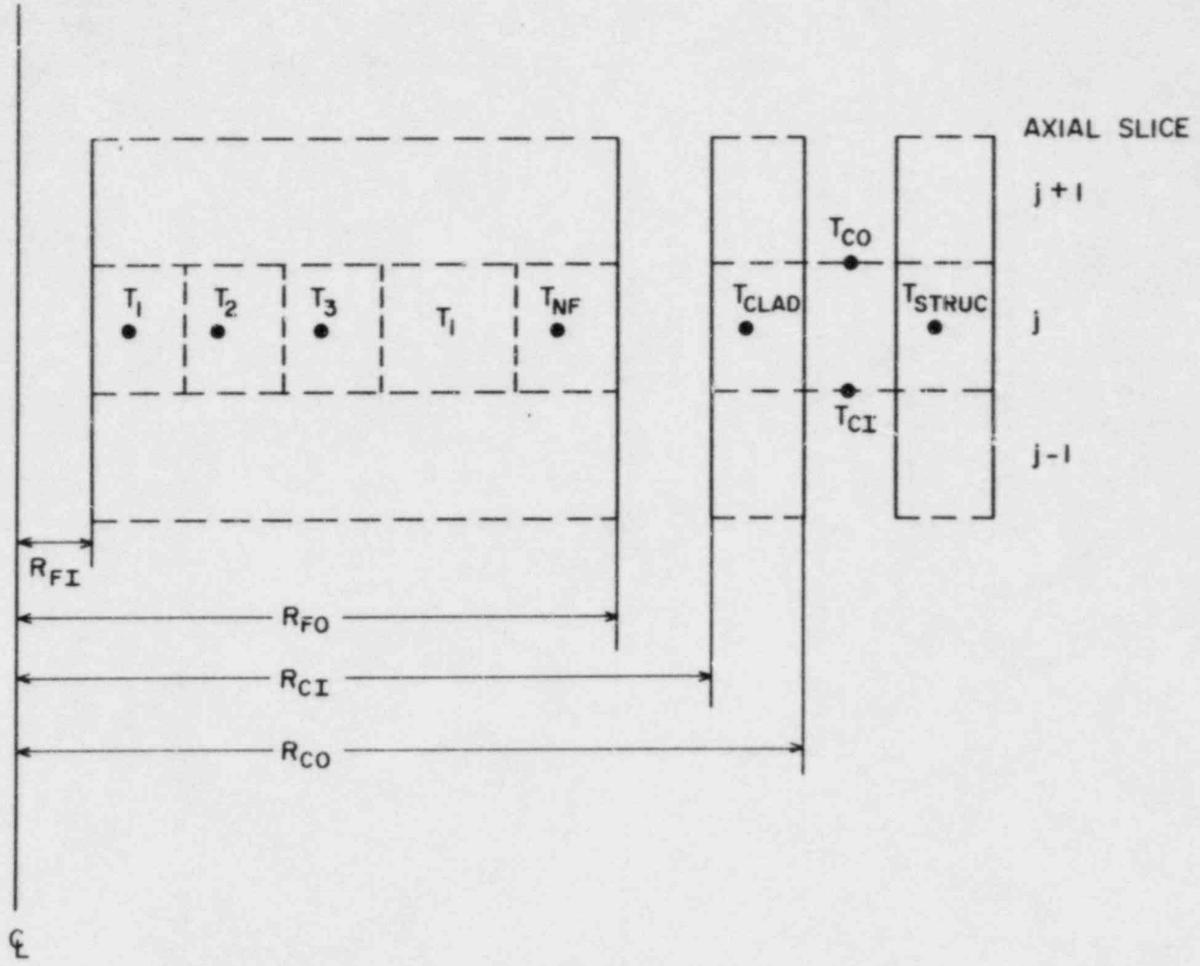

Figure 3.1-5 Radial Noding in an Axial Slice of a Core Channel

$$\Delta R = \frac{(R_{FO} - R_{FI})}{NF} \qquad (3.1\text{-}6c)$$

where, R_{FI} = inner fuel radius at temperature, T_{REF}

R_{FO} = outer fuel radius at temperature, T_{REF}

α_i = coefficient of thermal expansion for node i,

T_i = average temperature in the ith node.

In the equal area method, the radii are given by:

$$R_1 = R_{FI}(1 + \alpha_1 (T_1 - T_{REF})) \qquad (3.1\text{-}7a)$$

$$R_i = [(R_{i-1}^2) + \Delta R(1 + \alpha_{i-1}(T_{i-1} - T_{REF}))^2]^{1/2} \qquad (3.1\text{-}7b)$$

and

$$\Delta R = \frac{[R_{FO}^2 - R_{FI}^2]^{1/2}}{NF} \qquad (3.1\text{-}7c)$$

The restructuring of the fuel is calculated for an axial slice during the steady-state only. Grain growth is assumed to divide the fuel into three regions: unrestructured, equiaxed grain growth, and columnar grain growth. The transition temperatures for equiaxed grain growth, T_{EG}, and columnar growth, T_{CG}, are user input. If the fuel pin restructures, the inner fuel radius is determined by taking the mass balance of fuel in each slice:

$$R'_{FI} = [R^2_{EG} + (\rho_{EG}/\rho_{CG})(R_{UN}^2 - R_{EG}^2) + (\rho_{UN}/\rho_{CG})(R_{FI}^2 - R_{UN}^2)]^{1/2}, \qquad (3.1\text{-}8)$$

where R_{EG} is the first node in the equiaxed grain region, R_{UN} is the first node in the unrestructured region, and ρ_{UN}, ρ_{EG}, ρ_{CG} are the densities in the unrestructured, equiaxed grain, and columnar grain regions respectively. The new inner fuel radius, R'_{FI}, is re-evaluated at the reference temperature, TREF, before being used in the radii equations.

There is only one node in the clad, therefore the cladding radii are given by:

$$R_{NF+2} = R_{CLI}(1 + \alpha_{CL}(T_{CL} - T_{REF})), \quad (3.1\text{-}9a)$$

$$R_{NF+3} = R_{NF2} + (R_{CLO} - R_{CLI})(1 + \alpha_{CL}(T_{CL} - T_{REF})), \quad (3.1\text{-}9b)$$

where R_{CLI} and R_{CLO} are the clad inner and outer clad radii at the reference temperature.

Thermal expansion effects are not accounted for in the coolant channel flow area or the structure.

3.1.2.2 FUEL-CLAD GAP

The gap between the fuel and cladding is determined explicitly by subtracting the outer fuel radius and inner clad radius as calculated at the operating temperature. If this distance is negative, the outer fuel radius is set equal to the inner fuel radius and the gap is taken to be zero.

Heat transfer across the gap is modeled in terms of a gap conductance. The gap conductance is computed if the gap is of finite size; for a closed gap, the conductance is user input.

For the case of a finite gap, heat is transported across the gap by conduction through a mixture of fill gas and fission gasses (xenon and krypton) and thermal radiation between the outside surface of the fuel and the inside surface of the clad. Heat transfer via free convection of the gasses in the gap is considered negligible.

With these assumptions, the heat flux at the outer fuel surface (per unit length) across a finite gap is given by

$$q = 2\pi R_{NF+1}(T_{NF} - T_{NF+2})(h_{cond} + h_{rad}) \quad (3.1\text{-}10)$$

where,

$$h_{rad} = \bar{\varepsilon}\sigma \left(\bar{T}^3_{NF} + \bar{T}^2_{NF+2} \quad T_{NF+2} + \bar{T}^2_{NF+2}\, \bar{T}_{NF} + \bar{T}^3_{NF+2}\right) \tag{3.1-11}$$

$$\bar{\varepsilon} = \left[\frac{1}{\varepsilon_{NF}} + \frac{R_{NF+1}}{R_{NF+2}} \left(\frac{1}{\varepsilon_{NF+2}} - 1\right)\right]^{-1} \tag{3.1-12}$$

$$h_{cond} = k_{mix}/(R_{NF+2} - R_{NF+1}) \tag{3.1-13}$$

$$k_{mix} = 0.5 \left[\sum_{i=1}^{N} x_i\, k_i + \frac{1}{\sum_{i=1}^{N} x_i/k_i}\right] \tag{3.1-14}$$

The emissivities (ε_{NF}, ε_{NF+2}) of the fuel and cladding and the thermal conductivity of the gasses (k_i) are user input. The mole fractions of the gases (x_i) are determined by user input models if fission gas is released.

If there is no gap, the heat flux at the outer fuel surface is given by

$$q = 2\pi\, R_{NF+1}\, (T_{NF} - T_{NF+2})\, h_{cont}, \tag{3.1-15}$$

where h_{cont}, the contact resistance, is user input.

3.1.2.3 TOTAL REACTOR CORE POWER

The total reactor core power (which includes the fission and decay heat contributions) is divided among the core coolant channels and the bypass channel. Therefore the total reactor power, P5TOT(t), is written as

$$P5TOT(t) = \sum_{k=1}^{N6CHAN} P5FISS(k,t) + \sum_{k=1}^{N6CHAN} P5DCY\,(k, t) + P5BYPS(t) \tag{3.1-16}$$

where,

$$P5FISS(k,t) = F5PFIS(k) \cdot F6TPOW(k) \cdot P5PTOT(\emptyset) \cdot n(t) \quad (3.1\text{-}17)$$

$$P5DCY(k,t) = F5PDCY(k) \cdot F6TPOW(k) \cdot P5TOT(\emptyset) \cdot d(k,t) \quad (3.1\text{-}18)$$

$$P5BYPS(t) = F6BYP \cdot P5TOT(\emptyset) \cdot (F5PFISS(N6CHAN+1) \cdot n(t) + F5PDCY(N6CHAN+1) \cdot d_B(t)), \quad (3.1\text{-}19)$$

where,

F6TPOW(k) = Fraction of total power allocated to the k-th channel,

F5PFIS(k) = Fraction of power from fission and gamma heating in the k-th channel,

F5PDCY(k) = Fraction of power from decay heating in the k-th channel,

F6BYP = Fraction of power in the bypass channel,

n(t) = normalized time-dependent factor for fission and gamma heating,

d(k,t) = normalized time dependent factor for decay heating in the k-th channel,

$d_B(t)$ = normalized time-dependent factor for decay heating of the bypass channel.

It is required that,

$$\sum_{k=1}^{N6CHAN} F6TPOW(k) + F6BYP = 1 \quad (3.1\text{-}20)$$

and

$$F5PFIS(k) + F5PDCY(k) = 1 \quad (3.1\text{-}21)$$

The power deposited in a channel is further subdivided into four terms:

1) Portion deposited in the fuel (or blanket) pellets, F5PWR5(k)

2) Portion deposited in the cladding, F5PWR6(k),

3) Portion deposited in coolant, F5PWR1(k),

4) Portion deposited in structure, F5PWR7(k)

These power fractions are normalized so that

$$F5PWR5(k) + F5PWR6(k) + F5PWR1(k) + F5PWR7(k) = 1 \qquad (3.1\text{-}22)$$

for all channels.

3.1.2.4 IN-CHANNEL SPATIAL POWER NORMALIZATION

An axial variation along the length of the channel is specified by a profile supplied by the user. The axial distribution profile is stored in the F5PAX array. The data are taken to apply at the nodal midpoints. These relative axial distribution data are then normalized such that:

$$\frac{1}{Z_T} \sum_{j=1}^{N5ASEC} F5PAX_j \, \Delta Z_j = 1, \qquad (3.1\text{-}23)$$

where Z_T is the total axial height of the channel, N5ASEC, is the total number of axial slices in the channel, and ΔZ_j is the height of the j-th axial slice.

The radial power within a fuel or blanket pellet is allowed to vary in a user specified manner. The pin radial profile is stored in the F5PRAD array. The user-input radial power shape is normalized such that:

$$\frac{\sum_{i=1}^{N5NFR} F5PRAD_i \cdot A_i}{\sum_{i=1}^{N5NFR} A_i} = 1 , \qquad (3.1\text{-}24)$$

where N5NFR is the number of radial nodes in the pin and A_i is the area of the i-th node.

Any power deposited in the cladding, coolant, or structural material is assumed to be distributed uniformly in the radial direction.

3.1.2.5 STEADY-STATE ALGORITHMS

Axial heat conduction is neglected in calculating the in-core steady-state temperature distribution. This assumption not only permits the calculation to be done by marching from one axial level to the next, but also permits calculating the coolant temperature distribution independently from the fuel rod and structure temperature calculations. In the steady-state, the coolant enthaply (or temperature) calculations are calculated before determining the fuel rod and structure temperatures.

3.1.2.5a COOLANT HYDRAULIC CALCULATION

The core region is subdivided into N6CHAN parallel channels. These channels represent either fuel, blanket, or control rods. A bypass channel is also included. At steady-state, there are two options that may be used to obtain the fraction of the total flow through these channels. The first option requires that the flow fraction be specified by the user through the parameters F_k and F_{BP}. These are given by the following equations:

$$F_k = \frac{W_k}{W_{total}} \quad , \qquad k = 1,\ldots, \text{N6CHAN} \, , \tag{3.1-25a}$$

and

$$F_{BP} = \frac{W_{BP}}{W_{total}} \quad . \tag{3.1-25b}$$

In the second option, these flow fractions are calculated by assuming the same total pressure drop for each channel. Knowing the total pressure drop and using an iterative procedure, the fraction of the total flow in each channel can be computed from the momentum equations. In either case, it is required that

$$\sum_{k=1}^{N6CHAN} F_k + F_{BP} = 1 \quad . \tag{3.1-26}$$

For the case of single-phase sodium, the flow is assumed to be one-dimensional and incompressible. The momentum equation for the axial pressure distribution is,

$$\frac{dP}{dZ} = - g\rho - \frac{G_k|G_k|f_k}{2\rho\, D_{hk}} - G_k^2 \frac{d}{dZ}\left(\frac{1}{\rho}\right) \tag{3.1-27}$$

Rewriting the above equation in finite-difference form, the pressure at any axial slice is computed from

$$P_{j+1} = P_j - \left[g\rho + \frac{f_k\, G_k|G_k|}{2\rho\, D_{hk}}\right]_j \Delta Z_j - G_k^2 \left[\frac{1}{\rho_{j+1}} - \frac{1}{\rho_j}\right] \tag{3.1-28}$$

In the case where a core inlet module is attached at the bottom of the active core, the coolant flow is assumed to be isothermal; hence no energy equation is solved for this region. The momentum equation then contains three additional loss coefficients:

$$P_1 = P_e - \sum_{n=1}^{3} \frac{K_n\, G_k\, G_k}{2\rho} - \left[g\rho + \frac{f_k\, G_k|G_k|}{2\rho\, D_{hk}}\right]\Delta L_k \quad , \tag{3.1-29}$$

where

K_1 = loss coefficient due to area expansion,

K_2 = loss coefficient due to area contraction,

K_3 = loss coefficient of inlet orifice.

The loss coefficients are input values provided by the user. The ΔL_k and D_{hk} are the length and hydraulic diameter of this section.

On the top of the core, an additional loss coefficient k_4 is imposed in the core outlet module such that the computed pressure drop in each channel satisfies the overall force balance

$$P_d = P_{\text{last slice}} - \frac{k_4}{2\rho} G_k|G_k| - \Delta L_4 \, g\rho \quad . \tag{3.1-30}$$

The value of k_4 or G_k is adjusted internally in SSC according to the options discussed before, so that the calculated P_d is made to agree with that determined from the upper plenum, since the pressure at d (see Figure 3.1-1) is given by

$$P_d = P_a + \rho g(Z_a - Z_d) \quad . \tag{3.1-31}$$

This additional loss factor k_4 will be retained in the transient computations.

3.1.2.5b COOLANT ENERGY TEMPERATURE CALCULATIONS

Since axial heat conduction is neglected all the power deposited in a particular axial level within a channel can be considered to be deposited directly into the coolant for calculational purposes. Therefore, using donor-cell differencing in space and assuming the flow is uni-directional, the coolant temperature at axial level i is given by

$$T_i = T_{i-1} + Q_{CO}/(Wc_p) \tag{3.1-32}$$

where

T_{i-1} = temperature upstream of axial location, i.

Q_{CO} = total power (w) deposited in axial slice i-1.

W = channel coolant flow rate,

c_p = specific heat of the coolant in axial slice i-1.

Because c_p is defined as a function of the average temperature in the axial slice, i.e.,

$$c_p = c_p\left((T_i + T_{i-1})/2\right), \tag{3.1-33}$$

an iterative procedure is used to determine T_i. The procedure is terminated when

$$\left|\frac{T_i^{n+1} - T_i^n}{T_i^{n+1}}\right| \leq \text{F5CRIT}, \tag{3.1-34}$$

where F5CRIT is user supplied and n = iteration index. After T_i is determined, the procedure is repeated for the next axial level in a marching fashion.

3.1.2.5c FUEL TEMPERATURE CALCULATIONS

After the coolant temperatures are determined the temperatures in the fuel pin are determined by applying the steady-state heat conduction equation

$$\frac{1}{r}\frac{d}{dr}\, r\, k_i(\overline{T}_i)\frac{d}{dr} T_i(r) = Q_i \quad , \quad i = 1,\ldots,NF+2 \tag{3.1-35}$$

over the cladding, gap, and fuel pin radial nodes at a particular axial level in a coolant channel. Q_i is the power density (w/m^3). [For a fission gas plenum the equation is applied only over the clad]. The heat conduction equation is then solved analytically to form

$$T_i(r) = \frac{Q_i}{4k_i(T_i)} [r_{i+1}^2 - r^2]$$

$$+ \left[\frac{\pi Q_i \, r_{i+1}^2 - q^s_{i+1}}{2\pi k_i(T_i)} \right] \ell n \, (r/r_{i+1}) + T^s_{i+1} \qquad (3.1\text{-}36)$$

where, q^s_{i+1} = heat flow per unit axial length at the i+1 interface,

T^s_{i+1} = temperature at the i+1 interface.

Eq. (3.1-36) is integrated over each node to obtain the average temperature in the node as

$$\bar{T}_i = \left\{ -\left[\frac{Q_i}{8k_i} \right] (r_{i+1}^4 - r_i^4) \right.$$

$$+ C_1[r_{i+1}^2 (\ell n \, r_{i+1} - 1/2) - r_i^2 (\ell n \, r_i - 1/2)]$$

$$\left. + C_2[r_{i+1}^2 - r_i^2] \right\} / (r_{i+1}^2 - r_i^2) \qquad (3.1\text{-}37a)$$

where

$$C_1 = [\pi Q_i \, r_{i+1}^2 - q^s_{i+1}]/(2\pi \, k_i) \qquad (3.1\text{-}37b)$$

$$C_2 = T^s_{i+1} - \left\{ -\left[\frac{Q_i}{4k_i} \right] r_{i+1}^2 + C_1 \, \ell n \, r_{i+1} \right\} \qquad (3.1\text{-}37c)$$

The surface heat fluxes are obtained from the steady state heat balance,

$$q^s_{i+1} = \sum_{j=1}^{i} \pi Q_j \, (r_{j+1}^2 - r_j^2) \qquad (3.1\text{-}38)$$

The surface temperature at the outer clad surface is determined using the applied convective boundary condition,

$$T^s_{NF+3} = \frac{q^s_{NF+3}}{2\pi r_{NF+3} h_{cool}} + T_{cool} \qquad (3.1\text{-}39)$$

where,

h_{cool} = convective clad-to-coolant heat transfer coefficient,

T_{cool} = bulk average coolant temperature at that axial level in the channel.

The temperature at the clad inner surface is then determined by evaluating Eq. (3.1-36) at that surface,

$$T^S_{NF+2} = T_{NF+2}\,(r_{NF+2}) \quad . \tag{3.1-40}$$

The gap conductivity equation is used to obtain the fuel outer surface temperature,

$$T^S_{NF+1} = \frac{q^S_{NF+1}}{[2\pi r_{NF+1}\, h_{gap}]} + T^S_{NF+2} \quad . \tag{3.1-41}$$

The remaining surface temperatures are obtained by marching inward from the outermost fuel node and evaluating Eq. (3.1-36) at the appropriate surface, i.e.,

$$T^S_{i+1} = T_{i+1}(r_{i+1}) \;,\; i = (NF-1),\ldots,\, 1 \tag{3.1-42}$$

Since the material properties are all functions of the average temperature, an iterative strategy is used to solve the equations. The iterations are terminated when

$$\left|\frac{\bar{T}_i^{\,n} - \bar{T}_i^{\,n-1}}{\bar{T}_i^{\,n}}\right| \leq F5CRIT, \quad i = 1,\, NF+2 \tag{3.1-43}$$

where n = iteration index.

After the temperatures are converged a check is made to see if any fuel temperatures exceed the user specified restructuring temperatures. If the fuel pin restructures, the process is repeated with the new material properties, but no further restructuring is allowed.

3.1.2.5d STRUCTURE TEMPERATURE CALCULATIONS

In SSC, the effect of the wire wrap and any duct wall associated with the channel is accounted for in the structure temperature calculation. For calculational purposes, a lumped element equation is used and the average temperature of the wire and structure combined is given by

$$T_{STRUC} = Q_{STRUC}/UA_{TOT} + T_{cool} \quad , \tag{3.1-44}$$

where,

T_{cool} = bulk coolant temperature for this axial level of this channel,

Q_{STRUC} = total power deposited directly into the structure,

UA_{TOT} = overall heat transfer coefficient,

= $U_{wire} A_{wire} + U_{STRUC} A_{STRUC}$,

U_{wire}, A_{wire} U_{STRUC}, A_{STRUC} = the overall heat transfer coefficient and total heat transfer area for the wire and structure respectively.

As was the case for the fuel pin, the structure material properties are temperature dependent and an iterative procedure is employed to solve for the temperatures. As before, the iterations are terminated when

$$\left| \frac{T_{STRUC}^{n} - T_{STRUC}^{n-1}}{T_{STRUC}^{n}} \right| \leq F5CRIT, \tag{3.1-45}$$

where n = iteration index. This procedure is repeated for all axial levels of all channels.

3.1.2.6 TRANSIENT ALGORITHMS

In transient calculations, the structure, coolant, and fuel rod temperatures are coupled at a particular axial level. As in the steady-state, axial heat conduction is neglected and the flow is assumed to be uni-directional in the channel. These assumptions do permit the transient energy equations to be solved using a fully-implicit finite difference scheme in time on an axial level basis in marching fashion.

3.1.2.6.a COOLANT HYDRAULIC CALCULATIONS

The fraction of total coolant flow entering a channel, prior to the initiation of transients, is established by the design of the orifice pattern. During transients, this fractional flow in a channel will be altered by the buoyancy effect. A model for the computation of the flow pattern inside the reactor core is developed here. This flow redistribution is then used to compute the enthalpy change and the pressure drop in each of the flow channels.

Calculations of flow redistribution in the reactor vessel are based on the following momentum equation for one-dimensional incompressible flow:

$$\frac{\partial}{\partial t}(W) + \frac{\partial}{\partial z}(W \cdot v) + A\frac{\partial p}{\partial z} + f \cdot \frac{\rho v^2}{2}\frac{A}{D_h} g\rho \cos(g,W) = 0. \qquad (3.1\text{-}46)$$

In deriving the above equation, it was assumed that the control volume in the flow circuit satisfies

$$\frac{d \ln A}{dz} = 0 \quad , \qquad (3.1\text{-}47)$$

where W is the coolant flow rate (kg/s), v is the velocity (m/s), p is the pressure (N/m^2), A is the flow area (m^2), D_h is the hydraulic diameter

(m), z is the vertical coordinate (m), and ρ is the fluid density (kg/m^3).

The Moody friction coefficient f is expressed in the form

$$f = c_1(Re)^{-c_2}, \tag{3.1-48}$$

where c_1 and c_2 are constants determined by the flow regime.

The differential form of the momentum Equation (3.1-46) can be applied for any of the parallel channels from the elevation e (bottom of the core) to the elevation d (top of the core) in Figure 3.1-1 by integrating through different axial regions. We obtain

$$(p_e - p_d)_j = \left(\frac{L}{A}\right)_j \frac{dW_j}{dt} + \left(\frac{W}{A}\right)_j^2 \left[\frac{1}{\rho_d} - \frac{1}{\rho_e}\right]_j$$

$$+ W_j|W_j|^{(1-c_2)} I_{f,j} + W_j|W_j| I_{k,j} - g I_{g,j}, \tag{3.1-49}$$

where j denotes the j-th channel, and

$$\left(\frac{L}{A}\right)_j = \left(\frac{L}{A}\right)_{inlet} + \left(\frac{L}{A}\right)_{core} + \left(\frac{L}{A}\right)_{outlet} \tag{3.1-50}$$

$$I_{f,j} = \frac{1}{2}\left[(fL/(\rho DA^2))_{inlet} + (1/(DA^2)\int \frac{f}{\rho}\, dz)_{core}\right. \tag{3.1-51}$$

$$\left. + (fL/(\rho A^2))_{outlet}\right]_j$$

$$I_{k,j} = \left[(K/(2\rho A^2))_{inlet} + (K/(2\rho A^2))_{outlet}\right]_j \tag{3.1-52}$$

$$I_{g,j} = \left[(L\rho)_{inlet} + \int_{core} \rho dz + (L\rho)_{outlet}\right]_j \tag{3.1-53}$$

Note: similar equations are obtained for the bypass channel.

The flow redistribution in various channels in the vessel is calculated from the pressure-drop equation by using two more assumptions:

1) No radial pressure variation in the lower and upper plena,

2) At any instant,

$$\sum_{j=1}^{N6CHAN} W_j(t) + W_{BP}(t) = W_{vessel}(t) \quad , \tag{3.1-54}$$

where W_{vessel} is the summation of total flow rate(s) leaving the loop(s) and entering the vessel lower plenum, and the subscript BP denotes bypass. Equations (3.1-49) and (3.1-54) together with the loop hydraulic equations discussed in Section 3.2.9 constitute a set of differential and algebraic equations to solve for the time rates of change of the various flow rates and the instantaneous pressures. The advancement in time of the hydraulic differential equations is handled by a predictor-corrector integration algorithm of the Adams type (see Chapter 4).

3.1.2.6b COOLANT TEMPERATURE EQUATION

The governing ordinary differential equation for the coolant is developed by applying the coolant energy equation over the node, integrating over the node, and using donor cell differencing in space. The governing finite difference for the coolant equation is:

$$\begin{aligned}(\rho c_p)\, V_{cool} \left(\frac{T_{co}^{k+1} - T_{co}^{k}}{\Delta t}\right) &= Wc_p \,(T_{ci}^{k+1} - T_{co}^{k+1}) \\ &+ UA_{STRUC}\,(\overline{T}_{STRUC}^{k+1} - \overline{T}_{cool}^{k+1}) \\ &+ (NRODS)\, q^{s}_{NF+3}\, \Delta Z \\ &+ Q_{cool}\, V_{cool}\end{aligned} \tag{3.1-55}$$

where,

ρ = density of coolant

c_p = specific heat of coolant

T_{co}^{k+1} = coolant temperature at outlet to axial slice at time k+1

T_{co}^{k} = coolant temperature at outlet to axial slice at time k

Δt = timestep

W = average channel flow rate

T_{ci}^{k+1} = coolant temperature at inlet to axial slice at time k+1

UA_{STRUC} = overall heat transfer coefficient between structure and coolant

$\bar{T}_{STRUC}^{k+1}$ = average structure temperature at time k+1

$\bar{T}_{cool}^{k+1}$ = bulk coolant temperature at this axial slice

$= (T_{co}^{k+1} + T_{ci}^{k+1})/2$

NRODS = number of fuel rods associated with this coolant channel

q^s_{NF+3} = heat flux between fuel rod cladding and coolant at time k+1

ΔZ = height of axial slice

Q_{cool} = total volumetric power deposited directly in coolant

V_{cool} = total volume of coolant in axial slice.

3.1.2.6c FUEL PIN TEMPERATURE EQUATIONS

The average temperatures in the cladding and the radial nodes of the fuel pin are calculated by applying Fourier's law over the nodes, integrating over the node, and using a finite difference procedure in time to form,

$$(\rho cp)_i \frac{(\bar{T}_i^{k+1} - \bar{T}_i^{k})}{\Delta t} \quad \frac{-[q^s_{i+1} - q^s_i]}{A_i} + Q_i(t) \quad i=1,\ldots,NF,\ i=NF+2 \qquad (3.1\text{-}56)$$

where, $A_i(t) = \pi(r_{i+1}^2 - r_i^2)$.

The surface heat fluxes, q^s_i's, are determined by using a weighted residuals procedure in space. Specifically, it is assumed that the temperature distribution within a radial node can be approximated by:

$$T_i(r,t) \simeq \tilde{T}_i(r,t) = \bar{T}_i(t)\, F_{i,1}(r) + q^s_{i+1}(t)\, F_{i,2}(r) + T^s_{i+1}(t)\, F_{i,3}(r) \quad i=1,\ldots,NF,\ldots, i=NF+2 \tag{3.1-57}$$

where, for $r_1 \neq 0$

$$F_{i,1}(r) = \frac{(r^2 - r_{i+1}^2) - 2r_{i+1}^2\, \ell n(r/r_{i+1})}{I_{i,1} - 2r_{i+1}^2\, I_{i,2}} \tag{3.1-58a}$$

$$F_{i,2}(r) = \frac{1}{2\pi k_i}\left\{\frac{(r^2 - r_{i+1}^2) - 2r_{i+1}^2\, \ell n\,(r/r_{i+1})}{I_{i,1} - 2r_{i+1}^2\, I_{i,2}}\right\} - \ell n\,(r/r_{i+1}) \tag{3.1-58b}$$

$$F_{i,3}(r) = -\left\{\frac{(r^2 - r_{i+1}^2) - 2r_{i+1}^2\, \ell n\,(r/r_{i+1})}{I_{i,1} - 2r_{i+1}^2\, I_{i,2}}\right\} + 1 \tag{3.1-58c}$$

and for $r_1 = 0$

$$F_{i,1}(r) = 0, \tag{3.1-59a}$$

$$F_{i,2}(r) = (r^2 - r_2^2)\,/4\pi k_1\,(r_1^2 - r_2^2) \tag{3.1-59b}$$

$$F_{i,3}(r) = 1 \tag{3.1-59c}$$

where,

$$I_{i,1} = \frac{(r_{i+1}^4 - r_i^4) - 2r_{i+1}^2\,(r_{i+1}^2 - r_i^2)}{2(r_{i+1}^2 - r_i^2)} \tag{3.1-60a}$$

$$I_{i,2} = \frac{(r^2_i - r^2_{i+1}) - 2r^2_i\, \ell n\,(r_i/r_{i+1})}{2(r^2_{i+1} - r^2_i)} \tag{3.1-60b}$$

It is required that these equations satisfy all boundary conditions and all interface continuity conditions. Specifically,

a) a convective boundary at the clad-coolant interface,

$$q^s_{NF+3} = -2\pi r_{NF+3}(T^s_{NF+3} - T_{cool}) \cdot h_{cool} \qquad (3.1\text{-}61a)$$

b) the continuity of heat flux at the fuel clad gap,

$$q^s_{NF+1} = -2\pi r_{NF+2}\, k_{NF+3} \frac{\partial}{\partial r} \tilde{T}_{NF+2}(r_{NF+2},t) \qquad (3.1\text{-}61b)$$

c) the temperature drop at the fuel clad gap

$$q^s_{NF+1} = 2\pi r_{NF+1}\, h_{gap} \quad (T^s_{NF+1} - \tilde{T}_{NF+2}(r_{NF+2},t)) \qquad (3.1\text{-}61c)$$

d) continuity of heat flux at a fuel nodal interface

$$q^s_i = -2\pi r_i k_i \frac{\partial}{\partial r} \tilde{T}_i(r,t)|_{r_i}, \qquad i = 2,NF \qquad (3.1\text{-}61d)$$

e) continuity of temperature at a fuel nodal interface

$$T^s_i = \tilde{T}_i(r_i,t) \qquad i = 2, NF \qquad (3.1\text{-}61e)$$

f) adiabatic boundary condition for the innermost node

$$0 = -2\pi r_1 k_1 \frac{\partial}{\partial r} \tilde{T}_1(r,t)\,|_{r_1} \qquad (3.1\text{-}61f)$$

Eqs. (3.1-56) and Eqs. (3.1-61) provide 3(NF+1) equations for determining the 3(NF+1) unknowns,

$$\bar{T}_i(t),\ q^s_{i+1}(t),\ T^s_{i+1}(t), \quad i = 1,\ NF,\ i = NF+2.$$

3.1.2.6d STRUCTURE TEMPERATURE EQUATION

The structure temperature equation in finite difference form is

$$(\rho c_p)\, V_{STRUC} \frac{(\bar{T}_{STRUC}{}^{k+1} - \bar{T}_{STRUC}{}^{k})}{\Delta t} = UA_{STRUC}\,(\bar{T}_{cool}{}^{k+1} - \bar{T}_{STRUC}{}^{k+1}) + Q_{STRUC} \qquad (3.1\text{-}62)$$

3.1.2.6e SOLUTION OF THE TRANSIENT TEMPERATURE EQUATIONS

Eqs. (3.1-55), (3.1-56), (3.1-61) and (3.1-62) are assembled to form a matrix equation in the 3(NF+1)+2 unknowns: T_{co}^{k+1}, $\bar{T}_{STRUC}^{k+1}$, $\bar{T}_i^{k+1}$, q_{i+1}^{s}, T_{i+1}^{s}, i = 1,NF, i = NF+2. The resulting coefficient matrix has a bandwidth of seven and is solved using a standard banded inversion routine. The solution procedure is then marched to the next axial level via T_{co}^{k+1}, and the process repeated for all axial levels of all channels.

3.1.2.7 TRANSIENT FISSION HEATING

The time-dependent portion of the fission power contribution is calculated by solving the space-averaged, one-energy group reactor kinetics equations. The one-energy group assumption is reasonable, particularly for a fast reactor. The space-averaged model is quite adequate since the core of an LMFBR responds, due to the relative smallness of the core and the large neutron migration area, more uniformly than a light water reactor core to changes in reactivity.

The point-kinetics equations written in terms of the prompt neutron generation time (ℓ) may be expressed (source term neglected) as:

$$\frac{dN}{dt} = \frac{\rho - \beta T}{\ell} N + \Sigma_i \lambda_i C_i \,, \qquad (3.1\text{-}63)$$

$$\frac{dC_i}{dt} = \frac{\beta_i N}{\ell} - \lambda_i C_i, \qquad (3.1\text{-}64)$$

where

N = neutron density (which is proportional to the power),

ρ = total reactivity ($\Delta k/k$),

β_T = total effective delayed neutron fraction = $\sum_i \beta_i$,

ℓ = prompt neutron generation time (s),

λ_i = decay constant of the i-th delayed neutron group (s^{-1}),

C_i = density of the i-th effective delayed neutron precursor,

β_i = fraction of the i-th effective delayed neutron group,

t = time (s),

By rewriting N and C_i in normalized form such that

$$n(t) = \frac{N(t)}{N(0)}; \; c_i(t) = \frac{C_i(t)}{C_i(0)}; \text{ where } C_i(0) = \frac{\beta_i}{\ell_i} N(0) \qquad (3.1\text{-}65)$$

Equations (3.1-63) and (3.1-64) become

$$\frac{dn}{dt} = \frac{\rho - \beta_T}{\ell} + \frac{1}{\ell} \sum \beta_i c_i \,, \qquad (3.1\text{-}66)$$

$$\frac{dc_i}{dt} = \lambda_i \, (n - c_i). \qquad (3.1\text{-}67)$$

The direct integration of these equations requires very small timestep sizes due to the small numerical value of the generation time (ℓ). To assure numerical stability and accuracy, step sizes of approximately (100 to 1000)$\cdot \ell$ are required. Typically, ℓ is about = 6×10^{-7} s, therefore, the step sizes of the order of 0.00006 to 0.0006 s would be required.

The simplest way to circumvent this problem is to utilize the prompt jump approximation (PJA). This approximation makes use of the very fact that ℓ is

extremely small. By assuming that ℓ approaches zero, the product ℓ dn/dt in Equation (3.1-66) also approaches zero. Thus, n may be directly solved for as

$$n = \frac{1}{\beta_T - \rho} \sum_i \beta_i C_i \quad . \tag{3.1-68}$$

This means that any distrubance in the reactivity (ρ) will be instantaneously reflected in the power (n). Thus, for a step change in ρ, n jumps immediately to some initial level dependent on the size of the reactivity insertion.

The PJA is in excellent agreement (to within < 0.1%) with the exact solution for values of ρ less than +50 cents. It should be noted that this approximation gets even closer to the exact solution when the prompt neutron generation time is smaller.

The main drawback of using the PJA is the fact that agreement to the exact solution diminishes as ρ approaches β_T. It can be seen from Equation (3.1-68) that n is discontinuous at $\rho = \beta_T$. To provide for these cases where ρ approaches β_T (or more conservatively, when ρ > 50 cents) an optional numerical method is included in SSC which solves the equations "exactly".

To provide an "exact" solution to Equations (3.1-66) and (3.1-67), without integrating them directly, the method proposed by Kaganove [Ref. 3.1-1] was used. Here, Equations (3.1-67) are solved for c_i in terms of dc_i/dt and substituted into Equation (3.1-66) such that

$$\frac{dn}{dt} = \frac{\rho n}{\ell} - \frac{1}{\ell} \sum_i \frac{\beta_i}{\lambda_i} \frac{dc_i}{dt} \tag{3.1-69}$$

The assumption is then made that over any integration step (Δt), the

normalized power (n) and reactivity (ρ) may be represented by second-order polynomials. Thus,

$$n(t) = n_0 + n_1 t + n_2 t^2 \qquad 0 \leq t \leq \Delta t, \tag{3.1-70}$$

$$\rho(t) = \rho_0 + \rho_1 t + \rho_2 t^2 \qquad 0 \leq t \leq \Delta t, \tag{3.1-71}$$

where

n_0 = value of n at the end of previous timestep,

ρ_0 = value of ρ at the end of previous timestep,

and n_1, n_2, ρ_1, ρ_2 are constants in to be evaluated.

Equation (3.1-67) is now integrated in a straightforward manner:

$$\int_0^t d\left[c_i(\mu)\, e^{\lambda_i \mu}\right] = \int_0^t \lambda_i e^{\lambda_i \mu}\, n(\mu)\, d\mu. \tag{3.1-72}$$

Then

$$c_i(t) = c_{io} e^{-\lambda_i t} + \lambda_i e^{-\lambda_i t} \int_0^t e^{\lambda_i \mu}\, n(\mu)\, d\mu \quad , \tag{3.1-73}$$

where

$$c_{io} = c_i(t)\,|_{t=0}.$$

Making use of Equation (3.1-70), Equation (3.1-73) becomes

$$c_i(t) = c_{io} e^{-\lambda_i t} + n_o \left(1 - e^{-\lambda_i t}\right) + \frac{n_1}{\lambda_i}\left(\lambda_i t - 1 + e^{-\lambda_i t}\right)$$

$$+ \frac{n_2}{\lambda_i^2}\left[\lambda_i^2 t^2 - 2\lambda_i t - 2\left(1 - e^{-\lambda_i t}\right)\right]. \tag{3.1-74}$$

Likewise, Equation (3.1-69) becomes

$$n(t) - n(o) = \frac{1}{\ell}\int_0^t \rho(\mu)\, n(\mu)\, d\mu - \frac{1}{\ell}\sum_i \frac{\beta i}{\lambda_i}\,[c_i\,(t) - c_{io}]. \qquad (3.1\text{-}75)$$

Upon substituting Equations (3.1-70) and (3.1-71) into Equation (3.1.75), one obtains

$$n_1 t + n_2 t^2 = \frac{1}{\ell}\left(\rho_o n_o t + \rho_o n_1 \frac{t^2}{2} + \rho_o n_2 \frac{t^3}{3} + \rho_1 n_o \frac{t^2}{2} + \rho_1 n_1 \frac{t^3}{3} + \rho_1 n_2 \frac{t^4}{4}\right.$$

$$\left. + \rho_2 n_o \frac{t^3}{3} + \rho_2 n_1 \frac{t^4}{4} + \rho_2 n_2 \frac{t^5}{5}\right) - \frac{1}{\ell}\sum_i \frac{\beta_i}{\lambda_i}\,[c_i(t) - c_{io}] \qquad (3.1\text{-}76)$$

The boundary conditions are then imposed that the integral Equation (3.1-76) be satisfied at the midpoint and end of the step (i.e., at $t=\Delta t/2$ and $t=\Delta t$). Thus, Equation (3.1-76) yields two equations in the unknowns n_1 and n_2. With the assumption that during any given timestep, the power and reactivity are functions of time only (i.e., decoupled), the solution is now complete. During a transient, the implementation of the solution in SSC will proceed as follows:

(a) using the predicted value of reactivity at $t=\Delta t$ and the two previous values, the two constants ρ_1 and ρ_2 in Equation (3.1-71) are calculated;

(b) using Equation (3.1-76) solved at $\Delta t/2$ and Δt, the constants n_1 and n_2 are calculated;

(c) the predicted power may then be calculated using Equation (3.1-70).

3.1.2.8 REACTIVITY CONTRIBUTIONS

The total reactivity at a given time, t, is the sum of an applied re-

activity, $\rho_a(t)$ (e.g., control rod movement), plus the sum of the various reactivity feedback contributions, $\rho_i(t)$:

$$\rho(t) = \rho_a(t) + \Sigma\ \rho_i(t) \quad . \tag{3.1-77}$$

As indicated in Figure (3.1-6), the total reactivity is then incorporated into the point-kinetics model and used in the evaluation of the normalized time-dependent factor for the fission and gamma heating. It should also be noted that the reactivity effects are inherently spatially-dependent. This is not only due to the fact that the temperatures vary spatially, but even for the same temperatures the magnitude of the effect will depend on the location within the reactor. Since the point-kinetics equations suppress any spatial dependence, an appropriately weighted spatial integration of the evaluated local reactivity feedback effects must be performed.

A survey of several references [3.1-2 through 3.1-6] and existing computer models [3.1-7,3.1-8] has identified the following contributions to the feedback effects:

- Doppler
- Sodium density and voiding
- Fuel axial expansion
- Structural expansion
- Bowing
- Fuel slumping

The first three effects will be discussed in more detail in subsequent subsections. Models are presented and equations developed for incorporation of these effects into the present version of SSC. The remainder of this section will briefly discuss the last three effects.

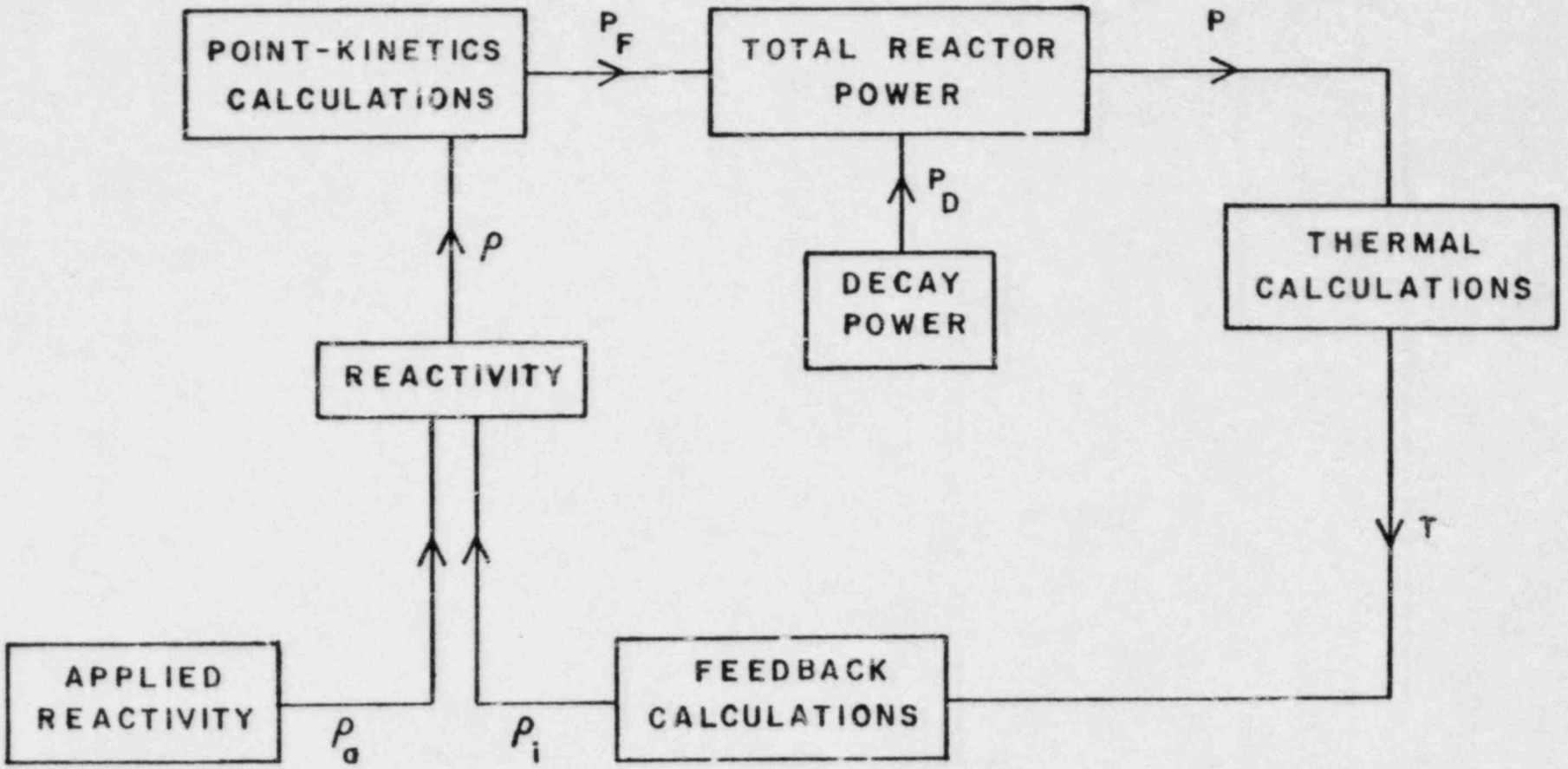

Figure 3.1-6 Reactivity Feedback Loop

Radial Structural Expansion

As the core heats up there is radial expansion of the fuel assemblies and core support structures which tends to effectively increase the pitch-to-diameter ratio of the fuel lattice, reducing the reactivity. However, this effect has a long time constant relative to the fuel, for example, since it is related to the structural components. From a normal operational viewpoint (e.g., taking the reactor from zero to full power), this effect will be much more important than for those transients that SSC will be analyzing.

Bowing

Bowing is caused by differential thermal expansion and is a result of radial temperature gradients. Positive reactivity can be added when fuel material bows towards the center of the reactor. To reduce this effect, spacers are placed between fuel elements and fuel assemblies. The temperature gradients cause stresses in the contacted material which is designed to be strong enough to prevent appreciable displacements.

Also, as with structural expansion this effect will have a relatively long time constant since it is the fuel assembly and not the fuel pins themselves that provide the structural strength [3.1-2].

Fuel Slumping

In the event of fuel melting, there is the possibility for fuel movement within the cladding material. If the fuel moves (slumps) towards the center of the core, then there will be positive reactivity added to the system. However, the current version of SSC does not treat the class of transients that

would lead to this condition; hence, fuel slumping in not considered further.

3.1.2.8a DOPPLER EFFECT

The Doppler effect is the most important and reliable prompt negative reactivity effect in current thermal and fast reactor designs which utilize high fertile (U_{238}) material concentrations. Probably one of the better understood reactivity phenomena, the Doppler effect is due to the increased kinetic motion of the fuel atoms, as measured by an increase in fuel temperature, resulting in the broadening of cross-section resonances and increased resonance absorption.

The Doppler coefficient is defined as the change in multiplication factor, k, associated with an arbitrary change in the absolute fuel temperature, T. Since ir fast reactors this coefficient is found to vary as the inverse of fuel temperature, a temperature independent Doppler parameter, α^{DOP}, can be generally defined as

$$\alpha^{DOP} = T\, dk/dt. \qquad (3.1\text{-}78)$$

Equation (3.1-78) may be integrated to yield

$$k^1 - k^2 = \alpha^{DOP} \ln T^1/T^2 , \qquad (3.1\text{-}79)$$

where T^1 and T^2 represent two different fuel temperatures and k^1 and k^2 are the resulting multiplication factors. Rigorously, reactivity is defined as

$$\rho = \frac{k - 1}{k} , \qquad (3.1\text{-}80)$$

and changes in reactivity, $\Delta\rho$, as

$$\Delta\rho = \rho^1 - \rho^2 = \frac{k^1 - k^2}{k^1 k^2} \qquad (3.1\text{-}81)$$

For small reactivity changes, the Doppler effect is of the order of 10^{-4}. With $k \approx 1$,

$$k^1 - k^2 \approx \rho^1 - \rho^2 , \tag{3.1-82}$$

the change in reactivity due to the Doppler effect $\Delta\rho^{DOP}$, can be written as

$$\Delta\rho^{DOP} = \alpha^{DOP} \ln \frac{T^1}{T^2} . \tag{3.1-83}$$

This equation may be applied locally or regionally depending on how the temperatures and Doppler coefficient are defined. Specificaly, in discrete notation, the local Doppler reactivity, ρ^{DOP}_{JK} is

$$\rho^{DOP}_{JK} = \alpha^{DOP}_{JK} \ln \frac{T_{JK}}{T^2_{JK}} , \tag{3.1-84}$$

where K represents the channel, J is the axial position in the channel K, and T_{JK} is the effective local temperature at position JK. This effective fuel temperature can be taken to be the volume-average fuel temperature which is defined as

$$T_{JK} = \frac{\sum_I V_{IJK} T_{IJK}}{\sum_I V_{IJK}} , \tag{3.1-85}$$

where V_{IJK} is the fuel volume in channel K, axial slice J, between radial mesh I and I-1, and T_{IJK} is the local fuel temperature at this position.

It should be noted that the Doppler coefficient in Equation (3.1-84) is shown to be a spatially-dependent variable. Although α^{DOP}_{JK} will be a constant with respect to fuel temperataure, there will be spatial variations due to different fuel types (e.g., enrichment, pin size, volume fractions of structural material, coolant, and fuel) and different sodium density. In the present model, α^{DOP}_{JK} will be a spatially-dependent parameter supplied by the user, Thus, the first concern relating to fuel type can be directly addressed.

The sodium density dependence is actually a neutron spectrum dependence--the harder the spectrum, the smaller the Doppler effect (since there are less neutrons in the resonance range). The less sodium present, owing to density decreases or voids, implies a harder spectrum. To treat this effect, an effective isothermal sodium void fraction, X^{NA}_{JK}, is defined

$$X^{NA}_{JK} = \frac{\rho^{NA}_{JK\,ref} - \rho^{NA}_{JK}}{\rho^{NA}_{JK\,ref}} \qquad (3.1\text{-}86)$$

where ρ^{NA}_{JK} is the local, time-dependent sodium density at position JK, and $\rho^{NA}_{JK\,ref}$ is the local reference sodium density at position JK. Thus, if β^{DOP}_{JK} and Ω^{DOP}_{JK} are the Doppler parameters with and without sodium present, respectively, then the net Doppler parameter can be approximated by

$$\alpha^{DOP}_{JK} = \beta^{DOP}_{JK}\,(1 - X^{NA}_{JK}) + \Omega^{DOP}_{JK}\,X^{NA}_{JK} \qquad (3.1\text{-}87)$$

To obtain an overall Doppler reactivity, ρ^{DOP}, for use in the point-kinetics equation, a summation of Equation (3.1-84) must be performed. Thus,

$$\rho^{DOP} = \sum_{J,K} \rho_{JK}^{DOP} = \sum_{J,K} \alpha_{JK}^{DOP} \ell n \frac{T_{JK}}{T_{JK}} . \qquad (3.1\text{-}88)$$

The values of the Doppler coefficients, α_{JK}^{DOP}, for each JK-th region must be supplied by the user in units of reactivity ($\Delta k/k$) for that mesh.

3.1.2.8b SODIUM DENSITY AND VOID EFFECTS

Heating of the sodium coolant decreases the coolant density and can ultimately lead to vaporization (voiding). These density decreases affect the reactivity of the reactor through two competing effects: increased leakage, which adds negative reactivity and is important away from the center of the core; and spectral hardening due to a decrease in the macroscopic sodium scattering cross-section which adds positive reactivity. The net effect depends primarily upon the location in the reactor.

In modeling this effect, both sodium density changes and voiding can be treated in a similar fashion. Basically, what is required along with the spatial sodium density distribution is a table of spatially-dependent sodium reactivity worths. The sodium density will be determined internally by SSC from knowledge of the sodium temperature distribution. However, the reactivity worths are user supplied.

There are several ways to present this reactivity effect depending on the form in which the reactivity worth data are known. For application in SSC,

the following equation, which can treat either sodium density or voiding reactivity effects, is used:

$$\rho^{NA} = \sum_{JK} \beta_{JK} M_{JK} , \qquad (3.1\text{-}89)$$

where ρ^{NA} is the overall sodium density and voiding reactivity for use in the point-kinetics equations, β_{JK} is the sodium reactivity worth in axial slice J, channel K, in units of reactivity per unit mass of sodium effectively voided, and M_{JK} is the effective mass of sodium voided in segment JK, and is defined in the following equation:

$$M_{JK} = (\rho^{NA}_{JK2} - \rho^{NA}_{JK1}) \cdot V^{NA}_{JK} \qquad (3.1\text{-}90)$$

In this equation, ρ^{NA}_{JK} is the local average, time-dependent sodium density and V^{NA}_{JK} is the local coolant volume in segment JK.

3.1.2.8c FUEL AXIAL EXPANSION EFFECT

Axial expansion of the fuel pellets tends to increase the active core height while decreasing the fuel density, resulting in a net decrease in reactivity. An upper limit to the magnitude of this effect is obtained if it is assumed that the fuel pellets are free to move within the cladding. However, the actual mechanisms for expansion are difficult to model, especially for ceramic fuel. Fuel pellet cracking or friction between the pellet surface and inner clad wall will reduce the expansion significantly. On the other hand, if the fuel pellets are not stacked in perfect contact within the clad, then there may be negative fuel expansion if the fuel pellets settle.

Physics calculations for CRBRP [3.1-9] indicate a maximum overall reactivity of -.18¢/mil of fuel axial expansion. The range of this effect is quoted to be +.025¢/mil to -.18¢/mil owing to the uncertainties previously discussed. For inclusion in SSC, the reactivity due to fuel axial expansion, ρ^{AX}, is based on a model which parallels the treatment of sodium density reactivity effects:

$$\rho^{AX} = \sum_{JK} C_{JK} \quad N^{*}_{JK} \tag{3.1-91}$$

where C_{JK} is the fuel reactivity worth in axial slice J, channel K, in units of reactivity per unit mass of fuel effectively voided from segment JK and N^{*}_{JK} is the effective mass of fuel voided in segment JK.

The user will supply values for the C_{JK} constants. An expression for the internal evaluation of N^{*}_{JK} is now derived based on the logic that as the fuel temperature increases, the fuel expands axially according to the following equations:

$$Z^{2}_{JK} = [1 + \alpha(T^{2}_{JK} - T^{1}_{JK})] Z^{1}_{JK} , \tag{3.1-92}$$

where α is the linear fuel expansion coefficient in units of cm/cm-K and T_{JK} is the fuel volume average temperature as evaluated by Equation (3.1-85). To conserve mass, an axial increase in the fuel length (FL) implies

a decrease in the fuel density, ρ^{FL}_{JK}, (ignoring other dimensional changes); thus

$$\overset{\cdot}{\rho}{}^{FL1}_{JK}\, Z^{1}_{JK} = \rho^{FL2}_{JK}\, Z^{2}_{JK} \qquad (3.1\text{-}93)$$

or

$$\rho^{FL1}_{JK} - \rho^{FL2}_{JK} = \rho^{FL1}_{JK} \cdot [\alpha(T^{2}_{JK} - T^{1}_{JK})/(1 + \alpha(T^{2}_{JK} - T^{1}_{JK}))] \qquad (3.1\text{-}94)$$

The difference in density times the original fuel volume (before expansion), V^{FL1}_{JK} will give the amount of fuel voided from location JK, N_{JK}:

$$N_{JK} = \rho^{FL1}_{JK}\, X^{FL}_{JK}\, V^{FL1}_{JK} \quad , \qquad (3.1\text{-}95)$$

where X^{FL}_{JK} is the fuel void fraction at location JK and follows from Equation (3.1-94) to be

$$X^{FL}_{JK} = \alpha(T^{2}_{JK} - T^{1}_{JK})/[1 + \alpha(T^{2}_{JK} - T^{1}_{JK})] \qquad (3.1\text{-}96)$$

The effective amount of fuel voided from location JK, N^{*}_{JK}, and the resulting net reactivity effect associated with fuel axial expansion are given by the following equations:

$$N^{*}_{JK} = e \cdot N_{JK} \quad , \qquad (3.1\text{-}97)$$

$$\rho^{AX} = e \cdot \Sigma\; C_{JK}\, N_{JK} \quad , \qquad (3.1\text{-}98)$$

where e is a user-supplied constant that accounts for the fact that the present model does not account for the uncertainties associated with the mode of

fuel expansion and does not explicitly evaluate the increase in reactivity because the fuel that was calculated to be voided from location JK [Equation (3.1-95)] actually causes a net increase in axial fuel height, reducing leakage. An estimate on the size of these effects is given in Reference [3.1-4]. A recommended upper limit for e is thus given to be 0.3.

3.1.2.9 DECAY HEATING

The time-dependent portion of the decay heat contribution can be handled in one of two ways:

(1) tabular look-up of user supplied data, or

(2) solution of user-supplied empirical relationships.

The decay heat calculations are handled in one subroutine (PDCY5T). In SSC, the default option of tabular look-up is used. Thus, paired points of time vs. decay heat fraction must be supplied on input. If the user wishes to supply empirical correlations, they must be inserted into PDCY5T at the appropriate place.

Both the relative magnitude and the time-dependent shape of the decay heating are allowed to be channel-dependent, as discussed earlier. The user provides F5PDCY(K) as well as d(K,t). An additional time-dependent function $d_B(t)$ for gamma heating of coolant in the bypass channel must also be provided. Both d(K,t) and $d_B(t)$ are normalized so that at steady-state their values are 1.0.

3.1.3 UPPER (OUTLET) PLENUM

In the upper (outlet) plenum, the coolant from the core exit and the bypass channel mixes with the coolant stored in the region. Along with this mixing process, the heat transfer between sodium and various structural metals and between sodium and the cover gas also takes place. An accurate treatment for this mixing process, coupled with the heat transfer, is required so that the sodium temperature at the outlet nozzle of the reactor vessel may be properly predicted. A detailed three-dimensional (in space) thermohydraulic treatment would be expensive for a system code. Therefore, a simplified treatment was developed.

A schematic of the contents of the outlet plenum is shown in Figure 3.1-7. The upper plenum contains a large volume of sodium, an annular bypass channel, a small region occupied by the cover gas, and three sections of metal. Fluid leaving the reactor core enters tne plenum from the bottom section, while a small percentage of cold bypass flow enters the plenum through the annular space formed by the thin thermal liner and the vessel wall. The vessel outlet flow is represented by an exit nozzle. The support columns, chimney of the outlet module, control rod drive mechanism, vortex suppressor plate, control assembly, cellular flow collector, baffle, and all other structures are lumped together and represented by a section of mass (m1) immersed in fluids. The cylindrical thermal liner is indicated as another mass (m2). The vessel closure head and other metals above the cover gas region are considered as mass m3. The cover gas region is connected to a large reservoir which represents its connections, such as the overflow tank, equalization line heater, and gas region of the loop pumps.

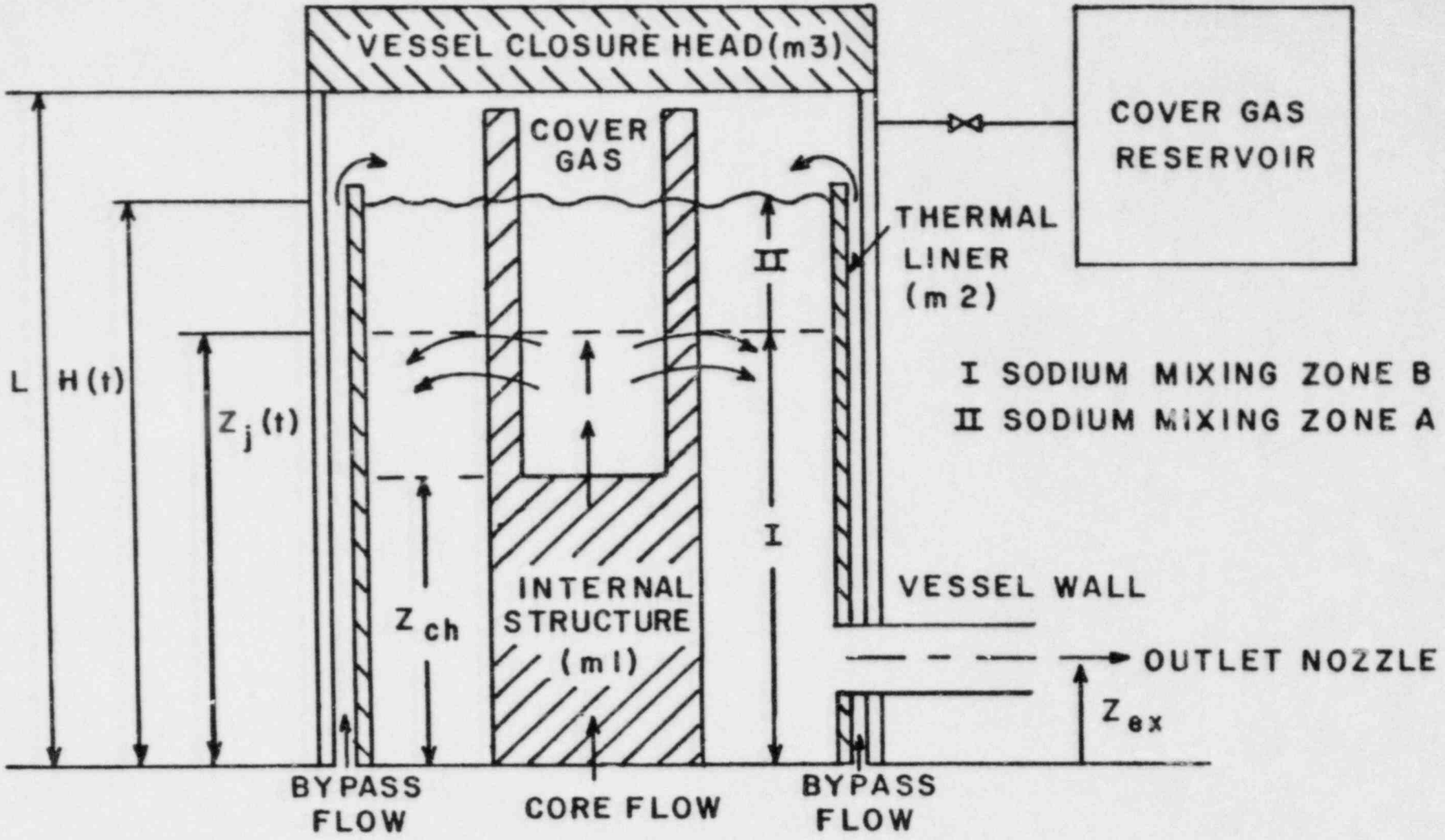

Figure 3.1-7 A Schematic of the Upper (Outlet) Plenum of a Reactor Vessel

A user of SSC can represent the outlet plenum described above with either a two-zone mixing model or a single-zone perfect mixing model, by setting the appropriate input option flag. In the equations that follow, the single-zone model is simply a sub-set of the two-zone model with the parameter (f) always held at zero.

For the two-zone mixing model, the maximum penetration of the average core exit flow is used as the criterion for dividing the sodium region into two zones. The upper mixing zone is denoted as zone A and the lower zone as zone B. The basic assumptions are

1) Core flows from different channels into the upper plenum are represented by a single equivalent flow. This flow is associated with the mass-average enthalpy of the different channel flows.
2) The maximum penetration distance, which is related to the initial Froude number, divides the upper plenum into two mixing zones. Full penetration is assumed for flow with positive buoyancy.
3) The mixing process in both zones is described by the lumped-parameter approach, i.e., complete mixing in each zone is assumed.
4) The cover gas obeys the perfect gas law, and it is initially in equilibrium with the gas in the reservoir.

At steady-state, the core exit flow is at a temperature higher than the mixed-mean sodium temperature of the outlet plenum. In other words, in accordance with our assumption (2) above, the core exit flow is assumed to penetrate the entire height of the outlet plenum. In this case, we have only one zone, as opposed to up to two zones during transients. The governing energy equations for this complete mixing at steady-state are written for each material as

sodium:

$$W_c(E_c - E_\ell) + W_{BP}(E_{BPE} - E_\ell) + U_g A_{\ell g}(T_g - T_\ell) + U_\ell A_{\ell m1}(T_{m1} - T_\ell) + U_\ell A_{\ell m2}(T_{m2} - T_\ell) = 0 \; ; \tag{3.1-99}$$

cover gas:

$$A_{\ell g}(T_\ell - T_g) + A_{gm1}(T_{m1} - T_g) + A_{gm2}(T_{m2} - T_g) + A_{gm3}(T_{m3} - T_g) = 0 \tag{3.1-100}$$

internal structure (m1):

$$U_\ell A_{\ell m1}\,(T_\ell - T_{m1}) + U_g A_{gm1}\,(T_g - T_{m1}) = 0 \tag{3.1-101}$$

thermal liner (m2):

$$U_\ell A_{\ell m2}\,(T_\ell - T_{m2}) + U_g A_{gm2}\,(T_g - T_{m2}) + (UA)_{BP}(T_{BPM} - T_{m2}) = 0 \tag{3.1-102}$$

vessel closure head (m3):

$$T_{m3} - T_{BPE} = 0 \; ; \tag{3.1-103}$$

bypass flow:

$$T_{BPM} = T_{m2} + (T_{BPI} - T_{BPE}) \left(\frac{WC}{UA}\right)_{BP} \tag{3.1-104}$$

$$T_{BPE} = T_{m2} + (T_{BPI} - T_{m2}) \exp\,(-UA/WC)_{BP} \; . \tag{3.1-105}$$

The above seven equations (3.1-99) through (3.1-105) are solved simultaneously to yield a complete solution of coolant mixing in the upper plenum.

During transients, we divide the outlet plenum by up to two zones. As mentioned earlier, this partition is based on the penetration height of the average core exit flow. The governing equations which determine the instantaneous sodim level and various temperatures are expressed for each material as

sodium level:

$$\frac{dH}{dt} = \frac{W_i - W_{ex}}{\bar{\rho} A_{g\ell}} + H\;[(1 - f)\,\alpha(T_b)\frac{dT_b}{dt} + f\,\alpha(T_A)\,\frac{dT_A}{dt}]; \tag{3.1-106}$$

sodium in the upper mixing zone A:

$$\frac{dE_A}{dt} = \frac{1}{\rho_A A_{g\ell} Hf} [W_{BP}(E_{BPE}-E_A) + \beta_1 W_C(E_B-E_A) + h A_{G\ell}(T_B-T_A)$$

$$+ U_g A_{g\ell}(T_g-T_A) + U_\ell f [A_{\ell m1}(T_{m1}-T_A) + A_{\ell m2}(T_{m2}-T_A)]]; \quad (3.1\text{-}107)$$

sodium in the lower mixing zone B:

$$\frac{dE_B}{dt} = \frac{1}{\rho_B A_{g\ell} H(1-f)} [W_C(E_C-E_B) + \beta_2 W_{BP}(E_A-E_B) + hA_{g\ell}(T_A-T_B)$$

$$+ U_\ell(1-f) [A_{\ell m1}(T_{m1} - T_B) + A_{\ell m2}(T_{m2} - T_B)]]; \quad (3.1\text{-}108)$$

cover gas:

$$\frac{dT_g}{dt} = \frac{U_g}{(MC)_g} [A_{g\ell}(T_A-T_g) + A_{gm1}(T_{m1}-T_g) + A_{gm2}(T_{m2}-T_g)$$

$$+ A_{gm3}(T_{m3}-T_g)]; \quad (3.1\text{-}109)$$

metal m1 (internal structure):

$$\frac{dT_{m1}}{dt} = \frac{1}{(MC)_m} [U_\ell A_{\ell m1}[f T_A + (1-f) T_B - T_{m1}] + U_g A_{gm1}(T_g-T_{m1})]; \quad (3.1\text{-}110)$$

metal m2 (thermal liner):

$$\frac{dT_{m2}}{dt} = \frac{1}{(MC)_{m2}} [U_\ell A_{\ell m2} [f(T_A-T_{m2}) + (1-f)(T_B-T_{m2})]$$

$$+ U_g A_{gm2}(T_g - T_{m2}) + (UA)_{BP}(T_{BPM} - T_{m2})] \quad (3.1\text{-}111)$$

metal m3 (vessel closure head):

$$\frac{dT_{m3}}{dt} = \frac{U_g A_{gm3}}{(MC)_{m3}} (T_g - T_{m3}) \quad . \quad (3.1\text{-}112)$$

The auxiliary equations required by the above governing equations are

$$T_{BPE} = T_{m2} + (T_{BPI} - T_{m2}) \exp (- UA/WC)_{BP} \quad (3.1\text{-}113)$$

$$T_{BPM} = T_{m2} + (T_{BPI} - T_{BPE}) \left(\frac{WC}{UA}\right)_{BP} \quad (3.1\text{-}114)$$

$$W_i = W_C + W_{BP} \quad , \quad (3.1\text{-}115)$$

$$f = 1 - z_j(t)/H(t) \quad , \quad (3.1\text{-}116)$$

$$\bar{\rho} = (1-f)\, \rho_B + f\, \rho_A \, , \quad (3.1\text{-}117)$$

and the liquid sodium densities, ρ_A and ρ_B, are obtained from the constitutive relationships for sodium. The contact areas between the cover gas and liquid or metals ($A_{g\ell}$, A_{gm1}, A_{gm2}, A_{gm3}) and between liquid and metals ($A_{\ell m1}$, $A_{\ell m2}$) are obtained by assuming that the cross-sectional areas in a direction perpendicular to the jet are constant during transients.

In the above equations, there are two control indices, β_1 and β_2, which take values of either 0 or 1 depending upon the relative location of the outlet nozzle and the maximum jet penetration height, z_j. Their values are

$$\beta_1 = 0 \text{ and } \beta_2 = 1 \qquad \text{for } z_j \geq (z_{ex} + \tfrac{1}{2} D) \quad , \quad (3.1\text{-}118a)$$

$$\beta_1 = 0 \text{ and } \beta_2 = 0 \qquad \text{for } (z_{ex} - \tfrac{1}{2} D) < z_j < (z_{ex} + \tfrac{1}{2} D) \quad , \quad (3.1\text{-}118b)$$

and

$$\beta_1 = 1 \text{ and } \beta_2 = 0 \qquad \text{for } z_j \leq (z_{ex} - \tfrac{1}{2} D) \quad . \quad (3.1\text{-}118c)$$

The maximum penetration height is taken from a correlation developed earlier [3.1-10].

It is given as

$$z_j = (1.0484\ Fr_o^{0.785})\ r_o + z_{ch} \quad , \quad (3.1\text{-}119)$$

where Fr_o is the local Froude number and is defined as

$$Fr_o = \left(\frac{W_C}{\pi r_o^2 \rho_C}\right)^2 \left[\frac{\rho_B}{g r_o(\rho_C - \rho_B)}\right] . \qquad (3.1\text{-}120)$$

For the case of full penetration, i.e., for $z_j(t) = H(t)$, f becomes zero. Equations (3.1-107) and (3.1-108) are then replaced by the following equations:

$$\frac{dE_B}{dt} = \frac{1}{\rho_B A_{g\ell} H}\left[W_C(E_C - E_B) + W_{BP}(E_{BPE} - E_B) + U_g A_{g\ell}(T_g - T_B)\right.$$

$$\left. + U_\ell \left[A_{\ell m1}(T_{m1} - T_B) + A_{\ell m2}(T_{m2} - T_B)\right]\right] , \qquad (3.1\text{-}121)$$

$$E_A = E_B . \qquad (3.1\text{-}122)$$

The cover gas mass is determined by assuming that the temperature of the gas in the reservoir remains constant and its pressure equals that of the cover gas in the vessel at any instant. The cover gas mass is then given by

$$M_g(t) = \frac{M_t\, V_g(t)\, T_{res}}{V_{res}\, T_g(t) + V_g(t)\, T_{res}} , \qquad (3.1\text{-}123)$$

where

$$V_g(t) = [L - H(t)]\, A_{g\ell} . \qquad (3.1\text{-}124)$$

These equations, when coupled with the boundary conditions [$W_C(t)$, $W_{BP}(t)$, $E_C(t)$, $T_{BPI}(t)$ and $W_{ex}(t)$], provide for a complete solution to the problem. This set of transient differential equations are solved together with the hydraulic equations using a predictor-corrector algorithm of the Adams type (see Chapter 4).

3.1.4 BYPASS FLOW CHANNEL

A bypass channel to represent coolant flow between the barrel and reactor vessel wall is included. The bypass channel is divided into two axial sections as shown in Figure 3.1-8. The lower section is adjacent to the active core region, and the upper section is separated from the outlet plenum by the thermal liner. The lower section is allowed to have heat generation due to gamma heating.

The momentum and energy equations of the bypass flow are treated in a manner similar to that of the core flow. Two loss coefficients (K_1 and K_2) are incorporated in the momentum equation such that the overall pressure drop through the channel can be balanced. At steady-state, the total pressure drop is given by

$$\Delta P = g[(\rho L)_1 + (\rho L)_2] + \frac{W^2}{2}\left[\left(\frac{fL}{\rho D_h A^2}\right)_1 + \left(\frac{fL}{\rho D_h A^2}\right)_2\right] \tag{3.1-125}$$

$$+ W^2\left[\Delta\left(\frac{1}{\rho A^2}\right)_1 + \Delta\left(\frac{1}{\rho A^2}\right)_2\right] + \frac{W^2}{2}\left[\left(\frac{K_1}{\rho A^2}\right)_1 + \left(\frac{K_2}{\rho A^2}\right)_2\right]$$

In Eq. (3.1-125), the subscripts 1 and 2 denote the lower and upper section, respectively. The loss coefficient k_1 is an input parameter, and k_2 is the computed value to establish the force balance at steady-state.

During transients the total pressure drop in the bypass channel is determined by the one-dimensional momentum equation:

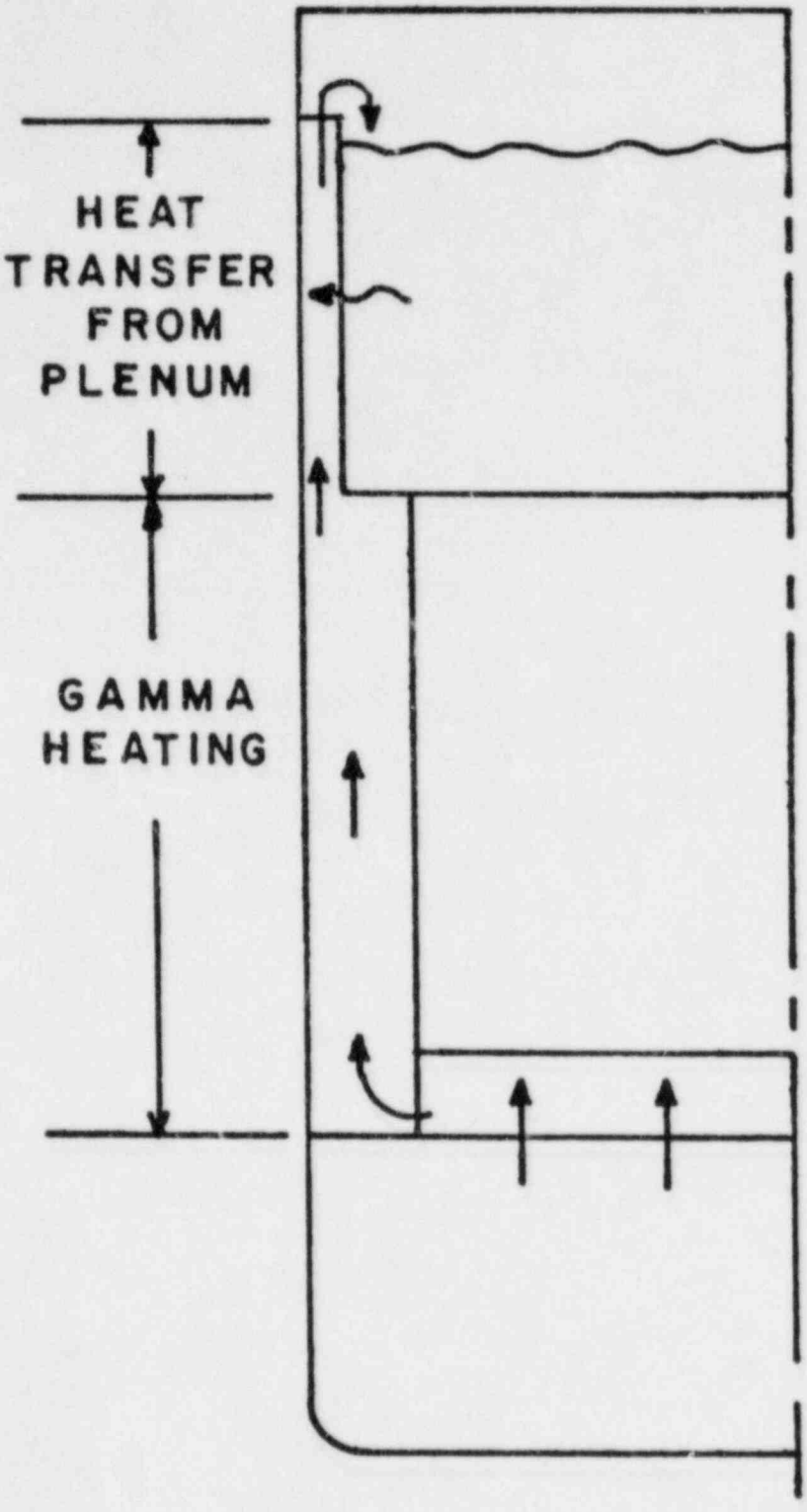

Figure 3.1-8 Bypass Flow Modeling Schematic

$$\Delta P = \frac{dW}{dt}\left[\left(\frac{L}{A}\right)_1 + \left(\frac{L}{A}\right)_2\right] + W^2 \left[\Delta\left(\frac{1}{\rho A^2}\right)_1 + \Delta\left(\frac{1}{\rho A^2}\right)_2\right]$$
$$+ \frac{W|W|}{2}\left[\left(\frac{fL}{A^2 \rho D_h}\right) + \left(\frac{fL}{A^2 \rho D_h}\right)_2\right] + g\left[(\rho L)_1 + (\rho L)_2\right]$$
$$+ \frac{W|W|}{2}\left[\left(\frac{fL}{\rho A^2}\right)_1 + \left(\frac{fL}{\rho A^2}\right)_2\right] . \qquad (3.1\text{-}126)$$

Fluid enthalpy at the exit of the lower sections is computed from the following equation:

$$\frac{\partial}{\partial t}(\rho E) = \frac{P_o \cdot F_{PBP} \cdot P(t)}{AL} - \frac{1}{A}\frac{\partial}{\partial z}(EW) , \qquad (3.1\text{-}127)$$

where A, L, F_{PBP} are the cross-sectional area, height, and fraction of power generation (at steady-state) of the lower section, respectively. In finite difference form, this equation becomes

$$E^{k+1}_{out} = \left[E^k_{in}(1 + A_3 W^k) + E^k_{out}(1 - A_3 W^k) - E^{k+1}_{in}(1 - A_3 W^{k+1}) + 2 P_o F_{PBP} P(t) \cdot A_3\right] / (1 + A_3 W^{k+1}), \qquad (3.1\text{-}128)$$

where

$$A_3 = \frac{\Delta t}{AL\bar{\rho}} \qquad (3.1\text{-}129)$$

$$\bar{\rho} = \frac{1}{2}(\rho^k_{in} + \rho^k_{out}). \qquad (3.1\text{-}130)$$

The computed E^{k+1}_{out} is the inlet enthalpy for computing the enthalpy rise in the upper section of the bypass channel. In the upper section, no internal heat generation is assumed, but heat transfer through the thermal liner is considered as discussed in Section 3.1.3. Calculation of enthalpy rise in the upper section is part of the upper plenum mixing model.

REFERENCES FOR SECTION 3.1

3.1-1 J.J. Kaganove, "Numerical Solution of the One-Group, Space-Independent Reactor Kinetics Equations for Neutron Density Given the Excess Reactivity", Argonne National Laboratory, ANL-6132, February 1960.

3.1-2 H. Hummel and D. Okrent, Reactivity Coefficients in Large Fast Power Reactors, American Nuclear Society, 1970.

3.1-3 J. Graham, Fast Reactor Safety, Academic Press, Inc., New York, 1971.

3.1-4 J. Yevick, Fast Reactor Technology and Plant Design, M.I.T. Press, Cambridge, MA, 1966.

3.1-5 R.G. Palmer and A. Platt, Fast Reactors, Temple Press Ltd., 1961.

3.1-6 The Technology of Nuclear Reactor Safety, Vol. I, T. J. Thompson and J.G. Beckerly, Editors, M.I.T. Press, Cambridge, MA, 1964.

3.1-7 F.E. Dunn, et al., "The SAS2A LMFBR Accident Analysis Computer Code", ANL-8138, 1974.

3.1-8 F.E. Dunn, et al., "The SAS2A LMFBR Accident Analysis Computer Code", ANL/RAS 75-17, April 1975.

3.1-9 Clinch River Breeder Reactor Plant, Preliminary Safety Analysis Report, Project Management Corporation.

3.1-10 J.W. Yang, "Penetration of Core Flow in Upper Plenum of an LMFBR", Trans. Am. Nucl. Soc. 23, 414, 1976.

3.2 HEAT TRANSPORT SYSTEM

3.2.1 SYSTEM DESCRIPTION

The heat transport system provides the vital function of removing reactor generated heat and transporting it to the steam generators while maintaining an adequate flow rate for controlling reactor temperatures within safe limits under all plant operating conditions. In this section of the report, a detailed analysis to predict the thermal and hydraulic response of the heat transport system under both pre-accident and transient conditions will be presented.

Figure 3.2-1 shows an example configuration of the heat transport system for a loop-type LMFBR plant. Only one circuit has been shown. It consists of the primary loop carrying radioactive liquid sodium and the intermediate loop carrying nonradioactive liquid sodium. The number of parallel heat transport circuits usually depends on total flow rate, allowable pressure drops, degree of plant reliability, size of available components, and allowable coolant velocities [3.2-1]. The Clinch River Breeder Reactor Plant (CRBRP) has three heat transport circuits operating in parallel [3.2-2].

Each primary loop contains a variable speed, centrifugal, liquid metal pump, a check valve, an intermediate heat exchanger (shell side), and the associated piping interconnecting these components. The pump circulates coolant through the reactor where it picks up the heat generated in the core and exits at a higher temperature. The coolant transfers this heat during its passage through the shell side of the intermediate heat exchanger and returns to the reactor to complete the cycle. All primary loops share a common heat

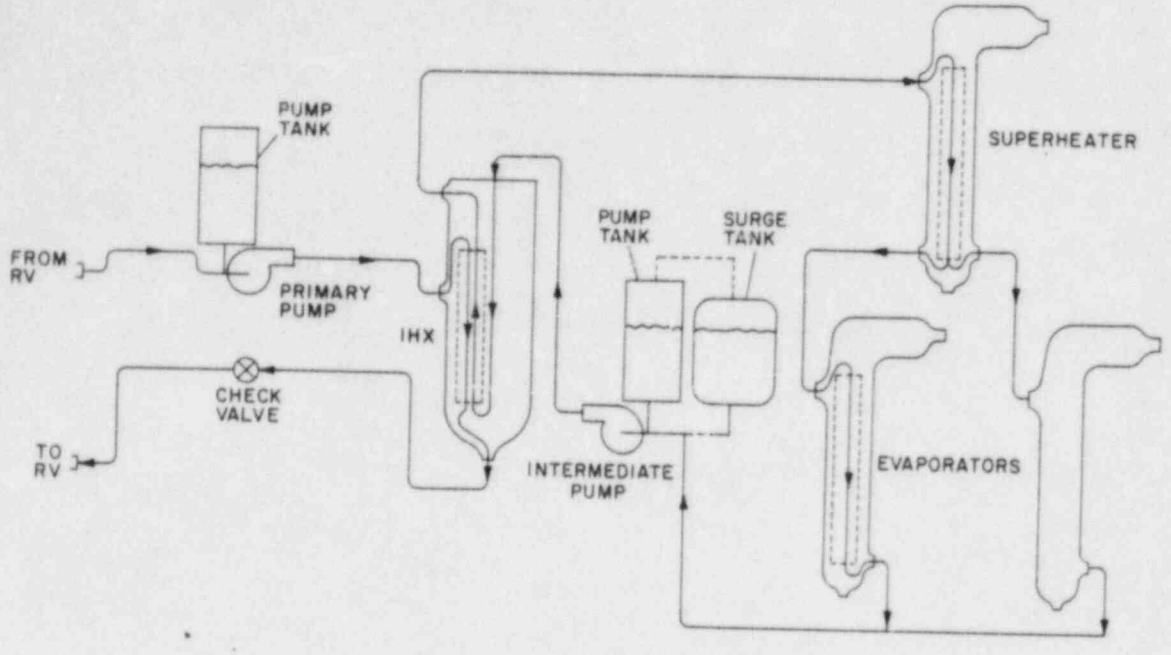

Figure 3.2-1 Example configuration of the heat transport system

source at the reactor core and a common flow path through the reactor vessel, but otherwise each circuit operates independently.

The primary and intermediate loops are thermally linked at the Intermediate Heat Exchanger (IHX). Here, the intermediate coolant, as it rises in the heat transfer tubes, picks up the heat from the coolant. It then passes to the shell side of the steam generator, where it gives up this heat to produce steam in the tubes, and returns to the IHX to complete the cycle. The coolant is circulated by a variable speed centrifugal pump. An expansion (surge) tank is also provided in the intermediate loop to accommodate coolant volume changes due to thermal expansion. In the case of the primary heat transport loops, the reactor vessel serves the purpose of the surge tank.

In the example configuration of Figure 3.2-1, which corresponds to the CRBRP design, heated intermediate coolant leaving the IHX flows through hot leg piping and enters the steam generation system superheater module. At the superheater exit, the piping consists of two parallel runs, each extending to an evaporator inlet. Cooled sodium from the evaporators flows through two parallel runs, joined at a tee, and continues as a single run to the pump situated in the cold leg and then back to the IHX. The expansion tank is located just upstream of the pump.

Transfer of reactor power by the heat transport system is achieved by varying system flow rates, which in turn are controlled by changing pump speeds. The piping runs are insulated on the outside to minimize heat loss.

3.2.2 ANALYSIS

For modeling purposes, the primary loop is understood to extend from the reactor vessel outlet to its inlet. The intermediate loop is assumed to start at the IHX secondary outlet, but does not include the shell side of the steam generator. The heat transport system calculations thus interface with the reactor calculations at the vessel inlet and outlet, and with the tertiary loop calculations at the steam generator.

The analysis is aimed at allowing considerable flexibility in the arrangement of components in the loop for future LMFBRs. In the CRBRP arrangement illustrated in Figure 3.2-1, the primary pump is placed in the hot leg. However, it could be located in the cold leg at the user's option. Also, the check valve could be anywhere in the loop, or be absent altogether. The figure also shows one superheater and two evaporators in the intermediate loop, with the intermediate pump in the cold leg and the expansion (surge) tank just upstream of it. The model could accommodate variations in this arrangement such as none or more than one superheater, and one or more evaporators at the user's option. Also, the pump and surge tank could be located away from each other.

3.2.2.1 GENERAL ASSUMPTIONS

The following basic assumptions are inherent in the analysis:

(1) one-dimensional (space) flow, i.e., uniform velocity and temperature profiles normal to the flow direction;

(2) single-phase liquid coolant, i.e., temperatures in the loop are

always below coolant saturation temperature;

(3) incompressible liquid, i.e., coolant properties are not pressure dependent;

(4) single mass flow rate model, i.e., the effect of time rate of change of density on mass flow rate distribution in space is neglected, so that at any instant of time, the mass flow rate would be uniform everywhere in a circuit, except at a free surface, or at a break where there is flow loss, or at a junction where flows meet, or at a branch where flows separate;

(5) axial heat conduction in walls is neglected.

3.2.2.2 MODEL FEATURES

Aside from its flexibility, the model has several other features. Some of these are:

(1) temperature-dependent material properties, expressed as curve-fitted polynomial functions of temperature,

(2) gravity effects included in detail,

(3) flow-dependent friction factors encompassing the full range of flow conditions from turbulent to laminar,

(4) loss coefficients included for area changes, etc.,

(5) heat transfer with pipe walls accounted for.

3.2.2.3 STEADY-STATE SIMULATION

Figure 3.2-2 shows a skeleton flow chart for the overall solution approach to the heat transport system. Certain boundary conditions and input data are necessary to start the calculations. These are the system geometry (i.e., pipe lengths, diameters, angles at nodes, loss coefficients, heat transfer tube dimensions, etc.), and certain reference parameters, such as the loop flow rates W_p and W_s, the coolant temperature at the reactor outlet $T_{1,1}$, the pressure at inlet to the primary loop P_1, the reactor pressure drop ΔP_{RV}, cover gas pressure in the pump tank P_{gas}, etc. Of these, W_p, W_s, $T_{1,1}$ are determined from overall plant thermal balance, and P_1 and ΔP_{RV} are obtained from the in-vessel simulation.

With this information, along with the constitutive relations, the calculation begins at the entrance of the primary loop and marches in the direction of coolant flow. The conservation equations for flow in pipes are solved first, unless an IHX is encountered (see Figure 3.2-2), in which case the energy and momentum equations at the IHX are solved. Following each component or pipe run, the boundary conditions are set for the next component or pipe run. This process continues until the outlet of the loop has been reached and temperatures and pressure drops in all piping runs and the IHX have been computed. At this point, the check valve pressure drop, pump pressure rise and operating speed, the height of coolant in the pump tank are all determined. The intermediate loop calculations now begin at the IHX secondary outlet, and a similar process continues until the steady-state thermal-hydraulic conditions in both loops are completely specified.

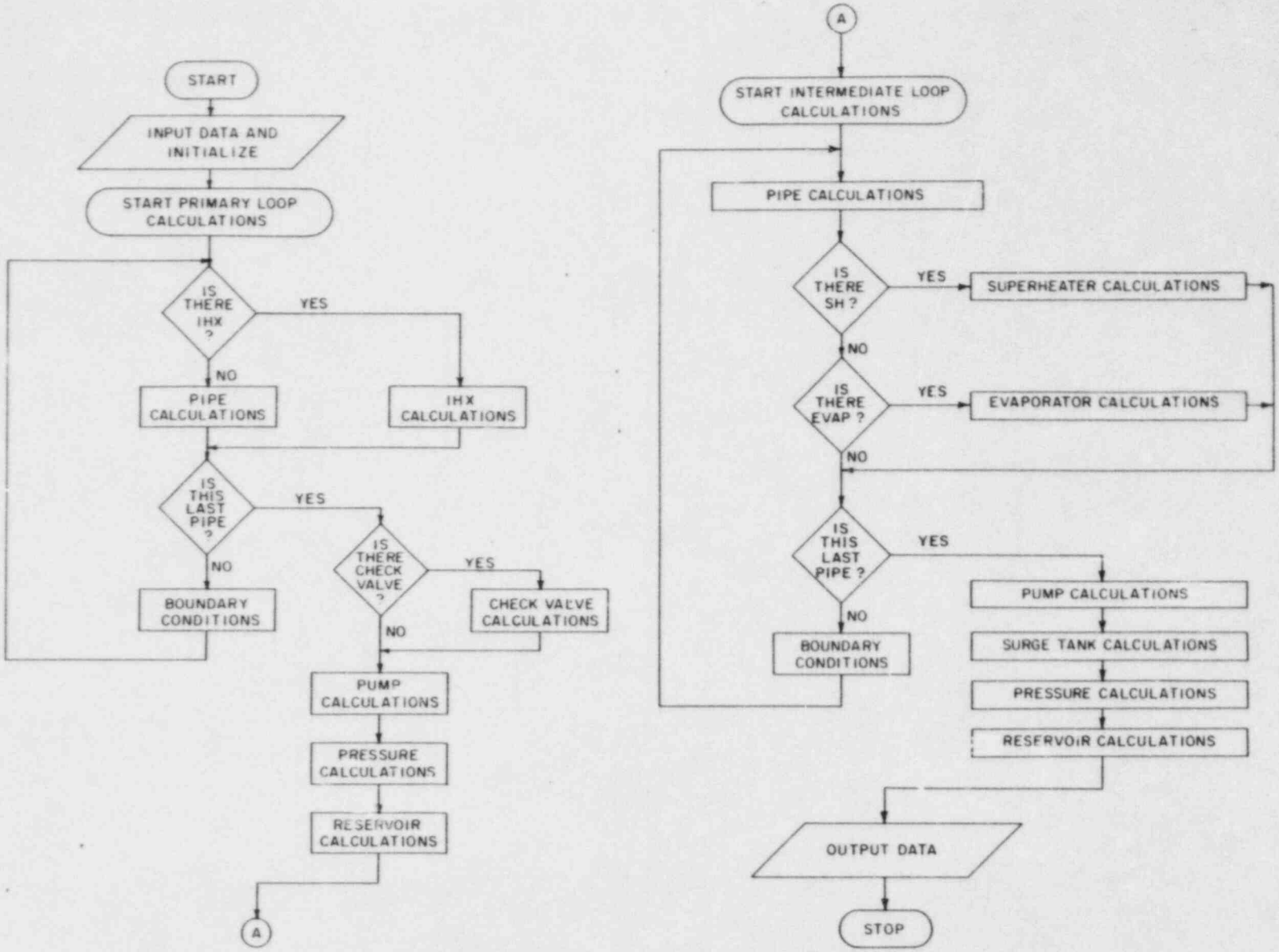

Figure 3.2-2 Flow diagram for steady state solution of heat transport system

3.2.2.4 TRANSIENT SOLUTION APPROACH

The simulation and solution approach is strongly influenced by the nature of the flowing medium within the range of conditions of interest to the model. For instance, for liquid sodium loops, the time-dependent energy and momentum equations can be decoupled since the effect of pressure on subcooled liquid sodium properties may be considered negligible. However, whereas the momentum equations are only loosely dependent on temperature through the sodium properties, the converse is not true, since convective terms in the energy equations are directly flow dependent. So, if the hydraulic equations are solved first with coolant properties evaluated at temperatures corresponding to the earlier time (one timestep previous), the energy equations can then be readily solved, using the flow rates calculated from the hydraulics at the advanced time. More details on hydraulic and thermal simulation procedures will be presented in subsections 3.2.9 and 3.2.10.

The next few subsections will be devoted to descriptions of the model equations for the individual components of the heat transport system.

3.2.3 COOLANT FLOW IN PIPING

By far the longest time the coolant spends in its passage through the heat transport circuit is in the piping runs interconnecting the different components. Hence, a thermal-hydraulic model for coolant flow in piping forms an important part of the overall system simulation model.

3.2.3.1 HEAT TRANSFER

A detailed model with discrete parameter representation has been formulated for the heat transfer process in the piping. This is preferable to a simple transport delay model as used in other codes [3.2-3, 3.2-4] for two reasons. First, the temperature signal is not only delayed in its passage from inlet to outlet of a pipe run, but also altered. Secondly, a detailed temperature distribution will aid in a more accurate determination of the gravitational heads and hence, the natural circulation capability of the heat transport system under loss of forced flow conditions.

Figure 3.2-3 shows the model configuration. In the axial direction the number of nodal interfaces (N) in a pipe section is user specified, the number being influenced by the pipe length and the coolant velocity at full flow. In the radial direction, there are two nodes - coolant and pipe wall. Perfect insulation (i.e., negligible heat losses) is currently assumed on the wall outer surface. As shown in the figure, the locations of coolant and wall temperatures form a staggered arrangement.

Governing Equations

The governing equations are obtained by the nodal heat balance method. The energy balance is applied over the control volume formed between two adjacent fluid nodal interfaces to obtain the coolant equation. The wall equation is related to the coolant equation through the heat flux term. These equations can be written for i = 1, N - 1, as follows:

Coolant:

$$\rho_{i\,i+1} A \Delta x \quad \frac{de_{i+1}}{dt} = W(e_i - e_{i+1}) - U_{cw} A_{cw} [T_{i\,i+1} - T_{w_i}], \qquad (3.2\text{-}1)$$

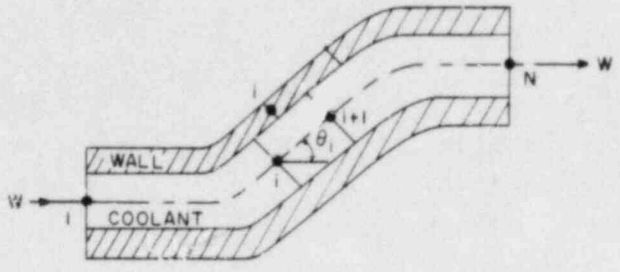

Figure 3.2-3 Nodel diagram for flow in piping

where e_{i+1} is the coolant enthalpy at the nodal interface i+1, T_{ii+1} is the average coolant temperature in the control volume between interfaces i and i+1, expressed as (using subscript notation ii + 1)

$$T_{ii+1} = \frac{T_i + T_{i+1}}{2} \tag{3.2-2}$$

ρ_{ii+1} is the coolant density corresponding to T_{ii+1}, W is the flow rate in the pipe, A is the cross-sectional area for flow given by $\pi D^2_i/4$, U_{CW} is the overall heat transfer coefficient between coolant and wall, evaluated at the midpoint between coolant nodal interfaces i and i+1, and A_{CW} is the area for heat transfer between coolant and wall, given by

$$A_{CW} = \pi D_i \Delta x. \tag{3.2-3}$$

Inherent in Equation (3.2-1) is the assumption that

$$\frac{de_i}{dt} \approx \frac{de_{i+1}}{dt} \approx \frac{de_{ii+1}}{dt} \tag{3.2-4}$$

Wall:

$$M_W C_{W_i} \frac{dT_{W_i}}{dt} = U_{CW} A_{CW} [T_{ii+1} - T_{W_i}] \tag{3.2-5}$$

where M_W = mass of wall for length Δx.

Finite Difference Forms

A fully implicit single-layer time integration scheme is applied to Equation (3.2-1) and the wall heat flux is allowed to be determined explicitly. With this, Equation (3.2-1) becomes

$$\begin{aligned} \overset{k}{\rho}_{ii+1} A\Delta x \frac{(e^{k+1}_{i+1} - e^{k}_{i+1})}{h} &= W^{k+1} (e^{k+1}_{i} - e^{k+1}_{i+1}) \\ &\quad - \overset{k}{U}_{CW} \overset{k}{A}_{CW} (\overset{k}{T}_{ii+1} - \overset{k}{T}_{W_i}), \end{aligned} \tag{3.2-6}$$

and Equation 3.2-5 becomes

$$M_w C_{w_i}^k \frac{(T_{w_i}^{k+1} - T_{w_i}^k)}{h} = U_{cw} A_{cw} (T_{i i+1}^k - T_{w_i}^k) \qquad (3.2\text{-}7)$$

where the index k represents previous time, (k+1) represents the current (advanced) time, and h is the size of the timestep.

The flow rate W^{k+1} in Equation (3.2-6) is known since hydraulic calculations precede thermal calculations. Equations (3.2-6) and (3.2-7) are now uncoupled and unknowns e^{k+1} and T^{k+1} can be determined algebraically in a marching fashion going from i=1 to N-1.

It is worth noting that Equations (3.2-6) and (3.2-7) are for forward flow only. However, the code has the formulation in terms of general node counters so that the equations and the marching direction in each pipe section are automatically adjusted depending on the flow direction, be it forward or reverse.

Overall Heat Transfer Coefficients

In Equations (3.2-1) and (3.2-5), U_{cw} represents the overall heat transfer coefficient between coolant and pipe wall, and it is defined, based on the resistance concept (see Figure 3.2-4), as

$$\frac{1}{U_{cw}} = \frac{1}{h_{film}} + r_{wall}. \qquad (3.2\text{-}8)$$

The film heat transfer coefficient is given in terms of Nusselt number Nu_c as

$$h_{film} = \frac{Nu_c k_c}{D_i} , \qquad (3.2\text{-}9)$$

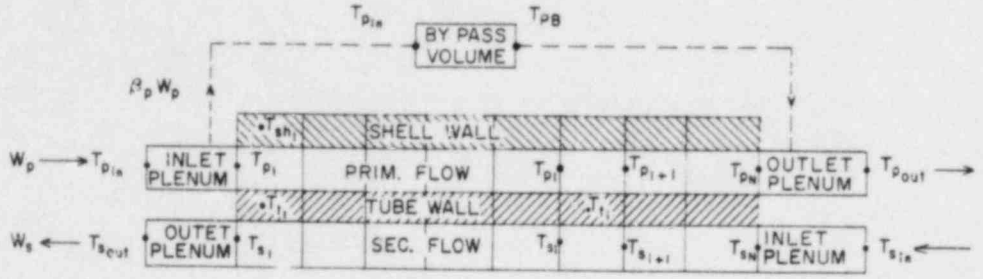

Figure 3.2-4 Nodal diagram for thermal balance

where Nu_c is obtained from established correlations (see Chapter 5).

The wall resistance term is obtained by considering half the wall thickness (since that is where T_{w_i} is defined), and is expressed as

$$r_{wall} = \frac{D_i}{2k_w} \ln \left(\frac{D_o + D_i}{2D_i}\right) \qquad (3.2\text{-}10)$$

where D_i, D_o are the pipe inner and outer diameters, respectively.

Since U_{cw} is dependent on material (k_c, k_w) and flow (Nu_c) properties, which are functions of temperature, it is evaluated at each nodal section of the pipe.

3.2.3.2 PRESSURE LOSSES

The hydraulic model essentially calculates the pressure losses in the pipe section as

$$\begin{aligned}(\Delta P_{f,g})_{pipe} &= \text{acceleration loss} + \text{frictional loss} \\ &\quad + \text{gravity loss} + \text{other losses.} \\ &= W^2(1/\rho_n - 1/\rho_1)/A^2 + W|W|/(2DA^2)\int_0^L f dx/\rho \\ &\quad + g\int_0^L \rho \sin\alpha dx + K\, W|W|/(\bar{\rho}A^2)\end{aligned} \qquad (3.2\text{-}11)$$

where f is a flow-dependent friction factor (see Chapter 5 for details). K; is a user-specified loss coefficient to account for losses due to bends, fittings, etc. Since f/ρ is a continuous function, $\int_0^L f/\rho\, dx$ is evaluated using Simpson's rule. However, $\rho\sin\alpha$, unlike f/ρ, is a discontinuous function,

dependent on the pipe geometry; hence $\int_0^L \rho \sin\alpha \, dx$ is evaluated rather as the summation $\Delta x \sum_{i=1}^{N-1} \rho_i \sin\alpha_i$, where $\rho_i = \rho(T_i)$.

The importance of these pressure loss evaluations will be seen later under the transient hydraulic simulation.

3.2.3.3 STEADY-STATE MODEL

For solving the steady-state, the energy equations are considerably simplified because of the absence of time derivatives. In fact, with the assumption of perfect insulation, the wall equation, i.e., Equation (3.2-5), disappears, and the coolant equation simply gives

$$T_i = T_1 \qquad \text{for } i = 1, N. \tag{3.2-12}$$

This equation also implies constant fluid properties over the pipe run.

The formulation for pressure losses in the piping is the same as for the transient, except that the acceleration term drops out, and f and ρ are constant, simplifying the evaluation of the frictional loss term. Since under steady-state, momentum balance yields

$$\text{pressure drop} = \text{pressure loss}, \tag{3.2-13}$$

there being no flow acceleration, the terms "loss" and "drop" can be used interchangeably. Generally, the term "drop" has been used in the steady-state analysis.

3.2.4 INTERMEDIATE HEAT EXCHANGER

3.2.4.1 DESCRIPTION AND SUMMARY

The IHX in an LMFBR serves to physically separate the radioactive primary coolant from the nonradioactive intermediate coolant while at the same time thermally connecting the two circuits in order to transfer the reactor-generated heat to the steam generator. Its location in each circuit of current loop-type reactor system designs was illustrated by the example configuration of Figure 3.2-1.

The IHX incorporates a liquid metal-to-liquid metal cylindrical shell-and-tube heat exchanger where primary coolant flows in the baffled shell and gives up its heat to secondary coolant flowing at a higher pressure in the tubes. The higher pressure in the secondary side is to assure no radioactive coolant enters the secondary circuit in the event of a leak in any of the heat transfer tubes. Secondary fluid in the tubes is a natural choice because it is more economical to put the higher pressure fluid in the tubes [3.2-1], besides the fact that primary coolant in the shell allows more design freedom [3.2-5]. All current designs use an essentially counterflow arrangement. However, the model to be described is equally valid for parallel flow as well.

The thermal response, in terms of temperature distribution in the IHX and heat transfer from primary to secondary coolant within the heat exchanger, is predicted by the thermal model, which involves dividing the heat transfer region into a user-specified number of nodes, and then applying energy balance over each node. The analysis includes mixing in plena, heat transfer with the wall, fouling, and primary bypass flow. Fouling resistance is included as a

user-specified parameter to allow the code to analyze the preaccident conditions of the plant at any stage of its operating life. The hydraulic response is obtained in terms of pressure drop characteristics on both primary and secondary sides of the IHX. The model includes variable friction factor in the heat transfer section, gravity heads, and losses due to contractions, expansions, etc. Also, a loss coefficient has been included in the hydraulic model in order to absorb uncertainties in the evaluation of various losses within the heat exchange unit.

3.2.4.2 ENERGY EQUATIONS

If a detailed model is needed to describe the heat transfer process in the piping, there is even greater justification for a detailed model here, apart from the need to evaluate the heat removal capability of the heat exchange unit accurately at all times. Figure 3.2-4 is a model diagram for the thermal model (under counterflow arrangement). All the active heat transfer tubes have been modeled by one representative tube. As in the piping, the coolant equations are derived using the nodal heat balance method.

Essential Features

Some features of the model are enumerated:

(1) user-specified number of equidistant axial nodes;

(2) variable material properties and heat transfer coefficients (functions of temperature, flow, etc.) which are evaluated locally;

(3) presence of bypass flow stream on primary side accounted for;

(4) ideal mixing plena at the inlet and outlet of each coolant stream;

(5) four radial nodes (secondary coolant, tube metal, primary coolant, shell wall);

(6) axial heat flow due to conduction in the metal wall is assumed negligible;

(7) fully developed convective heat transfer is assumed, i.e., entrance effects are neglected.

The tube and shell wall nodes (see Figure 3.2-4) lie in the midplane between the fluid nodal interfaces, giving rise to a staggered nodal arrangement. Representative time-dependent equations are noted below.

Plenum primary inlet:

$$\rho V_{in} \frac{d}{dt} (e_{p_1}) = W'_p (e_{p_{in}} - e_{p_1}), \tag{3.2-14}$$

where

$$e_{p_{in}} = e(T_{p_{in}}) \text{ and } e_{p_1} = e(T_{p_1}) , \tag{3.2-15}$$

V_{in} is the stagnant volume in the primary inlet plenum, and ρ is the average coolant density in the plenum. Further, from mass conservation, we have

$$W'_p = (1 - \beta_p) W_p , \tag{3.2-16}$$

where β_p is the fraction of flow bypassing the active heat transfer region.

Plenum primary outlet:

$$\rho V_{out} \frac{d}{dt} (e_{p_{out}}) = W'_p e_{p_N} + \beta_p W_p e_{PB} - W_p e_{p_{out}} . \tag{3.2-17}$$

Plenum primary bypass:

$$\rho V_{PB} \frac{d}{dt} (e_{PB}) = \beta_p W_p (e_{p_{in}} - e_{PB}). \tag{3.2-18}$$

Similar equations can be written for the inlet, outlet plena and downcomer on the secondary side.

Active Heat-Transfer Region

Primary coolant:

$$\rho V_p \frac{d}{dt}(e_{p_{i+1}}) = W'_p (e_{p_i} - e_{p_{i+1}}) - U_{pt}A_{pt}(T_{p_{i\,i+1}} - T_{t_i}) - U_{psh}A_{psh}(T_{p_{i\,i+1}} - T_{sh_i}) . \quad (3.2\text{-}19)$$

Secondary coolant:

$$\rho V_s \frac{d}{dt}(e_{s_i}) = W_s (e_{s_{i+1}} - e_{s_i}) + U_{st}A_{st}(T_{t_i} - T_{s_{i\,i+1}}) . \quad (3.2\text{-}20)$$

Tube wall:

$$M_t C_{t_i} \frac{d}{dt}(T_{t_i}) = U_{pt}A_{pt}(T_{p_{i\,i+1}} - T_{t_i}) - U_{st}A_{st}(T_{t_i} - T_{s_{i\,i+1}}). \quad (3.2\text{-}21)$$

Shell wall:

$$M_{sh} C_{sh_i} \frac{d}{dt}(T_{sh_i}) = U_{psh}A_{psh}(T_{p_{i\,i+1}} - T_{sh_i}). \quad (3.2\text{-}22)$$

In the above equations V_p, V_s are the control volumes between interfaces i and i+1 on the primary and secondary sides, respectively. U_{pt}, U_{st}, U_{psh} denote the overall heat transfer coefficients and A_{pt}, A_{psh} and A_{st} are the areas per length Δx for heat transfer between the primary coolant and tube wall, primary coolant and shell wall, and secondary coolant and tube wall, respectively, defined as

$$A_{pt} = \pi D_2 n_t \Delta x, \quad (3.2\text{-}23)$$

$$A_{st} = \pi D_1 n_t \Delta x, \quad (3.2\text{-}24)$$

$$A_{psh} = A_{sh} \Delta x/L, \quad (3.2\text{-}25)$$

where n_t = number of active heat transfer tubes, A_{sh} is the shell heat

transfer area, D_1 is the IHX tube inner diameter, D_2 is the IHX tube outer diameter, and L is the length of the active heat transfer region.

Equations (3.2-19) to (3.2-22), along with the plena equations, are integrated by a fully implicit single-layer scheme. The heat flux terms in Equations (3.2-19) and (3.2-20) are allowed to be determined explicitly, which uncouples them. These equations are then solved in a marching fashion without resorting to matrix inversion. Subsequently, the heat fluxes in Equations (3.2-21) and (3.2-22) are evaluated implicitly. The timestep control is achieved (1) by checking for Courant stability violations and (2) by regulating the relative change of the integrated variables from the standpoint of user-desired accuracy. This is required particularly since the heat flux terms, being allowed to lag in the coolant equations, could lead to unbounded solutions if no control of the timestep size was exercised.

The above equations, in the form shown, are valid for counterflow arrangement, positive flow only. However, they have been coded with general node counters to allow for reverse flow in either coolant stream, as well as a choice of parallel or counterflow arrangement. All functional relationships between enthalpy and temperature and vice versa were obtained from property relations (see Chapter 5).

Overall Heat Transfer Coefficients

In Equations (3.2-19) to (3.2-22), U_{pt}, U_{st}, and U_{psh} represent the overall heat transfer coefficients from primary fluid to tube wall, from secondary fluid to tube wall, and from primary fluid to shell wall, respectively, and are defined, based on the resistance concept, by:

$$\frac{1}{U_{pt}} = \frac{1}{h_{film,p}} + r_{wall,p} + \frac{1}{h_{foul,p}} \qquad (3.2\text{-}26)$$

$$\frac{1}{U_{st}} = \frac{1}{h_{film,s}} + r_{wall,s} + \frac{1}{h_{foul,s}}, \tag{3.2-27}$$

$$\frac{1}{U_{psh}} = \frac{1}{h_{film,p}}, \tag{3.2-28}$$

where the film heat transfer coefficients are calculated in terms of Nu by

$$h_{film,p} = \frac{Nu_{pt} \, k_p}{D_{h,p}}, \tag{3.2-29}$$

$$h_{film,s} = \frac{Nu_{st} \, k_s}{D_1}, \tag{3.2-30}$$

The Nusselt numbers, Nu_{pt} and Nu_{st}, are obtained from established correlations (see Chapter 5).

The wall resistance terms are obtained by dividing the tube wall thickness equally between primary and secondary sides, since T_t is defined at the midpoint of wall thickness.

$$r_{wall,p} = \frac{D_2}{2k_t} \ln (2D_2/(D_1 + D_2)) \tag{3.2-31}$$

and

$$r_{wall,s} = \frac{D_1}{2k_t} \ln ((D_1 + D_2)/2D_1), \tag{3.2-32}$$

k_t = thermal conductivity of tube wall.

Fouling is a time-dependent phenomenon, and the fouling resistances $1/h_{foul,p}$ and $1/h_{foul,s}$ are included as a user input quantity in order to lend capability to the model to better analyze the response of the heat exchange unit at any stage of its operating life.

The overall heat transfer coefficients, U_{pt} and U_{st}, are dependent on material (k_p, k_t, k_s) and flow (Nu_{pt}, Nu_{st}) properties, which are functions of temperature and, therefore, are evaluated at each nodal section along with the temperatures. Referring to Figure 3.2-4, for each i, k_t

would be evaluated at i on the tube wall node whereas all other variables (k_p, k_s, Nu_{pt}, Nu_{st}) would be evaluated at the midpoint between the fluid nodal interfaces i and (i+1). The Nusselt numbers are obtained from established correlations.

There are three options available to the user in which either

(1) both A_p and $D_{h,p}$ are supplied,

(2) A_p is user input and $D_{h,p}$ is calculated from

$$D_{h,p} = \frac{4A_p}{n_t \pi D_2} \text{ , or} \tag{3.2-33}$$

(3) both A_p and $D_{h,p}$ are calculated by the code as follows:

$$A_p = n_t \frac{\pi D_2^2}{4} \left[\frac{2\sqrt{3}}{\pi} (P/D_2)^2 - 1 \right] , \tag{3.2-34}$$

and $D_{h,p}$ is given by Equation (3.2-33). The Reynolds number for the primary side is defined as

$$Re = \frac{W_p D_{h,p}}{A_p \mu} , \tag{3.2-35}$$

where A_p is the flow area on the shell side. On the tube side, the Reynolds number is given by

$$Re = \frac{W_s D_1}{A_s \mu} , \tag{3.2-36}$$

where A_s, the flow area through the tubes, is given as

$$A_s = n_t \frac{\pi D_1^2}{4} . \tag{3.2-37}$$

3.2.4.3 PRESSURE LOSSES

Figure 3.2-5 illustrates a typical hydraulic profile of the IHX. The primary coolant rises in the inlet region, reverses, flows down around the tubes, and exits at the bottom through the outlet nozzle. The secondary (intermediate) coolant flows down the central downcomer into the bottom header (inlet plenum region) where it turns upward and distributes itself into the heat transfer tubes. The pressure losses on both primary and secondary sides of the IHX can be expressed as follows:

$$(\Delta P_{f,g})_{IHX} = \text{acceleration loss} + \text{frictional loss} + \text{gravity loss} + \text{inlet loss} + \text{exit loss} + \text{other losses.}$$

For the primary side this equation gives

$$(\Delta P_{f,g})_{IHX,p} = \frac{W_p'^2}{A^2_p}\left(\frac{1}{\rho_N} - \frac{1}{\rho_1}\right) + \frac{1}{2}\frac{W'_p|W'_p|}{D_{h,p}A_p{}^2}\int_0^L \frac{f}{\rho}\,dx + \Delta P_g + K_{p_{in}}\frac{W_p|W_p|}{(\rho A^2)_{in}} + K_{p_{out}}\frac{W_p|W_p|}{(\rho A^2)_{out}} + K_p\frac{W_p|W_p|}{\bar{\rho}A^2_p}, \quad (3.2\text{-}38)$$

where

$$\Delta P_g = g(\rho \sin\alpha\, \Delta x)_{\text{inlet plenum}} + g\int_0^L \rho \sin\alpha\, dx + g(\rho \sin\alpha\, \Delta x)_{\text{outlet plenum}} \quad (3.2\text{-}39)$$

$$W'_p = (1 - \beta_p)\, W_p\,, \quad (3.2\text{-}40)$$

and

$$\bar{\rho} = \frac{\rho_{in} + \rho_{out}}{2}\,. \quad (3.2\text{-}41)$$

K_{in} (K_{out}) is user specified and can represent expansion (contraction) loss from the inlet pipe to the inlet plenum and nozzle losses, or it can also

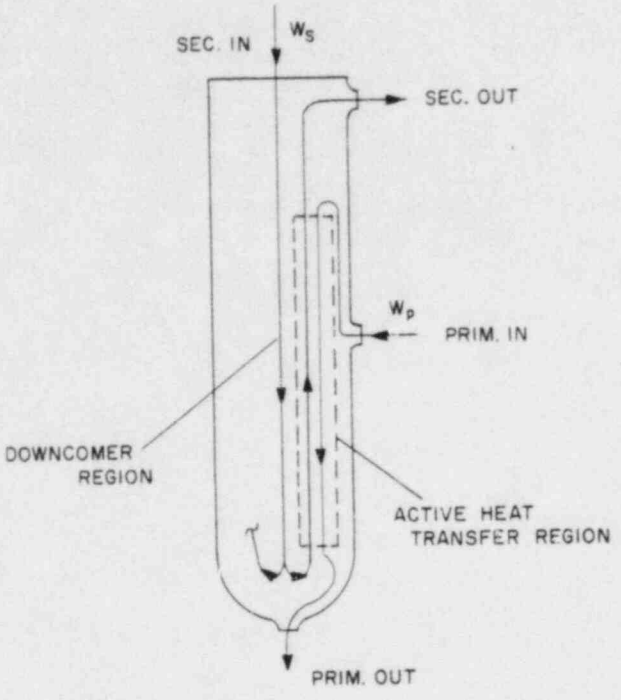

Figure 3.2-5 Hydraulic profile of IHX

include inlet plenum losses due to turning, flow distribution, etc. A_{in} represents the area of primary piping at the IHX inlet. K_p is an uncertainty absorber that is either calculated during steady state if $\Delta P_{IHX,p}$ is known from flow testing (or other means), or is input by the user if $\Delta P_{IHX,p}$ is not known. Once determined or known, the value of K_p remains constant for that particular transient. This is a useful parameter especially because of the difficult task of determining accurately all the losses in the complex internal geometry of the heat exchange unit.

Similarly, for the secondary side

$$(\Delta P_{f,g})_{IHX,s} = \frac{W^2_s}{A^2_s}\left(\frac{1}{\rho_1} - \frac{1}{\rho_N}\right) + \frac{1}{2}\frac{W_s|W_s|}{D_1 A_s{}^2}\int_0^L \frac{f}{\rho}\,dx + \Delta P_g$$

$$+ K_{s,in}\, W_s|W_s|/(\rho A^2_{in}) + K_{s,out}\, W_s|W_s|/(\rho A^2)_{out} \qquad (3.2\text{-}42)$$

$$+ \Delta P_{c,e} + K_s\, /W_s|W_s|/(\overline{\rho} A^2_s)$$

where

$$\Delta P_g = g(\rho \sin\alpha\, \Delta x)_{downcomer} + g(\rho \sin\alpha\, \Delta x)_{inlet\ plen}$$

$$+ g\int_0^L \rho \sin\alpha\, dx + g(\rho \sin\alpha\, \Delta x)_{outlet\ plen}\,, \qquad (3.2\text{-}43)$$

and

$$\Delta P_{c,e} = K_c \frac{W_s|W_s|}{(\rho A^2)_{tube\ in}} + K_e \frac{W_s|W_s|}{(\rho A^2)_{tube\ out}}\,. \qquad (3.2\text{-}44)$$

K_s in Equation (3.2-42) is the uncertainty absorber for the secondary side. The friction factor f is a function of Reynolds number (Re) and the relative roughness of the channel e/D_h. The same approach is used in the formulation of the hydraulics in the sodium-side of the steam generator heat exchangers.

3.2.4.4 STEADY STATE MODEL

Energy Equations

To start the calculations, the boundary temperatures at one end of the IHX, in this case $T_{p_{in}}$ and $T_{s_{out}}$, are assumed to be known. Applying thermal balance at the primary inlet plenum (see Figure 3.2-2) gives

$$W_p e_{p_{in}} - (\beta_p W_p e_{p_{in}} + W'_p e_{p_1}) = 0. \tag{3.2-45}$$

On simplification, this yields

$$T_{p_1} = T_{p_{in}} \tag{3.2-46}$$

Similarly, at the secondary outlet plenum,

$$T_s = T_{s_{out}}. \tag{3.2-47}$$

Thus, the boundary temperatures at one end of the active heat transfer section are known. Now, energy balance at each nodal section (see Figure 3.2-6) gives, for i=1, N-1:

primary fluid:

$$(1 - \beta_p)\, W_p\, (e_{p_i} - e_{p_{i+1}}) - U_{pt}A_{pt}\, (\frac{T_{p_i} + T_{p_{i+1}}}{2} - T_{t_i}) = 0 \tag{3.2-48}$$

tube wall:

$$U_{pt}A_{pt}(\frac{T_{p_i} + T_{p_{i+1}}}{2} - T_{t_i}) - U_{st}A_{st}\, (T_{t_i} - \frac{T_{s_i} + T_{s_{i+1}}}{2}) = 0; \tag{3.2-49}$$

secondary fluid:

$$(-L_{fd})\, W_s\, (e_{s_{i+1}} - e_{s_i}) + U_{st}A_{st}\, (T_{t_i} - \frac{T_{s_i} + T_{s_{i+1}}}{2}) = 0 \tag{3.2-50}$$

where

L_{fd} = 1 for parallel flow,

= -1 for counter flow,

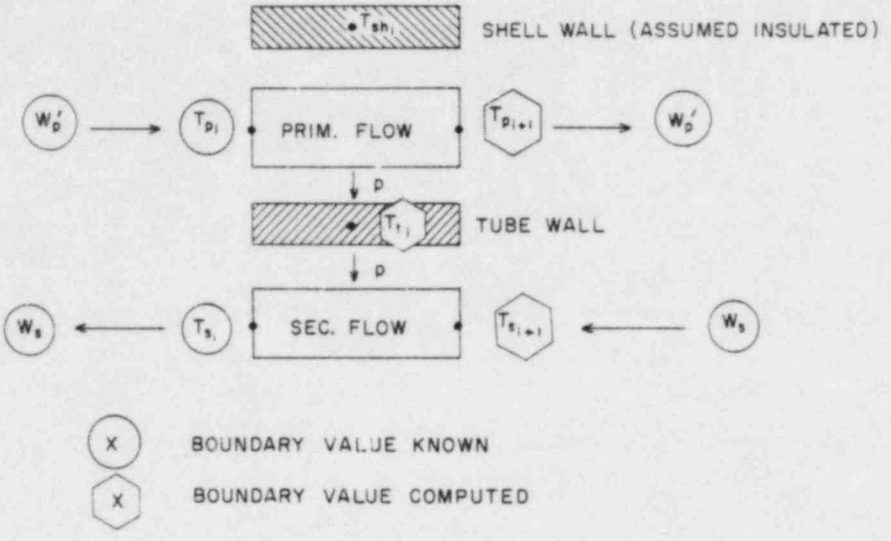

Figure 3.2-6 Steady state boundary conditions for an IHX nodal section

and

$$e_p = e(T_p),$$

$$e_s = e(T_s).$$

Equations (3.2-48) to (3.2-50), together with the functional relationships of the enthalpies to temperatures, form a system of coupled, independent, nonlinear algebraic equations that are solved iteratively for each i to determine $T_{p_{i+1}}$, $T_{s_{i+1}}$ and T_{t_i}. For the bypass mixing volume, referring back to Figure 3.2-4, we have

$$e_{pB} = e_{p_1},$$

or (3.2-51)

$$T_{pB} = T_{p_1},$$

and, at the primary outlet plenum:

$$e_{p_{out}} = (1 - \beta_p)\, e_{pN} + \beta_p\, e_{pB}. \quad (3.2\text{-}52)$$

This yields

$$T_{p_{out}} = T\,(e_{p_{out}}) \quad (3.2\text{-}53)$$

At the secondary outlet plenum:

$$e_{s_{in}} = e_{s_N},$$

or (3.2-54)

$$T_{s_{in}} = T_{s_N}.$$

With all temperatures thus obtained, an overall energy balance yields the heat transferred in the IHX as:

$$P_{loss,p} = W_p\ (e_{p_{in}} - e_{p_{out}}), \quad (3.2\text{-}55)$$

and

$$P_{gain,s} = W_s\ (e_{s_{out}} - e_{s_{in}}) \quad (3.2\text{-}56)$$

Equations (3.2-55) and (3.2-56) should yield results that match as closely as

possible. Also, the heat transferred at the IHX should equal the reactor heat plus heat addition at the pump, to within specified limits. If not, the appropriate iterated variable has to be reselected and the computations repeated until convergence is obtained (refer also to Section 4.1.2).

Pressure Drop

The formulation for hydraulics in the IHX is the same for the steady state as in the transient, except that "pressure drop" (ΔP_{IHX}) is used instead of "pressure loss", i.e., $(\Delta P_{f,g})_{IHX}$.

3.2.5 CENTRIFUGAL PUMP

Liquid metal pumps for LMFBRs are vertically mounted, free-surface, centrifugal pumps driven by a variable speed motor. The impeller is attached to the bottom of a long shaft while the drive motor and its bearings are located at the upper end. The shaft is surrounded by a tank which extends upward from the pump casing to the motor mounting. In order to protect the bearings of the motor, the level of sodium in this tank is maintained well below the bearings, and an inert gas such as argon is used in the region above the liquid level [3.2-6].

The sodium tank thus essentially sees only the inlet pressure to the pump at its lower end, and the cover gas pressure acting on the sodium free surface at its upper end. Hence, for modeling purposes, the pump is most conveniently divided so that a free-surface pump tank is located just upstream of the pump impeller (see Figure 3.2-7). The impeller is modeled in terms of (1) homologous head and torque relations which describe the pump characteristics, and (2) angular momentum balance to determine the impeller speed during transients. The behavior of the free surface in the pump tank is described by a

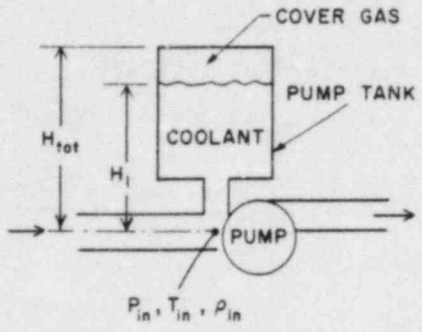

Figure 3.2-7 Schematic diagram for the pump model

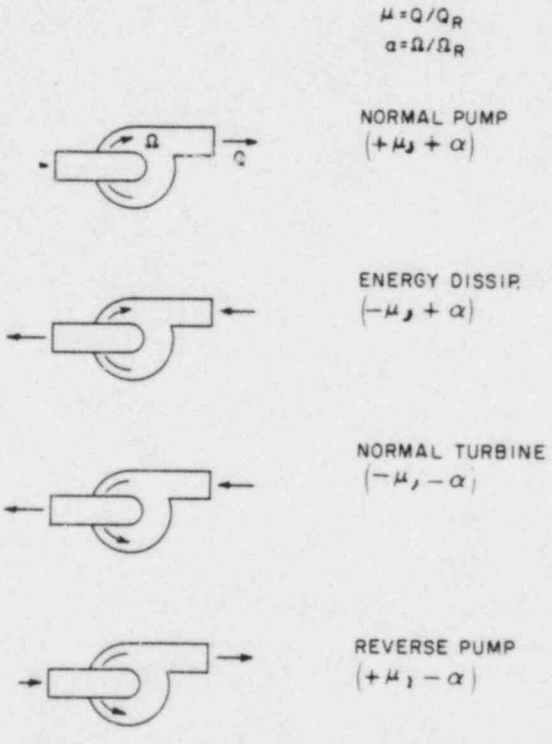

Figure 3.2-8 Pump configurations under different regimes of operation

mass balance at the tank. The pump equations are solved together with the hydraulic equations in the loop to account for the interaction between the impeller and the flow resistance in the circuit.

3.2.5.1 IMPELLER DYNAMICS

Homologous characteristics: Any given full-flowing turbomachine has definite relationships between head and discharge, torque and discharge, horsepower and discharge, etc. for any given speed. These are the pump characteristics relating the different parameters. However, there are very few complete sets of data available. Also, we need characteristics for all ranges of flow and speed conditions. Here, homologous theory [3.2-7] can be used to advantage in two ways. First, it permits the results of model tests to be used with units of the same specific speed. Secondly, by using dimensionless, homologous relationships, one can use one set of relationships to represent a whole series of different pumps having nearly the same specific speed.

In a severe accident such as a double-ended pipe break in the cold leg of a primary heat transport loop, the pump can go through several regimes of operation. These are illustrated in Figure 3.2-8. If the pump parameters are made dimensionless through division by the appropriate rated values as follows:

$$h = H/H_R,\ \mu = W/W_R,\ \alpha = \Omega/\Omega_R,\ \beta = T_{hyd}/T_R, \qquad (3.2\text{-}57)$$

where H_R is the pump head (m) at rated conditions, W_R is the pump volumetric flow rate (m^3/s) at rated conditions, Ω_R is the pump rotational speed (rpm) at rated conditions and T_R is the pump torque (N-m) at rated conditions, then these variables can be related by homologous curves, which are dimensionless extensions of the four-quadrant pump characteristics.

Homologous curves for head discharge can be drawn by plotting

$$\frac{h}{\alpha^2} \text{ vs. } \frac{\mu}{\alpha} \text{ in the range } 0 \leq \left|\frac{\mu}{\alpha}\right| \leq 1,$$

$$\frac{h}{\mu^2} \text{ vs. } \frac{\alpha}{\mu} \text{ in the range } 0 \leq \left|\frac{\alpha}{\mu}\right| < 1;$$

and, for torque-discharge, by plotting

$$\frac{\beta}{\alpha^2} \text{ vs. } \frac{\mu}{\alpha} \text{ in the range } 0 \leq \left|\frac{\mu}{\alpha}\right| \leq 1,$$

$$\frac{\beta}{\mu^2} \text{ vs. } \frac{\alpha}{\mu} \text{ in the range } 0 \leq \left|\frac{\alpha}{\mu}\right| < 1.$$

Figures 3.2-9 and 3.2-10 show these curves encompassing all four quadrants and all regions of pump operation. The curves can be read either in tabular form, as is done in the RELAP3B code, [3.2-8] or in the form of curve-fitted polynomials. In this analysis, the latter approach has been used. The polynomial relations are of the following form (up to 5th order):

$$\frac{\beta}{\alpha^2} \text{ or } \frac{h}{\alpha^2} = a_1 + a_2 \frac{\mu}{\alpha} + a_3 \left(\frac{\mu}{\alpha}\right)^2 + a_4 \left(\frac{\mu}{\alpha}\right)^3 + \ldots \qquad (3.2\text{-}58)$$

$$\text{in the range } 0 \leq \left|\frac{\mu}{\alpha}\right| \leq 1 ,$$

$$\frac{\beta}{\mu^2} \text{ or } \frac{h}{\mu^2} = a_1 + a_2 \frac{\alpha}{\mu} + a_3 \left(\frac{\alpha}{\mu}\right)^2 + a_4 \left(\frac{\alpha}{\mu}\right)^3 + \ldots \qquad (3.2\text{-}59)$$

$$\text{in the range } 0 \leq \left|\frac{\alpha}{\mu}\right| \leq 1 ,$$

where a_1, $a_2 \ldots a_6$ are user-specified constants for each polynomial. There are seven sets of polynomials for head discharge and seven sets for torque discharge. This is a very convenient representation and avoids tabular look-ups during computation. The code has default coefficients for a pump with specific speed 1800 (gpm units). This is in the range of specific speeds

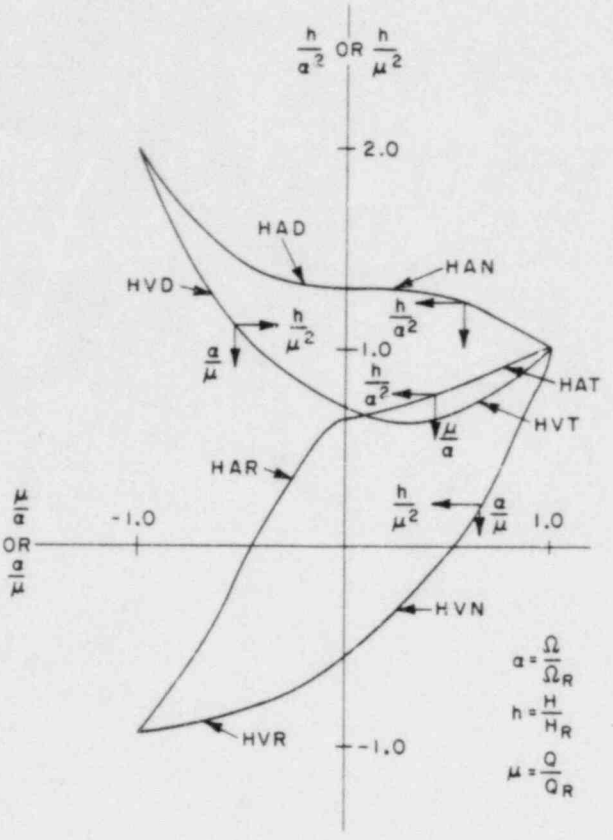

Figure 3.2-9 Complete homologous head curves

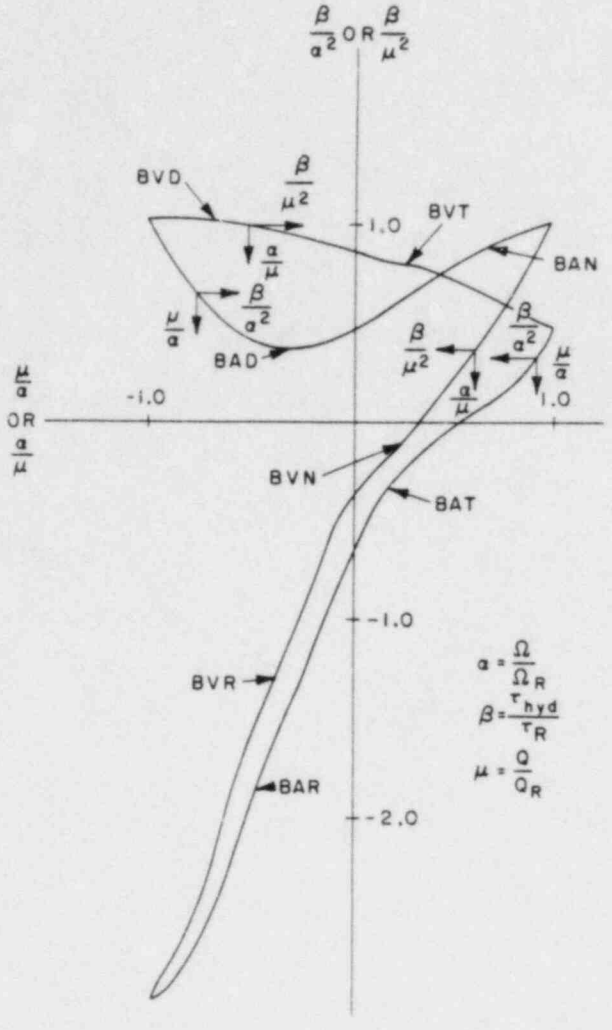

Figure 3.2-10 Complete homologous torque curves

for LMFBR pumps. They have been obtained by curve-fitting the data points in [3.2-7] for all regions except reverse pump, where the values are not available. The reverse pump region corresponds to positive flow and negative impeller rotational speed (see Figure 3.2-8) and can occur during the later stages ($t > 60$ s) of the transient following pipe break, without pony motor. Values for this regime were generated from the Karman Knapp circle diagram [3.2-9] and then curve-fitted.

Once the characteristics are available in this fashion, the head H and torque T_{hyd} can be determined, knowing rated values, operating speed, and flow rate at any time during a transient. The head then yields the pressure rise across the pump as

$$(PRISE)_{pump} = \rho_{in}\, gH\ , \qquad (3.2\text{-}60)$$

where ρ_{in} is the density of coolant at the pump inlet.

Angular Momentum Balance

The hydraulic torque is used to determine the operating speed of the impeller. At any time during the transient, the rotational speed of the pump is obtained by integrating

$$I\ \frac{d\Omega}{dt} = T_m - T_{hyd} - T_{fr}, \qquad (3.2\text{-}61)$$

where I is the moment of inertia of shaft, impeller and rotating elements inside the motor, T_m is the applied motor torque (= 0 during coastdown), T_{hyd} is the hydraulic load torque due to fluid at the impeller, T_{fr} is frictional torque, and Ω is the angular speed of the pump (rad/s).

3.2.5.2 PUMP TANK (RESERVOIR)

Mass conservation at the pump tank (reservoir) yields the equation describing the level of coolant free surface below the cover gas as

$$A_{res} \frac{d}{dt} (\rho Z_R) = W_{in} - W_{out} , \qquad (3.2\text{-}62)$$

where A_{res} is the cross-sectional area of the pump tank, W_{in} is the mass flow rate into the pump, W_{out} is the mass flow rate out of the pump, Z_R is the height of coolant in the pump tank, and ρ is the density of coolant in the pump tank.

Assuming negligible gas flow to and from the cover gas volume in the reservoir (see Figure 3.2-11) and applying the ideal gas law, the pressure of cover gas is determined from

$$P_{gas} = \frac{m_{gas} R_{gas} T_{gas}}{A_{res} (Z_{tot} - Z_R)} \qquad (3.2\text{-}63)$$

where Z_{tot} is the total height of the pump tank. The temperature of the cover gas is assumed to be the same as that of the coolant below it.

The inlet pressure to the pump impeller is governed by the behavior of coolant and cover gas in the pump tank, as follows:

$$P_{in} = P_{gas} + \rho g Z_R + K_{res} (W_{in} - W_{out}) \, | \, (W_{in} - W_{out}) \, | , \qquad (3.2\text{-}64)$$

where K_{res} is a user-specified loss coefficient for the tank orifice. Knowing P_{in} and $(PRISE)_{pump}$ from Equations (3.2-64) and (3.2-60), respectively, the pressure at pump discharge is simply obtained as the sum

$$P_{out} = P_{in} + (PRISE)_{pump} . \qquad (3.2\text{-}65)$$

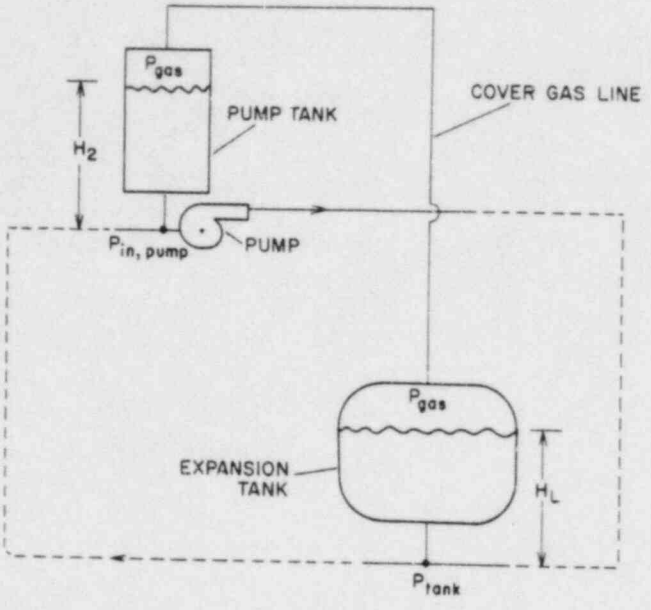

Figure 3.2-11 Schematic arrangement of surge and pump tanks

3.2.5.3 STEADY-STATE MODEL

The aim of the steady-state pump model is two-fold:

(1) to determine the pump operating conditions from its characteristics, and

(2) to determine the level of sodium in the pump tank.

Impeller

In the current approach, it was felt more logical to determine pump operating speed during steady state by matching pump head with load (total hydraulic resistance) in the circuit. Thus, for the primary loop, the required pressure rise across the pump is obtained from

$$(PRISE)_{pump} = \sum_j \Delta P_j + \Delta P_{CV} + \Delta P_{RV}, \qquad (3.2\text{-}66)$$

where the ΔP_j's are the pressure drops in the piping runs and the IHX. ΔP_{CV} and ΔP_{RV} are, respectively, the pressure drops in the check valve and the reactor vessel.

Similarly, for the intermediate loop

$$(PRISE)_{pump} = \sum_j \Delta P_j + \Delta P_{IHX}\text{'s} + \Sigma\Delta P_{SG}\ , \qquad (3.2\text{-}67)$$

where $\Sigma\Delta P_{SG}$ is the shell side pressure drop in all steam generator heat exchangers.

Pump head is related to $(PRISE)_{pump}$ by

$$H = (PRISE)_{pump}/(\rho_{in} g). \qquad (3.2\text{-}68)$$

Knowing the head and flow rate, the pump operating speed can be obtained from the homologous head curve. Equation (3.2-58) can be rearranged to give

$$a_1\alpha^5 + a_2\mu\alpha^4 + (a_3\mu^2 - h)\alpha^3 + a_4\mu^3\alpha^2 + a_5\mu^4\alpha + a_6\mu^5 = 0 \qquad (3.2\text{-}69)$$

This is a fifth degree polynomial equation in α, and is solved by a Newton's

iteration method specially adapted for polynomials [3.2-10]. Pump steady-state operating speed can now be obtained from Equation (3.2-57), since both α and Ω_R are known.

Pump Tank

The cover gas pressure in the tank at steady state is assumed known. For the primary loop, the gas pressure is generally equal to the gas pressure in the reactor vessel. In the case of the secondary loop, the gas pressure is generally equal to that in the surge tank. Thus, static pressure balance yields the height of coolant in the pump tank:

$$Z_R = (P_{in} - P_{gas}) / (\rho_{in} g), \qquad (3.2\text{-}70)$$

where P_{in}, ρ_{in} are, respectively, the pressure and coolant density at the pump inlet.

3.2.5.4 PONY MOTOR OPTION

While the arrangement of the primary and intermediate loops is intended to be such that natural circulation will provide sufficient heat transport for safe decay heat removal in the event of loss of all pumping power, the pumps may be equipped with pony motors (as is the case with CRBRP) supplied with normal and emergency power to provide forced circulation decay heat removal. Therefore, a pony motor option has been included in the pump model. The pony motor is assumed to come into play when the main motor coasts down to a user-specified fraction of its rated speed. Once the pony motor takes over, the angular momentum balance equation, i.e., Equation (3.2-61), is bypassed since the pump speed remains constant. All other calculations remain the same. Options are also available for delayed pony motor trip and for subsequent restart if desired.

3.2.6 CHECK VALVE

A check valve in the heat transport system serves two purposes:

(1) to prevent thermal shock and flow reversal in a non-operating loop, and

(2) to allow operation of the plant while one loop is out of commission.

The valve generally closes on reverse flow. The most common type utilizes a pivoted disk which closes against a seat if flow is reversed.

The modeling approach for the check valve is similar to that employed in the RELAP3B code [3.2-8]. The flow-dependent pressure losses are assumed to be represented by

$$\Delta P_{CV} = c_i \frac{W|W|}{\rho_{CV}} \quad , \tag{3.2-71}$$

where ρ_{CV} is the coolant density at the check valve location. The model allows for three regions of operation for the valves, hence, three pressure loss coefficients are required:

(1) c_1 for positive flow with valve open,

(2) c_2 for negative flow with valve open,

(3) c_3 for negative flow with valve in closed position,

where c_1, c_2, c_3 are user-specified constants, in addition to P_{CV}, the back pressure required to close the valve.

For positive flow, the valve remains open at all times. On reverse flow, the valve remains open as long as ΔP_{CV} with $c_i = c_2$ is less than P_{CV}. So far, both valves behave identically, but from the closed position, type 1

valve opens when ΔP_{CV} with $c_i = c_2$ is less than P_{CV}, whereas type 2 valve opens when ΔP_{CV} with $c_i = c_3$ is less than P_{CV}. At the user's option, the valve can also remain open in the failed position on reverse flow.

3.2.7 SURGE TANK

The expansion (surge) tank in each intermediate loop serves to accommodate the coolant volume change due to thermal expansion over the operating range. Figure 3.2-11 shows a schematic diagram of the expansion tank and pump tank. Much like the reactor vessel upper plenum in the primary system, the surge tank adds another free surface in the intermediate loop. During steady-state operation, the pressure in the loop at the location of the surge tank is evaluated (assuming that the level in the tank is known) by

$$P_{tank} = P_{gas} + \rho g Z_L \ . \qquad (3.2\text{-}72)$$

Here, ρ is the density of coolant at the tank location, and P_{gas} is the pressure of cover gas in the surge tank.

Equation (3.2-72) gives the starting point for evaluating all other pressures in the intermediate loop, once pressure drops in the different piping runs and components have been computed.

During a transient, the equations are very similar to those for the pump tank and will not be repeated here.

3.2.8 PIPE-BREAK MODEL

During a pipe-break accident in an LMFBR, the coolant flow in the system is coupled to the break discharge rate. Since a coolant pipe is usually surrounded by an outer pipe, the discharge fluid, depending on the gap size between pipes, may expand freely or be space limited.

In most existing codes [3.2-3, 3.2-4, 3.2-11] only two limiting types of breaks are considered. One is the small leak for which a discharge coefficient of 0.611 is used. The other is the guillotine break with large separation distance so that the flow interaction between the two sides of the break can be neglected. The medium size breaks are treated as either small leaks or guillotine breaks. Furthermore, the effect of the sleeve or guard pipe flow confinement is not considered.

The existing models result in a high prediction for the discharge rate. However, this may not necessarily result in a conservative impact on the reactor core since higher discharge rates result in an optimistic (i.e., earlier) reactor scram time. This effect may be illustrated in Figure 3.2-12, which is a sketch of the flow rate and power versus time. For a predicted fast coolant loss, one predicts an early scram operation which is usually initiated by a low flow sensing device. With a slower coolant loss, the scram may be initiated at a later time, or it may not occur at all. Thus, it is important to employ a realistic rather than a "conservative" model to determine the discharage rate.

The model to be described [3.2-13] covers the entire range of break/pipe area ratios (from small leaks to guillotine breaks with large separation distance) as well as gap/pipe area ratios (from free-jet flow to confined flow).

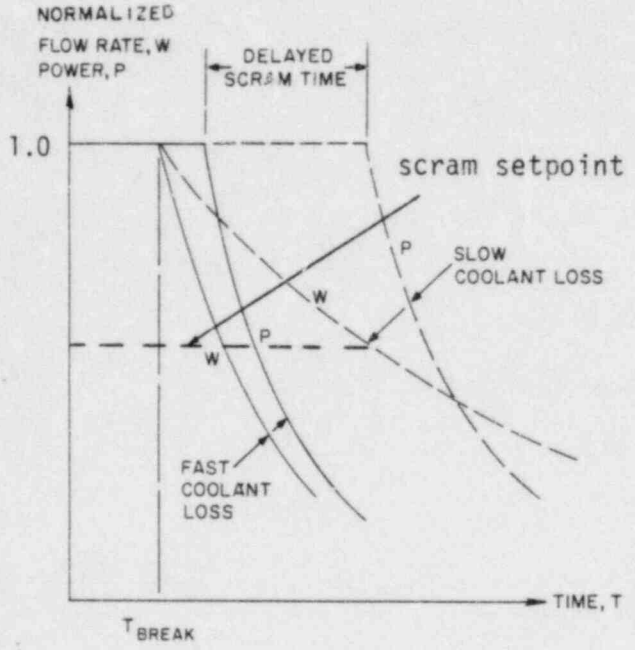

Figure 3.2-12 Effect of flow rate on scram time

The flow in the break region is considered to be quasi-steady and incompressible, and gravity effects are neglected. When the break area is small compared to the space between the coolant and outer pipes, the discharge fluid is assumed to behave as a free jet. When the break area is large such that the discharge fluid is limited by the gap space, confined flow theory accounting for dissipation pressure losses are employed.

3.2.8.1 FREE-JET DISCHARGE

Consider the case of small break/gap area ratio in Figure 3.2-13(a). The jet then expands freely (i.e., with a free stream surface) and the following conservation equations apply:

$$(v_1 - v_2)\, A_p = v_j\, (A_3 + A_4), \tag{3.2-73}$$

$$(p_1 - p_2)\, A_p = \rho(v^2_2 - v^2_1)\, A_p + \rho v^2_j\, (A_4 - A_3), \tag{3.2-74}$$

$$p_\alpha + \frac{1}{2}\rho v^2_\alpha = p_j + \frac{1}{2}\rho v^2_j,\ \alpha = 1,2, \tag{3.2-75}$$

where A, p, ρ and v denote area, pressure, density and velocity, respectively. Here, A_p denotes the inside cross-sectional area of the pipe.

The pressure-velocity relations for upstream and downstream pipe flows are given in the form

$$F_\alpha\,(p_\alpha, v_\alpha) = 0,\ \alpha = 1,2. \tag{3.2-76}$$

In addition, if the discharge coefficient based on two-dimensional free streamline analysis [3.2-13] without wall impingement effect is employed, one deduces

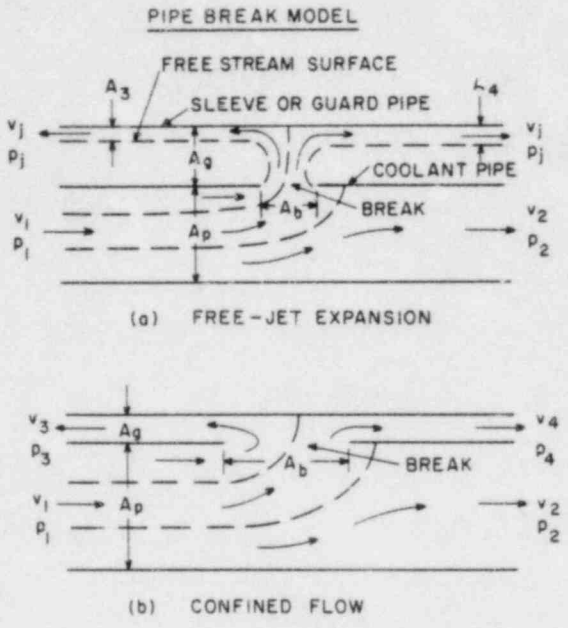

Figure 3.2-13 Illustration of pipe break flowfields

$$(2/\pi)[(1 + r^2_1)\tanh^{-1}r_1 - (1 + r^2_2)\tanh^{-1}r_2$$
$$- (1/2)(r^2_1 - r^2_2)\tanh^{-1}((r_1 + r_2)/2)] \qquad (3.2\text{-}77)$$
$$+ (r_1 + r_2)[1 + (r_1 + r_2)^2/4]^{0.5}$$
$$= A_b/A_p,$$

where $r_1 = v_1/v_j$ and $r_2 = v_2/v_j$.

For a given geometry and p_j, Equations (3.2-73) to (3.2-77) may be solved for p_1, p_2, v_1, v_2, v_j, A_3 and A_4. If coolant is discharged from both sides of pipe, v_2 is negative. The contraction (discharge) coefficient may be defined as $C_c = (A_3 + A_4)/A_b$. The discharge rate is then given by $Q = C_c A_b v_j$.

Equations (3.2-73) to (3.2-76) are applicable for jet discharge between two pipes as well as between two plane walls. Equation (3.2-77) is based on two-dimensional (planar) flow considerations. However, two-dimensional results have been known to be very good approximations for circular geometry, [3.2-13, 3.2-14] and it is expected that Equation (3.2-77) is a valid first approximation for various break configurations. It should be emphasized, however, that the impingement effect of the outer wall on the discharge coefficient has not been considered.

It may be noted that, using Equations (3.2-73) and (3.2-75), one may replace Equation (3.2-74) by

$$(v_1 + v_2)(A_3 + A_4) = 2v_j(A_4 - A_3). \qquad (3.2\text{-}78)$$

3.2.8.2 CONFINED FLOW

When the break/gap area ratio is large, the discharge rate is limited by the gap space as shown in Figure 3.2-13(b). Confined flow is accompanied by

significant dissipation losses in pressure. The governing equations are

$$(v_1 - v_2)\, A_p = (v_3 + v_4)\, A_g; \tag{3.2-79}$$

$$p_1 + \frac{1}{2}\rho v^2_1 = p_\beta + \frac{1}{2}\rho v^2_\beta + k_{1\beta}\frac{1}{2}\rho v^2_1, \quad \beta = 2,3,4\ ; \tag{3.2-80}$$

$$F_\alpha(p_\alpha, v_\alpha) = 0, \qquad \alpha = 1,2,3,4\ ; \tag{3.2-81}$$

where $k_{1\beta}$ denotes the loss coefficient from stream 1 to stream β, and Equation (3.2-81) represents a pipe flow relation for each stream. For a given geometry, Equations (3.2-79) to (3.2-81) may be solved for p_α and v_α, where α = 1,2,3 and 4.

The loss coefficients need to be determined by experiment. Meanwhile, however, a momentum principle employed by Taliev and described by Ginzberg [3.2-15] for converging and diverging pipe flows may be generalized to the present configuration to obtain the idealized formulas for the loss coefficients.

Consider the control volume for each separate stream as shown in Figure 3.2-14. The effective average pressure at a separating stream surface is assumed to be of the form $p = p_1 + k\rho v^2_1/2$, where k is a correction coefficient. For example, consider stream 1-2 shown at the bottom of Figure 3.2-14. A momentum balance for the control volume yields

$$p_1 A_{12} + (p_1 + k_b \frac{1}{2}\rho v^2_1)(A_2 - A_{12}) + \rho v^2_1 A_{12} = p_2 A_2 + \rho v^2_2 A_2. \tag{3.2-82}$$

Simplified by the continuity relation of $v_1 A_{12} = v_2 A_2$, Equation (3.2-82) becomes

$$p_1 - p_2 = \rho v_2 (v_2 - v_1)(1 + \frac{1}{2} k_b\, v_1/v_2); \tag{3.2-83}$$

similarly, for streams 1-3 and 1-4, one obtains

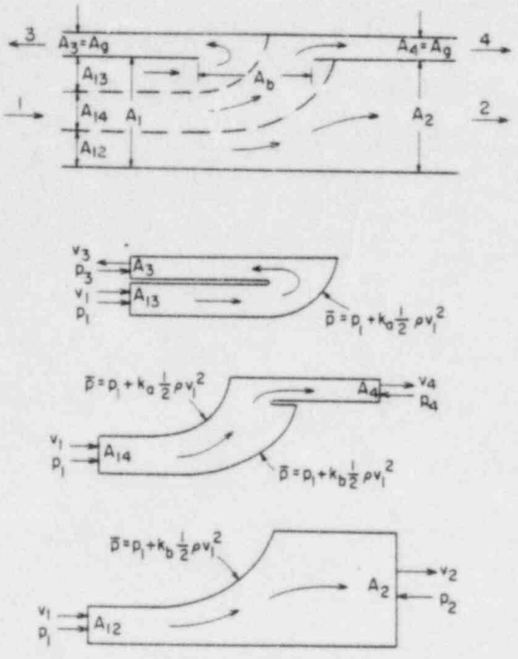

Figure 3.2-14 Control volumes for confined flow

$$p_1 - p_3 = \rho v_3(v_3 + v_1) \cdot (1 - \frac{1}{2} k_a v_1/v_3), \tag{3.2-84}$$

$$p_1-p_4 = \rho v_4(v_4-v_1) + \frac{1}{2} \rho v_1 [(k_b-k_a)v_3 + k_b v_4-k_a v_1] \tag{3.2-85}$$

Comparison of Equations (3.2-83) to (3.2-85) with Equation (3.2-80) yields

$$k_{12} = (1 - \frac{v_2}{v_1})^2 + k_b \left(\frac{v_2}{v_1} - 1\right) , \tag{3.2-86}$$

$$k_{13} = (1 + \frac{v_3}{v_1})^2 - k_a \left(\frac{v_3}{v_1} + 1\right) , \tag{3.2-87}$$

$$k_{14} = (1 - \frac{v_4}{v_1})^2 + [(k_b - k_a) \frac{v_3}{v_1} + k_b \frac{v_4}{v_1} - k_a] . \tag{3.2-88}$$

The correction factors k_a and k_b remain to be determined from experiments. Presently, however, the idealized values of $k_a = 0$ and $k_b = 0$ are assumed.

If the fluid is discharged from both sides of the pipe (v_2 is negative), then there exists only one separating stream surface, and the analysis is modified accordingly . Consider stream 2 to mix with part of stream 1 to exit at stream 4. Then, following the momentum principle, Equations (3.2-83) to (3.2-85) are replaced by

$$p_1 - p_2 = k_d \frac{1}{2} \rho v^2_1 , \tag{3.2-89}$$

$$p_1 - p_3 = \rho v_3(v_3 + v_1) (1 - \frac{1}{2} k_c v_1/v_3), \tag{3.2-90}$$

$$\begin{aligned} p_1 - p_4 = {} & \rho [v_4(v_4 - v_1) - v_2(v_3 + v_4)] \\ & + \frac{1}{2} \rho v_1 \left[K_1 v_1 \frac{v_3 + v_4}{v_1 - v_2} - k_c (v_3 + v_1)\right] , \end{aligned} \tag{3.2-91}$$

and Equations (3.2-86) to (3.2-88) are replaced by

$$k_{12} = \left(1 - \frac{v_2}{v_1}\right)^2 + k_d \ , \tag{3.2-92}$$

$$k_{13} = \left(1 + \frac{v_3}{v_1}\right)^2 - k_c \left(\frac{v_3}{v_1} + 1\right) \ , \tag{3.2-93}$$

$$k_{14} = \left(1 - \frac{v_4}{v_1}\right)^2 - \frac{2v_2(v_3 + v_4)}{v^2_1} + k_d \frac{v_3 + v_4}{v_1 - v_2} - k_c \frac{v_3 + v_1}{v_1} \ . \tag{3.2-94}$$

Again, k_c and k_d are correction factors which are to be determined experimentally. These are presently given the idealized value of zero.

The equations for confined flow are applicable for both circular pipes and plane walls. However, for the unsymmetrical case such as a circular break on the inner pipe, it is implied in the analysis that the discharge fluid spreads out circumferentially to fill the cross-sectional gap area between the inner and outer pipes.

3.2.9 GUARD VESSEL

As a safety feature to minimize the effects of a pipe-break accident, guard vessels are provided around the reactor vessel, IHX, primary pump and all piping which is below the elevation of the tops of the guard vessels. Their volumes are such that the reactor vessel coolant level does not fall below the outlet nozzle, so that the core is always submerged in coolant. If a break occurs such that coolant spills into a guard vessel, the vessel will

eventually fill up to the break height. Any level rise above that will create back pressure against further leakage.

A sample configuration of a guard vessel for a break in the reactor vessel inlet region is shown in Figure 3.2-15. At any time during the transient following a pipe break within a guard vessel, the volume of sodium collected in the guard vessel can be determined by

$$V_{GV} = \int_0^t \frac{W_b}{\rho} \, dt \ , \tag{3.2-95}$$

where W_b, the break flow rate (for the case illustrated), is

$$W_b = W_{2,1} - W_{3,1} \ , \tag{3.2-96}$$

and ρ is the coolant density at the break.

To determine the height of sodium in the guard vessel (Z_{GV}), a detailed knowledge of the configuration and dimensions of the annular and bottom space between the component and its guard vessel is required. However, a simpler and more general approach is to have a functional relationship between Z_{GV} and V_{GV} in the form of a polynomial equation as follows:

$$Z_{GV} = c_1 + c_2 (V_{GV} - V_{min}) + c_3 (V_{GV} - V_{min})^2 \qquad \text{if } V_{GV} > V_{min} \ , \tag{3.2-97}$$

and

$$Z_{GV} = 0 \qquad \text{if } V_{GV} \leq V_{min} \ ,$$

where c_1, c_2, c_3 are user-input coefficients depending on the geometry of the guard vessel space. V_{min} is the volume required to fill up to the lowest elevation of piping in the guard vessel. This is also a user-input quantity and will be different for different guard vessels. V_{GV} is limited

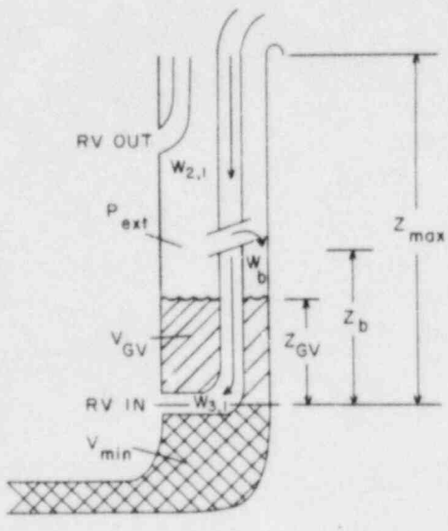

Figure 3.2-15 Guard vessel configuration for break in the inlet region of the reactor vessel

by V_{max}, the maximum capacity of the guard vessel. It seems reasonable to assume V_{max} to be the same for all guard vessels based on the volume contained in the upper plenum between the operating level and the minimum safe level. Z_{GV} is limited by Z_{max}, the height of the guard vessel. This can be different for different guard vessels.

With Z_{GV} known from Equation (3.2-97), the pressure external to the break can be determined by

$$\begin{aligned} P_{ext} &= P_{atm} && \text{if } Z_{GV} \leq Z_b \text{ ;} \\ &= P_{atm} + \rho g\,(Z_{GV} - Z_b) && \text{if } Z_{GV} > Z_b \end{aligned} \qquad (3.2\text{-}98)$$

3.2.10 TRANSIENT HYDRAULIC SIMULATION

The equations describing the behavior of pumps, free surface levels, pressure losses in different components, and flow rates in the loops together constitute the hydraulic model for the heat transport systems. Since the primary and intermediate systems are only thermally coupled, their hydraulic equations do not have to be solved together, even though it is advantageous to solve them at the same time.

In this section, the hydraulic model will be presented for the primary system only. Similar analysis is performed for the intermediate loop. Figure 3.2-16 is a sample configuration for a two loop simulation. A break occurs near the reactor vessel in one of the simulated loops and the remaining intact loops are lumped together as the other loop. Note that the code has a general formulation.

The model equations are now described.

Momemtum: the uniform mass flow rate model implies that at any instant in

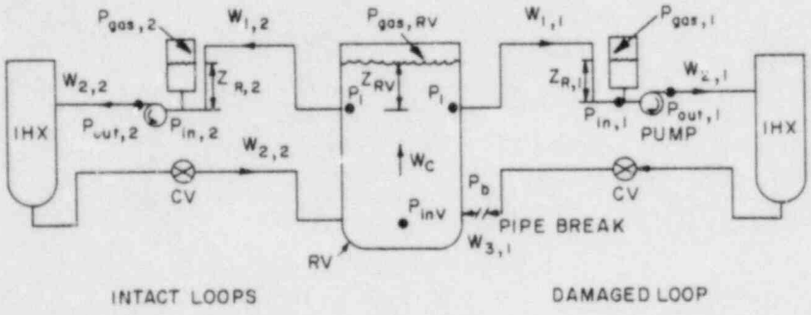

Figure 3.2-16 Hydraulic profile of PHTS for test case

time, flow rates are constant throughout the loops except at a free surface, or junction where several flows meet, or a break where there is flow loss. With this as background, the flow rates have been indicated in Figure 3.2-16. Volume-averaged momentum equations can be written relating the time rate of change of the mass flow rate in a constant mass flow rate section to the end pressure and total losses in that section. These are

$$\frac{dW_{1,1}}{dt} \sum_{1,1} \frac{L}{A} = P_1 - P_{in,1} - \sum_{1,1} \Delta P_{f,g} , \qquad (3.2\text{-}99)$$

$$\frac{dW_{2,1}}{dt} \sum_{2,1} \frac{L}{A} = P_{out,1} - P_{in,b} - \sum_{2,1} \Delta P_{f,g} , \qquad (3.2\text{-}100)$$

$$\frac{dW_{3,1}}{dt} \sum_{3,1} \frac{L}{A} = P_{out,b} - P_{inV} - \sum_{3,1} \Delta P_{f,g} , \qquad (3.2\text{-}101)$$

$$\frac{dW_{1,2}}{dt} \sum_{1,2} \frac{L}{A} = P_1 - P_{in,2} - \sum_{1,2} \Delta P_{f,g} , \qquad (3.2\text{-}102)$$

$$\frac{dW_{2,2}}{dt} \sum_{2,2} \frac{L}{A} = P_{out,2} - P_{inV} - \sum_{2,2} \Delta P_{f,g} . \qquad (3.2\text{-}103)$$

Here, $P_{in,b}$ and $P_{out,b}$ represent the pressure just upstream and downstream of the break, respectively and $\Sigma \Delta P_{f,g}$ is the summation of frictional and gravitational losses through the respective flow segment.

Pump: The pressure in the loop at the pump exit is obtained from Equation (3.2-65) in the pump model description.

Reservoir: The inlet pressure to the pump is obtained from Equation (3.2-64). Level changes are described by Equation (3.2-62).

Reactor Vessel (RV): The primary loop has interfaces with the RV at inlet to

loop and inlet to RV. The level of sodium in the upper plenum is determined by

$$A_{RV} \frac{d}{dt} (\rho Z_{RV}) = W_c - W_{1,1} - n\, W_{1,2} \quad , \tag{3.2-104}$$

where

$$W_c = W_{3,1} + n\, W_{2,2} \, . \tag{3.2-105}$$

P_1, the pressure at the inlet to the loop, is given by

$$P_1 = P_{gas,RV} + \rho g Z_{RV} \quad . \tag{3.2-106}$$

Equations (3.2-104) and (3.2-106), as well as the equation for $P_{gas,RV}$, are described in more detail in Section 3.1.

An equation to determine the vessel inlet pressure, which utilizes information from the primary loop hydraulic equations, as well as from the vessel coolant dynamics, must be included as part of primary loop hydraulic model. The equation is obtained as follows (again, a two loop simulation is used for illustrative purposes):

Mass conservation at vessel inlet yields

$$W_c = n\, W_{2,2} + W_{3,1} \quad . \tag{3.2-107}$$

or differentiating both sides,

$$\frac{dW_c}{dt} = n \frac{dW_{2,2}}{dt} + \frac{dW_{3,1}}{dt} \tag{3.2-108}$$

From the loop hydraulics

$$\frac{dW_{2,2}}{dt} = \frac{P_{out,2} - P_{inV} - \sum_{2,2} \Delta P_{f,g}}{\sum_{2,2} \frac{L}{A}} \tag{3.2-109}$$

and, assuming break after pump:

$$\frac{dW_{3,1}}{dt} = \frac{P_{out,b} - P_{inV} - \sum_{3,1} \Delta P_{f,g}}{\sum_{3,1} \frac{L}{A}} \qquad (3.2\text{-}110)$$

The core flow can be expressed as

$$W_c = \sum_j W_j \quad , j = 1, (N6CHAN + 1) \ , \qquad (3.2\text{-}111)$$

where (N6CHAN + 1) represents the number of channels simulated in the core, including bypass. Differentiating both sides of Equation (3.2-111) and substituting along with Equations (3.2-109) and (3.2-110) in Equation 3.2-108, one obtains

$$\sum_j dW_j/dt = n(P_{out,2} - P_{inV} - \sum_{2,2} \Delta P_{f,g})/ \sum_{2,2} L/A + (P_{out,b} - P_{inV} - \sum_{3,1} \Delta P_{f,g})/ \sum_{3,1} L/A \qquad (3.2\text{-}112)$$

Also, applying momentum balance across the core yields

$$\sum_j dW_j = \Sigma [P_{inV} - P_1 - \Sigma \Delta P_{f,g}]/(\Sigma\ L/A)_j, \qquad (3.2\text{-}113)$$

Substituting into Equation (3.2-112) and simplifying yields the vessel inlet pressure as

$$P_{inV} = (A + B + C)/[\sum_j \frac{1}{(\Sigma \frac{L}{A})_j} + \frac{n}{\sum_{2,2} \frac{L}{A}} + \frac{1}{\sum_{3,1} \frac{L}{A}}], \qquad (3.2\text{-}114)$$

where

$$A = \Sigma[(P_1 + (\Sigma\ \Delta P_{f,g})_j)/(\Sigma L/A)_j], \qquad (3.2\text{-}115)$$

$$B = n[(P_{out,2} - \sum_{2,2} \Delta P_{f,g})/ \sum_{2,2} L/A], \qquad (3.2\text{-}116)$$

$$C = [(P_{out,b} - \sum_{3,1} \Delta P_{f,g})/ \sum_{3,1} L/A]. \qquad (3.2\text{-}117)$$

Equations (3.2-99) to (3.2-106), together with the equations for the pump, break, guard vessel, vessel inlet pressure, etc., form a system of ordinary differential equations and associated algebraic equations to be solved together to yield the flow rates, pressures, and free-surface levels in the system. These equations are advanced in time using a predictor-corrector algorithm of the Adams type (see Chapter 4).

The solution procedure is shown in Figures 3.2-17 and 3.2-18 by means of simple flow charts. Only the main calculations involved during each timestep are indicated. During each step, several detailed subroutines, which are not shown here, are called.

3.2.11 TRANSIENT THERMAL SIMULATION

On the primary side, the loop thermal calculations interface directly with the reactor vessel at the loop inlet and outlet. On the intermediate side, the coupling is through the heat fluxes at the steam generator.

As mentioned earlier, since the wall equations are decoupled from the coolant equations in each module, the solution can march in the direction of flow. Figures 3.2-19 and 3.2-20 show flow charts for the simulation procedure. To keep the illustration simple, the overall logic shown is for forward flow only; however, the code has the more general logic to handle reverse flow as well.

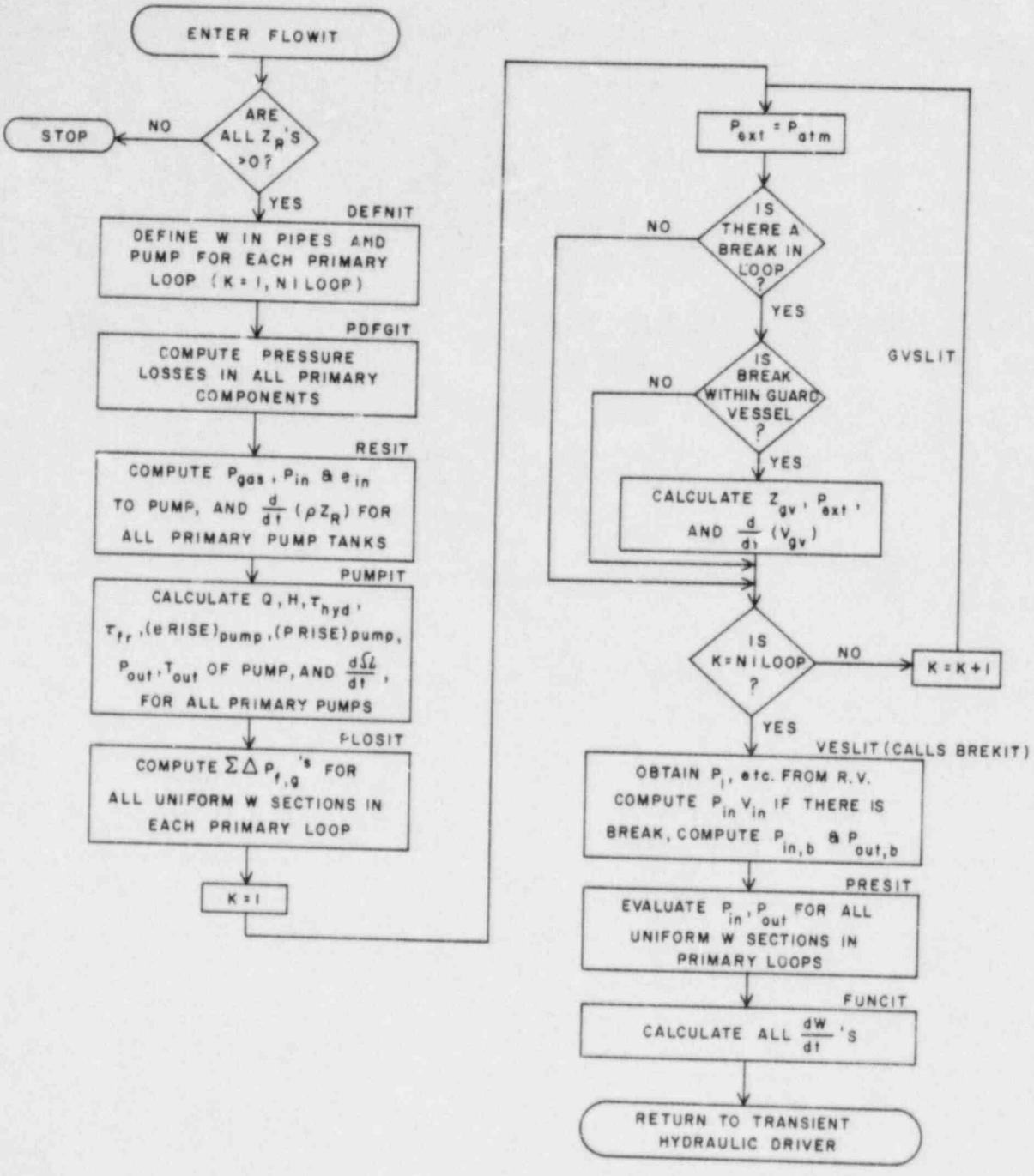

Figure 3.2-17 Flow diagram for transient hydraulic simulation (primary system)

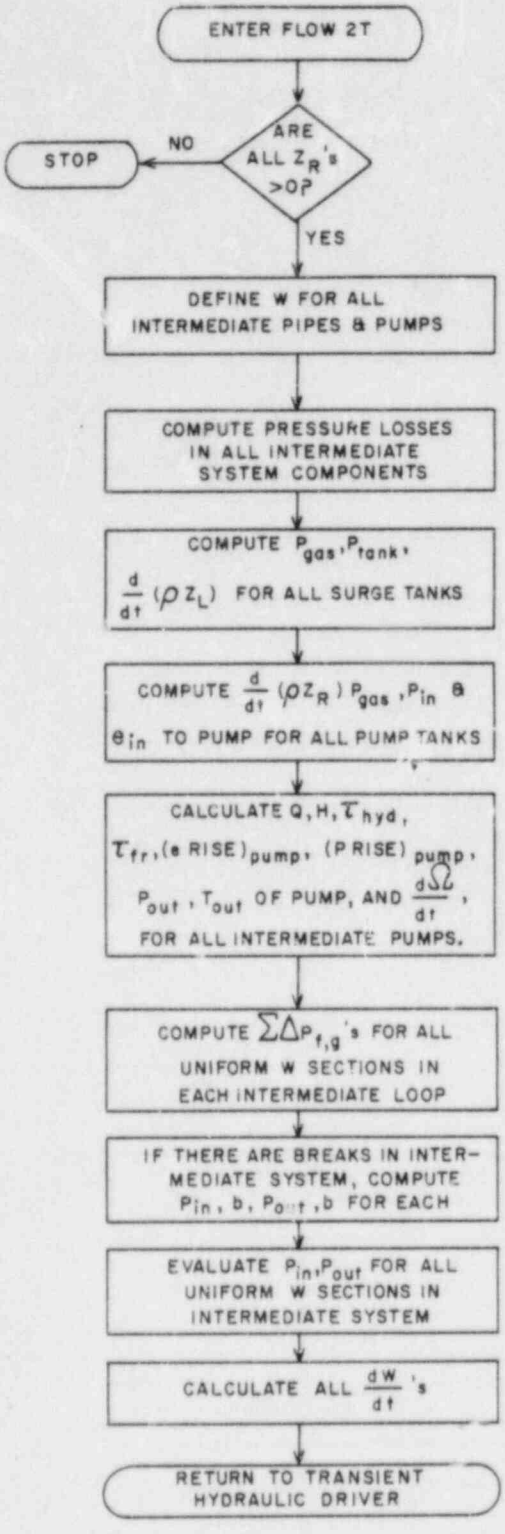

Figure 3.2-18 Flow diagram for transient hydraulic simulation (intermediate system)

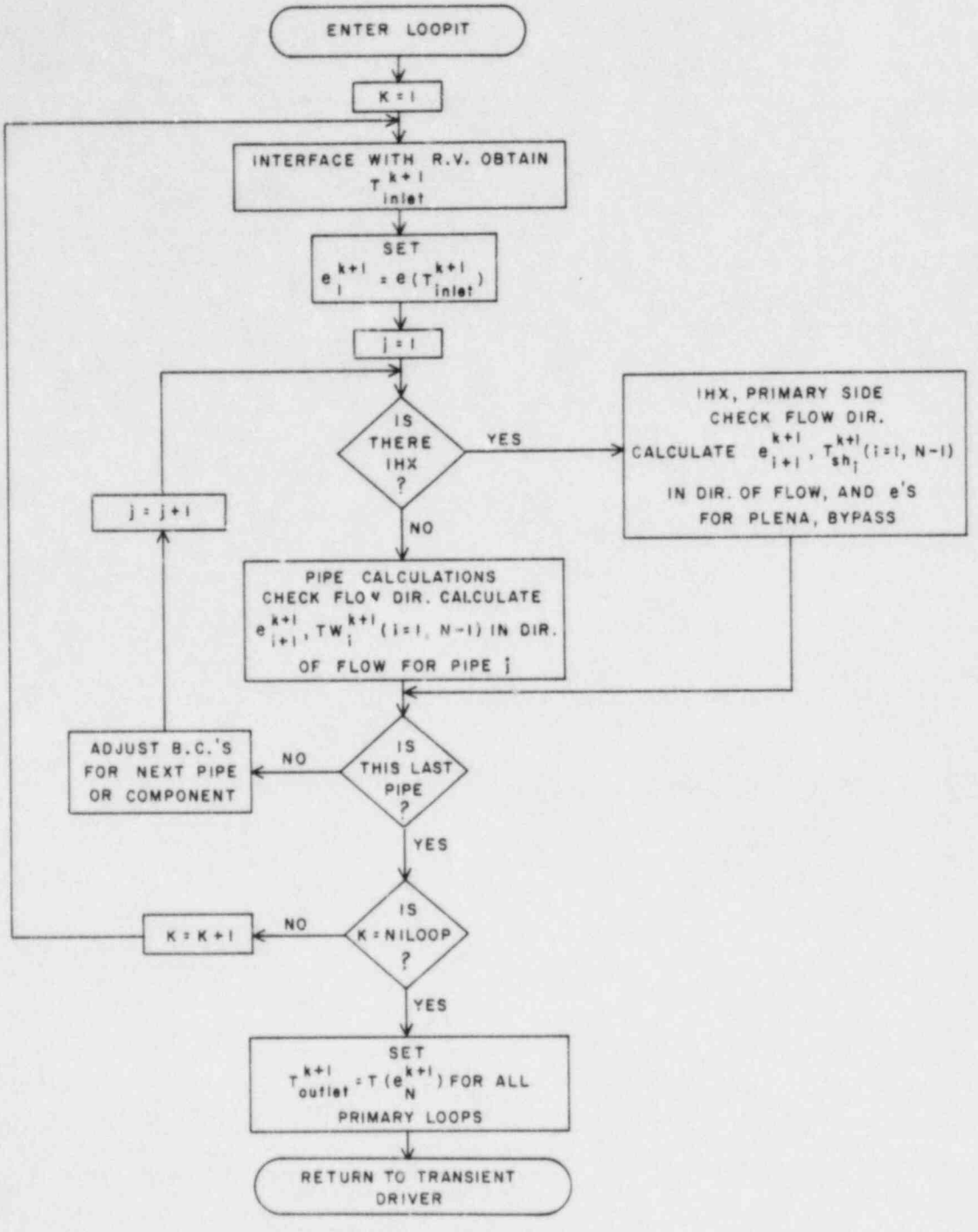

Figure 3.2-19 Flow diagram for transient thermal simulation (primary system)

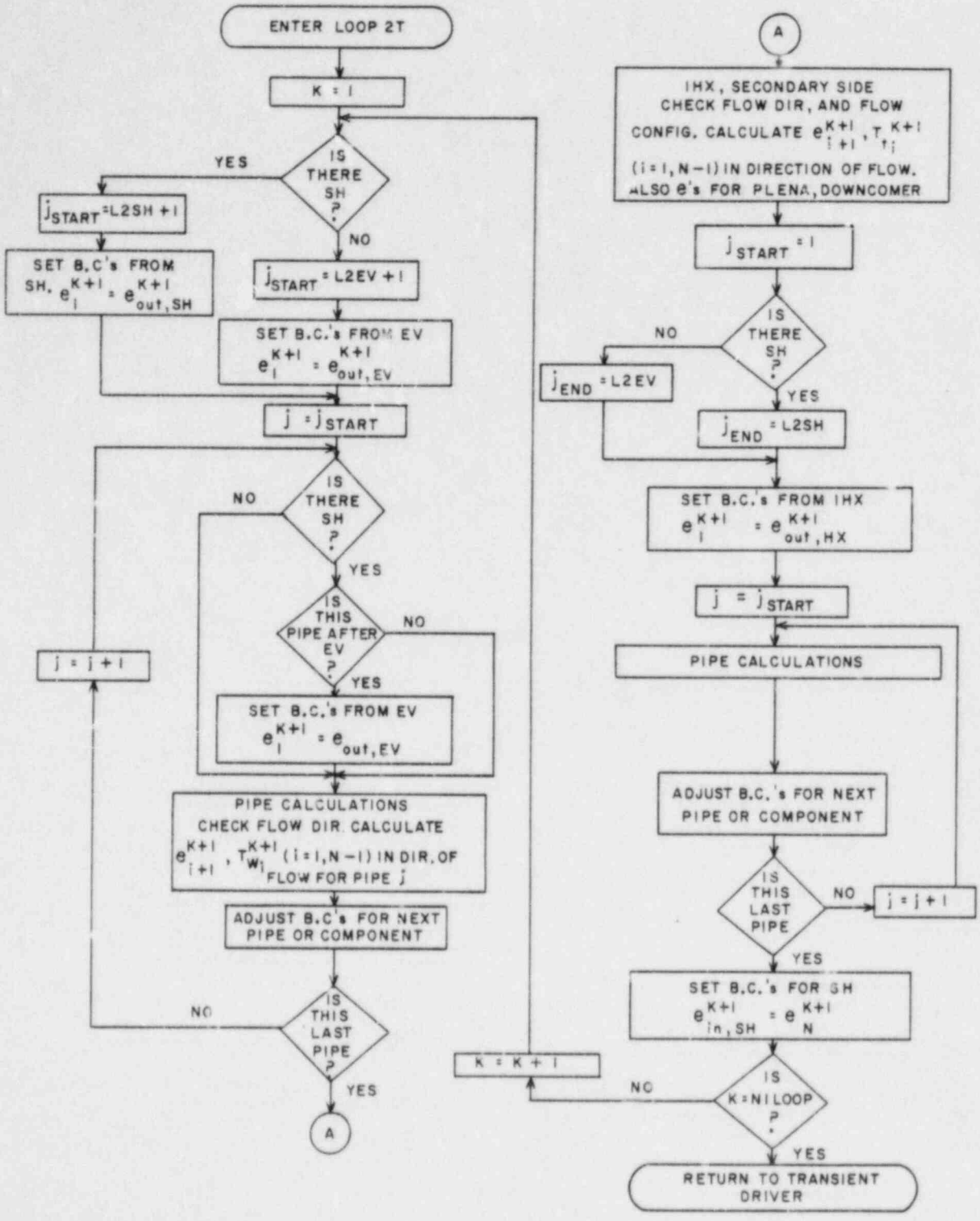

Figure 3.2-20 Flow diagram for transient thermal simulation (intermediate system)

REFERENCES FOR SECTION 3.2

3.2-1 W. L. Chase, "Heat-Transport Systems", in Fast Reactor Technology: Plant Design, Ch. 4, edited by J. G. Yevick, The M.I.T. Press, Cambridge, MA, 1966.

3.2-2 Clinch River Breeder Reactor Plant, Preliminary Safety Analysis Report, Project Management Corporation.

3.2-3 S. L. Additon, T. B. McCall, and C. F. Wolfe, "IANUS - Outline Description", Westinghouse Advanced Reactors Division, Waltz Mill, Pennsylvania, FPC-939.

3.2-4 "LMFBR Demonstration Plant Simulation Model, Demo", Westinghouse Advanced Reactors Division, WARD-D-0005 (Rev 3), February 1975.

3.2-5 W. H. McAdams, Heat Transmission, 2nd Edition, McGraw-Hill, New York, 1942.

3.2-6 N. J. Palladino, "Mechanical Design of Components for Reactor Systems", in The Technology of Nuclear Reactor Safety, Vol. 2, Ch. 14, edited by T. J. Thompson and J. G. Beckerley, the M.I.T. Press, Cambridge, MA, 1973.

3.2-7 V. L. Streeter and E. B. Wylie, Hydraulic Transients, McGraw-Hill, New York, 1967.

3.2-8 "RELAP 3B Manual, A Reactor System Transient Code", Brookhaven National Laboratory, RP 1035, December 1974.

3.2-9 B. Donsky, "Complete Pump Characteristics and the Effects of Specific Speed on Hydraulic Transients", Trans. ASME, J. Basic Eng., pp. 685-696, December 1961.

3.2-10 E. Isaacson and H. B. Keller, Analysis of Numerical Methods, John Wiley & Sons, Inc., New York, 1966.

3.2-11 B. A. Martin, A K. Agrawal, D. C. Albright, L. A. Epel, and G. Maise, "NALAP: An LMFBR System Transient Code", BNL-50457, July 1975.

3.2-12 V. Quan and A. K. Agrawal, "A Pipe-Break Model for LMFBR Safety Analysis", BNL-NUREG-50688, 1977.

3.2-13 J. S. McNown and E. Y. Hsu, "Application of Conformal Mapping to Divided Flow", Proc. Midwest Conf. Fluid Dynamics, pp. 143-155, 1951.

3.2-14 H. Rouse and A. H. Abul-Fetouh, "Characteristics of Irrotational Flow Through Axially Symmetric Orifices", J. Appl. Mech. 17, pp. 421-426, 1950.

3.2-15 I. P. Ginzburg, Applied Fluid Dynamics, Chap. VI, NTIS N63-21073, 1963.

3.3 THE STEAM GENERATOR SYSTEM (MINET)

The representation of the steam generation system in SSC is handled within a computational package, designated MINET, which is coupled and interfaced to SSC. MINET is based on a momentum integral network method, which is an extension of the momentum integral method [3.3-1]. This method uses a two-plus equation representation of the thermal-hydraulic behavior of a system of heat exchangers, pumps, pipes, valves, tanks, etc. It is computationally faster than the three equation methods used in RELAP [3.3-2] and its descendents, yet represents the compression and expansion of water/steam due to changes in enthalpy and pressure.

The MINET representation of a system is as one or more networks of accumulators, segments, and boundaries. Networks are linked together via heat exchangers only, i.e., heat can transfer between networks, but fluids cannot. Accumulators are used to represent tanks or other voluminous components, as well as locations in the system where significant flow divisions or combinations occur. Segments are composed of one or more pipes, pumps, heat exchangers, (inside or outside of tubes), and/or valves, each represented by one or more nodes. Boundaries are simply points where the network interfaces with the user or the SSC code.

MINET calculations are performed at two levels, i.e., the network level (accumulators), and the segment level. Equations conserving mass and energy are used to calculate the pressure and enthalpy within accumulators. An integral momentum equation is used to calculate the segment average flow rate. In-segment distributions of mass flow rate and enthalpy are calculated using local equations of mass and energy. The segment pressure is taken to be the linear average of the pressure at both ends.

With few exceptions, the steam generator network is a closed system, accessed through the boundary modules. The exceptions are certain variables which are control system related, e.g., pump speed. Boundary modules in the hot network interface only with intermediate loop parameters, and are not accessible to the user. Water/steam network boundary modules receive user input information regarding pressure or flow rate and temperature (used only if in-flow). MINET calculations advance the other module variable (flow rate or pressure) and temperature (if outflow).

The current MINET version uses a homogeneous equilibrium model of two phase flow, supplemented by various two phase correlations. Extension of the method to include better representation of the two phase phenomena, whether through slip, drift, or two fluid models, is a good possibility. This is because the intricacies of these models are less likely to strain the numerics of MINET than codes where local pressures are calculated via time-dependent equations.

The MINET package is extensive and utilizes many equations and variables. Most of these variables are listed and defined in Table 3.3-1.

3.3.1 MINET METHOD PHYSICS

The computational speed and power of the MINET method results largely from the local suppression of sonics in flow segments. It is implicitly assumed that the propagation of pressure waves in pipes, pumps, heat exchangers, and valves takes place on a time scale much smaller (milliseconds) than the transient of interest (seconds to minutes). Of course, such an assumption would be incorrect regarding the large break loss-of-coolant accident (LOCA) often postulated for light water reactor primary loops. However, for steam generating

systems, one is generally more interested in representing slower transients and overall plant behavior than large break LOCA's. Thus, for a feed or steam line break, one concentrates on monitoring the inventory loss and maintaining a reasonably accurate average pressure so as to properly update the conditions feeding back toward the reactor.

Table 3.3-1 - Variables Used in MINET Models

A_h - heat transfer area in heat exchanger h

A_i - flow area for node i

A_m - heat transfer area in segment m

A_s - heat transfer area attributable to subsystem s

A_{max_v} - maximum (full open) flow area through valve v

At_h - tube cross-sectional area in heat exchanger h

A_v - flow area through valve v

Cpt_i - specific heat of heat exchanger tube material in node i

D_{eq} - equivalent hydraulic diameter

Dh_h - hot side tube diameter in heat exchanger h

Dws_h - water/steam side tube diameter in heat exchanger h

E_b - enthalpy at boundary module b

E_i - node average enthalpy for node i

E_{IM} - enthalpy entering segment from bordering module IM

E_j - enthalpy at nodal interface j

E_{mi} - enthalpy at inlet interface of segment m

E_{mo} - enthalpy at outlet interface of segment m

E_n - average enthalpy in accumulator n

E_{OM} - enthalpy in segment outlet bordering module OM

f_i - friction factor in node i

fa_h - heat transfer area correction factor for heat exchanger h

fk_m - impedance coefficient for segment m

$f\ell_n$ - liquid level in accumulator n

FM_{sm} - fraction of flow in segment m attributable to subsystem s

fv_n - volume fraction of liquid in accumulator n

FV_{sn} - fraction of flow through accumulator n attributable to subsystem s

fv_v - stem power factor for valve v (area = $(stem)^{fv_v} \cdot A_{max_v}$)

g - gravitational constant

H_p - head for pump p

hf_h - heat transfer fouling coefficient for heat exchanger h

hh_i - overall heat transfer coefficient from hot side to tube wall (w/s side) in node i

$h\ell_i$ - local heat transfer coefficient on hot side, node i

Hr_p - head for pump p at rated frequency and flow rate

hws_i - heat transfer coefficient on water/steam side in node i

i - node number

I_m - inertial term for segment m

j - interface number

k - current time step number

k_i - heat exchanger tube conductivity in node i

K_v - loss coefficient for valve v

ℓ - advanced time step number

M_d - number of segments in network d

Mf_d - first segment number in network d

$M\ell_d$ - last seghment number in network d

n - node number relative to the first node in segment; accumulator number

N_d - number of accumulators in network d

N_m - numbers of nodes in segment m

Nb_d - number of boundary modules in network d

Nbi_d - number of inlet boundary modules in network d

Nbo_d - number of outlet boundary modules in network d

Nf_m - first node in segment m

NH_m - number of heat exchangers in segment m

$N\ell_m$ - last node in segment m

Ns_d - number of subsystems in network d

P_b - pressure at boundary module b

P_{IM} - pressure in module at inlet of segment M

P_m - pressure in segment m

P_{mi} - pressure at inlet of segment m

P_{mo} - pressure at outlet of segment m

P_n - pressure in accumulator n

P_{OM} - pressure in module at outlet of segment M

Pi_b - pressure at inlet boundary module

Po_b - pressure at outlet boundary module

Q_i - heat transfer rate into node i

Q_n - heating rate in accumulator n

QA_h - total heat transfer rate in heat exchanger h

QA_m - total heat transfer rate in segment m

QA_s - total heat transfer rate in subsystem s

QH - energy dumped into the hot network from the rest of the intermediate loop

Qh_i - heat transfer rate from hot side to tube wall, water/steam side

QHWS - energy removed through the heat exchangers to the water/steam side

Qv_s - heating in subsystem s from accumulators

QWS - energy removed through water/steam side boundary modules

Q_{ws_i} - heat transfer rate from tube wall to water/steam side

r_m - pressure change across segment m

S_v - stem position for valve v

Sd_v - demanded stem position for valve v

t - time

Th_i - hot side temperature in node i

Tw_i - tube wall temperature, water/steam side, node i

Tws_i - water/steam side temperature, node i

V_i - volume of node i

V_n - volume of accumulator n

W_b - mass flow rate at boundary module b

W_i - mass flow rate at node i

W_j - mass flow rate at nodal interface j

W_m - segment m average mass flow rate

W_m^{est} - estimated advanced time mass flow rate for segment m

W_{mi} - segment m inlet mass flow rate

W_{mo} - segment m outlet mass flow rate

Wc_m - choked mass flow rate limit for segment m

Wi_b - mass flow rate at inlet boundary module b

Wo_b - mass flow rate at outlet boundary module b

W_p - mass flow rate through pump p

Wr_p - reference flow rate through pump p

W_v - mass flow rate through valve v

Z_{mi} - elevation at inlet of segment m

Z_{mo} - elevation at outlet of segment m

α_i - pressure loss factor for node i

α_m - pressure loss factor for segment m

α_p - coefficient of heat variation for pump p

β_m - pressure loss term for segment m

δ_{ip} - 1 if pump at node i, otherwise, = 0

δ_{iv} - 1 if valve at node i, otherwise, = 0

ΔPa_i - pressure change due to acceleration

ΔPf_i - pressure change due to friction

ΔPg_i - pressure change due to gravity

ΔPk_m - pressure change due to form loss

ΔP_{nm} - presure difference between segment m junction and accumulator n average pressure

ΔP_p - pressure change across pump p

ΔP_v - pressure change across valve v

ΔX_i - length of node i

ΔZ_i - elevation change across node i

ξ - relative convergence criteria

ρ - density

ρ_n - accumulator n average density

ρt_i - tube wall density in node i

Ω_n - interior angle between vertical at a radian to the liquid level in a cylindrical accumulator

τ_i - tube wall temperature time constant in node i

τ_p - pump coastdown time constant to pump p

τ_v - valve time constant for valve v

ω_p - impeller speed in pump p

ωd_p - demanded impeller speed in pump p

ωr_p - reference impeller speed in pump p

χ - fluid quality

3.3.1.1 MODEL FUNDAMENTALS

The calculation of pressures in MINET centers on the accumulators. Here, equations for the conservation of mass and energy are used to advance accumulator pressure and enthalpy

$$V_n \frac{d\rho_n}{dt} = \sum^{\text{Inlets}} W_{mo} - \sum^{\text{Outlets}} W_{mi} \quad , \tag{3.3-1}$$

and

$$V_n \frac{d(\rho_n E_n)}{dt} = \sum^{\text{Inlets}} W_{mo} E_{mo} - \sum^{\text{Outlets}} W_{mi} E_{mi} + Q_n + V_n \frac{dP_n}{dt} \tag{3.3-2}$$

The equation of state is used to express the density time derivative in terms of pressure and enthalpy,

$$\frac{d\rho_n}{dt} = \left(\frac{\partial \rho_n}{\partial P_n}\right) \frac{dP_n}{dt} + \left(\frac{\partial \rho_n}{\partial E_n}\right) \frac{dE_n}{dt} \tag{3.3-3}$$

Note that the mass flow rate and enthalpy exiting the accumulators are those entering the segment, and the same parameters exiting the segment are inlet values for the accumulators.

Segment inlet and outlet pressures are calculated from those in bordering modules. If a boundary module is at the end of a segment, the pressure at that end is equal to the boundary module pressure. For the case of an accumulator at the segment end, the pressure differential between the accumulator port where the segment connects and the position where the accumulator average pressure is defined must be calculated. As accumulators are considered to be stagnant, i.e., zero flow rate, only elevation head needs to be considered:

$$P_{mi} = P_{IM} - \rho g \, (Z_{mi} - Z \, (P_{IM})), \tag{3.3-4}$$

$$P_{mo} = P_{OM} - \rho g \, (Z_{mo} - Z \, (P_{OM})). \tag{3.3-5}$$

When the accumulator contents are taken to be homogeneously distributed, the accumulator average pressure is defined at the center. If the accumulator contents are separated into liquid and vapor regions, the accumulator average pressure is located near the middle of the liquid region. Eqs. (3.3-4) and (3.3-5) still apply, but greater care must be taken because the density differences between the region necessitate evaluating the elevation head in two pieces, above and below the liquid level.

The segment pressure is taken to be the average of the pressures at both ends, i.e.,

$$P_m = (P_{mi} + P_{mo})/2 \tag{3.3-6}$$

It is at this segment average pressure that saturation properties are calculated for the entire segment, a step that results in significant computational savings.

Similarly, a segment average flow rate, W_m can be defined as

$$W_m = \sum_{i=Nf_m}^{N\ell_m} \left(\frac{\Delta X_i}{A_i} W_i \right) / I_m \quad , \tag{3.3-7}$$

where I_m is the segment inertia, defined as

$$I_m = \sum_{i=Nf_m}^{N\ell_m} \frac{\Delta X_i}{A_i} \quad . \tag{3.3-8}$$

This segment average flow rate is advanced using the segment integral momentum equation:

$$I_m \frac{dW_m}{dt} = P_{mi} - P_{mo} + r_m \quad , \tag{3.3-9}$$

where r_m is the total pressure change across the segment:

$$r_m = \sum_{i=Nf_m}^{N\ell_m} (\Delta Pg_i + \Delta Pf_i + \Delta Pa_i + \delta_{iv}\, \Delta P_v + \delta_{ip}\, \Delta P_p + \Delta Pk_m). \tag{3.3-10}$$

The first three terms on the right hand side of Eq. (3.3-10) are pressure changes due to gravity, friction, and acceleration:

$$\Delta Pg_i = -\rho_i g \Delta Z_i, \tag{3.3-11}$$

$$\Delta Pf_i = -f_i |W_i| W_i \, \Delta X_i / 2\rho_i A_i^2 \, D_{eq}, \tag{3.3-12}$$

and

$$\Delta Pa = \left\{ \frac{W_j^2}{\rho_j} - \frac{W_{j+1}^2}{\rho_{j+1}} \right\} / A_i^2. \tag{3.3-13}$$

The fourth and fifth terms are the contributions due to valves and pumps in the segment, and will be discussed in later sections. The sixth term is the form loss pressure change, and is used as a catch-all for losses due to bends, obstructions, etc. In MINET this term is calculated as

$$\Delta Pk_m = -fk_m |W_m| W_m, \tag{3.3-14}$$

when fk_m is a user input segment impedance coefficient. In practice, this coefficient is selected to match pressures and flow rates to steady state operating conditions, and is maintained at the same value for transient calculations.

The enthalpy of flow entering a segment from an accumulator or boundary module is determined by conditions in that bordering module. If the flow is coming from a boundary module or an accumulator with homogeneously distributed contents, the segment inlet enthalpy is set to the enthalpy in the bordering module. If the flow is entering from an accumulator with two separated regions, each at saturation conditions, the segment inlet enthalpy is set to saturated liquid or vapor enthalpy, depending on whether the segment connects below (liquid) or above (vapor) the liquid level.

In-segment distributions of mass flow rate and enthalpy are calculated using nodal mass and energy equations:

$$V_i \frac{d\rho_i}{dt} = W_j - W_{j+1} \quad , \tag{3.3-15}$$

$$V_i \frac{d(\rho_i E_i)}{dt} = W_j E_j - W_{j+1} E_{j+1} + Q_i + V_i \frac{dP_m}{dt} \tag{3.3-16}$$

where, for a segment node:

$$\frac{d\rho_i}{dt} = \left(\frac{\partial \rho_i}{\partial P_m}\right) \frac{dP_m}{dt} + \left(\frac{\partial \rho_i}{\partial E_i}\right) \frac{dE_i}{dt} \tag{3.3-17}$$

At this point, all of the basic equations essential to MINET have been written. While the core group of equations has been completed, some auxiliary equations are needed for the various modules.

3.3.1.2 PIPE MODEL

Pipes are the simplest of the modules. All of the equations needed to represent them were covered in the previous section.

3.3.1.3 PUMP MODEL

The pressure change across a pump is proportional to the pump head,

$$\Delta P_p = \rho_p g H_p \ . \tag{3.3-18}$$

The intricate relationship between the pump head, the relative pump speed, and the relative mass flow rate, is generally available in the form of homologous pump curves. For the simple pump model currently used in MINET, quadratic characteristics are assumed, and the pump head is given by:

$$H_p = Hr_p \left\{ (1 + \alpha_p)\left(\frac{\omega_p}{\omega r_p}\right)^2 - \alpha_p \left(\frac{W_p}{Wr_p}\right)^2 \right\} . \qquad (3.3\text{-}19)$$

3.3.1.4 VALVE MODEL

Representation of valves depends on whether choking conditions exist. If the flow is unchoked, a form loss is calculated for the valve,

$$\Delta P_v = -K_v |W_v| W_v / 2\rho_v A_v^2, \qquad (3.3\text{-}20)$$

where K_v is the loss coefficient. The valve flow area is calculated from the valve stem position, and user input maximum flow area and stem power coefficient:

$$A_v = (S_v)^{fv} \, Amax_v \quad . \qquad (3.3\text{-}21)$$

The user has three options on choke flow calculations, including neglecting the possibility. If the Henry and Fauske [3.3-3] or Moody [3.3-4] models are specified, they are used to calculate the choked mass velocity G_c (=W/A). The valve flow area given by Eq. (3.3-21) is used to multiply this choked mass velocity to get a choked mass flow rate. If the mass flow rate through the valve at a given time is below the choked flow rate, calculations proceed normally.

In the case when the mass flow rate exceeds the choked flow limit, the mass flow rate must be set to the choke flow rate for the next step. Because this contradicts the segment integral momentum equation, care must be taken to isolate any valve where choking is allowed in a segment by itself. Then the segment momentum equation is overwritten with the choke flow limit.

$$W_m = Wc_m. \qquad (3.3\text{-}22)$$

3.3.1.5 ACCUMULATOR

While much of the accumulator behavior is represented by Eqs. (3.3-1) and (3.3-2), additional equations are needed. Because the heating term, Q_n, in Eq. (3.3-2) is a user input and distributed uniformly throughout the accumulator, it is not a problem.

If the user wants the contents of an accumulator separated into saturated liquid and vapor regions, he does so by indicating an initial liquid level between 0.0 and 1.0. For accumulators with uniform cross sectional area (dA/dz = 0.0), e.g., an upright drum, the volume fraction, fv_n, is equal to the level fraction, $f\ell_n$.

The quality, x, can be calculated as

$$x = 1/\left(1 + \frac{\rho_f}{\rho_g}\left(\frac{fv_n}{1 - fv_n}\right)\right) , \qquad (3.3\text{-}23)$$

when ρ_f and ρ_g are saturated liquid and vapor density, respectively.

One of the input options allows the user to specify accumulators as horizontal cylinders. In the case where the contents of a horizontal cylinder are separated into two saturated regions, the relationship between the liquid level and the volume fraction occupied by liquid is not trivial. We define interior angle Ω_n (Figure 3.3-1) as the angle between the vertical and a vector running from the volume center line to the liquid level at the accumulator wall, such that

$$f\ell_n = \frac{1 - \cos \Omega_n}{2} \qquad (3.3\text{-}24)$$

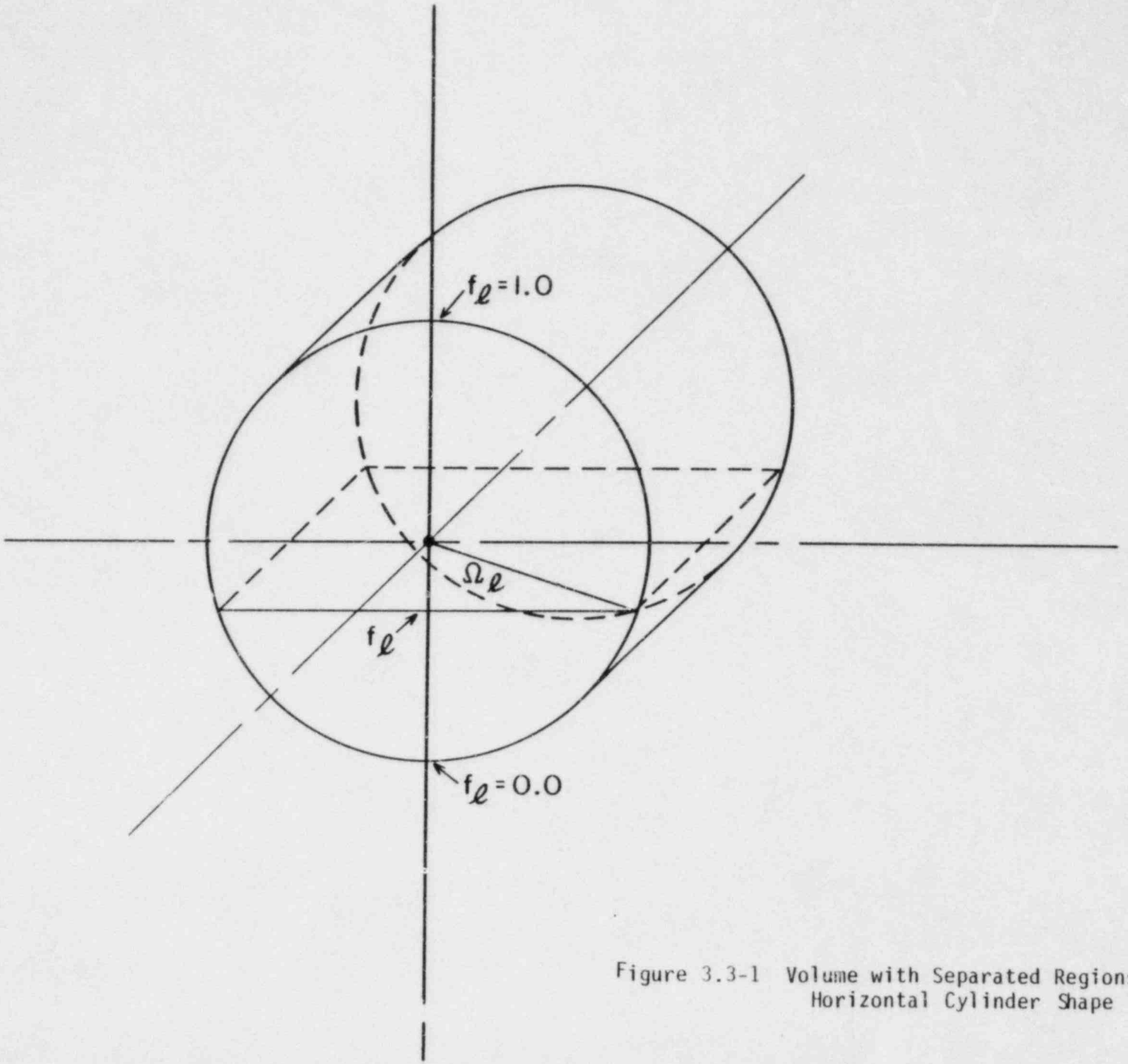

Figure 3.3-1 Volume with Separated Regions and Horizontal Cylinder Shape

It can be shown that the volume fraction occupied by the liquid region is related to interior angle Ω_n by the expression:

$$fv_n = (\Omega_n - \frac{\sin 2\Omega_n}{2})/\pi \qquad (3.3\text{-}25)$$

During steady state calculations, where $f\ell_n$ is user input, Eq. (3.3-24) is solved for Ω_n, Eq. (3.3-25) provides fv_n, and Eq. (3.3-23) gives the quality, which in turn is used to set the volume average enthalpy. In the transient calculations, the enthalpy is advanced directly, and the same three equations are used in the reversed order to obtain the liquid level, $f\ell_n$.

3.3.1.6 HEAT EXCHANGERS

Heat exchangers are among the most difficult plant components to represent, principally because of the complexity of two phase flow and heat transfer phenomena. A secondary complicating factor is the dependence of heat transfer on geometrical considerations, given the variety of heat exchanger designs. In addition to the heat exchangers designed for power plant use, there are several more exotic designs used in experimental systems. Representation of the experimental heat exchangers is desirable because much of the data useful for code verification comes from such units.

3.3.1.6.1 HEAT EXCHANGER MODULE BASICS

It is assumed that a single tube can be used to represent the heat exchanger. The unit cell consists of the fluid inside the tube, the tube wall, and the fluid outside the tube, yet attributable to that tube, as shown in Figure 3.3-2.

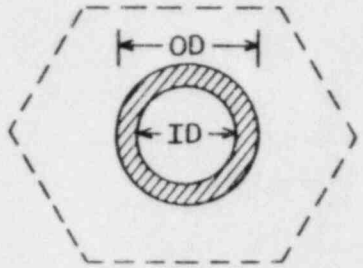

Figure 3.3-2 The Heat Exchanger Unit Cell

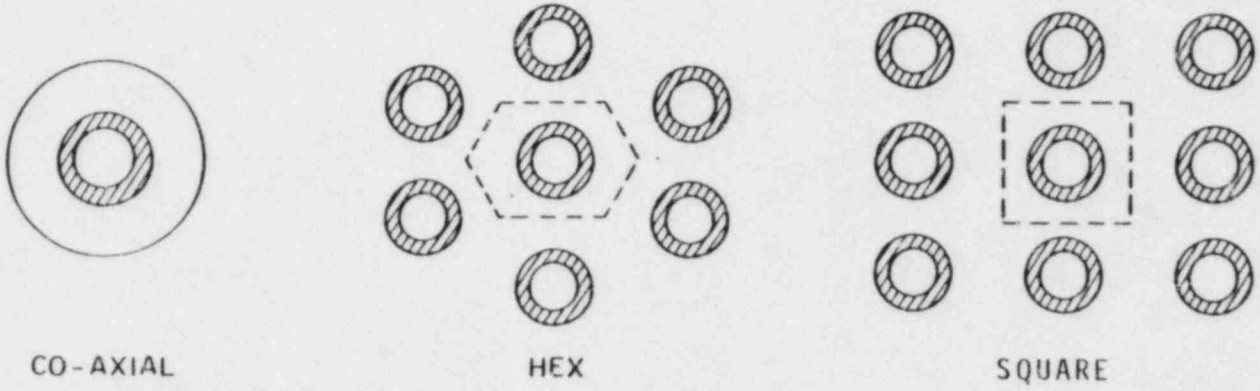

Figure 3.3-3 Heat Exchanger Tube Configuration Options

The tube wall temperature is defined at the water/steam side of the tube, principally because of the sensitivity of the nucleate boiling heat transfer correlation to that temperature rather than the tube centerline temperature. The heat flux from the tube wall to the water/steam side is defined as

$$Qws_i = hws_i \, (Tw_i - Tws_i). \tag{3.3-26}$$

On the hot side, the corresponding expression is

$$Qh_i = hh_i \, (Tw_i - Th_i), \tag{3.3-27}$$

where hh_i is the overall heat transfer coefficient:

$$hh_i = \left(\frac{2k_i}{Dh_h}\right) \ell n \, \frac{Dh_h}{Dws_h} + \frac{1}{h\ell_i} + \frac{1}{hf_h} \tag{3.3-28}$$

In order to represent the various heat transfer phenomena encountered on the water/steam side of the heat exchanger, it is necessary to use several heat transfer correlations, each with a specified range of applicability. At "jump" conditions, the code switches from one correlation to the next, often with a resulting discontinuity in the heat transfer coefficient. The manner in which this entire correlation switching process is integrated in the heat exchanger analysis is of major importance to the stability, accuracy, and reliability of the model.

In the MINET heat exchanger model, the heat transfer correlation selection problem is treated using fixed length nodes. For the special case where two heat transfer regimes may occur in one node, a moving "level" is introduced. For a "level" node, the heat transfer calculations are done separately below and above the jump level, and volume weighted to provide the total node heat transfer rate.

3.3.1.6.2 HOT FLUID TYPE AND LOCATION

The user inputs the hot side fluid type, either sodium or water, and whether it flows inside or outside of the tube. Note that the tube wall temperature is always calculated on the tube side away from the hot fluid.

3.3.1.6.3 TUBE CONFIGURATION

While heat exchanger tubes are usually aligned in a hex arrangement, other configurations are possible, particularly in experimental units. For this reason, the three grid arrangements shown in Figure 3.3-3 are available as user input for each heat exchanger.

The flow area, A_o, for the outside region of the unit cell must be determined from the tube configuration, the tube outer diameter (OD), and the pitch to diameter ratio (POD). Results for the three SSC options are given in Table 3.3-2.

Table 3.3-2. Flow Areas for Heat Exchanger Tube Configurations

Grid Descriptions*	A_o
Co-Axial (1)	$\pi\ OD^2\ (POD^2 - 1)/4$
Square (4)	$OD^2\ (POD^2 - \pi/4)$
Hex (6)	$OD^2\ (2\sqrt{3}\ POD^2 - \pi)/4$

*Note: The number given parenthetically indicates the number of equidistant tubes that are closest to the reference (center) tube (see Fig. 3.3-3). This number is required as input for each heat exchanger.

3.3.1.6.4 CO/COUNTER CURRENT FLOW

While most heat exchangers are counter current flow, there are limited instances where co-current flow exists. Therefore, a co/counter current flow option (multiplier) is available as a user input for each heat exchanger.

3.3.1.6.5 HELICAL COIL OPTION

Two parameters are input for each heat exchanger for the purpose of representing helical coil heat exchangers. The coil diameter is used to modify the friction factor, and is ignored if set to zero (straight tube). The ratio of tube length to heat exchanger length is used to calculate the node length inside the coil, and is useful for coils in a pool. For straight tubes or coaxial helical coils, this factor is set to one, and the heat exchanger length is used to obtain node length inside and outside the tube.

3.3.1.7 PARALLEL FLOW PATHS

There are numerous instances where a number of parallel flow paths are essentially the same, e.g., heat exchanger tubes. As very significant computational advantages can be gained by taking advantage of such parallel paths, MINET was developed accordingly. The user inputs the number of parallel units represented by each module. This parameter is used to determine the fraction of the total flow through a module attributable to a single unit.

3.3.2 MINET STEADY STATE CALCULATIONS

In order to provide maximum flexibility with regard to the type of systems that can be represented using MINET, it was necessary to expand on the

traditional steady state marching schemes. Much of the analysis is now performed at a global level, and the process of marching through the modules has become an intermediate step.

3.3.2.1 BOUNDARY CONDITIONS

Each boundary module has two ports so that it can be doubly connected. The first port connects the module to the end of a network segment. For a boundary module on the hot side, the second port connects to one of the intermediate loops, as indicated through user input. Boundary modules on the water/steam side are "grounded", indicating user-input boundary conditions.

The convention regarding steady state boundary conditions is for enthalpy (or temperature) and mass flow rate to be input for inlet boundary modules, and pressure to be input for outlet boundary modules. On the hot side, intermediate loop mass flow rates, temperatures, and pressures are used similarly for the boundary modules, using the linkage indicated by the two boundary module ports.

3.3.2.2 STEADY STATE GLOBAL CONSIDERATIONS

MINET interfaces with SSC at the intermediate loop, as shown in Figure 3.3-4. A section of the intermediate loop, including all heat exchangers connecting to the steam generating system, and connecting piping, is effectively pulled into the steam generator network. At the completion of steam generator steady state calculations, the pressure change and inertia of that part of the intermediate loop are returned to the intermediate loop calculations for use in its momentum equation.

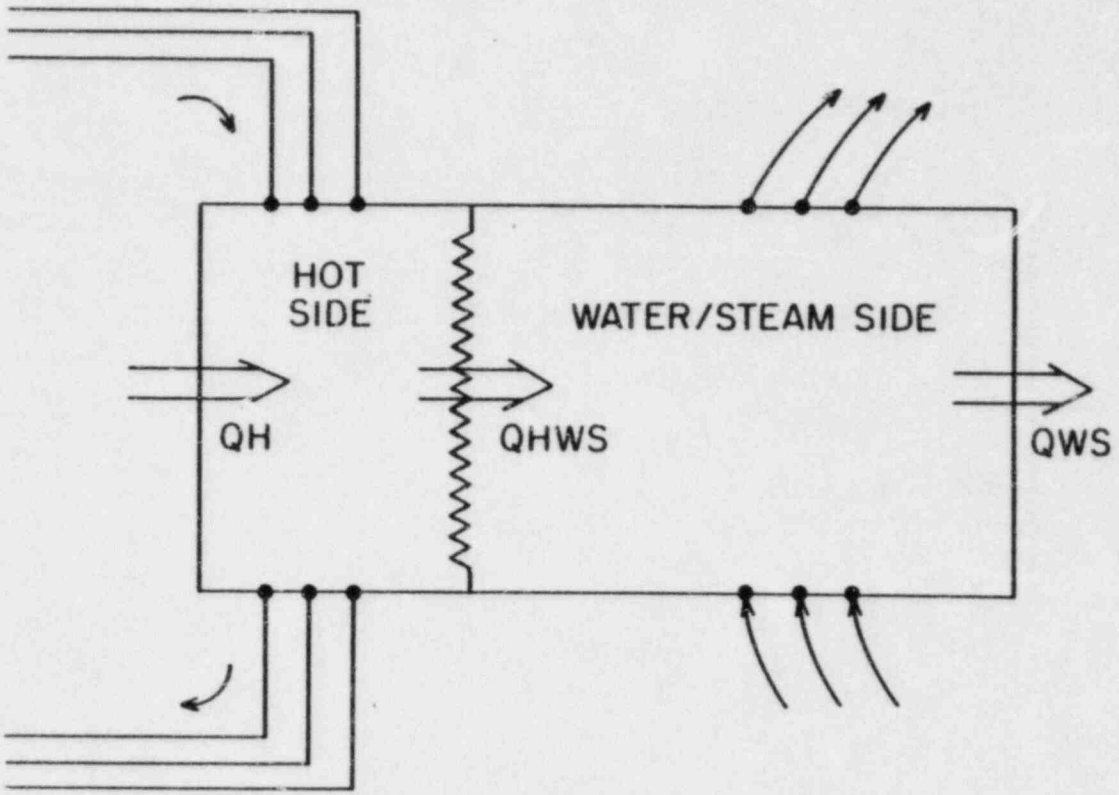

Figure 3.3-4 The MINET Steam Generator Network for SSC

Under steady state conditions, the entire network, as well as the hot and water/steam sides, must obey conservation of mass and energy. The amount of energy dumped into the hot side of the network, QH, is given by:

$$QH = W(E(T_{in}) - E(T_{out})).$$

This energy, plus any added by heating in the accumulators, is the amount to be removed through the heat exchangers to the water/steam side, QHWS. Any additional heat generated in accumulators on the water/steam side is added to QHWS to get the total energy removed through the water/steam side boundary modules, QWS.

3.3.2.3 STEADY STATE ITERATIVE PROCESS

Global calculations need to be performed only once in the steady state process. However, much of the steady state calculational process is iterative. The strategy employed is outlined in Figure 3.3-5.

Sub-system analysis constrains the amount of heat that must be transferred to a specific section of the network. It is performed for a given distribution of pressure and mass flow rate.

Enthalpies and energy transfer in the network segments and accumulators are calculated for the same mass flow rate and pressure distribution. A convergence flag is set to "true" if the results of this calculation are sufficiently close to previous values.

Segment modules are then analyzed in the order they appear within segments. The main purpose of this step is to evaluate segment pressure drops.

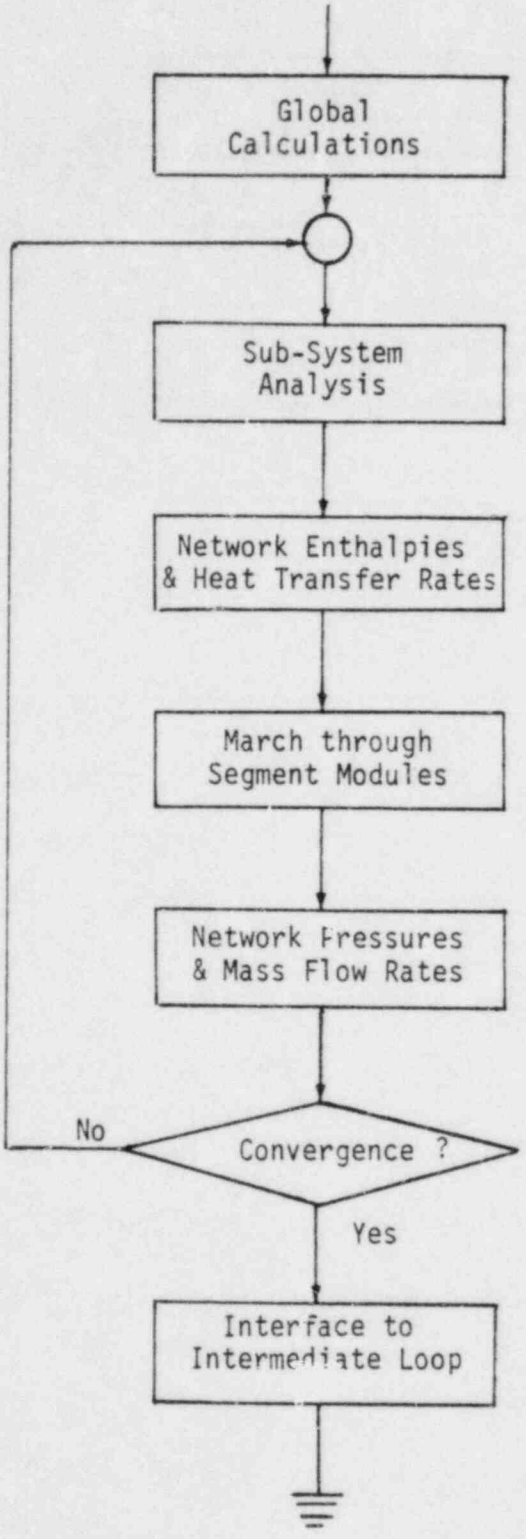

Figure 3.3-5 Steady State Solution Strategy

The pressure drops at current pressures, mass flow rates, and enthalpies are then used to determine new system pressures and mass flow rates. An internal iteration is used in this process.

If the convergence flag was not set to "true" in the enthalpy and energy transfer calculation, the new mass flow rate and pressure distribution are returned for sub-system analysis, etc. If the convergence flag was set "true", steady state calculations are completed, and the results are interfaced back to the intermediate loop.

3.3.2.3.1 SUB-SYSTEM ANALYSIS

A sub-system may be defined as a part of the system that, for given pressures and mass flow rates, requires a fixed heat input for system equilibrium to be maintained. In its simplest form, the system shown in Figure 3.3-4 has two subsystems, the hot and water/steam networks.

For each accumulator with separated regions within a network, one additional sub-system is introduced. This is because the flows exiting a separated region accumulator do so at saturation enthalpies. Thus, for such an accumulator to maintain an equilibrium, the fluid energy entering must compensate for the saturated flow exiting.

Examples of such sub-systems include the steam drum and recirculation loop in CRBRP and the aspirator and downcomer in the Three Mile Island once-through steam generators. In operating plants, conditions must be tuned until such sub-systems are in equilibrium. In MINET steady-state calculations, it is assumed that such tuning has been performed by the plant control system, the plant operator, or at least on paper by the plant designer. Thus, it is inferred that for the system to be operating as the user indicates, the heat

input to any sub-system must satisfy the sub-system energy balance or the plant would not be at steady-state.

Accumulators with separated regions are not allowed on the hot side of the network. This is because (1) the hot side of the network should be sub-cooled under steady-state conditions, (2) the part of the intermediate loop within the network is borrowed, more or less, and to include such a key component in the network would handicap intermediate loop calculations, and (3) to allow for such a remote possibility would greatly complicate the network calculations.*

Knowledge of the heat input required by each subsystem is an important step in determining the steady state conditions. However, for some of the more intricate systems, the fraction of flow from each accumulator, FV_{sn}, and segment, FM_{sm}, contributing to each sub-system must also be determined. For sub-systems terminating at separated region accumulators, these fractions are determined simply by back-tracking upstream from the accumulator inlet ports, noting where the flow came from. The remaining network side subsystem is credited with the remainder of the flow fractions. These fractions indicate how much of the heat received by each segment or accumulator counts toward fulfilling the subsystem heating requirements.

While subsystem heating requirements and flow fractions do much to constrain heat transfer rates, ambiguous situations can still arise, particularly in representing parallel heat exchangers. In this case two or more units could transfer varying amounts of heat so long as together they transfer the necessary amount. The technique used in the SSC/MINET steam generator network to resolve these ambiguities is based on the available heat transfer area.

*This limitation is eliminated in a version under development.

Thus, if two heat exchangers of equal size must make up the heat requirement for a subsystem, each is assumed to provide half of the heat.

The total sub-system heat transfer area and accumulator heating must be determined, to be used in the network enthalpy and heat transfer rate calculations to follow. Given that we know the total heat transfer area of each segment as the sum of the heat transfer area of each heat exchanger in the segment, we can write the subsystem heat transfer area as

$$A_s = \sum_{m=1}^{M} FM_{sm} A_m \ . \qquad (3.3\text{-}30)$$

The total heat received by each sub-system as a result of heating in the accumulators is

$$Qv_s = \sum_{n=1}^{N_d} FV_{sn} Q_n \ . \qquad (3.3\text{-}31)$$

3.3.2.3.2 SYSTEM ENTHALPY AND ENERGY TRANSFER (ENET)

In the ENET section, the accumulator enthalpies, segment inlet and outlet enthalpies, segment energy transfer, and sub-system energy transfer are calculated. This is done first for the water/steam network, then for the hot network. A single matrix equation is used to simultaneously solve for all variables on one side on the network. For a network consisting of M_d segments, N_d volumes, and Ns_d sub-systems, there are $3M_d + N_d + Ns_d$ equations and unknowns, as shown in Tables 3.3-3 and 3.3-4.

The equations conserving energy in the segments and accumulators are straight-forward. In the segment inlet enthalpy equation, the enthalpy of the flow entering the segment is set to the module enthalpy of bordering boundary modules or homogeneous accumulators. When the flow is entering a segment from a separated region accumulator, the segment inlet enthalpy is set to the satu-

Table 3.3-3

Equations Used in ENET Matrices

Equation Type	Number Used	Equation
Segment Energy	M_d	$W_m(E_{mo} - E_{mi}) = QA_m$
Segment Inlet Enthalpy	M_d	$E_{mi} = E_{IM}$
Volume Energy	N_d	$\sum_{\text{Inlets}} W_{mo}E_{mo} - \sum_{\text{Outlets}} W_{mi}E_{mi} = Q_n$
Total Heat Removal	1	$\sum_{}^{Ns_d} QA_s = \begin{cases} QWS & ; \text{ w/s side} \\ QHWS & ; \text{ hot side} \end{cases}$
Separated Region Accumulator	Ns_d-1	$E_n = E(P_n, F\ell_n)$
Segment Heat Transfer Rate		$QA_m = \begin{cases} \sum_{s=1}^{Ns_d} \frac{FM_{sm}A_m}{A_s}(QA_s - QV_s) & ; \text{ w/s side} \\ \sum_{h=1}^{NH_m} QA_h & ; \text{ hot side} \end{cases}$

Table 3.3-4

Variables Used In ENET Matrix Equation

Variable	Variable Name	Number Defined
E_{mi}	Segment Inlet Enthalpy	M_d
E_{mo}	Segment Outlet Enthalpy	M_d
E_n	Accumulator Enthalpy	N_d
QA_m	Segment Heat Transfer Rate	M_d
QA_s	Sub-System Heating Required	Ns_d

rated liquid or vapor enthalpy, depending on whether the connecting port is below or above the liquid level in the accumulator. In the total heat removal equation, the total heat input to all of the subsystems on the side is set equal to the total heat to be removed from that side. The separated region accumulator equation uses the user-input liquid level to calculate the accumulator average enthalpy.

Of the six ENET equation types, only the segment heat transfer rate equations differ significantly between the two networks. For the water/steam network, the segment heat transfer rate is set equal to the sum of the heating contributions made to each subsystem. The contribution is calculated as the total heat required from segments in the subsystem, QA_S-Qv_S, multiplied by the ratio of the segment heat transfer area contributing to that subsystem, $FM_{sm} \cdot A_m$, to the total heat transfer area in the subsystem, A_S. On the hot side, results from the water/steam network calculations imply the heat transfer rate per heat exchanger, which can be used to calculate hot side segment heat transfer rates.

Once the new segment enthalpies and heat transfer rates have been calculated, hot side segment enthalpies, heat transfer rates, and mass flow rates are used to calculate hot network inlet and outlet enthalpies for each heat exchanger. Because the process of marching through the segment modules is executed first for the water/steam network, these hot network enthalpies are needed before they would normally be calculated.

3.3.2.3.3 MODULE MARCH

The step of marching through all of the modules in each segment is necessary for the correct calculation of the segment pressure loss, r_m. Because the pressure loss terms are sometimes dependent on the square of the mass flow

rate, two segment loss parameters, α_m and β_m are calculated such that

$$r_m = \beta_m - (\alpha_m + fk_m)|W_m|W_m. \tag{3.3-32}$$

Five of the six terms of Eq. (3.3-10) are represented by α_m and β_m, the other being the segment form loss, $fk_m|W_m|W_m$. Gravitational losses, which are independent of flow rate, accelerative losses, which are small, and the pump contribution at reference speed and zero flow rate are included in the β_m term.

$$\beta_m = \sum_{i=Nf_m}^{N\ell_m} \Delta Pg_i + \Delta Pa_i + \delta_{ip}\,\rho_i g\,Hr\,(1 + \alpha_p) \tag{3.3-33}$$

Frictional losses, valve form losses, and the pump contribution proportional to the normalized flow rate, are included in α_m:

$$\alpha_m = \sum_{i=Nf_m}^{N\ell_m} f_i/2\rho_i A_i D_i + \delta_{ip}\rho_i g\,Hr\,\alpha_p/Wr_p{}^2 + \delta_{iv}\,K_v/2\rho_i A_v{}^2 \tag{3.3-34}$$

Several of the pressure changes are dependent on local density, which is a function of segment pressure and local enthalpy. In MINET it is currently assumed that, during the steady state, enthalpy is constant across pipes, pumps, and valves. Only in the heat exchangers does the enthalpy vary with position.

As the water/steam network segments are analyzed first, it is at that time the enthalpy distribution is determined for both sides of the heat exchanger. Later, when the hot network segments are analyzed, the heat exchanger enthalpy distribution is already known, and only the evaluation of pressure losses is necessary.

At the onset of calculations for a given heat exchanger, flow rates, pressures, inlet and outlet enthalpies, and total heat transfer rate are already known. To force the heat transfer rate, as indicated by correlations,

tube conductivities, and heat transfer areas, to provide the required total heat transfer rate, an area correction factor, Fa_h, is used. Fa_h is used to factor the total heat transfer area up or down, as needed.

The steady state iterative process for heat exchangers is shown in Figure 3.3-6. Three levels of iteration are included in the figure, the outermost being on the heat exchanger area correction factor, Fa_h. The nodal iteration is performed to obtain a combination of nodal heat flux and node average properties that are consistent. The inner level of iteration is for the tube wall temperature that produces heat transfer from the tube wall to the water/steam side equal to the heat transfer from the hot side to the tube wall. In the case of a "level" node, there is yet another iterative process for the fraction of the node at which the level enthalpy is reached.

3.3.2.3.4 SYSTEM PRESSURES AND FLOW RATES (PRFLOW)

The system pressure and flow rate calculation is the last major step of the steady state calculations. Using current pressure losses, which are dependent on current enthalpies, pressures, and mass flow rates, the system pressures and mass flow rates are adjusted, first for the water/steam side network, then for the hot network. The equations and variables used in the PRFLOW matrix equation are shown in Tables 3.3-5 and 3.3-6, respectively. Because the segment momentum equation contains a nonlinear term ($|W_m|W_m$), the solution is iterative.

For a network with M_d segments, N_d accumulators, and Nb_d boundary modules, there are $3M_d + N_d + Nb_d$ equations and unknowns. Segment flow rate, inlet and outlet pressure, accumulator pressure, flow rate at Nbo_d outlet boundary modules, and pressure at Nbi_d inlet boundary modules are calculated.

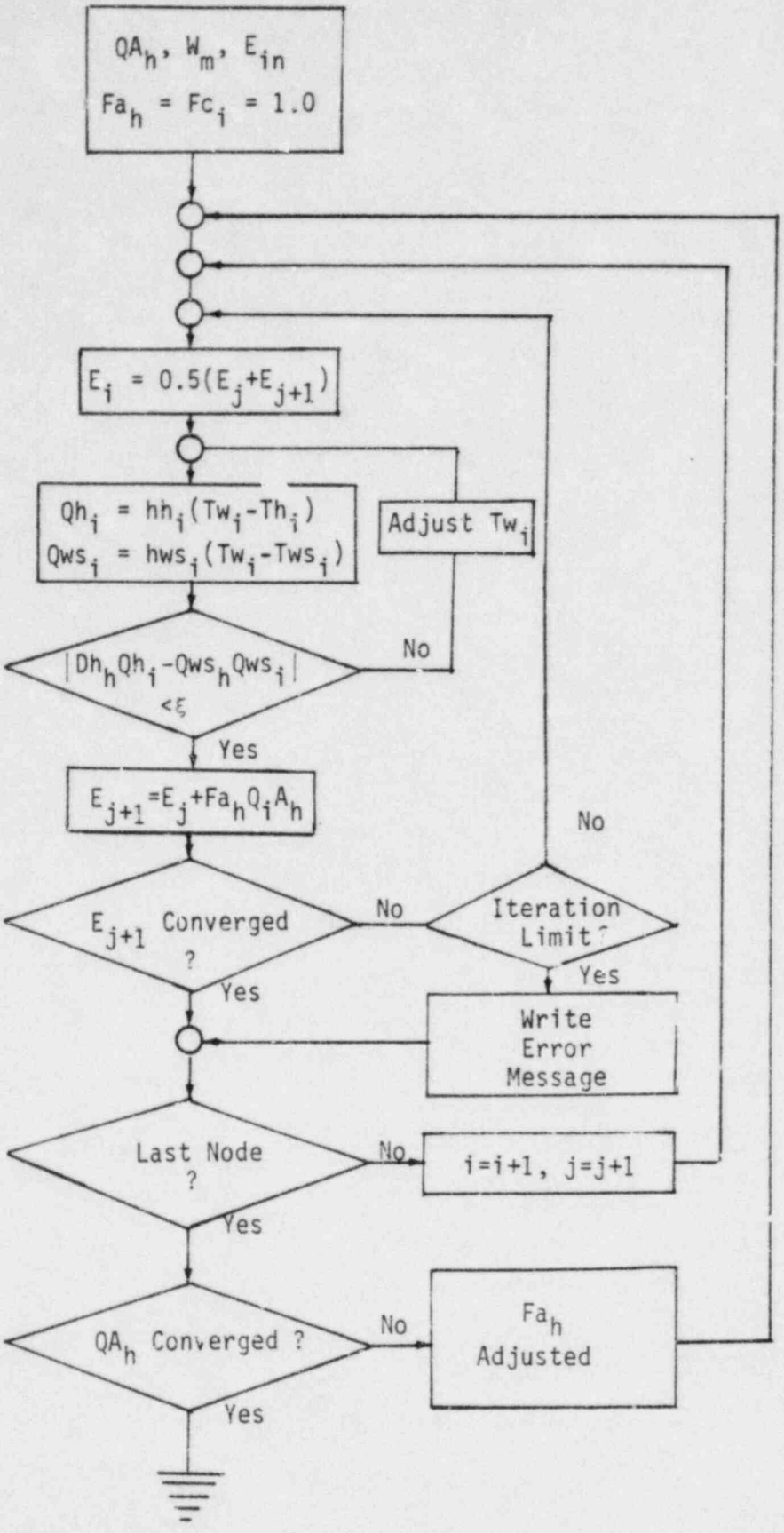

Figure 3.3-6 Heat Exchanger Iterative Process

Table 3.3-5

Equations Used in PRFLOW Matrices

Equation Type	Number Used	Equation
Accumulator Mass Balance	N_d	$\sum_{\text{Inlets}} W_m - \sum_{\text{Outlets}} W_m = 0$
Segment Momentum Balance	M_d	$P_{mo} - P_{mi} + (\alpha_m + Fk_m)\lvert W_m \rvert W_m = \beta_m$
Segment Inlet Pressure	M_d	$P_{mi} = \begin{cases} P_n + \Delta P_{nm}, & \text{if Accumulator} \\ P_b, & \text{if Boundary Module} \end{cases}$
Segment Outlet Pressure	M_d	$P_{mo} = \begin{cases} P_n + \Delta P_{nm}, & \text{if Accumulator} \\ P_b, & \text{if Boundary Module} \end{cases}$
Boundary Module Flow	Nb_d	$W_b = W_m$

Table 3.3-6

Variables Used in PRFLOW Matrix Equation

Variable	Variable Name	Number Solved For
W_m	Segment Flow Rate	M_d
P_n	Accumulator Pressure	N_d
P_{mi}	Segment Inlet Pressure	M_d
P_{mo}	Segment Outlet Pressure	M_d
Pi_b	Inlet Boundary Module Pressure	Nbi_d
Wo_b	Outlet Boundary Module Flow Rate	Nbo_d

Conservation of mass requires the net flow into any accumulator be zero under steady state conditions. The segment integral momentum equation is written using α_m and β_m, as defined in Eqs. (3.3-33) and (3.3-34). Pressure at the segment inlets and outlets are defined by the bounding pressures, either from an accumulator or boundary module, and any gravitational pressure differences resulting from elevation differential. Finally, the mass flow rate through a boundary module is constrained to the mass flow rate in the connecting segment.

3.3.3 MINET TRANSIENT ANALYSIS

MINET transient analysis is performed at two levels, the segment level and the network (accumulator) level. First, the response of the segments to changes in the bordering modules is determined, and stored in the segment response matrices. These matrices are used in conjunction with changes in boundary conditions, and current accumulator conditions, to advance accumulator pressures and enthalpies. Segment parameters are then advanced. This process is done twice per step, once for the water/steam network, then again for the hot network.

The calculational process used in the MINET transient analysis is shown schematically in Figure 3.3-7. Steps in this process will be discussed in the sections that follow.

3.3.3.1 INTERMEDIATE LOOP TO NETWORK INTERFACE

As discussed previously, MINET interfaces with the intermediate loop of the SSC LMFBR representation, replacing a section of that loop in the calculational process (see Figure 3.3-4). Temperatures, pressures, and mass flow

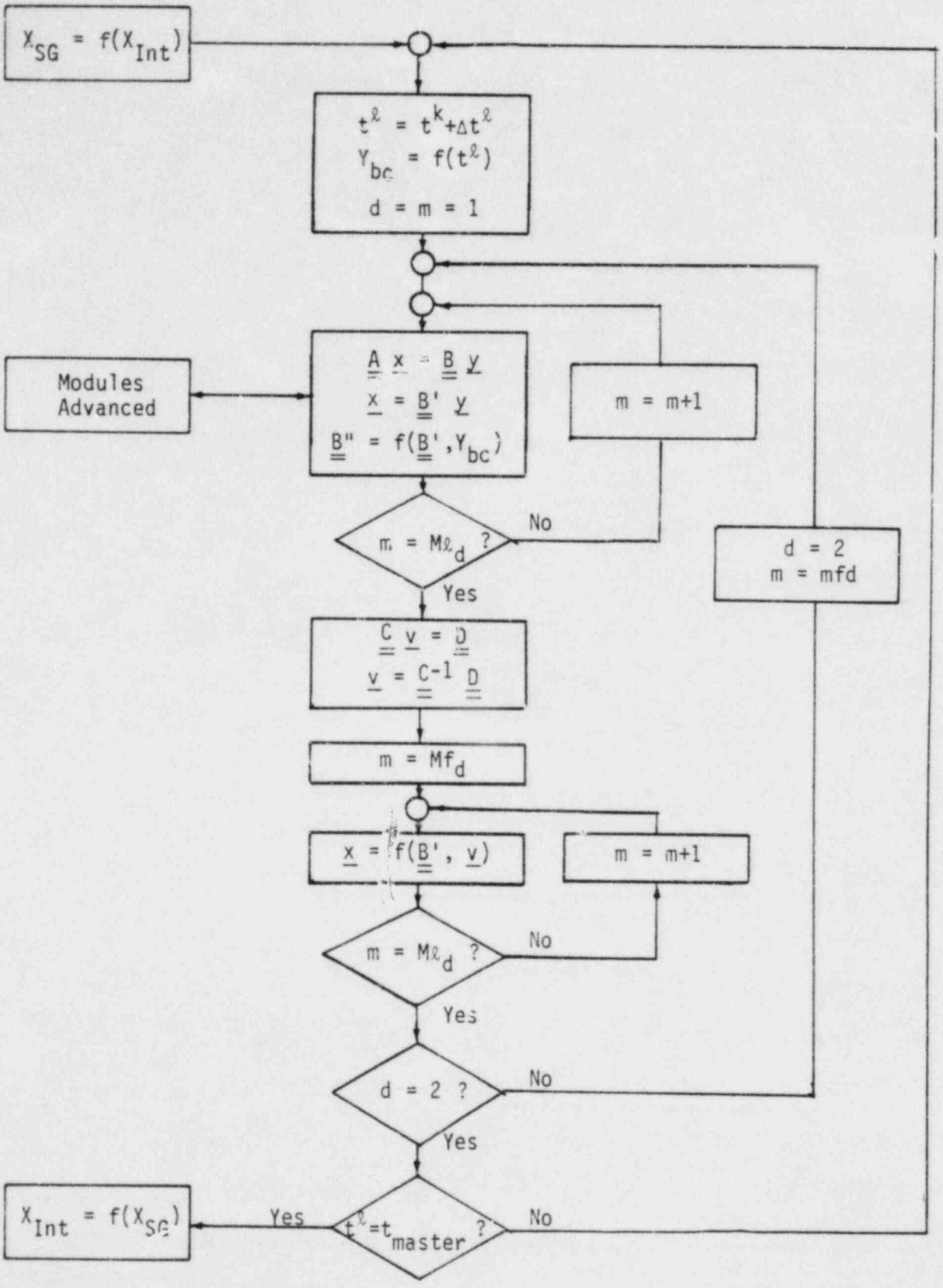

Figure 3.3-7 MINET Transient Calculational Process

rates at connecting points are used to define current values for the steam generator hot side boundary modules. Mass flow rates are used for inlet and pressures for outlet boundary modules. Intermediate loop temperatures provide steam generator enthalpies for both inlet and outlet hot side boundary modules. Only if flow is entering the network will a given enthalpy actually be used. Further, if flow is exiting the network, the enthalpy for that boundary module will be updated.

3.3.3.2 TIME STEP PREPARATION

At the beginning of a time step, several parameters including the time step size, must be set. The time step to be taken, Δt^{ℓ}, advances the steam generator variables from current (t^{k}) values to advanced time values (t^{ℓ}).

Most of the equations are integrated implicitly in time, which allows time steps larger than the equation time constants to be used without introducing instabilities. However, the heat exchanger tube wall temperature is treated explicitly in the wall heat conduction equation, and thus, that equation has a limiting time constant τ_i:

$$\tau_i = \rho t_i \, Cpt_i At_h / fa_h \, (Dh_h \, hh_i + Dws_h \, hws_i) \qquad (3.3\text{-}35)$$

The second significant task in preparing for a time step is the updating of boundary modules and accumulator heating. The only means of updating these required parameters at present is via user input (value vs. time tables), which are interpolated to get current values. If the user has chosen to control any pumps or valves in similar fashion, the appropriate tables are used at this time to update the corresponding pump speeds or valve positions.

There are two alternate means of controlling pump speeds and valve positions. A limited control option is available in the steam generator, which

manually trips and coasts down pumps or releases and resets safety valves on pressure settings. These limited control options are used to update pump speeds or valve positions when that module is updated. A more sophisticated control is available via the PPS/PCS system. However, PPS/PCS information is available only at the master clock time step, and the interfacing is done upon entry into and exit out of the steam generator.

3.3.3.3 SEGMENT CALCULATIONS

In this part of the transient calculations, the segment response matrix must be determined for the current segment pressures, local enthalpies, mass flow rates, heat fluxes, as well as pump speeds and valve positions. The segment response matrix indicates the response of local enthalpies and mass flow rates to current conditions and changes in pressure and enthalpy in bordering modules.

3.3.3.3.1 LOADING THE SEGMENT EQUATIONS

At this point in the calculations, values are known, for most variables, at the k step. Time, boundary module parameters, accumulator heating, and, depending on the control option specified, pump speeds and valve positions, are known for the ℓ step. The segment matrix equation is to be used, in conjunction with the global solution, to advance local enthalpies and mass flow rates to the advanced time step, ℓ. The equation is of the form

$$\underline{\underline{A}}\ \underline{x} = \underline{\underline{B}}\ \underline{y}, \qquad (3.3\text{-}36)$$

where, for a segment with N_m nodes, $\underline{\underline{A}}$ is a $2N_m + 2$ square matrix, $\underline{\underline{B}}$ is a $(2N_m + 2) \times 5$ matrix, $\underline{x}$ is a $2N_m + 2$ vector, and $\underline{y}$ is a 5 vector. The $\underline{x}$ vector is composed of nodal interface values:

$$\underline{x} = \text{col}\ \{\Delta E_{mi}, W_{mi}, \ldots, \Delta E_j, W_j, \ldots, \Delta E_{mo}, W_{mo}\}\ . \tag{3.3-37}$$

Vector $\underline{y}$ is made up of changes in the enthalpy and pressure in the modules connecting to the inlet and outlet of the segment, and unity:

$$\underline{y} = \text{col}\ \{\Delta E_{IM}, \Delta P_{IM}, \Delta E_{OM}, \Delta P_{OM}, 1\} \tag{3.3-38}$$

The $2N_m + 2$ equations loaded into matrices $\underline{\underline{A}}$ and $\underline{\underline{B}}$ depend on the conditions within the segment at step k. One momentum equation or choke flow constraint must be used for each segment,

$$I_m \frac{dW_m}{dt} = P_{mi} - P_{mo} + \beta_m - fk_m|W_m|W_m - \sum_{i=Nf_m}^{N\ell_m} \alpha_i |W_i| W_i , \tag{3.3-39}$$

$$\text{if } W_m^{est} < Wc_m ,$$

or

$$W_m = Wc_m , \qquad \text{if} \qquad W_m^{est} \geq Wc_m , \tag{3.3-40}$$

where W_m^{est} is the segment flow rate estimated with P_{mi} and P_{mo} remaining constant. Zero, one, or two equations must be written to constrain the segment end enthalpy when flow is entering the segment:

$$E_{mi} = E_{IM}, \quad \text{if} \quad W_{mi} \geq 0, \tag{3.3-41}$$

and

$$E_{mi} = E_{OM}, \quad \text{if} \quad W_{mo} \leq 0. \tag{3.3-42}$$

Mass must be conserved in each of the nodes

$$V_i \left(\frac{\partial \rho_i}{\partial E_i}\right) \frac{dE_i}{dt} = W_j - W_{j+1} - V_i \left(\frac{\partial \rho_i}{\partial P_m}\right) \frac{dP_m}{dt} \tag{3.3-43}$$

This accounts for N_m mass equations, giving $N_m + 1$, $N_m + 2$, or $N_m + 3$ equations, depending on the direction of flow at the segment end. The remaining $N_m + 1$, N_m, or $N_m - 1$ remaining equations come from the nodal energy equations.

That $N_m + 1$, N_m, or $N_m - 1$ equations are needed is seemingly in conflict with the ready availability of energy equations for the N_m nodes. At this pont it is enthalpies at the nodal interfaces that are required, and the relationship between the constraint of these enthalpies and the nodal energy equations is not trivial.

The nodal energy equation can be written as:

$$V_i \left\{ \rho_i + E_i \left(\frac{\partial \rho_i}{\partial E_i} \right) \right\} \frac{dE_i}{dt} = W_j E_j - W_{j+1} E_{j+1} + Q_i + V_i \left\{ 1 - E_i \left(\frac{\partial \rho_i}{\partial P_m} \right) \right\} \frac{dP_m}{dt} \quad (3.3\text{-}44)$$

Before loading a conservation of mass equation, Eq. (3.3-43), into the matrix equation, the node average enthalpy time derivative term must first be eliminated. The nodal energy equation, Eq. (3.3-44) can be used to isolate the node average enthalpy time derivative:

$$\frac{dE_i}{dt} = \frac{\left\{ W_j E_j - W_{j+1} E_{j+1} + Q_i + V_i \left[1 - E_i \left(\frac{\partial \rho_i}{\partial P_m} \right) \right] \frac{dP_m}{dt} \right\}}{V_i \left\{ \rho_i + E_i \left(\frac{\partial \rho_i}{\partial E_i} \right) \right\}} \quad (3.3\text{-}45)$$

This expression is substituted into eq. (3.3-43) to obtain a conservation of mass equation used for all nodes. Equation (3.3-45) is eventually used to advance all of the node average enthalpies.

In order to use Eq. (3.3-44) to advance the nodal interface enthalpy, the derivative of node average enthalpy with respect to time has to be expressed in terms of the interface enthalpies. If the obvious replacement is made, i.e.,

$$\frac{dE_i}{dt} = 0.5 \left(\frac{dE_j}{dt} + \frac{dE_{j+1}}{dt} \right) \quad (3.3\text{-}46)$$

a not so obvious result occurs. Because the time constant for enthalpy transport is relatively long, a non-physical numerical "rocking" occurs, in which

outlet enthalpies swing rapidly in response to changes in inlet enthalpy.

The donor-cell differencing scheme is used in lieu of the averaging indicated by Eq. (3.3-46). The assumption is that the rate of change in enthalpy throughout the node (except the inlet section) is uniform in response to changes in inlet enthalpy, and thus,

$$\frac{dE_{j+1}}{dt} = \frac{dE_i}{dt} \tag{3.3-47}$$

The donor cell differenced form of the conservation of energy is written:

$$V_i\left\{\rho_i + E_i\left(\frac{\partial\rho_i}{\partial E_i}\right)\right\}\frac{dE_{j+1}}{dt} = W_jE_j - W_{j+1}E_{j+1} + Q_i + V_i\left[1 - E_i\left(\frac{\partial\rho_i}{\partial P_m}\right)\right]\frac{dP_m}{dt} \tag{3.3-48}$$

Thus, for a node with flow entering one end and exiting the other, Eq. (3.3-48) effectively projects changes in outlet enthalpy in response to changes in the inlet enthalpy, for current nodal conditions. This is true regardless of whether the flow direction is the same as steady state (forward flow), or the opposite (reversed flow). Of course, when the flow is reversed, the j-th interface is the node outlet, and Eq. (3.3-48) is written for dE_j/dt:

$$V_i\left\{\rho_i + E_i\left(\frac{\partial\rho_i}{\partial E_i}\right)\right\}\frac{dE_j}{dt} = W_jE_j - W_{j+1}E_{j+1} + Q_i + V_i\left[1 - E_i\left(\frac{\partial\rho_i}{\partial P_m}\right)\right]\frac{dP_m}{dt} \tag{3.3-49}$$

When flow is not passing through a node, it is either entering (converging) or exiting (diverging) both ends. Neither condition is stable, i.e., likely to continue through the time step. For a diverging flow node, we assume the rate of change in enthalpy is uniform throughout the node, and therefore load both Eq. (3.3-48) and Eq. (3.3-49) into the matrix equation.

For a converging flow node, the enthalpy at both interfaces is determined from outside the node. Thus it is unnecessary to use the nodal energy equation to constrain interface enthalpy.

Thus, a node contributes zero, one, or two constraints on interface enthalpy, depending on whether the flow is converging, through, or diverging, respectively. For a converging flow segment, there must be one more converging node than diverging node. Similarly, a diverging flow segment must contain one more diverging flow node than converging node. A flow-through segment has an equal number of converging and diverging nodes. Therefore, the nodal energy equations account for $N_m - 1$, N_m, or $N_m + 1$ constraints, as are required.

The nodal equations are thus loaded into the matrices of Eq. (3.3-36) in implicit form, i.e.,

$$y^{\ell} = f(x^{\ell}). \tag{3.3-50}$$

The loading logic is summarized in Table (3.3-7).

With the complexity involved in choosing the equation to be used in loading the segment matrix equation, care must be taken that mass and energy are conserved for each node. Because the nodal mass conservation equations are, in fact, responding to changes in node average enthalpy and segment pressure, and adjusting mass flow rates accordingly, mass is indeed being conserved. Energy is also being conserved, since Eq. (3.3-45) is subsequently used (see Section 3.3.3.6) to advance the node average enthalpy.

3.3.3.3.2 SOLVING FOR THE SEGMENT RESPONSE MATRIX

Once the matrices of Eq. (3.3-36) have been loaded, the segment response matrix is available as:

$$\underline{\underline{B}}' = \underline{\underline{A}}^{-1} \underline{\underline{B}}.$$

Table 3.3-7 Logic Used in Loading Segment Matrix Equation

Row	I	Load
1	$W_{mi}^{k}>0$	$\Delta E_{mi}^{\ell} = E_{IM}^{\ell} - E_{mi}^{k} + \Delta E_{IM}^{\ell}$
.	.	.
.	.	.
.	.	.
.	.	.
2n-1	$W_{j}^{k}<0$	$(C_3-W_j^k)\Delta E_j^{\ell} - C_7 W_j^{\ell} + W_{j+1}^{k}\Delta E_{j+1}^{\ell} + C_8 W_{j+1}^{\ell} = -C_4\Delta P_m^{\ell} + Q_i^k - \left(\frac{\delta Q_i}{\delta W_i}\right) W_i^k$
2n	Any	$-C_5 W_j^k \Delta E_j^{\ell} + \left\{1-C_5 E_j^k - C_6\right\} W_j^{\ell} + C_5 W_{j+1}^k \Delta E_{j+1}^{\ell} + \left\{C_5 E_{j+1}^k - C_6 - 1\right\} W_{j+1}^{\ell} = (C_2 - C_4 C_5)\Delta P_m^{\ell} + C_5 Q_i^k - 2C_6 W_i^k$
2n+1	$W_{j+1}^{k}>0$	$-W_j^k \Delta E_j^{\ell} - C_7 W_j^{\ell} + (W_{j+1}^k + C_3)\Delta E_{j+1}^{\ell} + C_8 W_{j+1}^{\ell} = -C_4\Delta P_m^{\ell} + Q_i^k - \left(\frac{\delta Q_i}{\delta W_i}\right) W_i^k$
.	.	.
.	.	.
.	.	.
.	.	.
$2N_m+1$	$W_{mo}^{k}<0$	$\Delta E_{mo}^{\ell} = E_{OM}^{k} - E_{mo}^{k} + \Delta E_{OM}^{\ell}$
$2N_m+2$	$W_m^{est} \geq Wc_m^k$	$\sum_{i=Nf_m}^{N\ell_m} \left\{\left[\frac{\Delta X_i}{A_i \Delta t^{\ell}} + \left(\alpha_i^k + Fk_m \frac{\Delta X_i / A_i}{I_m}\right)\lvert W_i^k\rvert\right]\frac{(W_j^{\ell} + W_{j+i}^{\ell})}{2}\right\} = \frac{I_m W_m^k}{\Delta t^{\ell}} + P_{IM}^{\ell} - P_{OM}^{\ell} + \beta_m^k$
	$W_m^{est} > Wc_m^k$	$\sum_{i=Nf_m}^{N\ell_m} \left\{\frac{\Delta X_i}{2A_i}(W_j^{\ell} + W_{j+1}^{\ell})\right\} = I_m Wc_m^k$

Table 3.3-7 (Continued)

where

$$C_1 = \frac{V_i}{\Delta t}\left(\frac{\partial \rho_i}{\partial E_i}\right)^k, \quad C_2 = \frac{V_i}{\Delta t}\left(\frac{\partial \rho_i}{\partial P_m}\right)^k, \quad C_3 = \frac{V_i}{\Delta t}\left[\rho_i + E_i\left(\frac{\partial \rho_i}{\partial E_i}\right)\right] - \frac{\partial Q_i}{\partial E_i}, \quad C_4 = \frac{V_i}{\Delta t}\left[E_i\left(\frac{\partial \rho_i}{\partial P_m}\right) - 1\right],$$

$$C_5 = C_1/C_3, \quad C_6 = C_5\left(\frac{\partial Q_i}{\partial W_i}\right)/2, \quad C_7 = E_j^k + \left(\frac{\partial Q_i}{\partial W_i}\right)/2, \quad C_8 = E_{j+1}^k - \left(\frac{\partial Q_i}{\partial W_i}\right)/2$$

While the expression of the segment response matrix as the inverse of matrix $\underline{\underline{A}}$ times matrix $\underline{\underline{B}}$ is simple enough, the computation involved can be significant, especially for large matrices. Because of the large number of zeros in the $\underline{\underline{A}}$ matrix, MINET loads and solves the segment matrix equation in close-packed form. This step saves data storage space and significantly increases computational speed. Since a form of Gaussian elimination is still used to solve for the segment response matrix, there is little need to detail the process beyond making the following points.

1) Matrix $\underline{\underline{A}}$ is stored and solved as a six column matrix with $2N_m + 1$ rows plus a $2N_m + 2$ column matrix with one row (the momentum equation).
2) While the entries of matrix $\underline{\underline{A}}$ change somewhat under various flow conditions, the solver is general enough to handle any situation.
3) The solver is several times faster than full Gaussian elimination.

3.3.3.3.3 BOUNDARY ADJUSTED SEGMENT RESPONSE MATRIX

Before continuing on to evaluate the segment response matrices for the other segments, two steps are taken. First, matrix $\underline{\underline{A}}$ is discarded (data storage area de-allocated), as it is no longer useful. Second, advanced time (step ℓ) values are already known for the boundary modules, and these values are factored into the segment response matrix at this time. For a boundary module at the segment inlet with pressure and enthalpy specified as boundary conditions, these changes can be factored into column 5 of the matrix:

$$\{B^k_{i,5} = B^k_{i,5} + B^k_{i,1}\,\Delta E^{\ell}_{IM} + B^k_{i,2}\,\Delta P^{\ell}_{IM}\}, \quad i = 1,\ldots,2N_m + 2 \tag{3.3-52}$$

When mass flow rate is the bondary condition for the inlet boundary module, the change in pressure must be inferred from the equation for W_{mi} (after ΔE_{IM}^{ℓ} is factored in),

$$\Delta P^{\ell}_{IM} = \{W^{\ell}_{IM} - B_{2,5} - B_{2,3}\,\Delta E^{\ell}_{OM} - B_{2,4}\,\Delta P^{\ell}_{OM}\}/B_{2,2} \qquad (3.3\text{-}53)$$

This change in pressure is then factored into all of the rows.

$$\{B^{k}_{i,5} = B^{k}_{i,5} + (W^{\ell}_{IM} - B_{2,5})B_{i,2}/B_{2,2}\}\,, \quad i = 1,\ 2N_m + 2 \qquad (3.3\text{-}54)$$

$$\{B^{k}_{i,3} = B^{k}_{i,3} - B_{2,3}\cdot B_{i,2}/B_{2,2}\}\,, \quad i = 1,\ 2N_m + 2 \qquad (3.3\text{-}55)$$

$$\{B^{k}_{i,4} = B^{k}_{i,4} - B_{2,4}\cdot B_{i,2}/B_{2,2}\}\,, \quad i = 1,\ 2N_m + 2 \qquad (3.3\text{-}56)$$

If the mass flow rate is specified for a boundary module at the outlet end of a segment, it is the last row of the segment response matrix that is used to infer the change in outlet pressure. For the case when both ends of a segment connect to boundary modules, only the fifth column of the boundary adjusted segment response matrix is effectively non-zero, and the advancement of segment parameters to step & could be done immediately.

All of the segments in a network side are completed, and the boundary adjusted segment response matrices are stored, before the network accumulator pressure and enthalpy calculations are performed. First, however, the module advancement process, performed while the segment matrix equation is being loaded, will be discussed.

3.3.3.4 MODULE CONDITIONS UPDATE

In the transient calculations, the module level variables, e.g., heat exchanger tube wall temperatures, are advanced at the same time that the segment equations are being loaded. This saves on data storage space and reduces code complexity.

Essentially, there are two types of module level characteristics that must be known for segment level calculatons to proceed correctly. These are pressure drops and heat transfer rates.

As was the case in steady state calculations, the pressure losses are broken into two parts, a constant term, β_m (see Eq. (3.3-33)), and a term proportional to the square of the mass flow rate, $\alpha_m|W_m|W_m$ (see Eq. (3.3-34)). However, during transients, there is often wide variation in local mass flow rate, and the use of a segment loss factor, α_m, is impractical. Instead, a local loss factor, α_i, is evaluated for each node and is loaded into the segment momentum equation (see last row in Table 3.3-7). This local α_i is defined consistently with Eq. (3.3-32), i.e.,

$$\alpha_i = \frac{fi}{2\rho_i A_i D_i} + \delta_{ip}\,\rho_i g\,Hr\,\alpha p/Wr_p^2 + \delta_{iv}\,K_v/2\rho_i A_v^2 \qquad (3.3\text{-}57)$$

Pressure losses due to gravity, friction, and acceleration are evaluated at each segment node, for current time enthalpies, mass flow rates, and pressures. For the pump and valve modules (one node each), an additional contribution is made to the pressure drop, consistent with Eqs. (3.3-18) - (3.3-21). In order to evaluate these pressure drop terms accurately, advanced time values of relative pump speed and valve stem position are needed. If a speed or valve position has already been set, the module calculation can proceed. If alternate means of controlling pump speeds and valve position, either via the limited internal control or the more extensive PPS/PCS control system, were specified, the speed or position must yet be advanced in time.

For a pump, the relative demand speed, ωd_p^{ℓ}, is first calculated. The advanced time relative pump speed, ω^{ℓ}, is calculated via the differential equation

$$\tau_p \frac{d\omega_p{}^{\ell}}{dt} = \omega d_p{}^{\ell} - \omega_p{}^{k}, \qquad (3.3\text{-}58)$$

where τ_p is the user input pump time constant. If the relative pump speed drops below the user-input pump seizure speed, it is set to zero. The relative demand speed can be tripped, i.e., changed from 1 to 0, at a user input time, either through the limited MINET control option, or the PPS/PCS system. More sophisticated control of the pump demand speed requires use of the PPS/PCS system models.

For a valve, the relative demand stem position, S_d is first calculated. The advanced time valve stem position is calculated using the differential equation

$$\tau_v\left(\frac{dS}{dt}\right)^{\ell} = S_d{}^{\ell} - S^{k}, \qquad (3.3\text{-}59)$$

where τ_v is the appropriate user-input time constant. The stem position is limited by the user-input minimum "leak" position and full open. The limited steam generator internal controller is useful for safety valves which open (S_d = 1.0) and close (S_d = 0.0) at set pressures and time constants (τ_{vo} and τ_{vc}). When the valve position is actively controlled, the PPS/PCS system must be used to determine the demand position, S_d, and the time constant is often taken to be zero.

The calculation of current time heat transfer rates is a more involved process, partly because the tube wall temperature depends on conditions in two otherwise disconnected segments. Because the time constants in the heat transfer process are not small, explicit treatment of the heat transfer rate, $Q_i{}^{k}$, and the tube wall temperature, $T_w{}^{k}$, is possible.

When heat exchangers are first analyzed during the water/steam segment marches, the heat transfer rate is evaluated using current fluid characteristics and tube wall temperatures,

$$Q_i^k = \pi Dh \Delta X_i \cdot h_i^k(E_i^k, P_m^k, Tw_i^k) \cdot (Tw_i^k - T(E_i^k, P_m^k)). \tag{3.3-60}$$

later, when the heat exchangers are treated on the hot side, the heat transfer rate is again calculated using Eq. (3.3-60). In each case, the dependence of the heat flux on fluid enthalpy and mass flow rate are evaluated so that heat flux can be integrated implicitly with respect to these variables:

$$Q_i^{\ell} = Q_i^k + \frac{dQ_i}{dE_i}^k \Delta E_i^{\ell} + \frac{dQ_i}{dw_i}^k \Delta W_i^{\ell} \tag{3.3-61}$$

Only after the current heat transfer rates have been calculated for both the water/steam side and the hot side is the tube wall temperature advanced

$$Tw_i^{\ell} = Tw_i^k - \frac{\Delta t^k fa_h \ (Dh_h \ Qh_i^k + Dws_h \ Qws_i^k)}{At_h \ \rho t_i \ Cpt_i} \tag{3.3-62}$$

The explicit treatment of the tube wall temperatures greatly simplifies the calculational process, effectively decoupling the two network sides briefly while system variables are being advanced. However, it also introduces the time constant given in Eq. (3.3-35), which follows directly from Eqs. (3.3-60) and (3.3-62).

In the case of a "level" node, the level is adjusted during water/steam side calculations to the position where the level enthalpy is currently attained. Partial node conditions are then used to calculate the heat transfer rates below and above the level. These partial node heat transfer rates are then node fraction weighted to determine the nodal heat transfer rate.

On the hot side of the "level" node, it is first necessary to determine the new hot side level enthalpy, corresponding to the level position recently calculated on the water/steam side. In this case, algebraic equations for the node average enthalpy and the partial node average enthalpies are used to calculate the level enthalpy and the partial node average enthalpies. These enthalpies are used to calculate partial node heat transfer rates, through the partial node equivalent to Eq. (3.3-60). The nodal heat transfer rate is again calculated as the node-fraction weighted average of the partial node heat transfer rates. Partial node tube wall temperatures are advanced separately, and node fraction weighted to obtain node average tube wall temperature, which is used only when the level changes nodes.

3.3.3.5 NETWORK ACCUMULATOR CALCULATIONS

Once the segment response matrices have been determined for all of the segments in one network, the accumulator pressures and enthalpies can be determined. Conservation equations for mass and energy in each of the N_d network accumulators are coupled in the matrix equation,

$$\underline{\underline{C}}\ \underline{V} = \underline{D}, \tag{3.3-63}$$

where $\underline{\underline{C}}$ is a $2N_d$ square matrix, $\underline{D}$ is a $2N_d$ vector, and $\underline{V}$ is the $2N_d$ vector

$$\underline{V} = \text{col}\ \{\Delta E_1, \Delta P_1, \ldots, \Delta E_{N_d}, \Delta P_{N_d}\}\ . \tag{3.3-64}$$

The individual equations loaded into Eq. (3.3-63) are implicit forms of Eqs. (3.3-1) and (3.3-2), with Eq. (3.3-3) used to eliminate the density time derivatives.

$$\frac{V_n}{\Delta t}\left(\frac{\partial \rho_n}{\partial E_n}\right)^k \Delta E_n{}^{\ell} + \frac{V_i}{\Delta t}\left(\frac{\partial \rho_n}{\partial P_n}\right) \Delta P_n{}^{\ell} = \sum^{\text{Inlets}} W_{mo} - \sum^{\text{Outlets}} W_{mi} \qquad (3.3\text{-}65)$$

$$\frac{V_n}{\Delta t}\left[\rho_n + E_n\left(\frac{\partial \rho_n}{\partial E_n}\right)^k\right]\Delta E_n{}^{\ell} + \frac{V_n}{\Delta t}\left[E_n{}^k\left(\frac{\partial \rho_n}{\partial P_n}\right)^k - 1\right]\Delta P_n{}^{\ell} \qquad (3.3\text{-}66)$$

$$= \sum^{\text{Inlets}} W_{mo}{}^{\ell} E_{mo}{}^{\ell} - \sum^{\text{Outlets}} W_{mi}{}^{\ell} E_{mi}{}^{\ell} + Q_n{}^{\ell}$$

The process of loading Eqs. (3.3-65) and (3.3-66) into Eq. (3.3-63) is straightforward, with the exception of the inflows and outflows. Here the segment response matrices must be used to obtain the advanced time segment inlet and outlet mass flow rate and enthalpy as a function of changes in bordering pressures and enthalpies. As a simplification, for this part of the process it is assumed that the change in pressure at the segment boundary is equal to the change in pressure in the bordering accumulators (even though the absolute pressures may be different). Thus, for a segment taking flow out of accumulator 1 and into accumulator 2, the second row of the segment response matrix is retrieved (accumulator outflow is segment inflow). Then, for the first accumulator mass equation, the first four columns of the segment response matrix, row 2, are added to the first four columns of matrix C, row 1. This accounts for changes in the mass flow rate going into the segment in response to changes in enthalpy and pressure in the inlet and outlet bordering accumulator. The fifth column entry of row 2 of the segment response matrix is then subtracted from the first row of vector D. Note that if the segment were connected at this outlet to a boundary module instead of an accumulator, the third and fourth columns of the segment response matrix would be ignored.

Loading Eq. (3.3-66) is slightly more difficult because the flow energy terms must be linearized.

$$W^{\ell}E^{\ell} = E^{k}W^{\ell} + W^{k}\Delta E^{\ell}. \qquad (3.3\text{-}67)$$

Rows must be extracted from the segment response matrix for both W^{ℓ} and ΔE^{ℓ}, and substituted in Eq. (3.3-67). Second order "Δ" terms are dropped. The remaining terms are then loaded into Eq. (3.3-63).

After equations for all accumulators in the network have been loaded into the matrices, Eq. (3.3-63) is solved for vector $\underline{V}$. This is done using full Gaussian elimination, as these matrices are generally small and have mostly non-zero elements.

$$\underline{V} = \underline{\underline{C}}^{-1}\,\underline{D} \qquad (3.3\text{-}68)$$

Vector $\underline{V}$ contains changes in the network accumulator enthalpies and pressure during the time step.

3.3.3.6 ADVANCING NETWORK VARIABLES

Accumulator enthalpies and pressures are advanced using the changes indicated in vector $\underline{V}$. If the contents of the accumulator are separated, the new level is then calculated. Using vector $\underline{V}$ and the boundary module adjusted segment response matrix, all of the nodal interface enthalpies and mass flow rates are then advanced.

The advancement of segment inlet and outlet enthalpy and mass flow is straightforward, as they are equal to the values for the just advanced interface enthalpies and mass flow rate at the inlet and outlet of the segment. Similarly, the boundary module enthlapies and mass flow rates can be advanced, where appropriate, using segment inlet and outlet enthalpies and flows.

Segment inlet/outlet pressures and boundary module pressure are not always as easy to advance. If the segment connects to a volume, the segment inlet/outlet pressure is calculated using the advanced accumulator pressure and elevation head. In the case where the pressure option was chosen as the user input parameter for the boundary module, the pressure at the boundary module is advanced already, and the adjoining segment pressure is adjusted to match it. It is the case where one or both ends of the segment connect to boundary modules and where mass flow rate boundary conditions were specified that is most difficult. For such a boundary module at the segment inlet, Eq. (3.3-53) must be used (these matrix B entries are carefully preserved). A similar expression is used when a mass flow rate boundary condition is specified at the segment outlet. When a segment has mass flow rate boundary conditions on both ends, Eq. (3.3-53) and the equivalent at the segment outlet are coupled and solved for the pressure at both ends.

Once the segment inlet and outlet pressures have been advanced, a new segment average pressure is calculated. This advanced time pressure is compared against the current value, thus giving the change over the time step, to be used in advancing the node average enthalpies. The node average energy equation used is the linearized form of Eq. (3.3-45):

$$\Delta E_i = \left\{ -C_4 \Delta P_m^{\ell} + W_j^{\ell} E_j^{\ell} - W_{j+1}^{\ell} E_{1+1}^{\ell} + Q_i^{k} + \left(\frac{\partial Q_i}{\partial W_i} \right) \Delta W_i^{\ell} \right\} / C_3 \qquad (3.3\text{-}69)$$

where C_3 and C_4 are as given in Table (3.3-7). If the flow is passing through the node at the beginning of the step, the node average enthalpy is over-written with the linear average of the junction enthalpies on either end. This is a standard step in the donor-cell differencing scheme used for the

flow-through nodes. Thus, Eq. (3.3-69) is actually used (and is critical) only for converging and diverging flow nodes.

3.3.3.7 INTERFACING BACK TO THE INTERMEDIATE LOOP

When the MINET transient calculations reach the advanced master clock time, it is necessary to return information useful to the SSC intermediate loop calculations. The outlet mass flow ratio are returned, but are not used by SSC, because sodium is assumed to be incompressible. The pressure drop across each of the intermediate loops are returned in lieu of absolute pressures. Lastly, the hot side boundary enthalpies are converted to temperature and returned as the temperatures into and out of the steam generator section of the intermediate loop. Note that unless flow has reversed in the intermediate loop, the temperature into the steam generator will be the same as when it was passed in at the beginning of the step.

3.3.4 MINET - PPS/PCS INTERFACE

The PPS/PCS module requires input from MINET in order to control steam generator and other plant functions, such as reactor power. As this information is required for specific components, such as the steam drum, additional user input is required to identify which of the modules represent these components. If a particular component is not represented, the user inputs "999" as the identity, and a dummy signal is sent to the PPS/ PCS for the non-existent component.

In order to represent some steam generator system pump speeds and valve positions, it is necessary to identify the specific component, e.g., feedwater pump, from amongst the otherwise indistinguishable modules. If the component is identified as "999", the signal returning from the PPS/PCS system for the missing component is ignored.

REFERENCES FOR SECTION 3.3

3.3-1. J. E. Meyer, "Hydrodynamic Models for the Treatment of Reactor Thermal Transients," Nucl. Sci. Eng. 10, 269, 1961.

3.3-2. "RELAP 3B Manual, A Reactor System Transient code," Brookhaven National Laboratory, RP 1035, Dec. 1974.

3.3-3. R. E. Henry and H. K. Fauske, "The Two-Phase Critical Flow of One-Component Mixtures in Nozzles, Orifices, and Short Tubes", Trans. ASME J. Heat Transfer, 93, 179 (1971).

3.3-4. F. J. Moody, "Maximum Flow Rate of a Single Component. Two-Phase Mixture", Trans. Amer. Soc. Mech. Engrs., Journal of Heat Transfer, 87, 134-142 (1965).

3.4 MODELING OF PLANT PROTECTION AND PLANT CONTROL SYSTEMS

3.4.1 INTRODUCTION

The dynamic simulation of protected transients in liquid-metal-cooled fast breeder reactors (LMFBRs), is an integral part of the overall design, development and safety evaluation. The overall plant system response to a variety of operational, incidental and accidental transients requires mathematical modeling of the entire plant including the interactions of the plant protection system (PPS) and plant instrumentation and control systems (PCS).

Limited modeling of the PPS and PCS has been developed and incorporated in a number of system simulation codes [3.4-1, 3.4-2, 3.4-3, 3.4-4]. These models are normally highly plant dependent and often inadequate in their representation of the actual plant conditions.

The aim of this chapter is to present a fairly generalized and detailed modeling of the plant protection and control systems that has been developed and incorporated into the Super System Code (SSC). These models have been formulated to be more easily adaptable to plants of similiar design and characteristics.

The detailed description of the plant protection system is given in the following section (3.4.2). Section 3.4.3 describes the plant control systems for various plant systems, while Section 3.4.4 discusses the interaction of plant protection and control systems and the numerical interfacing with SSC.

3.4.2 PLANT PROTECTION SYSTEM

The function of the LMFBR Plant Protection System (PPS) is to assure that the results of all postulated conditions do not exceed the specified safety limits of the reactor system. It should provide the required protection by sensing the need for, and carrying to completion, reactor scrams, pump trips, turbine-generator set trips and subsequent isolation.

Safety limits are imposed on important process variables required to reasonably protect the integrity of each of the physical barriers which guard against the uncontrolled release of radioactivity. The maximum safety settings for automatic protective devices are related to variables on which safety limits have been placed. A maximum safety setting shall be so chosen that automatic protective action will correct the most severe abnormal situation anticipated before a safety limit is exceeded. Thus, the safety limit on reactor power would be the power level at which operation is deemed to become unsafe, while the maximum safety setting would be the power level at which a scram is initiated. The maximum safety setting must take into account the measurement and instrumentation uncertainties associated with the process variables.

The PPS can be thought of as a control system, which, in routine operation, remains an observer acting only if the plant system reaches the limit of permissible operation (maximum safety setting). The PPS includes the Shutdown System(s) and the Engineering Safety Features.

The PPS does not directly include the reactor operator in implementing a protective function. However, manual shutdown devices are considered part of the PPS.

In the present model, the PPS function is divided into two separate modes namely; manual and automatic, mode as shown schematically in Figure 3.4-1 and described in the following sections.

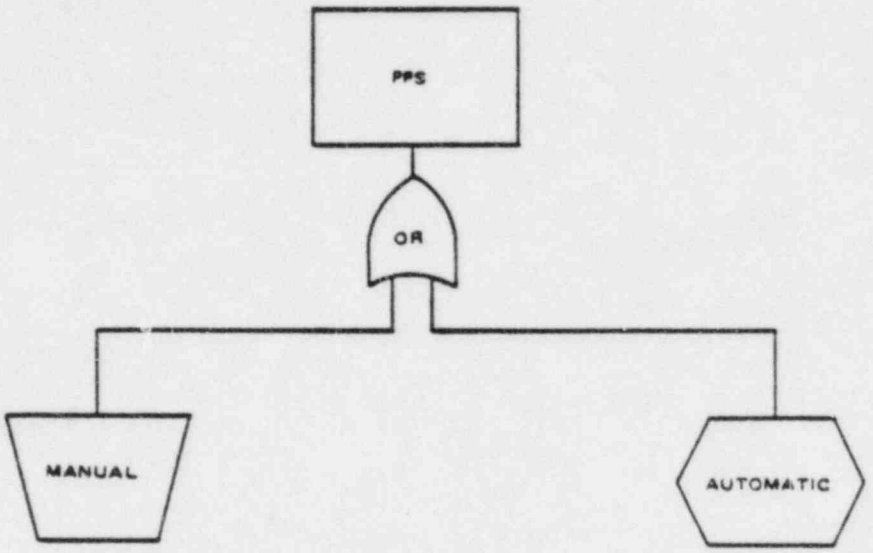

Figure 3.4-1 PPS Operation Logic

3.4.2.1 MANUAL MODE

In the manual mode, the model simulates the operator's action through which various shutdown systems can be activated.

To achieve this, the user must switch the PPS mode to manual and provide the time at which the derived shutdown system must be activated. It is important to note that the manual action can also be used to initiate a transient anywhere in the shutdown systems. The following systems can be manually activated (together or individually) through input:

(1) Primary control rods,

(2) Secondary control rods,

(3) Primary, intermediate and tertiary pump motors, and

(4) Turbine-generator set.

Manual activation is achieved through two coupled input data parameters; namely the manual switch flag and the time at which the manual action is desired. For example the user can input the following shutdown sequences:

Primary Scram at t = 0.10 s

Secondary Scram at t = 1.90 s

Primary Pump Trip (Loop 1) at t = 2.0 s

Primary Pump Trip (Loops 2 and 3) at t = 2.2 s

Secondary Pump Trip (Loops 1,2, and 3) at t = 2.5 s

Recirculation Pump Trip (Loops 1,2, and 3) at t = 2.5 s

Feedwater Pump Trip (Loop 1,2, and 3) at t = 3 s

Turbine Trip at t = 0.0 s

It must be noted that the manual switch does not necessarily exclude automatic action, if automatic conditions are satisfied prior to the time of manual trip. In order to exclude any possible automatic actions, the user should also set a long automatic time delay (see Section 3.4.2.5).

3.4.2.2 AUTOMATIC MODE

In the automatic mode, important system variables are processed through PPS subsystem trip functions for possible protective action in response to selected instrumentation signals.

The response of process sensors and transmitters is modeled using a first order approximation of the form [3.4-5, 3.4-6]:

$$T_m \frac{dX_m}{dt} = X_a - X_m \qquad (3.4\text{-}1)$$

where, T_m = time constant of the measuring device, (s),

X_m = measured (sensed) process variable, and

X_a = actual value of the process variable (e.g., flux amptitude, primary loop sodium flow rate, temperature, etc.,.

The time constants of the measuring devices are normally determined experimentally and are highly dependent on the characteristics of the measuring instrument. Table 3.4-1 summaries some typical instrumentation time constants.

Every important process variable is monitored by the PPS computer and the measured signal as given by Equation (3.4-1) is processed by the reactor shutdown subsystems.

Various plants use different process variables with different safety settings for the PPS subsystem trip equations. In order to represent a fairly generalized model of the PPS for LMFBRs of different design and configuration, SSC provides twenty functions, fifteen of which are chosen based on the review of the current LMFBR designs in the United States. The remaining five functions are left blank in order to provide the user with sufficient freedom for accommodation of other trip functions.

Table 3.4-1 Typical Sensor and Transmitter Time Constants

Measured Variable	T_m(s)
Neutron Flux	0.05
Pump Speep	0.02
Flow Rate	0.50
Temperature	2.00
Pressure	0.15
Liquid Level	0.50

The following is the list of the trip functions and their associated mathematical relations as they appear in the code.

(1) High Neutron Flux subsystem generates a reactor scram signal for significantly large positive reactivity insertion, that is:

$$\phi_m(t) \geq \phi_{max} \tag{3.4-2}$$

where $\phi_m(t)$ is the measured (normalized) neutron flux amplitude and ϕ_{max} is the specified safety setting (user supplied input).

(2) Flux-Delayed-Flux subsystem generates a reactor scram signal for rapid reactivity disturbance, either positive or negative, which may occur anywhere in the load range. For positive reactivity ($\rho>0$), the Laplace transform is:

$$L^{-1}[A_1 \phi_m(s)/(A_2 + s)] + A_3 \phi_m(t) + A_4 \alpha_{pm}(t) + A_5 \leq 0 \tag{3.4-3}$$

and according to the convolution theorem:

$$L^{-1}[F_1(s) \cdot F_2(s)] = \int_0^t f_1(t') \cdot f_2(t - t')dt' \tag{3.4-4}$$

Therefore, Equation (3.4-5) can be transformed into the time domain to obtain:

$$A_1 \int_0^t \phi_m(t') e^{-A_2 (t - t')} dt' + A_3 \phi_m(t) + A_4 \alpha_{pm}(t) + A_5 \leq 0 \qquad (3.4\text{-}5)$$

where α_{pm} is the measured (normalized) primary loop pump speed or total reactor coolant flow rate, and A_1, A_2. . ., A_5 are constants associated with the maximum safety settings.

For negative reactivity disturbances ($\rho<o$), a similiar relationship exists; except the constants associated with the maximum safety settings are different.

Equation (3.4-5) is an integral equation which can be easily transformed into a differential equation by the following definition:

$$I(t) = \int_0^t \phi_m(t') e^{-A_2 (t - t')} dt' \qquad (3.4\text{-}6a)$$

and

$$\frac{dI}{dt} = \phi_m(t) - A_2 \int_0^t \phi_m(t') e^{-A_2 (t - t')} dt' \qquad (3.4\text{-}6b)$$

or alternatively:

$$\frac{dI}{dt} = \phi_m(t) - A_2 I(t) \qquad (3.4\text{-}7a)$$

Equation (3.4-7a) is an ordinary differential equation in time, with the

initial condition given by:

$$I(t = 0) = \phi_m(t = 0)/A_2 \qquad (3.4\text{-}7b)$$

Therefore, Equation (3.4-5) can be readily evaluated as a function of time by first solving Equation (3.4-7) and substituting the results for I into Equation (3.4-5).

(3) Flux- $\sqrt{\text{Pressure}}$ subsystem provides protection against positive reactivity excursions and/or reduction in the pressure at the reactor inlet plenum over the desired load range, the trip equation is of the form:

$$C_1 \phi_m(t) + C_2 [P_m(t)]^{1/2} + C_3 \leq 0 \qquad (3.4\text{-}8)$$

where $P_m(t)$ is the measured (normalized) pressure and C_1, C_2, C_3 are constants associated with the maximum safety settings.

(4) Primary to Intermediate Speed Ratio subsystem generates a reactor scram signal for imbalance in heat removal capability between the primary and intermediate circuits of the same loop. The protective function is of the form:

$$D_1 \alpha_{pm}(t) - D_2 [D_3 \alpha_{pm}(t) + D_4 \alpha_{im} + D_5] + D_6 \leq 0 \qquad (3.4\text{-}9)$$

where $\alpha_{im}(t)$ is the measured (normalized) intermediate loop pump speed and D_1, D_2, . . ., D_6 are constants associated with the maximum safety settings.

(5) Pump Electrics subsystem provides protection for loss of AC power to any of the plant's coolant pump motors.

(6) Reactor Vessel Level subsystem generates a reactor scram signal for low reactor vessel sodium level, that is:

$$L_m(t) \leq L_{min} \qquad (3.4\text{-}10)$$

where $L_m(t)$ is the measured reactor vessel sodium level; and L_{min} is the minimum sodium level for PPS action.

(7) Steam to Feedwater Flow Ratio subsystem generates a reactor scram signal for large imbalances between the steam and feedwater flow rate for each heat transport system loop, that is:

$$|W_{fm}(t) - W_{sm}(t)| \geq \Delta \qquad \text{(Any Loop)} \qquad (3.4\text{-}11)$$

Where $W_{fm}(t)$ is the measured feedwater flow rate; $W_{sm}(t)$ is the measured steam flow rate, and Δ(kg/s) is the maximum difference in the flow rates for PPS action.

(8) IHX Primary Outlet Temperature subsystem generates a reactor scram signal if the IHX outlet sodium temperature exceeds a specified setpoint; that is:

$$T_{ixm}(t) \geq T_{max} \qquad \text{(Any Loop)} \qquad (3.4\text{-}12)$$

where $T_{ixm}(t)$ is the measured IHX outlet sodium temperature and T_{max} is the maximum safety setting.

(9) Flux-Total Flow subsystem provides protection against increasing and decreasing flow and power level over the load range. The trip equation is of the form:

$$F_1 \cdot \sum_{j=1}^{n} W_{pm,j}(t) + F_2 \cdot \phi_m(t) + F_3 \leq 0 \qquad (3.4\text{-}13)$$

where $W_{pm,j}(t)$ is the measured (normalized) sodium flow rate in the j-th primary loop, n is the total number of the primary loops and F_1, F_2, F_3 are constants associated with the maximum safety settings.

(10) Primary to Intermediate Flow Ratio subsystem provides protection against

large imbalance in the heat removal capability of the primary and intermediate circuits on the same loop. The trip equation is of the form:

$$G_1 W_{pm}(t) + G_2[G_3 W_{pm}(t) + G_4 W_{im}(t) + G_5] + G_6 \leq 0 \qquad (3.4\text{-}14)$$

where $W_{im}(t)$ is the measured (normalized) sodium flow rate in the intermediate loop, and $G_1, G_2, \ldots G_6$ are constants associated with the maximum safety settings.

(11) Steam Drum Level subsystem generates a reactor scram signal for high and low steam drum water levels as governed by the following trip equation:

$$H_m(t) \begin{cases} \geq H_{max} \\ \\ \leq H_{min} \end{cases} \quad \text{(Any Loop)} \qquad (3.4\text{-}15)$$

where $H_m(t)$ is the measured (normalized) steam drum water level, H_{max} is maximum water level and H_{min} is minimum water level for PPS action.

(12) High Evaporator Outlet Temperature subsystem generates a reactor scram signal for high sodium temperature at the outlet of any evaporator(s), that is:

$$T_{em}(t) \geq T_{emax} \quad \text{(Any Loop)} \qquad (3.4\text{-}16)$$

where $T_{em}(t)$ is the measured sodium temperature at the outlet of any evaporator, and T_{emax} is the maximum safety setting for PPS action.

(13) High Reactor Vessel Outlet Nozzle Temperature subsystem generates a reactor scram signal for high sodium temperature at any of the reactor outlet nozzles, that is:

$$T_{rm}(t) \geq T_{rmax} \qquad (3.4\text{-}17)$$

where $T_{rm}(t)$ is the measured sodium temperature at the reactor outlet nozzle, and T_{rmax} is the maximum safety setting.

(14) Low Primary Loop Flow subsystem generates a reactor scram signal for low primary loop sodium flow rate, that is:

$$W_{pm}(t) \leq W_{p,min} \qquad \text{(Any Loop)} \qquad (3.4\text{-}18)$$

where $W_{p,min}$ is the normalized minimum primary loop sodium flow rate for PPS action.

(15) Low Intermediate Loop Flow subsystem generates a reactor scram signal for low intermediate loop sodium flow rate, that is:

$$W_{im}(t) \leq W_{i,min} \qquad \text{(Any Loop)} \qquad (3.4\text{-}19)$$

where $W_{i,min}$ is the minimum normalized intermediate loop sodium flow rate for PPS action.

(16-20) Blank: these five functions are left blank to allow the user flexibility to simulate PPS trip functions applicable to other designs/plants.

3.4.2.3 PRIMARY AND SECONDARY SHUTDOWN SYSTEMS

In LMFBRs, the shutdown system consists of two independent, redundant systems capable of providing sufficient negative reactivity for neutronic shutdown, namely; primary and secondary control rod systems.

The primary rods are used for both power regulation and reactor shutdown; while the sole purpose of the secondary control rods is reactor shutdown.

In the present model, any number of the above shutdown subsystems can be assigned to either one of the shutdown systems, but not to both. For example,

subsystems 1, 3, 5, 8, 9, 12 can be assigned to the primary rods while the remaining subsystems can be assigned to the secondary rods. This option is provided through the input data and is discussed in Table 7-7 (Records 8016-8019) and Figure 7-10.

Manual operation of the primary and/or secondary shutdown systems is also included as was described in Subsection 3.4.2.1.

3.4.2.4 SIGNAL SUPPRESSION

A user of SSC can selectively suppress automatic reactor scram actions based on any or all of the PPS subsystem for both primary and secondary shutdown systems.

For example, subsystems 1, 3, 5, 8, 9, 12 can be assigned to the primary system; subsystems 2, 4, 6, 7, 10, 11, 13, 14 and 15 can be assigned to the secondary system. Additionally, if desired, the user could suppress possible primary system scrams due to subsystems 1, 5 and 8, for instance; and also suppress possible secondary system scrams due to subsystems 4, 7, 10 and 13. This is achieved by assigning the desired operative protective functions. Therefore, protective functions that would be operative in this example for the primary and secondary shutdown systems are 3, 9, 12; and 2, 6, 11, 13, 14 respectively.

3.4.2.5 SIMULATION OF INHERENT TIME DELAYS DURING SHUTDOWN

In order to be able to simulate the PPS system parallel to the real plant operation, the effect of instrumentation and mechanical time lags must also be included.

There are two types of automatic time delays: (1) scram time delay, and (2) trip time delay. The scram time delay is defined as the time from the automatic generation of the scram signal to the time at which control rod movement begins. The trip time delay is the time span from when the control rod movement begins, to the time when the pumps and turbines are tripped; as shown schematically in Figure 3.4-2.

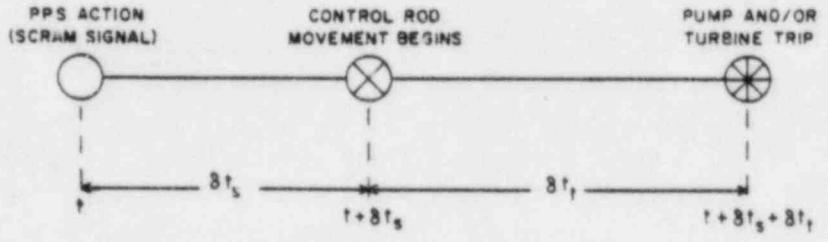

Figure 3.4-2 Schematic of the Shutdown Time Lags

These time delays can vary anywhere from 0 to ∞; and must be supplied through input data.

3.4.3. PLANT CONTROL SYSTEMS

Adequate modeling of Plant Control Systems (PCS) for the study of Anticipated Transients Without Scram (ATWS) is of considerable significance in the design, operation and safety evaluation of LMFBR systems. In order to assess the system response to such transient events, detailed models for plant control systems must, therefore, be provided in any large system simulation code.

The plant control system incorporates the manual and automatic controls that maintain the plant at the desired level of power, temperature, pressure, and flow conditions for startup, load changing, rated power, standby and shutdown conditions. These functions are usually accomplished using a two level feedback control system. The supervisory control (top level) uses the load demand signal as input. From this input, the power, temperature, pressure, flow and other setpoints are established electronically according to the desired part load profile. These demand setpoints are used by individual controllers (second level) which maneuver the control rods, pump drives or valves to attain the desired plant conditions.

3.4.3.1 UNIT CONTROLLER (Cascade)

A block diagram representation of a unit controller is shown in Figure 3.4-3. It is seen that the unit controller is composed of the setpoint generator, process measuring device, deadband and a proportional-integral-derivative (PID) module.

The setpoint generator allows for the generation of process setpoint either through the supervisory controller, $X_D(L)$ or a manual switch, X_{sp}. The process measuring device accounts for the instrumentation time lags, and is modeled by the first order system described earlier in section 3.4.2.2.

The deviation (error) signal (e) can then be calculated as:

$$e = \begin{cases} X_D\ (L) - X_m & \text{Automatic Mode} \\ X_{sp} - X_m & \text{Manual Mode} \end{cases} \qquad (3.4\text{-}20)$$

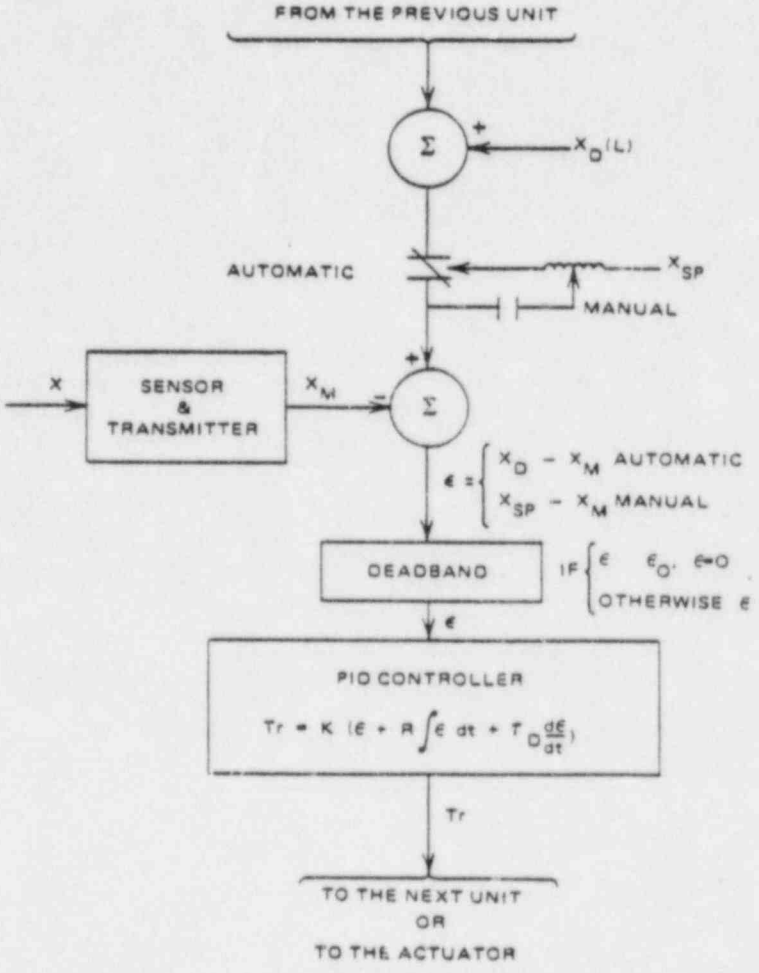

Figure 3.4-3 Block Diagram Representation of the Unit Controller

It is important to note that all of the controller variables are normalized with respect to their 100% load reference conditions, in order to remove any ambiguities of unit conversions.

There is normally a deadband around the setpoint, of width $2e_o$, over which the controller is insensitive to the changes in the error (deviation) signal, that is:

$$e = 0 \quad \text{if} \quad |e| \leq e_o \tag{3.4-21}$$

The error signal is then fed to a PID module to generate a corrective trim signal (Tr) as follows:

$$Tr = K \left(e + R \int e\, dt + T_D \frac{de}{dt}\right) \tag{3.4-22}$$

where K is the proportional gain, R is the integral repetition rate (s^{-1}) and T_D is the derivative time (s).

The controller response to increasing the integral rate is generally improved at the expense of a more oscillatory behavior. The addition of derivative action to the controller improves the response time significantly while reducing the oscillatory behavior. These modes of control are usually refered to as the lead-lag actions.

Setting the proportional gain to zero shuts off the entire cascade, while the integral reset rate, R, and the derivative time T_D can be set to zero selectively to shut off their respective modes.

In order to prevent undesirable oscillations and cyclic disturbances under certain control conditions, the controllers are usually designed to limit the excessive integral roll-up and roll-down [3.4-9]. This effect can be accounted for by bounding the value of the integral in Equation (3.4-22) to any positive (roll-up) and/or negative (roll-down) value.

The integral is transformed into a differential equation using the following definition:

$$I = \int e \, dt \tag{3.3-23}$$

Therefore,

$$\frac{dI}{dt} = e \quad ; \; I(t = o) = 0 \tag{3.4-24}$$

The derivative term of Equation (3.4-22) is approximated numerically as:

$$\frac{de}{dt} = \frac{e(t) - e(t - \Delta t)}{\Delta t} \tag{3.4-25}$$

where Δt is the integration timestep; $e(t)$ is the current error and $e(t - \Delta t)$ is the error at the end of the previous timestep.

The trim signal, Tr, is the controller output signal which is used as an input to the next unit controller (cascade) or as an input to the actuator as discussed in the following sections.

3.4.3.2 SUPERVISORY CONTROL

The supervisory controller uses the demanded power (load) signal and transforms it into a feedforward demand for the various plant controllers in order to maintain the desired operating conditions.

The desired operating conditions are determined by performing repeated steady state calculations at various power levels throughout the reactor automatic operating range assuming certain known turbine throttle conditions. These part load profiles of key plant variables are used as input for the transient calculations.

In order to increase the computational speed, the code calculates the load dependent setpoints as functions of plant load using polynomial approximations of the form:

$$X_D(L) = \sum_{i=0}^{2} C_i L \qquad (3.4\text{-}26)$$

where L is the fractional load and the C_i's are polynomial coefficients obtained from part-load profiles and supplied by the user through the input data.

3.4.3.3 REACTOR POWER CONTROL

The reactor power control system maneuvers the primary control rods as dictated by the plant's supervisory control in accordance with the reactor power control cascading mechanism.

Consider the point kinetics equations of Section 3.1.4:

$$\ell \frac{dN}{dt} = \beta(\rho/\beta - 1)N - \sum_{i=1}^{n} \ell\lambda_i C_i \qquad (3.4\text{-}27)$$

$$\ell \frac{dC_i}{dt} = \beta_i N - \ell\lambda_i C_i \qquad (3.4\text{-}28)$$

$$\beta = \sum_{i=1}^{n} \beta_i \qquad (3.4\text{-}29)$$

where ℓ is the prompt neutron generation time (s), N is the neutron flux amplitude (proportional to power), β_i is the fraction of the i-th delayed neutron group, λ_i is the decay constant of the i-th delayed neutron group (s^{-1}), ρ is the total reactivity (ρ/β is the total reactivity in dollars), and C_i is the density of the i-th effective delayed neutron precursor.

The total reactivity is the forcing function which causes the neutron flux amplitude to respond to changes in the reactor core, temperature, composition, and control rod movement. Thus;

$$\rho/\beta = (\rho/\beta)_{cr} + (\rho/\beta)_{fb} + (\rho/\beta)_{sd} \qquad (3.4\text{-}30)$$

where $(\rho/\beta)_{cr}$, $(\rho/\beta)_{fb}$ and $(\rho/\beta)_{sd}$ are the reactivity contributions due to reactor control rods, nuclear feedback effects and the cold shutdown margin of reactivity, respectively.

3.4.3.3.1 CONTROL ROD REACTIVITY

-- Rated Power Pre-Scram Operations

It was described earlier that in general the LMFBR shutdown system consists of two independent control rod systems namely; primary and secondary control rod banks.

The primary control rods are used to regulate reactor power during normal power operation and also shutdown if required, while the secondary control rods are used for reactor shutdown only. Therefore, during plant start-up, the secondary control rods are withdrawn (normally fully) and then the primary rods are withdrawn according to the precribed control rod banking strategy.

The pre-transient initialization in SSC is performed assuming the reactor is critical at a known initial reactor power.

The present model represents the primary control rods by an N-bank rod system which are assumed to be ganged according to a specified scheme. The reactivity worth of each rod bank is determined using the first order perturbation theory [3.4-10, 3.4-11]. The secondary control rods are all lumped into a single rod bank with a known rod worth and initial position.

The initialization procedure is as follows:

(1) Calculate the steady-state operating conditions at the known reactor power.

(2) Calculate all of the feedback reactivity contributions at the steady-state operating condition.

(3) Calculate the reactivity contribution of the secondary rods as:

$$(\rho/\beta)_{sr} = (\rho/\beta)_{sr_{max}} \cdot \left[Z_{in}/Z_{max} - \frac{1}{2\pi} \text{Sin} (2\pi Z_{in}/Z_{max}\right]_{sr} \qquad (3.4\text{-}31)$$

where $(\rho/\beta)_{sr_{max}}$ is the maximum worth of the secondary control rod bank in dollars, Z_{in} is the initial withdrawal position (m) and Z_{max} is the maximum withdrawal position (m). (These data must be supplied through input by the user).

(4) Calculate the reactivity requirements of the primary control rods by performing a reactivity balance satisfying the criticality condition at time zero of the transient using Equation (3.4-30). That is:

$$(\rho/\beta) = (\rho/\beta)_{cr} + (\rho/\beta)_{fb} + (\rho/\beta)_{sd} = 0 \qquad (3.4\text{-}32)$$

Hence:

$$(\rho/\beta)_{cr} = (\rho/\beta)_{pr} + (\rho/\beta)_{sr} = -\left[(\rho/\beta)_{fb} + (\rho/\beta)_{sd}\right] \qquad (3.4\text{-}33)$$

or

$$(\rho/\beta)_{pr} = -\left[(\rho/\beta)_{sr} + (\rho/\beta)_{fb} + (\rho/\beta)_{sd}\right]$$

where $(\rho/\beta)_{pr}$ is the total reactivity due to the primary control rod banks which is calculated as:

$$(\rho/\beta)_{pr} = \sum_{i=1}^{N} (\rho_i/\beta)_{pr_{max}} \cdot [Z_i/Z_{i_{max}} - \frac{1}{2\pi} \text{Sin} (2\pi Z_i/Z_{i_{max}})]_{pr} \qquad (3.4\text{-}34)$$

where N is the total number of primary control rod banks.

The maximum reactivity worth of each primary control rod bank, along with the initial positions of each bank are supplied through input, the code uses Equations (3.4-33) and (3.4-34) to readjust the position of the first primary rod bank to achieve criticality. Therefore,

$$(\rho_i/\beta)_{pr_{max}} \cdot [(Z_i/Z_{i_{max}}) - \frac{1}{2\pi} \text{Sin} (\frac{2\pi Z_i}{Z_{i_{max}}})]_{pr} =$$

$$- [(\rho/\beta)_{sr} + (\rho/\beta)_{fb} + (\rho/\beta)_{sd} +$$

$$\sum_{i=2}^{N} (\rho_i/\beta)_{pr_{max}} \cdot [(Z_i/Z_{i_{max}}) - \frac{1}{2\pi} \text{Sin} (2\pi Z_i/Z_{i_{max}})]_{pr}] \qquad (3.4\text{-}35)$$

must be solved iteratively for the initial position of the first primary rod bank, Z_1, using the user supplied position as the first guess. The solution is obtained using the Newton-Raphson's method for transcendental equations. If the reactivity balance is not achieveable, a message is printed and the calculation is terminated; the user must then reexamine the control rod worth and the cold shutdown margin of reactivity and repeat the calculations.

During transient operation (e.g., load changing), the primary control rod positions are regulated by the reactor power control and rod drive mechanism.

For example, for the CRBRP design, the reactor power control consists of three unit controllers (cascades) put in series, namely; the turbine inlet steam temperature, core mixed mean sodium temperature and the neutron flux. The output of the last cascade is sent to the power dead zone and saturation circuit limits of the control rod rates. Finally, the signal is divided into an analog magnitude signal and a digital direction signal for use as demands to the control rod drive mechanism actuator.

The multi-bank feature of the primary control rod system assumes the first primary rod bank (normally the fine rod bank) to be the first one to move up or down. The movement of the second bank will start when the first rod bank reaches the user supplied upper limit, $Z_{up,1}$ or the lower limit, $Z_{\ell w,1}$; similarly for the third, fourth and the N^{th} rod bank.

The input circuitry to each control rod bank accepts on- off inputs for IN, OUT and HOLD commands and provides the required action. The IN command steps a single rod down into the core at a predetermined rate. The OUT command steps a single rod up out of the core at a predetermined rate (not necessarily the same as the IN rate). The HOLD command maintains the rod in its present position (no motion). That is:

$$\frac{dZ_i}{dt} = \begin{cases} V_{down} & \text{IN Command} \\ 0 & \text{HOLD Command} \\ V_{up} & \text{OUT Command} \end{cases} \qquad (3.4\text{-}36)$$

In order to reduce instabilities in the reactor power calculations, the rod withdrawal or insertion rate is set proportional to the trim signal in the vicinity of the power dead zone.

The reactivity worth of the primary control rods are then calculated at every time step using Equation (3.4-34) and subsequently for calculation of the total reactivity from Equation (3.4-30), which is the used by the neutron kinetics Equations (3.4-27 through 3.4-29).

It is important to note that by definition, the cold shutdown margin of reactivity $(\rho/\beta)_{sd}$ is based on the fundamental requirement for reactor operation that there must always be sufficient control poison available to bring the reactor subcritical with some margin to spare.

-- Post-Scram Conditions

The pre-transient initialization procedure for primary and secondary control rods is performed independently of the nature of the transient at hand.

Immediately following reactor scram (primary and/or secondary), the power controller calculations are terminated and the position of primary and/or secondary control rods is calculated based on the scram dynamic behavior, which is highly design dependent.

In this model, the scram dynamic behavior is described by a series of high order polynomials. The polynomial coefficient can easily be altered to describe the dynamic behavior of the specific design under investigation.

In most LMFBR designs, control rods are designed to fall under the force of gravity (usually spring assisted) and the motion is damped as they approach full insertion.

The dynamic behavior of the primary control rods following reactor scram can be well represented by two sixth order polynomials of the form:

$$Z_i = Z_i(t = t_s) \cdot \sum_{k=0}^{6} a_k (t - t_s)^k \qquad (3.4\text{-}37)$$

where $Z_i(t=t_s)$ is the position of the i-th primary control rod bank at the time of scram (n), the a_k's are the polynomial coefficients and $(t-t_s)$ is time after reactor scram (s). The second polynomial is exactly the same as Equation (3.4-37) except for the values of a_k's. This equation describes the scram dynamics for rods which are partially inserted prior to scram (under this condition the spring effectiveness is significantly reduced for spring assisted type control rod designs).

The dynamic behavior of the secondary control rods is also represented by a sixth order polynomial which is similiar to Equation (3.4-37) with the exception that secondary control rods are assumed to be fully withdrawn prior to reactor scram and hence their position is only a function of time after the initiation of the secondary scram.

Having determined the control rod positions, the reactivity can be readily evaluated using Equations (3.4-34) and (3.4-31) for primary and secondary control rods.

The impact of stuck control rods (if any) for both primary and secondary control rod systems is also included as follows:

$$(\rho/\beta)_{pr} = (\rho/\beta)_{pstk} \quad \text{if} \quad (\rho/\beta)_{pr} < (\rho/\beta)_{pstk} \tag{3.4-38a}$$

$$(\rho/\beta)_{sr} = (\rho/\beta)_{sstk} \quad \text{if} \quad (\rho/\beta)_{sr} < (\rho/\beta)_{sstk} \tag{3.4-38b}$$

where $(\rho/\beta)_{pstk}$ is the worth of the stuck primary control rod in dollars, and $(\rho/\beta)_{sstk}$ is the worth of the stuck secondary control rods in dollars, as supplied by the user.

3.4.3.4 PRIMARY AND INTERMEDIATE FLOW-SPEED CONTROL

The LMFBR coolant sodium flow-speed control system adjusts the drive torque on the pump shaft as dictated by the plant's supervisory control in accordance with the sodium flow-speed control cascading mechanism.

The dynamics of coolant flow inside the primary or intermediate heat transport systems is governed by a momentum equation, which is essentially a pressure balance equation that gives the sodium flow rate as a balance of the frictional, gravitational, accelaration pressure losses and the pump pressure rise.

The dynamics of the pump is governed by the torque balance equation for the shaft and rotating assembly (see Section 3.2.5) as:

$$I \frac{d\Omega}{dt} = T_m - T_{hyd} - T_{fr} \qquad (3.4\text{-}39)$$

where I is the moment of inertia of shaft, impeller and rotating elements inside the motor, T_m is the applied motor torque (= 0 during coastdown), T_{hyd} is the hydraulic load torque due to the fluid at the impeller, T_{fr} is the frictional torque and Ω is the angular speed of the pump (rad/s).

During normal operation, the drive motor torque is adjusted by the controller action, in order to maintain the desired operating conditions. For example, a slight decrease in load causes a reduction in the motor torque which in turn leads to a decrease in pump speed and eventually the coolant flow rate through the variation in the pump head.

There are various methods of achieving pump speed control through adjustment of the drive motor torque[3.4-12]. They include: (1) changing the number of poles, (2) varying the hydraulic coupling, (3) changing the power

frequency, and (4) changing the external resistance. The method applied is strongly dependent on the motor type, and the adequacy of control over the desired operating regime. At present, the code allows for two options of speed control, namely; frequency and rheostatic external resistance techniques.

3.4.3.4.1 VARIABLE FREQUENCY METHOD

The drive motor torque of the squirrel cage induction motor can be written as [3.4-4, 3.4-11]:

$$T_{m,norm} = (a_1 s + \frac{b_1}{s})^{-1} \qquad (3.4\text{-}40)$$

where $T_{m,norm}$ is the normalized torque defined as:

$$T_{m,norm} = T_m/T_D \qquad (3.4\text{-}41)$$

T_D is the design torque, a_1, b_1 are constants characterizing the motor behavior and S is the slip ratio given by:

$$S = 1 - (w/w_s) \qquad (3.4\text{-}42)$$

w is the pump speed (rpm) and w_s is the synchronous speed (rpm) which is related to the frequency f(Hz), and the number of pairs of poles, p, by:

$$w_s = 60\ f/p \qquad (3.4\text{-}43)$$

The drive motor torque can be adjusted by varying the power frequency (f) through an external actuator. The dynamic behavior of the actuator can be well represented using a second order system of the form [3.4-5,3.4-6]:

$$\mu_1 \frac{d^2 f}{dt^2} + \lambda_1 \frac{df}{dt} + \beta_1 (f - f_0) = Tr \qquad (3.4\text{-}44)$$

where μ_1, λ_1, β_1 are constants characterizing the mechanical actuator, f_o is the initial steady state frequency, determined based on the zero trim, and Tr is the final trim signal from the last unit controller (cascade) of the pump flow-speed control system.

Initially, the plant is assumed to be operating at the desired power level. Therefore, the steady state form of Equation (3.4-39) can be written as:

$$T_m = T_{hyd} + T_{fr} \tag{3.4-45}$$

and then:

$$T_{m,norm} = \frac{T_{hyd} + T_{fr}}{T_D} = (a_1 S + b_1/S)^{-1} \tag{3.4-46}$$

which can be solved for S:

$$S = [1 - (1 - 4a_1 b_1 T^2_{m,norm})^{1/2}]/(2a_1 T_{m,norm}) \tag{3.4-47}$$

and therefore using equations (3.4-42) and (3.4-43) one obtains:

$$f = f_o = p\, w/60(1-S) \tag{3.4-48}$$

where w is the steady state pump speed ($w = 60\Omega/2\pi$).

3.4.3.4.2 VARIABLE EXTERNAL RESISTANCE METHOD

The drive motor torque of the wound rotor induction motor can be represented by [3.4-12]:

$$T_{m,norm} = (a_2 \frac{S}{R} + b_2 \frac{R}{S})^{-1} \tag{3.4-49}$$

where a_2, b_2 are motor characteristic constants and R is the external resistance parameter defined by:

$$R = 1 + (R_{ext}/R_m) \tag{3.4-50}$$

Here, R_{ext} is the variable resistance (ohms) provided by a liquid rheostat actuator and added in series to R_m, the motor resistance (ohms) which is related to the normalized liquid rheostat electrode position Z according to the following equation:

$$R_{ext} = R_{max} (1 - Z)^3 \tag{3.4-51}$$

where R_{max} is the maximum external resistance (ohms).

The variable liquid rheostat electrode position can also be simulated by a second order system of the form described earlier in Equation (3.4-44). That is:

$$\mu_2 \frac{d^2 Z}{dt^2} + \lambda_2 \frac{dZ}{dt} + \beta_2 (Z - Z_0) = Tr \tag{3.4-52}$$

Here μ_2, λ_2, β_2 describe the characteristics of the liquid rheostat actuator, and Z_0 is the initial steady state position of the electrodes determined based on zero trim.

It is important to note that the synchronous speed of the wound rotor induction motor is constant and the slip ratio, S, can only vary according to the changes in the rotor speed that is:

$$S = 1 - (w/w_s) \tag{3.4-53}$$

The initial steady state position is also determined based on the same approach described earlier for the squirrel cage motor. That is:

$$T_{m,norm} = \frac{T_{hyd} + T_{fr}}{T_D} = \left(a_2 \frac{S}{R} + b_2 \frac{R}{S}\right)^{-1} \quad (3.4\text{-}54)$$

which can be solved for R:

$$R = [1 + (1 - 4a_2 b_2 T^2_{m,norm})^{1/2}]S/(2b_2 T_{m,norm}) \quad (3.4\text{-}55)$$

and therefore using Equations (3.4-49) to (3.4-51) one obtains:

$$Z = Z_o = 1 - [R_m (R - 1)/R_{max}]^{1/3} \quad (3.4\text{-}56)$$

It is important to note that Z cannot exceed the value of one, which is its maximum position.

3.4.3.5 STEAM GENERATOR CONTROL

The purpose of the steam generator control system is to maintain the temperature, pressure, level, and pump speed at the desired value for both normal and off normal operating conditions. The steam generator control systems consist of (a) feedwater system and (b) turbine and pressure relief mechanisms.

There are generally two different types of steam generators which have been considered for LMFBR power plants; namely, recirculation type and the once-through design.

The recirculation type consists of a steam drum, evaporators, superheaters and a steam header. The feedwater flow rate and feedwater pump speed are controlled in order to maintain a desired control valve pressure drop and steam drum water level and minimize the difference between the feedwater flow into the drum and the saturated steam flow out of the drum. The steam flow rate out of the steam header is controlled based on near constant pressure at the first stage of the high pressure turbine. To enable the nuclear steam

supply system to follow turbine load reductions, which may include large step or ramp changes, an artificial steam load is incorporated. This load is created by dumping steam from the steam header to either condenser and/or atmosphere. The dump system is often controlled to give the required ramp load changes to prevent reactor scram. Following a turbine trip, the steam pressure relief system is switched to a closed loop pressure control mode based on constant header pressure.

The once-through design consists of a single unit sodium to water heat exchanger. The feedwater pump speed and control valves are also controlled to maintain the required valve pressure drop and steam flow rate at the main steam header. The turbine and pressure relief mechanisms are nearly identical for both recirculation and once-through steam generator designs.

In order to be able to represent the steam generator control adequately, a general multi-cascade valve controller and a general multi-cascade pump speed controller have been developed as will be discussed in the following subsections.

3.4.3.5.1 GENERAL MULTI-CASCADE VALVE CONTROLLER

The valve controller is modeled using the unit controller (cascade) strategy developed in Section 3.4.3.1. The number of cascades is dependent on the valve type and the system representation. The controller constants must be supplied by the user through input data.

The valve actuator dynamics is represented by a first order system accounting for deadzone and hysterisis effects as shown schematically in Figure 3.4-4,

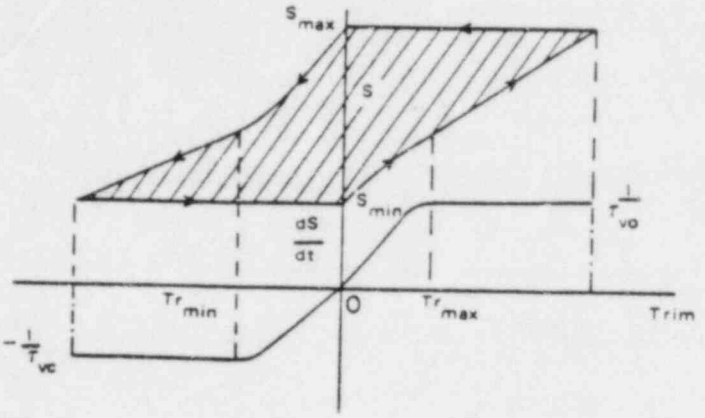

Fig. 3.4-4. Schematic Representation of Valve Deadzone and Hysteresis Effects

and mathematically represented by:

$$\frac{dS}{dt} = \begin{cases} \dfrac{Tr(t)}{Tr_{max}} \dfrac{1}{T_{vo}} & 0 \le Tr \le Tr_{max} \\ \dfrac{1}{T_{vo}} & Tr \ge Tr_{max} \end{cases} \Bigg\} \text{opening}$$

$$0 \qquad \text{stationary} \qquad (3.4\text{-}57)$$

$$\begin{cases} \dfrac{Tr(t)}{Tr_{min}} \dfrac{1}{T_{vc}} & Tr_{min} \le Tr \le 0 \\ -\dfrac{1}{T_{vc}} & Tr \le Tr_{min} \end{cases} \Bigg\} \text{closing}$$

where Tr is the actuator input forcing function (output trim signal from the last unit controller), Tr_{max} is the trim signal at which the valve actuator achieves its maximum opening speed (a positive number), Tr_{min} is the trim

signal at which the valve actuator achieves its maximum closing speed (a negative number), T_{vo} is the time in seconds to open the valve from its minimum opening, S_{min}, to its maximum opening, S_{max}, T_{vc} is the time in seconds to close the valve from its maximum opening, S_{max}, to its minimum opening, S_{min} (note T_{vo} is not necessarily equal to T_{vc}), and S is the fractional valve stem position (opening) which is bounded by:

$$S_{min} \leq S \leq S_{max} \tag{3.4-58}$$

In order to be able to simulate valve dynamics without the hysteresis effect, the user must input identical values for Tr_{max} and Tr_{min} (in both sign and magnitude).

The model also permits the simulation of uncontrolled valve closure caused by turbine trip conditions at any desired time into the transient.

3.4.3.5.2 GENERAL MULTI-CASCADE SPEED CONTROLLER

The feedwater pump speed controller is modeled using the same multi-cascade system, with the trim signal from the last unit controller as the forcing function to the pump drive actuator.

The feedwater drive system is represented by a much simpler model as compared to the sodium pump drives. This approach was chosen because the influence of the behavior of the feedwater pumps for operational transients is less significant than the sodium pumps.

The dynamic behavior of the feedwater pumps is therefore represented by the following first order system:

$$T_f \frac{d\alpha}{dt} = \alpha_d - \alpha \tag{3.4-59}$$

where T_f is pump time constant(s) (e-folding time), α is the normalized pump speed, and α_d is the normalized demanded speed given by the controller as:

$$\alpha_d = Tr + \alpha_0 \qquad (3.4\text{-}60)$$

Here Tr is the trim signal from the last unit controller (cascade) and α_0 is the initial pump speed. This definition of Equation (3.4-60) is in agreement with the steady state solution, where Tr = 0 and $\alpha_d = \alpha_0$ as required.

Following pump trip the demanded speed, α_d is set to zero and the pump speed will decay exponentially in accordance with Equation (3.4-59).

3.4.4. NUMERICAL METHODS AND OVERALL SYSTEM DYNAMICS

The mathematical models for dynamic simulation of plant protection and control systems discussed in the previous sections have been programmed and incorporated into the SSC computer code.

The proper sequence of calculations and the numerical integration techniques and coupling of the aforementioned models with SSC is discussed in this section.

3.4.4.1 NUMERICAL METHODS

Numerically the plant protection and control system models are assumed to be explicitly coupled with the SSC overall plant model. The integrations are performed assuming the plant is operating at steady state prior to the initiation of the transient (perturbation). However, for t>0, the updated actual

values of the process variables needed by the PPS-PCS models are used and the model equations are then integrated using the master clock timestep as determined by the SSC driver routine (see Chapter 4).

Close inspection of the model differential equations reveals that numerical stability can be insured so long as the value of the integrated function can be numerically and physically bounded to the value of its forcing function and/or the physical limits of the function itself. Keeping this definition in mind, it is seen that the only differential equations which can cause instability are those which possess short characteristic times such as (Equation 3.4-1) under the condition of small time constant T_m as compared to the integration timestep.

This problem can be remedied by either limiting the timestep to the characteristic time or bounding the value of the function to its forcing function. In the case of Equation (3.4-1) this implies setting $X_m = X_a$ if X_m exceeds X_a in magnitude. The former approach is used for equations where the characteristic time is readily available. Otherwise, numerical instability is prevented by bounding the value of the function.

The numerical integration of the differential equations is achieved using a fourth-order Runge-Kutta algorithm as described in References [3.4-4] and [3.4-13]. The numerical differentiation is performed using the backward difference scheme as was described in Equation (3.4-25).

The integration strategy used for the PPS-PCS as coupled to the SSC plant dynamic model has been very successfully tested and it was seen to be quite efficient and accurate for the cases of interest, which were taken to include abrupt and severe transients such as those reported in Reference [3.4-5].

3.4.4.2 OVERALL SYSTEM DYNAMICS

The plant protection and control system models described in the previous sections have been coded as various subroutines and incorporated into the SSC driver routine as shown in Figure 6-19 (PPCS8T).

It was mentioned earlier that the PPS-PCS calculations are explicit in nature, and therefore these subroutines are executed last in the sequence of transient calculations using the most recent values of the process variables just before the output process. The flow chart of each of the sub-drivers, along with its associated subroutines, is shown in Figures 6-22, 6-27, 6-28 and 6-29. The naming convention discussed in Section 6 is used in selecting program and subprogram names. Those with the digit "8" in the fifth position indicate the PPS-PCS modules.

REFERENCES FOR SECTION 3.4

3.4-1 W. H. Alliston, et al., "Clinch River Breeder Reactor Plant; LMFBR Demo Plant Simulation Model (DEMO)," CRBRP-ARD-0005, (1978).

3.4-2 D. L. Hetrick and G. W. Sowers, "BRENDA: A Dynamic simulator for a Sodium-Cooled Fast Reactor Power Plant," U.S. Nuclear Regulatory Commission, NUREG/CR-0244, (1978).

3.4-3 K. B. Cady, M. Khatib-Rahbar, G. F. Pavlenco, and J. R. Raber, "EPRI-CURL: Dynamic Analysis of Loop-Type LMFBRs", Electric Power Research Institute, Inc., EPRI-NP-1001 (1979).

3.4-4 M. Khatib-Rahbar, "System Modeling for Transient Analysis of Loop-Type Liquid-Metal-Cooled Fast Breeder Reactors," Cornell University Reactor Laboratory, CURL-53 (1978).

3.4-5 M. Khatib-Rahbar, A. K. Agrawal, and E. S. Srinivasan, "Feedback Control Systems for Non-Linear Simulation of Operational Transients in LMFBRs," in Proc. of the ANS/ENS Intrernational Meeting on Fast Reactor Safety Technology Meeting, Vol, III, 1316, Seattle, WA, August 19-23, (1979).

3.4-6 D. R. Coughanowr, and L. B. Koppel, Process Systems Analysis and Control, McGraw-Hill Book Co., New York (1965).

3.4-7 Clinch River Breeder Reactor Plant Preliminary Safety Analysis Report, Project Management Corporation (1975).

3.4-8 Fast Flux Test Facility Final Safety Analysis Reprt, HEDL-TI--7500 (1975).

3.4-9 "Operator's Manual for Vutronik Cascade Control Stations", Honeywell Industrial Division, Operator's Manual 37-01-05, Issue 2, Fort Washington, PA (1973).

3.4-10 J. R. Lamarsh, Introduction to Nuclear Reactor Theory, Addison-Wesley Publishing Co., Inc., Massachusetts (1961).

3.4-11 M. A. Schultz, Control of Nuclear Reactors and Power Plants, 2nd Edition, McGraw-Hill Book co., Inc., New York (1961).

3.4-12 P. L. Alger, Induction Machines, Gordon and Breach Science Publishers, New York (1970).

3.4-13 B. Carnahan, H. A. Luther, and J. O. Wilkes, Applied Numerical Methods, John Wiley & Sons, Inc., New York (1969).

4. NUMERICAL TECHNIQUES

The thermohydraulic transient simulation of an entire LMFBR system is, by its very nature, complex. Physically, the entire plant consists of many subsystems which are coupled by various processes and/or components. Mathematically, each subsystem constitutes a set of differential equations with appropriate boundary conditions. The connections between different subsystems are made through interface conditions. The numerical methods employed in the SSC-L code are discussed in this chapter.

4.1 STEADY-STATE SOLUTION

4.1.1 DESCRIPTION

The essential components and their arrangement in a loop-type LMFBR are schematically shown in Figure 4-1. Although only one set of loops is explicitly shown in this figure, any plant can, and does, have two or more sets of loops. In the SSC-L code, the number of such sets of loops is an input parameter. In actual running of the code, one can simulate most transients by one or two sets of loops.

As shown in Figure 4-1, the primary heat transport system (PHTS) consists of the reactor vessel and its internals, pump, primary side of the intermediate heat exchanger (IHX), check valve, and pipes connecting these major components. The centrifugal pump is a variable speed pump. It provides pumping head for offsetting the pressure losses due to friction, change in elvation, and other considerations. The absolute pressure in this closed loop is determined when the cover gas pressure is specified. Typically, the cover gas pressure is close to the atmospheric pressure.

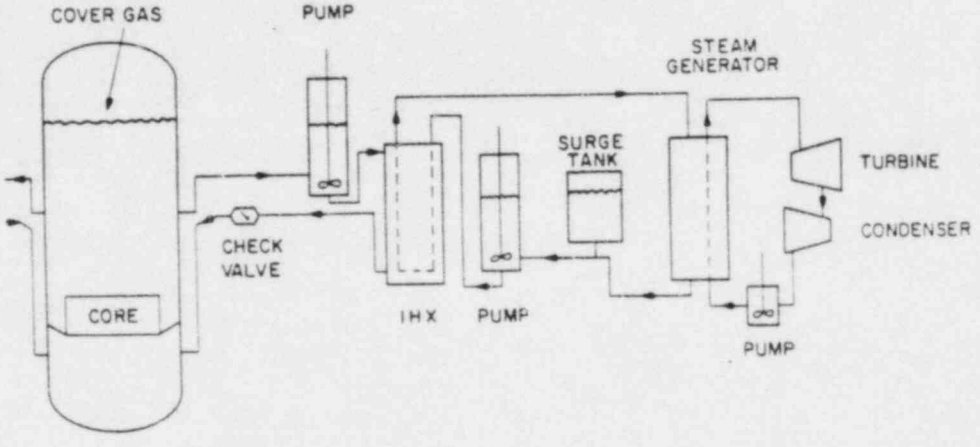

Figure 4-1 Sketch of the Heat Transport System

The intermediate heat transport system (IHTS) consists of the secondary sodium side of the IHX, sodium side in the steam generator, surge tank to accommodate change in sodium volume, pump, and pipes connecting these components. The hydraulic characterization of this closed loop is very similar to that of the PHTS.

The steam generating system, including the portion of intermediate loop in the evaporator and superheater region, is analyzed using the MINET package of subroutines. This package performs a thermal and hydraulic analysis of networks of pipe, pump, heat exchanger, valve, accumulator, and boundary modules, under both steady state and transient conditions.

4.1.2 NUMERICAL METHOD

The main objective of the SSC preaccident calculations is to provide a unique and stable plant-wide solution for the initialization of the transient analysis. The preaccident calculations for the entire plant including all of the essential components in the primary, secondary, and tertiary heat transport system can be time consuming if the overall conservation equations are solved simultaneously. One way to reduce demand on computing time is to take advantage of special features of the plant.

For example, the energy and momentum equations for liquid sodium can be decoupled since thermal properties are independent of pressure. Thus, the energy conservation equations for the primary and intermediate sodium loops can be solved first. The required pumping head is obtained by solving the momentum conservation equation. The energy and momentum equations for the water

loop, however, cannot be decoupled since the pressure-dependent nature of the two-phase water properties must be considered.

The resulting system of equations to be solved is a typical set of "m" nonlinear coupled algebraic equations with "n" unknowns (n>m). Certain groups of these equations representing the IHX and steam generator (on a component basis) must be solved iteratively. As the number of unknowns is greater than the number of independent equations, some plant variables must be known (i.e., specified) a priori. Since uncertainties may exist as to which operating conditions are known or unknown, the user is allowed some flexibility in the selection of plant variables which are input and those which are to be calculated.

The overall logic for the plant thermal and hydraulic steady-state balance is as follows:

1. Determine the unspecified primary loop parameter from the reactor power and two of the three parameters: primary loop mass flow rate, core inlet temperature, and core outlet temperature. A simple energy balance is used.
2. Iteratively solve for two of three intermediate loop parameters, the intermediate loop mass flow rate, the IHX inlet temperature, and the IHX outlet temperature. The third parameter is taken as user input. The two missing parameters are varied, while constrained by energy balance to one another, to give the proper heat transfer through the IHX.

3. Call the MINET package with intermediate loop mass flow rate, as well as hot and cold leg temperatures. The pipe inertia and pressure loss calculated in MINET and returned to the intermediate loop.
4. Determine the detailed in-core thermal and hydraulic balance.
5. Initialize:
   (a) primary loop hydraulics;
   (b) secondary loop hydraulics.
6. Initialize:
   (a) primary pump speed;
   (b) secondary pump speed

Since the calculation of the plant hydraulic balance (see steps 5 and 6 above) can be done on a per loop basis and requires no iteration or special techniques, it is not discussed further here. The detailed in-vessel balance is described in Section 3.1. However, the gross plant thermal balance warrants some discussion.

A plant schematic of an equivalent single-loop system is presented in Figure 4-2. The gross energy balance equations may be given by the following set of three independent equations:

$$Q = W_p [e(T_{Ro}) - e(T_{Ri})], \tag{4-1}$$

$$Q = U_I A_I \Delta T_I^{LM}, \tag{4-2}$$

$$Q = W_I [e(T_{Io}) - e(T_{Ii})], \tag{4-3}$$

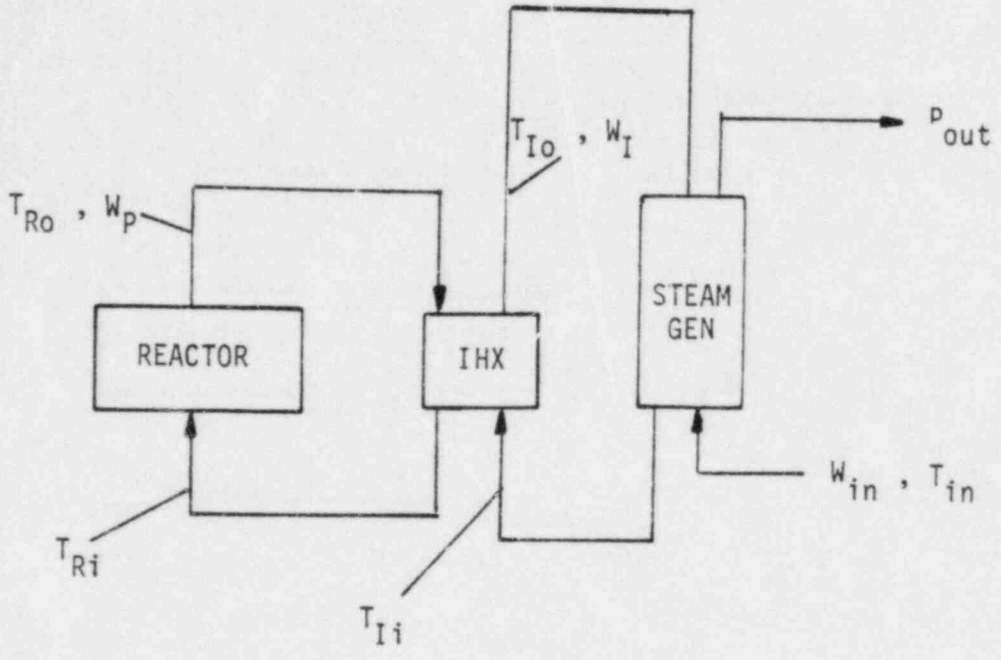

Figure 4-2 Plant Schematic

where ΔT^{LM} denotes the log-mean temperature difference and it is defined by the following expression:

$$\Delta T^{LM} = \frac{(\Delta T)_{outlet} - (\Delta T)_{inlet}}{\ell n \frac{(\Delta T)_{outlet}}{(\Delta T)_{inlet}}} \quad . \tag{4-4}$$

Equation 4-2 was obtained by assuming a once through heat exchanger, and that U_I, the overall heat transfer coefficient of the IHX is constant throughout the heat transfer portions. It is assumed to be known from empirical relationships.

In actual computations for the steady-state in SSC-L, Equation 4-2 is replaced by a series of nodal heat balances. The overall effective heat transfer coefficient for each of these nodes is computed as a function of flow conditions, temperature, and fouling. More details of the procedure can be found in Section 3.2.

4.2 INTEGRATION METHOD

The numerical integration in time of the entire system may be carried out in various ways. Two such integration strategies, geared to digital computer applications, are discussed further in this section: (1) intergration of all variables at a common timestep (i.e., a single timestep scheme, STS), or (2) integration of various processes/components at different timesteps (i.e., a multiple timestep scheme, MTS).

4.2.1 Single Timestep Scheme (STS)

The integration of the entire set of governing differential equations can be readily handled by advancing all time-dependent variables at a common timestep. This single timestep scheme (STS) is the simplest method from the standpoint of the computational logic involved.

In order to satisfy both stability and accuracy requirements, the timestep size (h) has to be the smallest of all h's for different processes. Depending on the integration method used, the smallest h may or may not be a function of time. In any case, the entire system is solved using a common, single value for h at any instant.

For the various processes/components modeled in the SSC-L simulation, estimates for characteristic integration timesteps are shown schematically in Figure 4-3. [As seen in Figure 4-3, the allowable timestep size spans several orders of magnitude and may be quite small.] Thus, although the logic is reduced, a penalty in terms of computational time spent in various parts of the

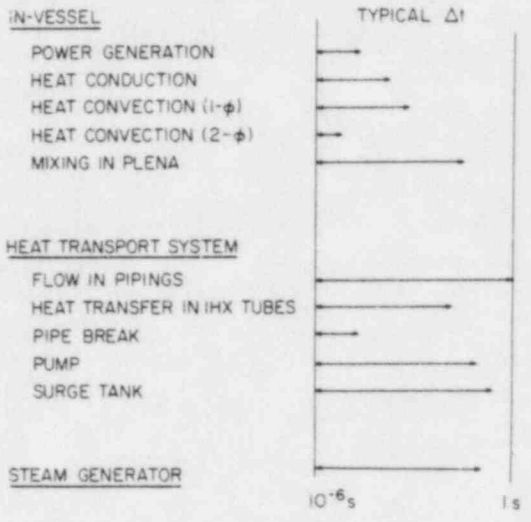

Figure 4-3 An Estimate of Timestep Sizes by Processes

system where variations are occurring less rapidly or where, by the nature of the particular process, a larger timestep could be allowed, must be paid. Indeed, for test cases run at BNL, factors of 5 in computational running times were seen between identical cases analyzed using the STS versus the MTS [4-1]. For this reason, the MTS method is used to handle the integration in time of the SSC-L code.

4.2.2 MULTIPLE TIMESTEP SCHEME (MTS)

A computationally more efficient integration strategy, which takes advantage of the fact that different components/processes may have widely varying timestep size requirements, is being used in the SSC-L code [4-1]. In this method, various portions of the overall system are advanced at different timesteps, all being controlled, however, by a master clock. This method is denoted as the multiple timestep scheme (MTS). It should be noted that the MTS is closely related to the method of fractional steps of Yanenko [4-2]. In this section, the division of the overall system into subsystems and the resulting timestep hierarchy and computational logic are discussed. Later sections address the individual subsystem integration method and timestep control, as well as the overall interfacing between subsystems.

The application of the MTS to the SSC code is based on physical considerations. For example, some of the subsystems or processes are known to respond rapidly while others change slowly. In general, hydraulic response is more rapid than energy/temperature response.

An important asumption used in the SSC-L code which has bearing here needs to be reiterated. In all regions of the system containing single-phase sodium

coolant (i.e., primary loops, intermediate loops, and reactor plena), the appropriate sodium properties are assumed to be functions of temperature only (i.e., not of pressure). Once this assumption is made and the sodium properties investigated, they are found to be slowly varying functions of temperature.

The convective energy equations are coupled to their respective sodium flow rates, and the flow rates are coupled to the plant temperatures. However, while the coupling of the convective energy equations to the sodium flow rates is very strong, the coupling of the flow rates to the temperatures is weak and enters only through the temperature-dependent nature of the sodium properties. Since the properties vary slowly, the possibility exists to solve for the sodium flow rates at a different timestep than the energy equations.

4.2.2.1 DIVISION OF OVERALL SYSTEM INTO SUBSYSTEMS

In the SSC-L code, the momentum equations governing the flow rates for the reactor vessel and all the sodium loops are handled separately. These momentum equations are advanced in time first. The sodium properties required are evaluated using the plant temperatures at the end of the previously completed timestep. For the purpose of the hydraulic equations only, these temperatures (and, consequently, the sodium properties used in the momentum equations) are assumed to remain constant during the hydraulic timestep. Subsequently, once all the energy equations have been advanced to the hydraulic time, the updated values of temperature are then used to calculate the sodium properties for the next hydraulic timestep.

Because of the existence of two phases on the tertiary side of the steam generators, the required water properties are highly pressure and temperature dependent. Thus, the thermal and hydraulic equations on the water side cannot be treated separately, but must be advanced in time simultaneously. Also included within this set of equations are the energy equations on the sodium side of the steam generators.

The remainder of the system energy equations are segmented into two groups. The first group encompasses all the energy equations in the primary and intermediate loops, inclusive of the IHX, but exclusive of those on the steam generator sodium-side. The in-vessel energy equations encompass the second group and include those dealing with heat conduction and power generation in the rods and those associated with the sodium coolant convection.

Thus, the various required computations can be grouped into four separate categories: (1) vessel and loop hydraulic calculations; (2) in-vessel sodium coolant energy, rod heat conduction and power generation calculations; (3) steam generator thermal and water-side hydraulic calculations; and (4) loop energy calculations.

With the preceding discussion in mind, Figure 4-4 should be referred to. Shown here is a schematic of the plant indicating the major components. Also shown are the names of those subroutines which are the main driver modules controlling the advancement in time of various blocks of the SSC-L transient segment.

The various driver modules are:

FLOW1T, FLOW2T — Drivers (called by the same DRIV1T module) for the vessel, primary and intermediate loop sodium coolant hydraulics.

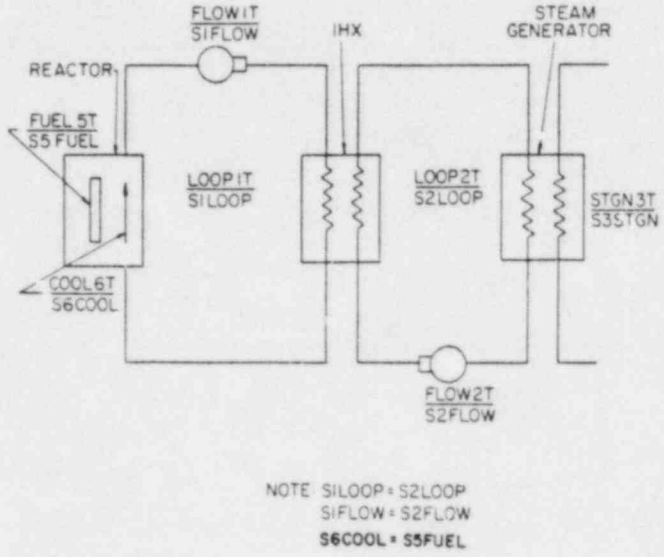

Figure 4-4 A Schematic of Transient Computational Modules and Respective Times

COOL6T, FUEL5T — Drivers for the in-vessel sodium coolant energy calculations and for the in-vessel rod heat conduction and power generation calculations, respectively.

STGN3T — Driver for the steam generator energy and water-side hydraulic calculations.

LOOP1T, LOOP2T — Drivers for the primary and intermediate loop energy calculations, respectively.

A further breakdown of all subroutines which are associated with each driver is provided in Chapter 6.

Also shown in Figure 4-4, listed under each subroutine name, is the respective variable name of the simulation time of that associated section of the code. For example, S5FUEL is the current time (s) at which in rod heat conduction and power generation calculations are being computed (driven by FUEL5T). Note, that since the primary and intermediate loop hydraulics are advanced at a common timestep, their respective simulation times are identical (i.e., S1FLOW = S2FLOW). The same is true for the primary and intermediate loop energy calculations (i.e., S1LOOP = S2LOOP), as well as for the in-vessel energy calculations (i.e., S5FUEL = S6COOL).

4.2.2.2 TIMESTEP HIERARCHY

In conjunction with the partitioning of the SSC-L transient segment as discussed above, a timestep hierarchy for the advancement in time of the entire system must be established. The variable name for the master clock, to which all sections must be advanced, is designated S9MSTR. The corresponding master timestep is designated S9DELT. Table 4-1 indicates the various trans-

Table 4-1

Code Sections with Corresponding
Simulation Times and Timestep Names

Section	Simulation Time (s)	Timestep (s)
Master Clock	S9MSTR	S9DELT
FLOW1T	S1FLOW	S1DELW
FLOW2T	S2FLOW	S2DELW
FUEL5T	S5FUEL	S5DELT
COOL6T	S6COOL	S6DELT
STGN3T	S3TIME	S3DELT
LOOP1T	S1LOOP	S1DELT
LOOP2T	S2LOOP	S2DELT

ient code sections, their corresponding simulation time variable names, and respective timestep names.

As in the partitioning of the SSC-L transient segment, knowledge of the system was used in the selection of the specific hierarchy of the various timesteps. Since the loop temperatures are assumed to respond more slowly, in general, than any other temperatures in the system, the respective timesteps at which those variables are advanced are set equal to the master clock timestep (i.e., S9DELT = S1DELT = S2DELT).

Although the hydraulic calculations are driven separately, the plant sodium temperatures are very tightly coupled to them. Thus, the hydraulic timestep must exert some influence on the master timestep, since S9DELT controls how rapidly the loop energy equations may advance. As discussed in the preceding section, the hydraulic calculations may be advanced for one timestep using the values of the sodium temperatures at the end of the previous timestep. Since the sodium temperatures depend strongly on the flow rates, the hydraulic calculations must be executed first during any given master timestep. Once the hydraulics are advanced one timestep (i.e., S1DELW = S2DELW), a check is immediately made. If the hydraulic timestep had to be reduced (as dictated by the hydraulic integration package's accuracy and/or stability requirements), the master timestep is also immediately reduced. If the hydraulic timestep may be increased, this is not allowed until the succeeding timestep, so the master timestep is not altered yet. The hydraulic timestep is by far the more restrictive of the two (i.e., S1DELW is more restrictive than S1DELT), because of the sensitive nature of the hydraulic equations. Thus, in general, once the hydraulic timestep is allowed to increase, the loop energy timestep immediately follows.

Summarizing for the hydraulic timestep limits then; S1DELW (which is the same as S2DELW) will never be less than, will most always equal, but occasionally may be greater than (for one time increment) the master timestep (S9DELT = S1DELT = S2DELT). It should also be noted again, that the hydraulic equations must be advanced first (i.e., before any other part of the system).

As discussed previously, the in-vessel calcuations consist of two sections: (1) sodium coolant convection calculations, and (2) rod heat conduction and power generation calculations. Since the calculations controlled by COOL6T (see Figure 4-4) are executed at the same timestep as those controlled by FUEL5T, the timestep hierarchy for these calculations is as follows:

$$S6DELT = S5DELT \leq S9DELT \quad .$$

The remaining section of the hierarchy to be assigned encompasses the steam generator calculations, driven by STGN3T. In the steam generator, both the thermal and water-side hydraulic calculations are advanced at a common timestep (S3DELT). Since the only interface with the steam generator is through the intermediate loop, the STGN3T calculations and its corresponding timestep are nested within the loop energy calculations. Thus, $S3DELT \leq S9DELT$.

The various criteria used for the timestep control of these four code sections, as well as the logic and computational algorithm involved, are discussed in detail in succeeding sections of this chapter.

4.2.3 INDIVIDUAL COMPONENT/PROCESS SOLVER

As presented in Section 4.2.2, the time integration of the entire SSC transient is divided into four sections.

(1) Primary and intermediate loop hydraulic calculations.

(2) In-vessel sodium coolant convection, rod heat conduction and power generation calculations.

(3) Steam generator energy (including the steam generator, sodium, and tube wall) and water-side hydraulic calculations.

(4) Primary and intermediate loop energy (exclusive of the steam generator sodium side) calculations.

The following discussion will proceed in the order just mentioned. Only the integration method used in the various components/processes will be mentioned here. For a description of the models and/or equations which represent any particular system, refer to the appropriate section in Chapter 3. The timestep control is discussed in Section 4.3.

The momentum equations describing the hydraulic response of the primary and intermediate loops are integrated explicitly. The integration scheme is a fifth-order predictor-corrector method [4-3] of the Adams type. Algorithms are provided within the package for automatically changing the step size (by factors of 2.0) according to the accuracy requested by the user. Checks are included to test for the stability of the numerical method and to test for accuracy requests which cannot be met because of round-off error.

The majority of the differential equations describing the thermal response in the vessel are handled by a first-order (i.e., single layer) semi-implicit integration scheme. By semi-implicit is meant a theta-differencing method where $\theta = 1/2$.

The energy equations in the lower plenum are handled by this first-order semi-implicit scheme. The differential equations in the upper mixing plenum encompass various energy and coolant level calculations. Since the equations also include the sodium level calculation which is important to the pressure

and hydraulic response, they are under control of the hydraulic integration package.

In the core region, the coolant energy equations are decoupled from the fuel heat conduction equations at the cladding wall. Once this decoupling is done, the time integration of the energy equations can be handled by a simple marching technique for each channel.

The transient heat conduction equations in the rod are handled by applying a first-order extrapolated Crank-Nicholson differencing scheme [4-5] to the descretized radial nodes. The solution proceeds inward from the cladding/coolant interface for each axial slice in each channel.

The method for advancing the transient neutron fission power utilizes either the prompt jump approximation or an "exact" solution to the point reactor kinetics equations as desired. This "exact" solution is a modified version of the method proposed by Kaganove [4-6].

The coolant energy equations are advanced using a first-order fully-implicit integration scheme. The solution proceeds up or down each channel depending on the direction of flow.

The steam generator thermal and water-side hydraulics equations are advanced using a first-order, semi-implicit integration scheme. The solution procedure involves marching first through the steam generator segments and secondly through the accumulators. The steam generator tube wall temperatures are lagged one timestep. This effectively decouples the sodium and water/steam sides and allows a simple marching procedure to be used. The accumulator conditions are advanced first. These conditions are then back-substituted so that the advanced steam generator water-side enthalpies and sodium temperatures in all control volumes and the advanced flow rates can be

solved for. Finally, the advanced conditions for the heat fluxes and tube wall temperatures are computed.

The loop energy equations are integrated by a first-order fully-implicit scheme. The wall heat fluxes are lagged one timestep. This decouples the energy equations and allows them to be solved in a simple marching fashion (in the direction of flow) without resorting to matrix inversions.

4.2.4 OVERALL INTERFACING

The advancement in time of the entire SSC transient segment has been divided into four sections, as discussed earlier in Section 4.2.2. Each section has its own individual timestep and uses various methods to handle the integration (see Section 4.2.3). Discussed here are the overall interface conditions required between these four sections and how they are computed. The impact of these interface conditions on the overall timestep control is addressed in Section 4.3.

The interface conditions are presented in the order in which they are required. Specifically:

(1) Primary and intermediate loop hydraulics interface conditions.

(2) In-vessel sodium coolant energy, rod heat conduction and power generation interface conditions.

(3) Steam generator interface conditions.

(4) Primary and intermediate loop energy interface conditions.

The primary and secondary loop hydraulics calculations interface with other SSC sections through various system temperatures and pressure-related conditions. As discussed in Section 4.2.2, the coupling of the hydraulic response to temperature variations is weak (through sodium properties), and,

consequently, temperature conditions updated at the end of the previous timestep are used during the succeeding hydraulic timestep. Thus, once this assumption is made, there are no interface conditions to be provided to the hydraulic calculations, and they become self-contained.

The rod heat conduction calculations interface with the in-vessel coolant energy calculations at the cladding-coolant boundaries. As discussed in Section 4.2.2.2, the coolant energy calculations are nested with the rod calculations and are executed simultaneously at each axial slice.

The in-vessel coolant energy equations require interface conditions of temperature at the vessel inlet nozzle(s). Since advanced values of the vessel inlet temperature(s) have not been calculated when the coolant energy equations are updated, extrapolations are required. Currently, since the pipe energy equations generally respond slowly, the value(s) of the vessel inlet temperature(s) is(are) used.

The required interface conditions at the steam generator boundaries are the intermediate loop sodium flow rate(s) and the intermediate loop temperature(s) at the steam generator heat exchanger sodium-side inlet(s). The intermediate loop flow rate(s) at the advanced steam generator time is already available, since the sodium loop hydraulics equations have been integrated previously.

The interface conditions required for the primary and intermediate loop energy calculations are (1) the vessel outlet temperature, (2) the sodium-side temperature(s) at the steam generator heat exchanger outlet(s), and (3) the sodium flow rate in each primary and intermediate loop. Since the loop energy equations are integrated last, all these required interface conditions from the other SSC transient sections are available at the advanced loop energy time (S1LOOP = S2LOOP = S9MSTR, see Section 4.2.2).

4.3 TIMESTEP CONTROL

To provide for the automatic control of the four separate timesteps utilized in the SSC transient segment, certain accuracy, numerical stability, and interface condition criteria must be established. The accuracy and numerical stability criteria apply to the specific integration method(s) (see Section 4.2.3) used in each of the four transient sections. The interface criteria apply to the boundary conditions (see Section 4.2.4) connecting the four sections to each other. In this section, the various criteria used to determine the timestep control are first discussed, then the specific algorithm used for the actual control of all timesteps in the SSC transient segment is described.

4.3.1 NUMERICAL STABILITY AND ACCURACY CRITERIA

As discussed in Section 4.2.3, all the integration methods used in SSC, with the exception of the primary and intermediate loop sodium hydraulics and reactor fission power generation (when using the prompt jump approximation - PJA) integration schemes are either of a fully-implicit or semi-implicit type.

Any scheme using an implicit technique is, by its very nature, inherently stable in a numerical sense.

The integration scheme used to advance the primary and intermediate loop hydraulic equations consists of a fifth-order predictor-corrector method of the Adams type. An algorithm is provided within the integration package to test for the stability of the numerical method. Thus, automatic control of the timesteps (i.e., S1DELW and S2DELW for the loop hydraulics and for the PJA, see Section 4.2.2.2) for numerical stability criteria is handled within the integration scheme itself. The user is allowed no control over these numerical stability criteria.

The accuracy criteria provided within SSC enable the user to select the degree of accuracy one desires for the various system variables being integrated. All accuracy criteria require a relative accuracy limit, which is supplied by the user. A value of the relative accuracy limit desired for each of the four transient sections must be input.

These relative accuracy limits are used such that any variable being integrated in any of the four transient sections is not allowed to change, in a relative sense, by more than the specified limit during any timestep. Thus, for any variable (Ω_{ij}) being integrated, the following holds:

$$\alpha_{ij} = |(\Omega_{ij}^{k+1} - \Omega_{ij}^{k})/\Omega_{ij}^{k}| \leq \alpha_i \qquad (4\text{-}6)$$

where:

α_{ij} = absolute relative deviation of variable Ω_{ij} from timestep k to k+1,

Ω_{ij}^{k+1} = value of Ω_{ij} at timestep k+1.

Ω_{ij}^{k} = value of Ω_{ij} at timestep k, and

α_i = relative accuracy limit specified for transient section i.

Table 4-2 lists the four SSC transient sections and the names of their corresponding α_i.

Within each transient section, after a timestep advancement has been completed, Equation 4-6 is applied to all variables just integrated. The maximum absolute relative change (α_{ij}-max) is selected and compared to the relative accuracy limit for that transient section. If the limit has been exceeded, the timestep for that section, which will be used during the next integration step, is decreased by a factor of 2.0. Conversely, if α_{ij}-max is less than a certain value (set equal to $\alpha_i/2.0$), the timestep for that section is allowed to increase by a (factor of 2.0) during the next integration step.

Table 4-2

SSC Transient Sections and
Corresponding Names for Accuracy Criterion Limits

Section	Relative Accuracy Criterion Limit (α_i)
FLOW1T FLOW2T	F1WMXA
COOL6T FUEL5T	F5MAXA
STGN3T	Controlled Internally
LOOP1T LOOP2T	F1EMXA

This evaluation of the various α_{ij}-max values from each transient section is performed after each timestep and forms the basis for the overall SSC automatic timestep control from an accuracy standpoint. For all sections integrated by fully-implicit or semi-implicit methods, the calculations of the specific α_{ij}-max values are handled in separate subroutines developed expressly for this purpose (see Chapter 6). The α_{ij} values for those variables integrated explicitly are calculated internally within the predictor-corrector package.

4.3.2 INTERFACE CONDITION CRITERIA

As discussed in Section 4.2.4, the four SSC transient sections are coupled together through various interface conditions at component/process boundaries. Some interface conditions involve variables which have already been computed (i.e., already advanced/updated in time) at the point in the execution logic when they are required. The remaining interface conditions involve variables whose advanced/updated values have not yet been computed at the point they are needed. Only these latter ("unknown") interface conditions need to be considered in establishing the interface condition criteria.

Listed in order of their requirement by the SSC transient sections, these "unknown" interface conditions (see Section 4.2.4 for a further discussion of how they are computed) are:

(1) For the primary and intermediate loop hydraulics calculations: None

(2) Rod heat conduction and power generation calculations: None

(3) In-vessel sodium coolant energy calculations: Sodium coolant temperature at vessel inlet nozzle(s),

(4) Steam generator energy and water-side hydraulics calculations: Intermediate loop temperature(s) at the steam generator heat exchanger sodium-side inlet(s).

(5) Primary and intermediate loop energy calculations: None.

At the end of each master clock step, all previously "unknown" interface conditions will have been computed. Thus, the values of the "unknown" interface conditions that were predicted during the just completed master clock timestep can be compared with the computed values for consistency. The following consistency check is made for each "unknown" interface conditions (Y_{ij}):

$$\Delta_{ij} = \left| \frac{p_{Y_{ij}}^{k+1} - c_{Y_{ij}}^{k+1}}{c_{Y_{ij}}^{k+1}} \right| \leq \Delta_i \quad , \tag{4-7}$$

where

Δ_{ij} = relative absolute deviation of interface condition Y_{ij} at end of timestep k+1.

$p_{Y_{ij}}^{k+1}$ = predicted value of Y_{ij} at end of timestep k+1 as used in transient section i.

$c_{Y_{ij}}^{k+1}$ = computed value of Y_{ij} at end of timestep k+1

Δ_i = relative absolute acceptance limit for interface conditions required by transient section i.

The values of Δ_i are specified by the user for all transient sections,

where appropriate.

Equation (4-7) is applied to all Y_{ij} at the end of each master timestep. The specific logic involved in implementing all these criteria is discussed in Section 4.2.4.

The purpose of the consistency checks performed using Equation (4-7) is to provide a means for establishing acceptance limit criteria for the "unknown" interface conditions. Whenever any Δ_{ij} fails to pass the consistency test (i.e., $\Delta_{ij} > \Delta_i$), the entire system time advancement is interrupted. The solution automatically reverts back to the end of the previously completed master clock integration step. The timestep in the transient section whose interface condition just failed the consistency test is decreased substantially. The solution of the overall system is then allowed to proceed once again.

4.3.3 MODIFICATIONS AT PRINT AND SUBSET INTERVALS

The discussion of the overall timestep control for SSC is now complete with the exception of modifications made at print and subset intervals. For print interval control, the user supplies the input data quantity S9PINT. This is the time interval (in seconds) at which the user desires various plant variables to be printed/stored. To ensure that the master clock time (S9MSTR, see Section 4.2.2.2) falls exactly on the print interval, modification to the master clock timestep (S9DELT) is occasionally necessary.

Additionally, whenever a subset interval time is reached, modification to the individual timestep for that transient section is required occasionally. As discussed in Section 4.2.2.2, the following subsets of timesteps are established within SSC:

(1) S6DELT = S5DELT $\leq$ S9DELT,

(2) S3DELT $\leq$ S9DELT.

As seen in Table 4-1, time step S6DELT corresponds to time S6COOL, S5DELT to S5FUEL, and S3DELT to S3TIME. Modifications to S5DELT and S3DELT are occasionally necessary to ensure that S5FUEL and S3STGN fall exactly on S9MSTR, respectively. The timestep control techniques used in SSC to handle modifications at both print intervals and subset intervals are identical.

A test is made before any transient section time is advanced to check if a print/subset interval would be exceeded using the current value of the timestep. If a print/subset interval would be exceeded, the following is done:

(1) The present allowed value of the affected timestep is stored.

(2) The affected timestep is set equal to the print/subset interval time minus the current time for the affected transient section.

(3) A control flag is set indicating that a modification (reduction) to the affected timestep has been made for reasons other than accuracy or stability.

(4) For the next integration step taken past the print/subset interval, the affected timestep is set equal to the presently allowed value for that timestep as dictated by accuracy, stability, and interface criteria.

4.3.4 ALGORITHM

The algorithm used in SSC to effect the overall automatic timestep control is shown in the logic diagram Figure 4-5. The various calculation drivers, transient section times, and timesteps are described in Section 4.2.2 and Table 4-1. Variables not identified in Table 4-1 include

- S9PRNT - time at which certain plant variables are to be printed/stored (seconds).
- S9PINT - Print interval increment (seconds).
- S9LAST - Problem termination time (seconds).

In Figure 4-5, the numbers in parentheses indicate the locations in the logic flow where the calculations for the four major sections of the SSC transient segment are executed. The remaining logic described in Figure 4-5 indicates how the criteria and modifications to the various SSC timesteps, discussed in Section 4.3.1 to 4.3.3, are implemented.

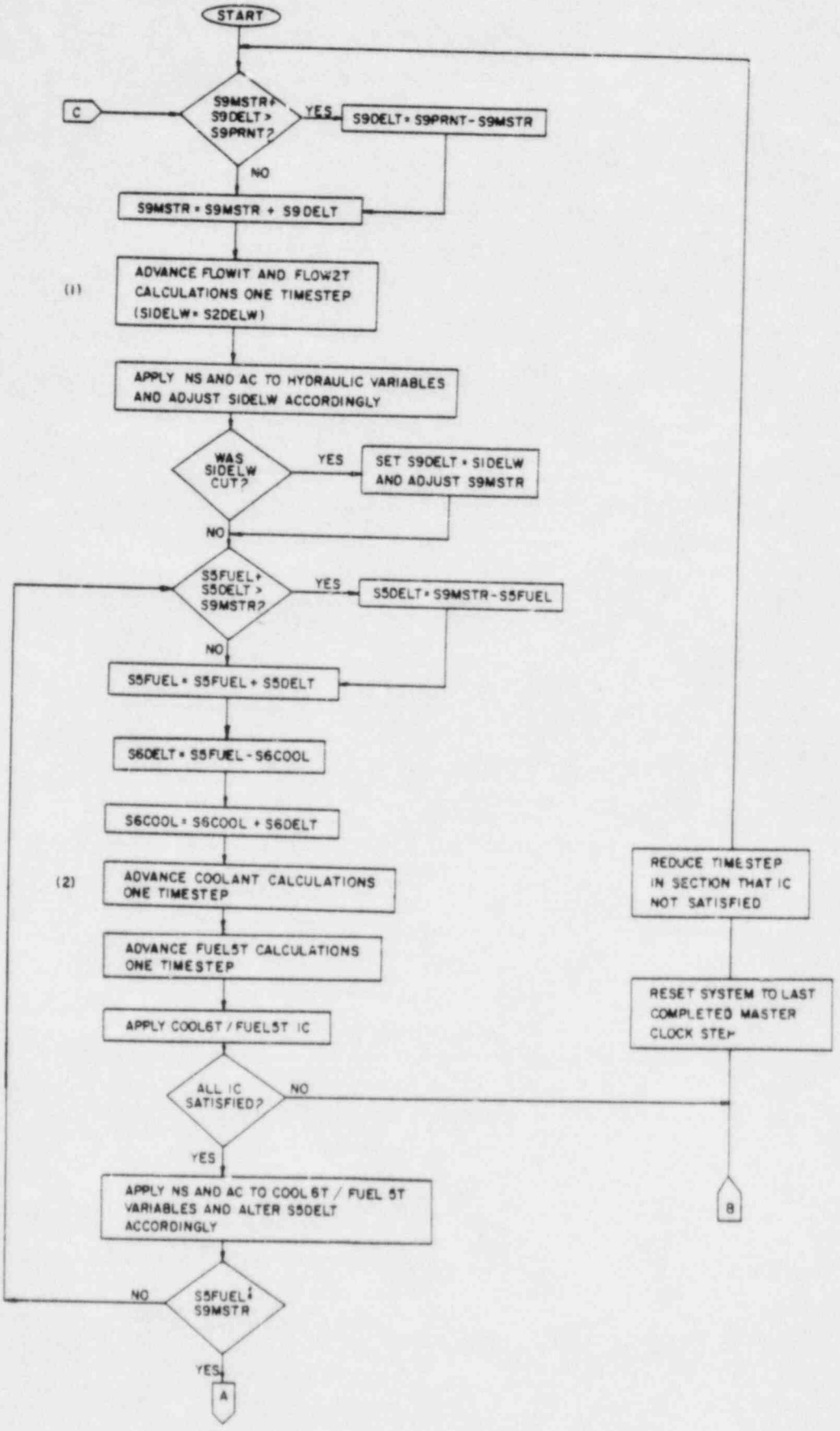

Figure 4-5 Logic Diagram for Overall SSC Timestep Control

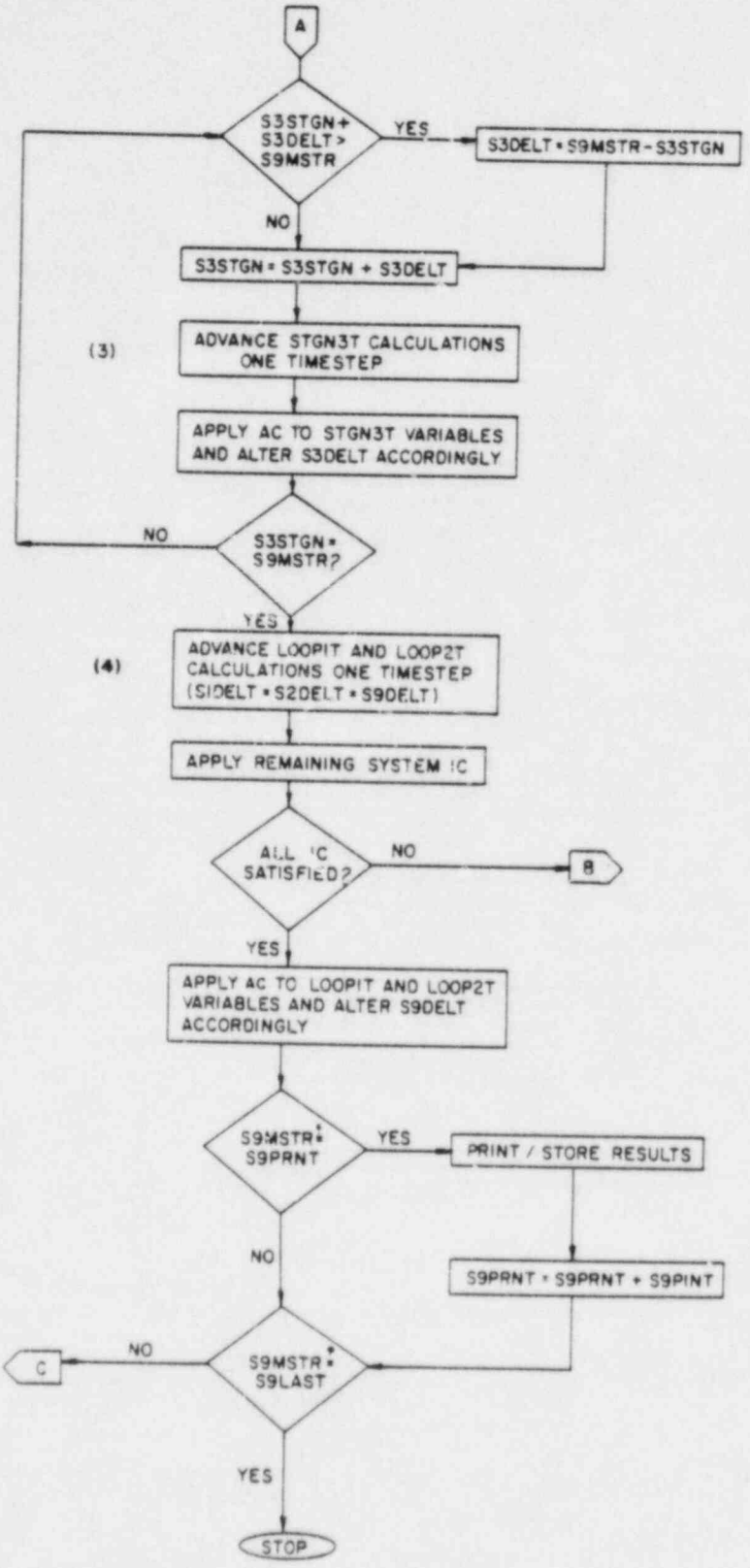

NOTE: NS AND AC – NUMERICAL STABILITY AND ACCURACY CRITERIA
AC – ACCURACY CRITERIA
IC – INTERFACE CRITERIA

Figure 4-5 (Cont'd) Logic Diagram for Overall SSC Timestep Control

REFERENCES FOR CHAPTER 4

4-1 J. G. Guppy, Application of Multiple Timestep Scheme in SSC-L, in Proc. ANS 1979 Winter Meeting, Vol. 33, p. 340, San Francisco, California, November 11-15, 1979.

4-2 N. N Yanenko, The Method of Fractional Steps, Springer-Verlag, New York, 1971.

4-3 F. T. Krogh, "Variable Order Integrators for the Numerical Solution of Ordinary Differential Equations," Jet Propulsion Laboratory Report, May 1, 1969.

4-4 M. Lees, "An Extropolated Crank-Ncholson Difference Scheme for Quasi-linear Parabolic Equations," Proceedings of the Symposium on Non-linear Partial Differential Equations, Academic Press, 1966.

4-5 A. C. Hindmarsh, "Linear Multistep Methods for Ordinary Differential Equations: Method Formulations, Stability, and the Methods of Nordsieck and Gear," UCRL-51186 Rev. 1, March 20, 1972.

4-6 J. J. Kaganove, "Numerical Solution of the One-Group, Space-Independent Reactor Kinetics Equations for Neutron Density given the Excess Reactivity," ANL-6132, 1960.

5. CONSTITUTIVE LAWS AND CORRELATIONS

A number of constitutive laws and correlations are required in order to execute the SSC code. The approach taken is based on providing the best available data into the code. The entire collection or part of these data may be overwritten by the user. This section describes collections of data that have been incorporated so far. All of the correlations and numerical values used are in SI units.

5.1 CONSTITUTIVE LAWS

The required thermophysical and transport properties for all of the materials of interest are provided for in the form of correlations. Reasonable values for the coefficients in these correlations are provided in SI units. These values may be changed by the user through input cards. Various constitutive laws are grouped according to materials.

5.1.1 CORE AND BLANKET FUEL

Thermal-conductivity (W/m K)

The thermal conductivity of mixed oxide [5-1] core (UO_2-20 w/o PuO_2) and blanket (oxide) materials is given by the following relation:

$$k(T,P) = \frac{k_0 (1-P)}{1 + (k_4 + k_5 P) P} \quad \frac{1}{k_1 + k_2 T} + k_3 T^3 \quad , \qquad (5\text{-}1)$$

where typical values for k_0, k_1, k_2, k_3, k_4 and k_5 are noted in Table 5-1, and P is the fractional porosity (= 1 - fractional density).

Table 5-1

Parameters in Fuel Thermal Conductivity
and Specific Heat Correlations

Parameter	Fuel material	Blanket material
k_o	113.3	113.3
k_1	0.78	0.78
k_2	0.02935	0.02935
k_3	6.60×10^{-13}	6.6×10^{-13}
k_4	1	1
k_5	10	10
P	input	input
c_o	194.319	194.319
c_1	1.3557×10^{-3}	1.3557×10^{-3}
c_2	-9.3301×10^{-7}	-9.3301×10^{-7}
c_3	2.4482×10^{-10}	2.4482×10^{-10}
c_4	502.951	502.951
c_5	0	0
c_6	0	0
T_1	3020.0	3020.0
T_2	3060.0	3060.0

Specific heat capacity (J/kg K)

The specific heat capacity of mixed-oxide [5-2] core and blanket materials is given by the following relations:

$$c_p(T) = c_o \left[1 + c_1 T + c_2 T^2 + c_3 T^3 + \frac{c_6}{T^2}\right] \qquad \text{for } T < T_1, \tag{5-2}$$

$$c_p(T) = c_p(T_1) + \frac{c_p(T_2) - c_p(T_1)}{T_2 - T_1} (T - T_1) \qquad \text{for } T_1 < T \leq T_2, \tag{5-3}$$

$$c_p(T) = c_4 + c_5 T \qquad \text{for } T > T_2, \tag{5-4}$$

where values of various parameters are noted in Table 5-1, and

$$c_p(T_1) = c_o \left[1 + c_1 T_1 + c_2 T_1^2 + c_3 T_1^3\right], \tag{5-5}$$

and

$$c_p(T_2) = c_4 + c_5 T_2 \quad . \tag{5-6}$$

Coefficient of thermal expansion (m/m K)

The average linear coefficient of thermal expansion from T_o to T for core and blanket materials is represented by the following equation [5-3, 5-4]:

$$\bar{\alpha}(T) = \alpha_0 + \alpha_1 T \qquad \text{for } T \leq T_3. \tag{5-7}$$

For higher temperatures, the average linear coefficient of thermal expansion is given by the following relation:

$$\bar{\alpha}(T) = \alpha_2 \qquad \text{for } T \geq T_4. \tag{5-8}$$

For intermediate temperatures,

$$\bar{\alpha}(T) = \bar{\alpha}(T_3) + \left[\frac{\bar{\alpha}(T_4) - \bar{\alpha}(T_3)}{T_4 - T_3}\right] (T - T_3) \qquad \text{for } T_3 < T < T_4, \tag{5-9}$$

where

$$\bar{\alpha}(T_3) = \alpha_0 + \alpha_1 T_3, \tag{5-10}$$

$$\bar{\alpha}(T_4) = \alpha_2, \tag{5-11}$$

and other parameters are noted in Table 5-2.

Density (kg/m^3)

The core and blanket fuel materials density is given by the following set of correlations:

$$\rho(T,P) = \frac{\rho_0(1 - P)}{[1 + \bar{\alpha}(T)\ (T - T_0)]^3} \qquad \text{for } T_0 \leq T \leq T_3, \tag{5-12}$$

$$\rho(T,P) = \rho(T_3, P) + \frac{\rho(T_4, P) - \rho\ (T_3, P)}{T_4 - T_3}(T - T_3) \qquad \text{for } T_3 < T \leq T_4, \tag{5-13}$$

$$\rho(T,P) = \frac{\rho_1}{[1 + \bar{\alpha}(T)\ (T - T_4)]^3} \qquad \text{for } T > T_4, \tag{5-14}$$

where P is the fractional porosity. The above correlations imply that (a) the core fuel density for different restructured regions have the same temperature dependence below fuel solidus temperature (T_3), and (b) the molten fuel density, i.e., density beyond its liquidus temperature (T_4), does not depend upon its pre-molten fractional density. The following two equations are noted for the sake of clarity:

$$\rho(T_3,P) = \frac{\rho_0(1 - P)}{[1 + \bar{\alpha}(T_3)(T_3 - T_0)]^3} \tag{5-15}$$

Table 5-2

Parameters in Fuel Coefficient of Thermal Expansion, Density and Emissivity Correlations

Parameter	Fuel material	Blanket material
α_0	5.7506×10^{-6}	5.7506×10^{-6}
α_1	2.997×10^{-9}	2.997×10^{-9}
α_2	3.1×10^{-5}	3.1×10^{-5}
T_0	295.4	295.4
T_3	3020.0	3020.0
T_4	3060.0	3060.0
ρ_0	11.04×10^{3}	10.0×10^{3}
ρ_1	8.733×10^{3}	8.744×10^{3}
P	input	input
e_0	0.75	0.75
e_1	5×10^{-5}	5×10^{-5}
T_5	400.0	400.0

and

$$\rho(T_4,P) = \rho_1 . \qquad (5\text{-}16)$$

The average linear coefficient of thermal expansion is already noted above; other parameters are noted in Table 5-2.

Emissivity (Dimensionless)

The core and blanket material emissivity [5-5] is given by the following correlations:

$$e = e_0 \qquad \text{for } T \leq T_5 \qquad (5\text{-}17)$$

and

$$e = e_0 + e_1 (T - T_5) \qquad \text{for } T > T_5 \qquad (5\text{-}18)$$

where e_0, e_1 and T_5 are given in Table 5-2.

5.1.2 CLADDING AND STRUCTURAL MATERIALS

For stainless steel, the default material for cladding and structure, the thermal conductivity (W/m-K) [5-6], specific heat (J/kgK) [5-6], and the average linear coefficient of thermal expansion (m/m-K) [5-7], are represented by polynomial fits of data. These equations, for temperatures up to melting point, are given by the following:

$$k(T) = k_0 + k_1 T + k_2 T^2 + k_3 T^3 \ , \qquad (5\text{-}19)$$

$$c_p(T) = c_0 + c_1 T + c_2 T^2 + c_3 T^3 \quad \text{and} \qquad (5\text{-}20)$$

$$\alpha(T) = \alpha_0 + \alpha_1 T + \alpha_2 T^2 \ , \qquad (5\text{-}21)$$

where values for various parameters for both cladding and structural materials are noted in Table 5-3. The structural or cladding material density is related to the average thermal coefficient of linear expansion as follows:

Table 5-3

Parameters for Cladding and
Structural Material Properties

Parameter	Cladding material	Structural material
k_0	9.01748	9.01748
k_1	1.62997×10^{-2}	1.62997×10^{-2}
k_2	-4.80329×10^{-6}	-4.80329×10^{-6}
k_3	2.18422×10^{-9}	2.18422×10^{-9}
c_0	380.962	380.962
c_1	0.535104	0.535104
c_2	-6.10413×10^{-4}	-6.10413×10^{-4}
c_3	3.02469×10^{-7}	3.02469×10^{-7}
ρ_0	8127.87	8127.87
α_0	1.7887×10^{-5}	1.7887×10^{-5}
α_1	2.3977×10^{-9}	2.3977×10^{-9}
α_2	3.2692×10^{-13}	3.2692×10^{-13}
T_0	298.15	298.15
e_0	0.55	0.55
e_1	2.5×10^{-4}	2.5×10^{-4}
T_1	400	400

$$\frac{\rho(T)}{\rho_0} = \frac{1}{[1 + \alpha(T)(T - T_0)]^3} , \qquad (5\text{-}22)$$

where ρ_0 is the density at temperature T_0.

The cladding and structural emissivity [5-8] are given by the following relations:

$$e = e_0 \qquad \text{for } T \leq T_1 \qquad (5\text{-}23)$$

and

$$e = e_0 + e_1(T - T_1) \qquad \text{for } T > T_1 , \qquad (5\text{-}24)$$

where values for e_0, e_1 and T_1 are also noted in Table 5-3.

5.1.3 CONTROL ROD MATERIAL

For the control rod material (boron carbide), the thermal conductivity (W/m-K), the specific heat (J/kg K), the average linear thermal coefficient of expansion (m/m-K), and the density (kg/m^3) are represented by polynomial fits [5-9]. These equations are:

$$k(T) = \frac{k_0 (1 - P)}{(1 + k_4 P)} \quad \frac{1}{k_1 + k_2 T} \qquad (5\text{-}25)$$

$$c_p(t) = c_0(1 + c_1 T + c_6/T^2) , \qquad (5\text{-}26)$$

$$\bar{\alpha}(T) = \alpha_0 + \alpha_1 T \qquad (5\text{-}27)$$

and

$$\rho(T) = \frac{\rho_0(1 - P)}{[1 + \bar{\alpha}(T)(T - T_0)]^3} \qquad (5\text{-}28)$$

These equations are similar in form to Equations (5-1), (5-2), (5-7) and (5-12), respectively. Values for the various parameters are noted in Table 5-4, and P is the porosity, which is an input quantity read in with the control rod geometric data. These correlations are valid in the temperature range from 500 K to 1250 K.

5.1.4 SODIUM

All of the required thermophysical properties for liquid sodium and sodium vapor are taken from Golden and Tokar [5-10]. These are noted as follows:

Thermal conductivity (W/m K)

The thermal conductivity of liquid sodium is given by the following equation:

$$k(T) = k_0 + k_1 T + k_2 T^2 \quad , \tag{5-29}$$

where

$$k_0 = 109.7 \ ,$$

$$k_1 = -6.4499 \times 10^{-2}$$

$$k_2 = 1.1728 \times 10^{-5} \ .$$

Specific heat capacity (j/kg K)

The specific heat capacity at constant pressure for liquid sodium is given by

$$c_p(T) = c_0 + c_1 T + c_2 T^2, \tag{5-30}$$

where

$$c_0 = 1630.22 \ ,$$

$$c_1 = -0.83354 \ ,$$

Table 5-4

Parameters for Control Rod Material Properties

Parameter	Value
k_0	334.13
k_1	21.6178
k_2	0.05381
k_3	0.0
k_4	2.2
k_5	0.0
c_0	1741.79
c_1	2.34856×10^{-4}
c_2	0.0
c_3	0.0
c_4	0.0
c_5	0.0
c_6	-46,634.7
α_0	-1.4886×10^{-3}
α_1	4.124×10^{-6}
ρ_0	2381.0
T_0	295.4

$$c_2 = 4.62838 \times 10^{-4} \quad .$$

Enthalpy (J/kg)

The enthalpy of saturated liquid sodium is given by

$$h_s(T) = h_0 + h_1 T + h_2 T^2 + h_3 T^3 \quad , \qquad (5\text{-}31)$$

where

$$h_0 = -6.7511 \times 10^4$$

$$h_1 = 1630.22 \quad ,$$

$$h_2 = -0.41674 \quad ,$$

$$h_3 = 1.54279 \times 10^{-4} \quad .$$

For unsaturated liquid sodium, the enthalpy is written as

$$h = h_s - \frac{p_s}{\rho_s} + \frac{p}{\rho} \quad , \qquad (5\text{-}32)$$

where the saturation vapor pressure (p_s) and the liquid sodium density (ρ_s) are given in the following equations. For incompressible sodium,

$$\rho(T,p_s) = \rho(T) = \rho_s(T) \quad ;$$

hence, Equation (5-32) becomes

$$h = h_s - \frac{p_s - p}{\rho} \quad . \qquad (5\text{-}33)$$

For most purposes, the liquid sodium enthalpy may be approximated by the saturation value.

In SSC we also need to compute liquid sodium temperature from its enthalpy value. Although it is computed iteratively in the code by inverting Equation (5-31), an approximate correlation is given by the following:

$$T = c_0 + c_1 h_s + c_2 h_s^2 + c_3 h_s^3 + c_4 h_s^4, \qquad (5\text{-}34)$$

where

$$c_0 = 55.5057 \ ,$$

$$c_1 = 5.56961 \times 10^{-4} \ ,$$

$$c_2 = 2.17341 \times 10^{-10} \ ,$$

$$c_3 = -7.27069 \times 10^{-17} \ ,$$

and

$$c_4 = 4.41118 \times 10^{-24} \ .$$

Saturation vapor pressure (Pa, i.e., N/m^2)

The saturation vapor pressure of sodium is expressed by the following two equations:

$$\log_{10} P_s = p_1 + p_2/T + p_3 \log_{10} T \qquad \text{for } T \leq T_1 \qquad (5\text{-}35)$$

and

$$\log_{10} P_s = p_4 + p_5/T + p_6 \log_{10} T \qquad \text{for } T > T_1 \ , \qquad (5\text{-}36)$$

where

$$p_1 = 11.35977 \ ,$$

$$p_2 = -5567.0 \ ,$$

$$p_3 = -0.5 \ ,$$

$$p_4 = 11.68672 \ ,$$

$$p_5 = -5544.97 \ ,$$

$$p_6 = -0.61344 \ ,$$

and

$$T_1 = 1144.2 \ .$$

The saturation temperature of liquid sodium as a function of pressure is given by the following equation [5-11]:

$$T_s = \frac{c_0}{\ell n(9.869 \times 10^{-6} p) - c_1} , \qquad (5\text{-}37)$$

where

$$c_0 = -12130.0 ,$$

$$c_1 = 10.51 ,$$

and p is the pressure in N/m^2.

Density (kg/m^3)

The density of saturated liquid sodium is given by the following relation:

$$\rho_s(T) = \rho_0 + \rho_1 T + \rho_2 T^2 + \rho_3 T^3 \qquad \text{for } T_1 \leq T \leq T_2 , \qquad (5\text{-}38)$$

where,

$$\rho_0 = 1011.597 ,$$

$$\rho_1 = -0.22051 ,$$

$$\rho_2 = -1.92243 \times 10^{-5} ,$$

$$\rho_3 = 5.63769 \times 10^{-9} ,$$

$$T_1 = 370.9 ,$$

and,

$$T_2 = 1644.2 .$$

The density of unsaturated liquid sodium is related to that of saturated liquid through a compressibility factor (β_T), as follows:

$$\rho(T,p) = \rho_s(T) \exp [\beta_T (p - p_s)] , \qquad (5\text{-}39)$$

where $\rho_s(T)$ is given by Equation (5-38) and p_s is given by Equations (5-35) or (5-36). If incompressibility is assumed, $\beta_T = 0$. Hence,

$$\rho(t,p) = \rho(T) = \rho_s(T) . \qquad (5\text{-}40)$$

Dynamic viscosity (Pℓ, i.e., N s/m^2)

The dynamic viscosity of liquid sodium is represented as

$$\log_{10}\eta = c_1 + \frac{c_2}{T} + c_3 \log_{10} T \quad , \tag{5-41}$$

where

$$c_1 = -2.4892 \quad ,$$

$$c_2 = 220.65 \quad ,$$

and

$$c_3 = -0.4925 \quad .$$

Heat of vaporization (J/kg)

The heat of vaporization, fitted over the range 1150 to 1500 K is given by the following equation [5-11]:

$$\lambda(T) = \lambda_0 + \lambda_1 T + \lambda_2 T^2 \quad , \tag{5-42}$$

where

$$\lambda_0 = 4.40241 \times 10^6 \quad ,$$

$$\lambda_1 = -17.5055 \quad ,$$

$$\lambda_2 = -0.380184 \quad .$$

Specific heat capacity (J/kg K)

The specific heat capacity at constant pressure for sodium vapor was fitted over the range 1150 to 1500 K, and is given by the equation [5-11]:

$$c_{pv}(T) = c_0 + c_1 T + c_2 T^2 \quad , \tag{5-43}$$

where

$$c_0 = 4.4015 \times 10^3 \quad ,$$

$$c_1 = -2.2987 \quad ,$$

$$c_2 = 6.347 \times 10^{-4} \quad .$$

Density (kg/m^3)

The density of sodium vapor is given by the following equation:

$$\rho_v = \frac{p\,A(T)}{T} \tag{5-44}$$

in which the factor A(T) was fitted over the range 1150 to 1600 K and is given by the equation [5-11]:

$$A(T) = a_0 + a_1 T + a_2 T^2 \ , \tag{5-45}$$

where

$$a_0 = 3.27317 \times 10^{-3} \ ,$$

$$a_1 = -8.72393 \times 10^{-7} \ ,$$

$$a_2 = 6.07353 \times 10^{-10} \ .$$

Enthalpy (J/kg)

At a given reference pressure p, the sodium saturation temperature T_s is first calculated. The liquid saturation enthalpy $h_\ell(T_s)$ and heat of vaporization $\lambda(T_s)$ are then calculated. The vapor enthalpy is then given by the equation

$$h_v(T) = h_\ell(T_s) + \lambda(T_s) + h_{v1}\,(T - T_s) + h_{v2}\,(T - T_s)^2 + h_{v3}\,(T - T_s)^3 , \tag{5-46}$$

where

$$h_{v1} = 4.4015 \times 10^3 \ ,$$

$$h_{v2} = -1.14935 \ ,$$

$$h_{v3} = 2.11567 \times 10^{-4} \ ,$$

$\lambda(T_s)$ is given by Equation (5-42), and $h_\ell(T_s)$ is given by Equation (5-31).

5.1.5 WATER/STEAM

The constitutive relations for water are currently given by correlations where the properties are evaluated as a function of enthalpy (H) and pressure (p) [5-12].

Enthalpy of saturated liquid (J/kg)

The enthalpy of saturated water is given by

$$H_\ell(p) = a_0 + a_1 p + a_2 p^2 + a_3 p^3 + a_4 p^4 + a_5 p^5 \quad , \tag{5-47}$$

where

$$a_0 = 5.7474 \times 10^5 \quad ,$$
$$a_1 = 2.09206 \times 10^{-1} \quad ,$$
$$a_2 = -2.8051 \times 10^{-8} \quad ,$$
$$a_3 = 2.38098 \times 10^{-15} \quad ,$$
$$a_4 = -1.0042 \times 10^{-22} \quad ,$$
$$a_5 = 1.6587 \times 10^{-30} \quad ,$$

and p is pressure in N/m^2.

Enthalpy of saturated vapor (J/kg)

The entalpy of saturated steam is given by

$$H_v(p) = b_0 + b_1 p + b_2 p^2 + b_3 p^3 + b_4 p^4 \quad , \tag{5-48}$$

where

$$b_0 = 2.7396 \times 10^6 \quad ,$$
$$b_1 = 3.7588 \times 10^{-2} \quad ,$$
$$b_2 = -7.1640 \times 10^{-9} \quad ,$$
$$b_3 = 4.2002 \times 10^{-16} \quad ,$$
$$b_4 = -9.8507 \times 10^{-24}.$$

Temperature of compressed liquid (K)

The temperature of compressed liquid is given by

$$T(H,p) = c_0(p) + c_1(p)H + c_2(p)H^2 + c_3(p)H^3 \qquad (5\text{-}49)$$

where

$$c_0(p) = c_{00} + c_{01}p \ ,$$

$$c_1(p) = c_{10} + c_{11}p \ ,$$

$$c_2(p) = c_{20} + c_{21}p \ ,$$

$$c_3(p) = c_{30} + c_{31}p \ ,$$

and the coefficients c_{ij} are given in Table 5-5.

Temperature of superheated vapor (K)

The temperature of superheated steam is given by

$$T(H,p) = d_0(p) + d_1(p)H + d_2(p)H^2 \ , \qquad (5\text{-}50)$$

where

$$d_0(p) = d_{00} + d_{01}p + d_{02}p^2 \ ,$$

$$d_1(p) = d_{10} + d_{11}p + d_{12}p^2 \ ,$$

$$d_2(p) = d_{20} + d_{21}p + d_{22}p^2 \ ,$$

and the coefficients d_{ij} are given in Table 5-6.

Density of compressed liquid (kg/m^3)

The density of compressed water is given by

$$D(H,p) = f_1 + f_2H^2 + f_3H^4, \text{ for } H \leq 6.513 \times 10^5 \text{ J/kg} \qquad (5\text{-}51)$$

or

$$D(H,p) = f_4 + \frac{f_5}{H - f_6}, \text{ for } H > 6.513 \times 10^5 \text{ J/kg} \qquad (5\text{-}52)$$

The coefficients f_j are given in Table 5-7.

Table 5-5

Values of Coefficients for
Temperature of Compressed Liquid Water

Coefficient	Value
c_{00}	2.7291×10^{2}
c_{01}	-1.5954×10^{-7}
c_{10}	2.3949×10^{-4}
c_{11}	-5.1963×10^{-13}
c_{20}	5.9660×10^{-12}
c_{21}	1.2064×10^{-18}
c_{30}	-1.3147×10^{-17}
c_{31}	-5.6026×10^{-25}

Table 5-6

Values of Coefficients for
Temperature of Superheated Water Vapor

Coefficient	Value
d_{00}	$6.5659 \times 10^{+2}$
d_{10}	-5.2569×10^{-4}
d_{20}	1.6221×10^{-10}
d_{01}	9.9066×10^{-5}
d_{11}	-3.4406×10^{-11}
d_{21}	1.8674×10^{-18}
d_{02}	-2.1879×10^{-12}
d_{12}	7.0081×10^{-19}
d_{22}	-1.4567×10^{-26}

Table 5-7

Values of Coefficients for Density of Compressed Liquid Water

Coefficient	Value
f_1	$999.65 + 4.9737 \times 10^{-7} \times p$
f_2	$-2.5847 \times 10^{-10} + 6.1767 \times 10^{-19} \times p$
f_3	$1.2696 \times 10^{-22} - 4.9223 \times 10^{-31} \times p$
f_4	$1488.64 + 1.3389 \times 10^{-6} \times p$
f_5	$1.4695 \times 10^{9} + 8.85736 \times p$
f_6	$3.20372 \times 10^{6} + 1.20483 \times 10^{-2} \times p$

Density of superheated vapor (kg/m^3)

The density of superheated steam is given by

$$D(H,p) = \frac{1}{g_0(p) + g_1(p)H} \quad , \tag{5-53}$$

where

$$g_0(p) = g_{00} + g_{01}p + g_{02}/p \quad ,$$

$$g_1(p) = g_{10} + g_{11}p + g_{12}/p \quad ;$$

and

$$g_{00} = -5.1026 \times 10^{-5} \quad ,$$

$$g_{01} = 1.1208 \times 10^{-10} \quad ,$$

$$g_{02} = -4.4506 \times 10^{+5} \quad ,$$

$$g_{10} = -1.6893 \times 10^{-10} \quad ,$$

$$g_{11} = -3.39[illegible] \times 10^{-17} \quad ,$$

$$g_{12} = 2.30[illegible]8 \times 10^{-1} \quad .$$

Specific heat of compressed liquid (J/m^3K)

The specific heat of compressed water is given by

$$c_p(H,p) = \frac{1}{a_0(p) + a_1(p)H + a_2(p)H^2} \quad , \qquad (5\text{-}54)$$

where

$$a_0(p) = a_{00} + a_{01}p \quad ,$$

$$a_1(p) = a_{10} + a_{11}p \quad ,$$

$$a_2(p) = a_{20} + a_{21}p \quad ;$$

and

$$a_{00} = 2.3949 \times 10^{-4} \quad ,$$

$$a_{01} = -5.1963 \times 10^{-13} \quad ,$$

$$a_{10} = 1.1932 \times 10^{-11} \quad ,$$

$$a_{11} = 2.4127 \times 10^{-18} \quad ,$$

$$a_{20} = -3.9441 \times 10^{-17} \quad ,$$

$$a_{21} = -1.6808 \times 10^{-24} \quad .$$

Specific heat of superheated vapor ($J/m\ K^3$)

The specific heat of superheat steam is given by

$$c_p(H,p) = \frac{1}{b_0(p) + b_1(p)H} \quad , \qquad (5\text{-}55)$$

where

$$b_0(p) = b_{00} + b_{01}p + b_{02}p^2 \quad ,$$

$$b_1(p) = b_{10} + b_{11}p + b_{12}p^2 \quad ;$$

and

$$b_{00} = -5.2569 \times 10^{-4} \quad ,$$

$$b_{01} = -3.4406 \times 10^{-11} \quad ,$$

$$b_{02} = 7.0081 \times 10^{-19} \quad ,$$

$$b_{10} = 3.2441 \times 10^{-10} \quad ,$$

$$b_{11} = 3.7348 \times 10^{-18} \quad ,$$

$$b_{12} = -2.9134 \times 10^{-26} \quad .$$

Viscosity of compressed liquid (Ns/m^2)

The viscosity of compressed water is given by

$$n(H,p) = c_0 + c_1X + c_2X^2 + c_3X^3 + c_4X^4 - (d_0 + d_1E + d_2E^2 + d_3E^3)(p - p_1) \quad H \leq H_1, \tag{5-56}$$

$$n(H,p) = e_0(H) + e_1(H)(p - p_1) \quad H_1 < H < H_2, \tag{5-57}$$

$$n(H,p) = f_0 + f_1Z + f_2Z^2 + f_3Z^3 + f_4Z^4 \quad H \geq H_2, \tag{5-58}$$

where

$$X = g_0(H - g_1),$$

$$E = g_2(H - g_3),$$

$$Z = g_4(H - g_5),$$

$$e_0(H) = e_{00} + e_{01}H + e_{02}H^2 + e_{03}H^3,$$

$$e_1(H) = e_{10} + e_{11}H + e_{12}H^2 + e_{13}H^3,$$

and the coefficients are given in Table 5-8.

Viscosity of superheated vapor (Ns/m^2)

The viscosity of superheated steam is given by

$$n(H,p) = (a_0 + a_1T) - D(b_0 + b_1T) \quad \text{for } T \leq 300 \text{ K}, \tag{5-59}$$

$$n(H,p) = (a_0 + a_1T) + (c_0 + c_1T + c_2T^2 + c_3T^3)D + D(d_0 + d_1T + d_2T^2 + d_3T^3)(e_0 + e_1D + e_2D^2) \quad \text{for } 300 < T < 375 \text{ K}, \tag{5-60}$$

$$n(H,p) = (a_0 + a_1T) - D(e_0 + e_1D + e_2D^2) \quad \text{for } T \geq 375 \text{ K}; \tag{5-61}$$

where

$$T = T_v(H,p) - 273.15,$$

$$D = D_v(H,p),$$

and the coefficients are given in Table 5-9.

Table 5-8

Values of Coefficients for
Viscosity of Compressed Liquid Water

Coefficient	Value
c_0	1.2995×10^{-3}
c_1	-9.2640×10^{-4}
c_2	3.8105×10^{-4}
c_3	-8.2194×10^{-5}
c_4	7.0224×10^{-6}
d_0	-6.5959×10^{-12}
d_1	6.763×10^{-12}
d_2	-2.8883×10^{-12}
d_3	4.4525×10^{-13}
e_{00}	1.4526×10^{-3}
e_{01}	-6.9881×10^{-9}
e_{02}	1.5210×10^{-14}
e_{03}	-1.2303×10^{-20}
e_{10}	-3.8064×10^{-11}
e_{11}	3.9285×10^{-16}
e_{12}	-1.2586×10^{-21}
e_{13}	1.2860×10^{-27}
f_0	3.0260×10^{-4}
f_1	-1.8366×10^{-4}
f_2	7.5671×10^{-5}
f_3	-1.6479×10^{-5}
f_4	1.4165×10^{-6}
H_1	2.76×10^{5}
H_2	3.94×10^{5}
p_1	6.8946×10^{5}
g_0	8.5813×10^{-6}
g_1	4.2659×10^{4}
g_2	6.4845×10^{-6}
g_3	5.5359×10^{4}
g_4	3.8921×10^{-6}
g_5	4.0147×10^{5}

Table 5-9

Values of Coefficients for
Viscosity of Superheated Water Vapor

Coefficient	Value
a_0	4.07×10^{-8}
a_1	8.04×10^{-6}
b_0	1.858×10^{-7}
b_1	5.9×10^{-10}
c_0	-2.885×10^{-6}
c_1	2.427×10^{-8}
c_2	-6.7893×10^{-11}
c_3	6.3170×10^{-14}
d_0	1.76×10^{2}
d_1	-1.6
d_2	4.8×10^{-3}
d_3	-4.7407×10^{-6}
e_0	3.53×10^{-8}
e_1	6.765×10^{-11}
e_2	1.021×10^{-14}

Conductivity of compressed liquid (W/m K)

The thermal conductivity of compressed water is given by

$$k(H,p) = a_0 + a_1 X + a_2 X^2 + a_3 X^3 \quad , \tag{5-62}$$

where

$$X = \frac{H}{5.815 \times 10^5}$$

and

$$a_0 = 5.7374 \times 10^{-1} \quad ,$$

$$a_1 = 2.5361 \times 10^{-1} \quad ,$$

$$a_2 = -1.4547 \times 10^{-1} \quad ,$$

$$a_3 = 1.3875 \times 10^{-2} \quad .$$

Conductivity of superheated vapor (W/m K)

The thermal conductivity of superheated steam is given by

$$k(H,p) = X + D\left(Z + \frac{cD}{T^{4.2}}\right) \quad , \tag{5-63}$$

where

$$T = T(H,p) - 273.15 \quad ,$$

$$D = D(H,p) \quad ,$$

$$X = z_0 + a_1 T + a_2 T^2 + a_3 T^3 \quad ,$$

$$Z = b_0 + b_1 T + b_2 T^2 \quad ,$$

and

$$c = 2.1482E5 \quad ,$$

$$a_0 = 1.76 \times 10^{-2} \quad ,$$

$$a_1 = 5.87 \times 10^{-5} \quad ,$$

$$a_2 = 1.04 \times 10^{-7} \quad ,$$

$$a_3 = -4.51 \times 10^{-11} \quad ,$$

$$b_0 = 1.0351 \times 10^{-4} \quad ,$$

$$b_1 = 4.198 \times 10^{-7} \quad ,$$

$$b_2 = -2.771 \times 10^{-11} \quad .$$

In addition to the properties listed above, various partial derivatives of many of the functions were required. These are obtained by analytically differentiating the appropriate correlations.

5.2 CORRELATIONS

The required pressure drop and heat transfer correlations for the range of interest are included in this section. Representative values for various curve-fitted parameters are noted in SI units.

5.2.1 FRICTION FACTOR CORRELATIONS

Fluid flow and heat transfer correlations for the entire flow regime are required by SSC. The following is a complilation of the friction factor correlations that have been selected or developed so far.

The pressure change due to friction is given by the following equations:

$$\frac{\Delta P}{\Delta L} = - \frac{f}{D_h} \frac{1}{2} \rho U^2 \quad , \tag{5-64}$$

where the hydraulic channel diameter, D_h, is defined as

$$D_h = \frac{4. \text{ (flow area)}}{\text{wetted perimeter}} \quad , \tag{5-65}$$

and U is the fluid velocity. The friction factor, f, depends on the Reynolds number Re and the surface roughness e. The friction factor for turbulent flow in a pipe is given in the Moody chart. The Moody chart is expressed as [5-13] the following transcendental equation:

$$1/\sqrt{f} = - 2.0 \log_{10} [(e/D_h/3.7 + 2.51/(Re\sqrt{f})] \quad . \tag{5-66}$$

For smooth pipes, i.e., for $e/D_h = 0$, the above equation simplifies to the following transcendental equation:

$$1/\sqrt{f} = 2.0 \log_{10} (Re \cdot \sqrt{f}) - 0.80 \quad , \tag{5-67}$$

which is the same as Prandtl's universal law of friction for smooth pipes [5-14].

Rather than the above-mentioned transcendental equation, a simplified form of the friction factor is desirable. The following explicit relation for f [5-15], which is accurate within ±5%, has been coded in SSC.

$$f = 0.0055 \left(1 + \left[20000 \cdot \frac{e}{D_h} + \frac{10^6}{Re}\right]^{1/3}\right) \quad . \tag{5-68}$$

For smooth pipes, the above equation reduces to

$$f = 0.0055 + 0.55(Re)^{-1/3} \quad , \tag{5-69}$$

which is very similar to the Koo correlation [5-16].

A comparison for computing efficiency in calculating f from either Equation (5-66) or Equation (5-68) was made. The approximate representation, Equation (5-68), was found to require 25% less machine time. Since the friction factor needs to be evaluated for each pipe section or node section, only Equation (5-68) for f has been incorporated in SSC.

The friction factor for laminar flow in pipes and heat exchangers is given by:

$$f = \frac{64}{Re} \quad . \tag{5-70}$$

The Reynolds number is evaluated at the bulk temperature of the fluid.

Three sets of correlations for friction factors of in-core assemblies are available:

a) Fuel Assemblies (L6ATYP ≠ 2 or 3)

$$f = \begin{cases} 64.0/Re & Re < 800 \\ (1.029 + 2837./Re^{1.24}) \cdot 0.316/Re^{.25} & Re \geq 800 \end{cases} \quad (5\text{-}71)$$

b) Blanket Assemblies (L6ATYP = 2)

$$f = \begin{cases} 110./Re & Re < 400 \\ \frac{110}{Re} \; 1 - \frac{(Re - 400.)}{4600.} & \\ + \; \frac{(Re - 400.)}{4600.} \cdot 0.48/Re^{0.25} & 400 \leq Re < 5000 \\ .48/Re^{0.25} & 5000 < Re \end{cases} \quad (5\text{-}72)$$

c) Control Assemblies (L6ATYP = 3)

$$f = \begin{cases} 84./Re & Re < 800 \\ 84./Re + (F6FRC1 \cdot Re^{-F6FRC2} - 84.\ Re) \cdot (Re - 800.)/1200. & 800 \leq Re < 2000 \\ F6FRC1 \cdot Re^{-F6FRC2} \cdot [1.034/PD^{1.24} + 29.7 \cdot (PD^{6.94}) \cdot (Re^{.086})/PWD^{2.239}]^{.885} & 2000 \leq Re \end{cases} \quad (5\text{-}73)$$

where, F6FRC12, F6FRC2 - user supplied constants

PD - assembly pitch to diameter ratio

PWD - wire wrap pitch to diameter ratio

For the inlet orifice region and bypass region, the following correction is used:

$$f = \begin{cases} 96.0/Re & Re < 2000 \\ F6FRC1 \cdot Re^{F6FRC2} & 2000 \leq Re \end{cases} \quad (5\text{-}74)$$

5.2.2 HEAT TRANSFER CORRELATIONS

The liquid metal heat transfer correlations for forced convection in a rod bundle have been develolped by West, Schad, Graber and Rieger, and Borishanskii. These correlations have been compared with the experimental data by Kazimi [5-20]. In view of the comparison, the modified Schad correlation is selected. The following correlation is valid for Pe > 10, i.e., for the turbulent flow regime:

$$Nu = [h_1 + h_2(P/D) + h_3(P/D)^2] \cdot (a + b\, Pe^c) \quad , \qquad (5\text{-}75)$$

where

$$h_1 = -16.15 \quad ,$$

$$h_2 = 24.96 \quad ,$$

$$h_3 = -8.55 \quad ,$$

and

$$a = 0, \qquad b = 1, \qquad c = 0.3 \qquad \text{for } Pe \geq 150 \quad ,$$

or

$$a = 4.496, \qquad b = 0, \qquad c = 0.3 \qquad \text{for } Pe < 150 \quad .$$

The above correlation also agrees well for the laminar flow regime.

For liquid metal flow in a pipe, Acki's correlation [5-21] for heat transfer is used:

$$Nu = 6.0 + 0.025\, (\bar{\phi}\, Pe)^{0.8} \quad , \qquad (5\text{-}76)$$

where

$$\bar{\phi} = \frac{0.014(1 - e^{-71.8x})}{x} \quad ,$$

$$x = \frac{1}{Re^{0.45}\, Pr^{0.2}} \quad .$$

In the laminar region,

$$Nu = 4.36 \qquad \text{for } Re \leq 3000 \ . \tag{5-77}$$

For the shell side in the intermediate heat exchanger, the Nusselt number is obtained from the Graber-Rieger correlation [5-22]:

$$Nu = A + B\, Pe^{C} \qquad 110 \leq Pe \leq 4300 \tag{5-78}$$

$$1.25 \leq P/D \leq 1.95$$

where

$$A = 0.25 + 6.2(P/D) \ ,$$

$$B = -0.007 + 0.032\,(P/D) \ ,$$

and

$$C = 0.8 - 0.024(P/D) \ .$$

The range of applicability is also indicated above. For $Pe < 110$, we use a constant value for Nu (evaluated using Equation (5-78) at $Pe = 110$).

The heat transfer correlations for water/steam are given for four different modes of heat transfer. The first mode of heat transfer is forced convection. The Nusselt number for this model is given as [5-23]:

$$Nu = 0.023\, Re^{0.8}\, Pr^{0.4} \tag{5-79}$$

The heat transfer for nucleate boiling is given as [5-24]:

$$h = S \cdot h_{NB} + F \cdot h_{c} \ , \tag{5-80}$$

where the nucleate boiling coefficient h_{NB} is given as:

$$h_{NB} = 0.00122 \left\{ \frac{K_{\ell}^{0.79}\, C_{\ell}^{0.45}\, \rho_{\ell}^{0.49}}{\Omega^{0.5}\, \mu_{\ell}^{0.29}\, \lambda_{fg}^{0.24}\, \rho^{0.24}} \right\} \Delta P^{0.75} \ , \tag{5-81}$$

where

C_{ℓ} = specific heat of liquid

K_{ℓ} = thermal conductivity of liquid

Ω = surface tension

λ_{fg} = latent heat of vaporization, and

ΔP = difference in saturation pressure corresponding to the wall superheat.

The Reynolds number correction factor F, and the nucleate boiling suppression factor S are represented as:

$$F = \begin{cases} 2.34 \left(\frac{1}{X_{tt}}\right)^{0.45} , & \frac{1}{X_{tt}} < 2. \\ 2.57 + 0.7643 \left(\frac{1}{X_{tt}}\right) , & \frac{1}{X_{tt}} \geq 2. \end{cases} \tag{5-82}$$

$$S = \begin{cases} 1.05 - 1.3 \times 10^{-5} Re , & Re \leq 2.5 \times 10^4 \\ 0.83 - 4.3 \times 10^{-6} Re , & 2.5 \times 10^4 < Re \leq 10^5 \\ 0.32 \exp(-1.92 \times 10^{-6} Re), & 10^5 < Re \leq 6 \times 10^5 \\ 0.09 , & Re > 6 \times 10^5 \end{cases} \tag{5-83}$$

and

$$Re = Re_\ell \quad F^{1.25} ,$$

where X_{tt} is the Lockhart/Martinelli [5.25] parameter:

$$\frac{1}{X_{tt}} = \left(\frac{x}{1-x}\right)^{0.9} \cdot \left(\frac{\rho_\ell}{\rho_v}\right)^{0.5} \cdot \left(\frac{\mu_v}{\mu_\ell}\right)^{0.1} \tag{5-84}$$

The convective coefficient h_c is calculated from the Dittus Boelter equation based on liquid thermodynamic properties [5.23].

The heat transfer for film boiling regime is given as [5.26]:

$$Nu = 0.0193 \, Re_\ell^{0.8} \, Pr_\ell^{1.23} \left(\frac{\rho_B}{\rho_g}\right)^{0.68} \left(\frac{\rho_\ell}{\rho_g}\right)^{0.068} , \tag{5-85}$$

where subscripts ℓ and g denote, respectively, liquid and vapor phase at saturation and subscript B indicates a bulk property of the steam/water mixture.

For superheated steam, the following heat transfer correlation for forced convection is used [5.27]:

$$Nu = 0.0133\ Re^{0.84}\ Pr^{0.333}. \qquad (5\text{-}86)$$

The steam/water quality at the DNB point is given by [5.28]:

$$X_{DNB} = \frac{4.38 \times 10^4\ \rho_\ell}{H_{\ell g}\ \rho_g\ \sqrt{G/1350.0}} \qquad \text{for } q > 6.3 \times 10^5, \quad (5\text{-}87)$$

or

$$X_{DNB} = \frac{4.38 \times 10^4\ \rho_\ell \cdot (5.3 \times 10^5/q)^{1.5}}{H_{\ell g}\ \rho_g\ \sqrt{G/1350.0}} \qquad \text{for } q < 6.3 \times 10^5 \quad (5\text{-}88)$$

where $H_{\ell g}$ is the latent heat of vaporization (J/kg), G is the mass flow rate per unit area (kg/s m^2), and q is in W/m^2.

REFERENCES FOR SECTION 5

5-1 LIFE-II Committee, ANL, Priv. Comm., 1973.

5-2 R.G. Gibbym, L. Leibowitz, J.F. Kerrisk and D.G Clifton, "Analytical Expresssions for Enthalpy and Heat Capacity for Uranium-Plutonium Oxide," HEDL-TME 73-60, June 1973.

5-3 B.F. Rubin, "Summary of (U, Pu) O_2 Properties and Fabrication Methods," GEAP-13582, November 1970.

5-4 M.F. Lyons, e. al., "UO_2 Properties Affecting Performance," Nucl. Eng. & Design 21, 167 (1972).

5-5 Thermophysical Properties of Matter, "Thermal Radioactive Properties of Non-Metallic Solids," Vol. 8 edited by Y.S. Touloukian, 1972.

5-6 "Mechanical and Physical Properties of the Austenitic Chromium-Nickel Stainless Steels at Elevated Temperatures," The International Nickel Company, Inc., New York, 1963.

5-7 C.S. Kim, "Thermophysical Properties of Stainless Steel," ANL 75-55, 1975.

5-8 J. Humphries, "On the Thermal Emittance of Stainless Steels," J. of British Nucl. Energy Soc. 13, 271 (1974).

5-9 "A Compilation of Boron Carbide Design Support Data for LMFBR Control Elements," HEDL-TME 75-19, 1975).

5-10 G.H. Golden and J.V. Tokar, "Thermophysical Properties of Sodium," ANL-7323, August 1967.

5-11 F.E. Dunn, G.J. Fischer, T.J. Heames, P.A. Pizzica, N.A. McNeal, W.R. Bohl and S.M. Prestein, "The SAS2A LMFBR Accident Analysis Computer Code," ANL-8138, October 1974.

5-12 W. Wulff, et al., "Development of a Computer Code for Thermal Hydraulics of Reactors (THOR)," Fifth Quarterly Progress Report, Sect. 3.2, BNL-NUREG-50534, July 1976.

5-13 C.F. Bonilla, "Fluid Flow in Reactor Systems," Nuclear Engineering Handbook, pp. 9-30, edited by H. Etherington, McGraw-Hill Book Company, Inc., New York, 1958.

5-14 H. Schlichting, Boundary Layer Theory, 4th Edition, p. 515, McGraw-Hill, Inc., New York, 1968.

5-15 S. Levy, "Fluid Flow," Ch. 15 in The Technology of Nuclear Reactor Safety, Vol. 2, edited by T.J. Thompson and J.G. Beckerly, the M.I.T. Press, Cambridge, Massachusetts, 1973.

5-16 W.H. McAdams, Heat Transmission, 2nd edition, McGraw-Hill, New York, 1942.

5-17 E.H. Novendstern, "Turbulent Flow Pressure Drop Model for Fuel Rod Assemblies Utilizing a Helical Wire-Wrap Space System," Nucl. Eng. & Design 22, 19 (1972).

5-18 R.A. Axford, "Summary of Theoretical Aspects of Heat Transfer Performance in Clustered Rod Geometries," LA-AC-9786, 1968.

5-19 R.A. Axford, "Two-Dimensional Multiregion Analysis of Temperature Fields in Reactor Tube Bundles," Nucl. Eng. & Design 6, 25 (1967).

5-20 M.S. Kazimi, "Heat Transfer Correlation for Analysis of CRBRP Assemblies," WARD-D-0034, April 1974.

5-21 S. Aoki, "Current Liquid-Metal Heat Transfer Research in Japan," Progress in Heat & Mass Transfer, Vol. 7, pp. 569-573, edited by O.E. Dwyer, Pergamon Press, Inc., Elmsford, New York, 1973.

5-22 H. Graber and M. Rieger, "Experimental Study of Heat Transfer to Liquid Metals Flowing In-Line Through Tube Bundles," Progress in Heat & Mass Transfer, Vol. 7, pp. 151-166, edited by O.E. Dwyer, Pergamon Press, Inc., Elmsford, New York, 1973.

5-23 F.W. Dittus and L.K. Boelter, Univ. of Calif. Publs. Eng. 2, 433 (1930).

5-24 J.G. Chen, "Correlation for Boiling Heat Transfer to Saturated Fluids in Convective Flow," I&EC Process Design and Development 5, 322 (1966).

5-25 R.W. Lockhart, and R.C. Martinelli, "Proposed Correlation of Data for Isothermal Two-Phase, Two-Component Flow in Pipes," Chem. Eng. Prog. 45 (1), 39 (1949).

5-26 A.A. Bishop, R.O. Sandberg and L.S. Tong, "Foreced Convection Heat Transfer at High Pressure after Critical Heat Flux," ASME Paper 65-HT-31, 1965.

5-27 J.B. Heineman, "An Experimental Investigation of Heat Transfer to Superheated Steam in Round and Rectangular Channels," ANL-6213, 1960.

5-28 R.B. Harty, "Modular Steam Generator Final Project Report," TR-097-330-010, September 1974.

6. CODE DESCRIPTION

6.1 SOFTWARE PRACTICES

At an early stage of the SSC development effort it was recognized that a set of well defined programming standards would be essential to the successful completion of the project. The choice of an acceptable standard was somewhat less obvious. At that time (prior to the formulation of the '77 standard) much of the published software standards literature for FORTRAN focused on the activity of the X3J3 standards subcommittee of the ANSI. However, no clear concensus appeared to be forthcoming. In this perspective, it was decided to proceed with the SSC development in close adherence to the then accepted language specification set forth in the "USA Standard FORTRAN ANSI X3.9-1966". With few exceptions this standard has been maintained throughout the code's development.

The interchange of computer software between dissimilar mainframes is often a major limiting factor in the dissemination of large codes. To bridge this problem, every effort has been made to minimize (or at least to localize) any mainframe dependent features found in SSC. These exceptions are clearly marked and are easily recognizable. The recommendations of the ANS STD.3-1971 form the basis of the coding practices followed in this area.

6.2 CODE STRUCTURE AND DATA MANAGEMENT

SSC is a deliberately structured ensemble of modules, each of which is determined by the component system/function it seeks to model. Modules are

interfaced through "inlet" and "outlet" junction points. This approach to system intergration has been found to facilitate the substitution of more advanced (or specialized) component models while minimizing inter-modular data coupling.

The SSC data structure is specified by the modules to which the data is associated. Labelled commons provide the basis of intra-modular communication.

Main memory storage is minimized through the use of a dynamic allocation scheme. Data which assumes a problem or system dependent length are stored in consecutive locations in a large fixed length block. The length of this block can be manipulated to obtain an optimal length for a given class of problems.

A symbolic naming scheme is used throughout SSC to avoid problems caused by naming ambiguities and degeneracies. To this end, all memory addressing is accomplished through a system of uniquely assigned identifiers (no two identifiers address the same memory location). Identifiers are restricted to six (6) or fewer characters. The first character specifies the physical property which describes the type of data stored. A list of all relevent characters is given in Table 6-1. The second character indicates the module to which the data belongs. These characters are listed in Table 6-2. The remaining characters (up to four (4) but at least one (1)) are assigned mnemonically. In a parallel fashion, procedure names are assigned according to a similar naming convention. Procedure identifiers are also restricted to six (6) or fewer characters. The last character (from Table 6-3) designates the main system division to which the procedure is resident. The next to last character indicates the module of which the procedure forms a part. These characters are found in Table 6-2. The remaining prefix of from two (2) to four (4) characters was assigned mnemonically to complete the procedure name.

TABLE 6-1
Initial Letters Used to
Indicate Type of Quantity and Units

A	Area	m^2
B	Mass	kg
C	Material properties; constants	(See Table 6-2)
D	Density	kg/m^3
E	Energy; enthalpy	J; J/kg
F	Fractions, factors	-
G	Mass flow rate per unit area	$kg/s\ m^2$
H	Heat Transfer Coefficient	W/m^2K
L	Control flags, counters, etc.	
M	Maximum allowable dimension	
N	Actual dimension specified	
P	Pressure; power	N/m^2; W
Q	Surface heat flux; miscellaneous	W/m^2; --
R	Reactivity; angular measure	k/k; radians
S	Time	s
T	Temperature	K (not C)
U	Velocity, angular velocity or speed	m/s; rpm
V	Volume	m^3
W	Mass flow rate	kg/s
X	Distance (length or radius)	m
Y	Distance (width or diameter)	m
Z	Distance (height or axial direction)	m

Table 6-2

Digits Used to Indicate
Major Modules (or Regions)

1	Primary loop.
2	Secondary loop.
3	Tertiary loop and steam generator.
5	Fuel (and blanket) rods.
6	Reactor core coolant volumes.
7	Reactor vessel, structure, etc.
8	Plant protection and control systems.
9	Global or general quantities, not pertaining to a specific module or modules (or regions).

NOTE: For entities pertaining to more than one region, the digit used is determined by whichever module creates or alters it.

For material properties constants (first character is "C"), the digits have a slightly different meaning:

1	Sodium.	6	Cladding of fuel rods.
2	Sodium vapor.	7	Steel, other structural material
3	Water or steam.		
4	Reactor fuel blanket.	8	Fission product/gap gas
5	Reactor Fuel.		

Also for material properties constants, the third character is meaningful; for example:

A	Coefficient of thermal expansion.		
C	Specific heat capacity.	K	Thermal conductivity.
D	Density.	N	Dynamic viscosity.
E	Emissivity.	P	Pressure.
H	Enthalpy.	T	Temperature.

Table 6-3

Final Letters Used for Procedure Names*

R	Routines of the input processor (reader) segment.
S	Routines of the steady-state segment.
T	Routines of the transient time-stepping segment.
U	Utility routines used by more than one program segment.
F	Functions other than those calculating material properties.
C	Routines calculating local conditions or correlations
*	The final letters of material properties functions generally correspond to those used for the third character for material properties constants (see Table 6-2).

6.3 FLOW CHARTS

The modularized structure of the SSC-L code lends itself to a natural sub-division. The code is divided into three major sequentially disjointed processes (i.e., MAIN9R, MAIN9S AND MAIN9T) as shown in Figure 6-1. These routines are the main driver programs and are called in succession by the controller routine. Each performs a unique set of tasks and is executed only once for any given case. It should be noted that this program structure is compatible with over-layed loader procedures found on most large computer systems (e.g., OVERLAY and SEGLOAD).

A set of sample segmented loader directives formulated for the CDC 7600 SEGLOAD utility is given in Appendix B.

The flow chart of each of the drivers, along with its associated subroutines, is shown in Figures 6-2 through 6-36. Note on these figures that any subroutine which calls subordinate routines that are continued on a subsequent figure is designated by an asterisk (*). A brief description of all subroutines used in SSC-L can be found in Appendix A.

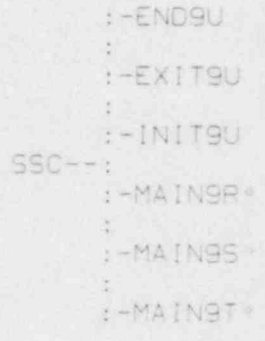

Figure 6-1 Main SSC Driver Programs

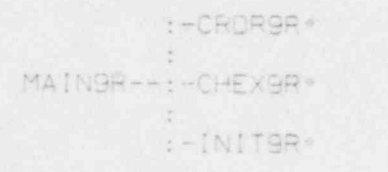

Figure 6-2 Main Input Processor Driver

Figure 6-3 Main Steady-State Segment Driver

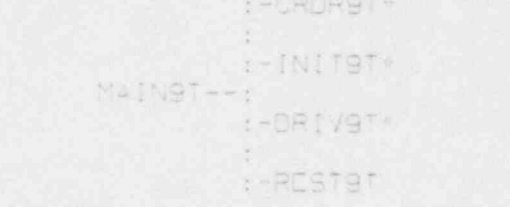

Figure 6-4 Main Transient Segment Driver

Note: (*) indicates that subordinate subroutines are contained in subsequent figures.

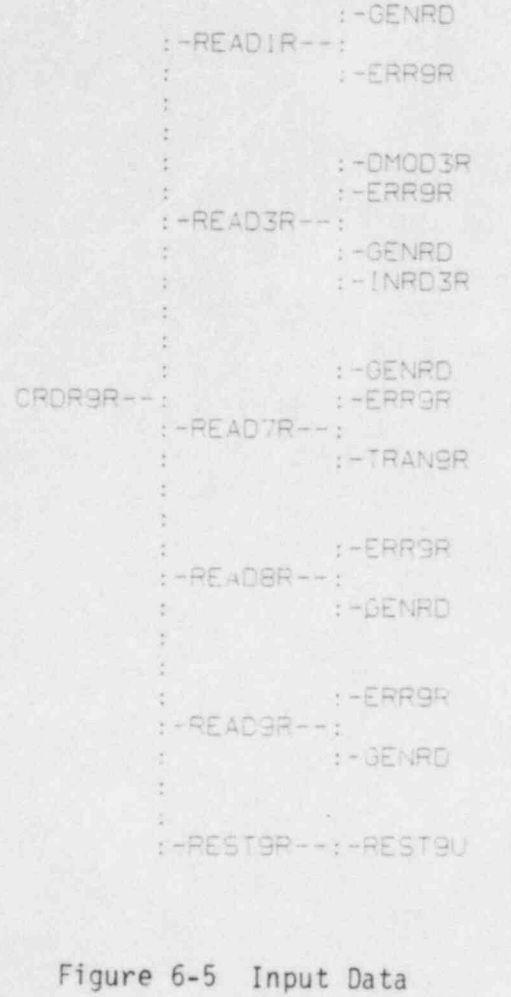

Figure 6-5 Input Data Read Subroutines

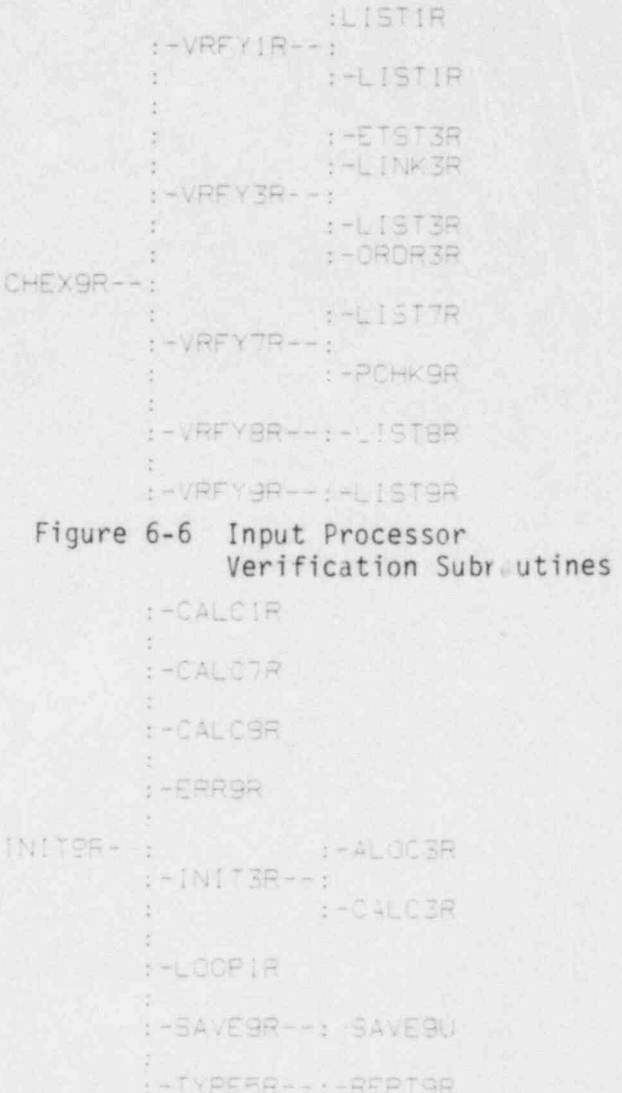

Figure 6-6 Input Processor Verification Subroutines

Figure 6-7 Input Processor Computational Subroutines

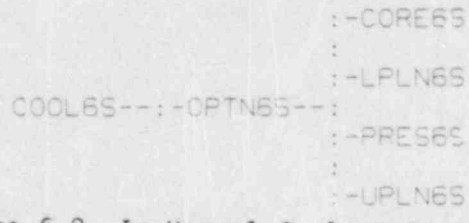

Figure 6-8 In-Vessel Coolant Steady-State Subroutines

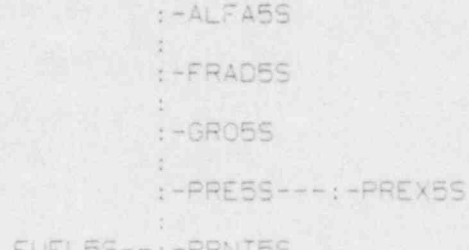

Figure 6-9 Fuel Heat Conduction Steady-State Subroutines

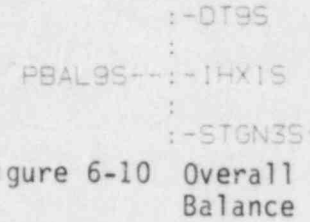

Figure 6-10 Overall Plant Thermal Balance Driver

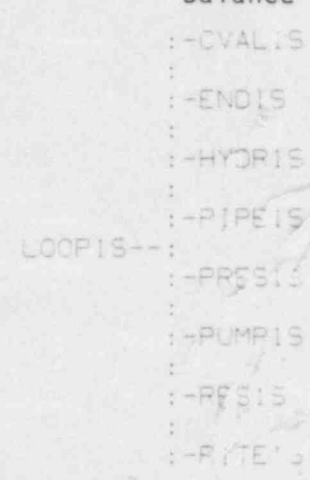

Figure 6-11 Primary Loop Steady-State Subroutines

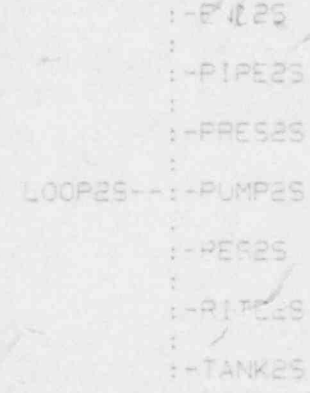

Figure 6-12 Secondary Loop Steady-State Subroutines

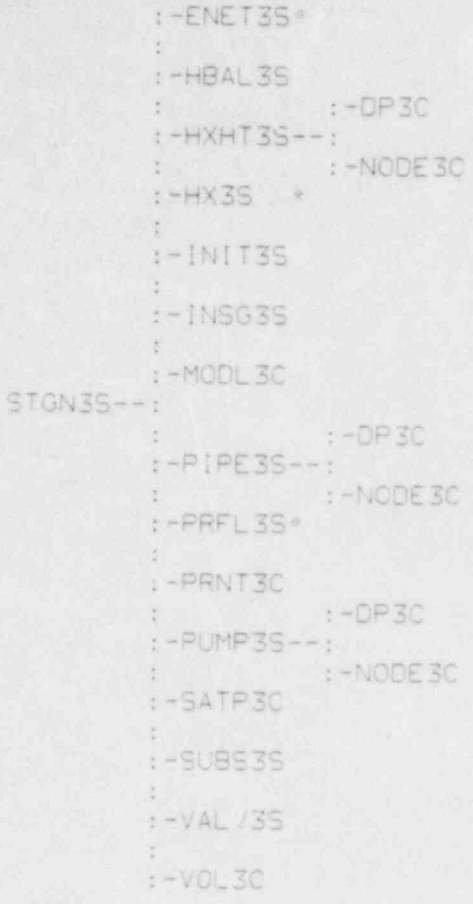

Figure 6-13 Steam Generator (SG) Steady-State (S-S) Driver

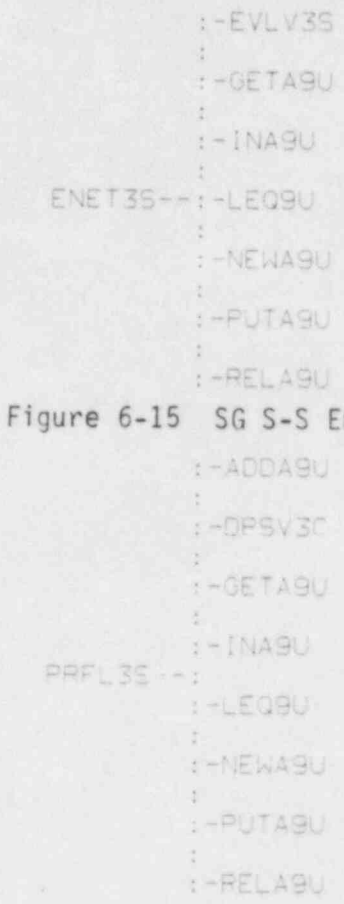

Figure 6-15 SG S-S Energy Balance

Figure 6-16 SG S-S Pressure and Mass Flow Balance

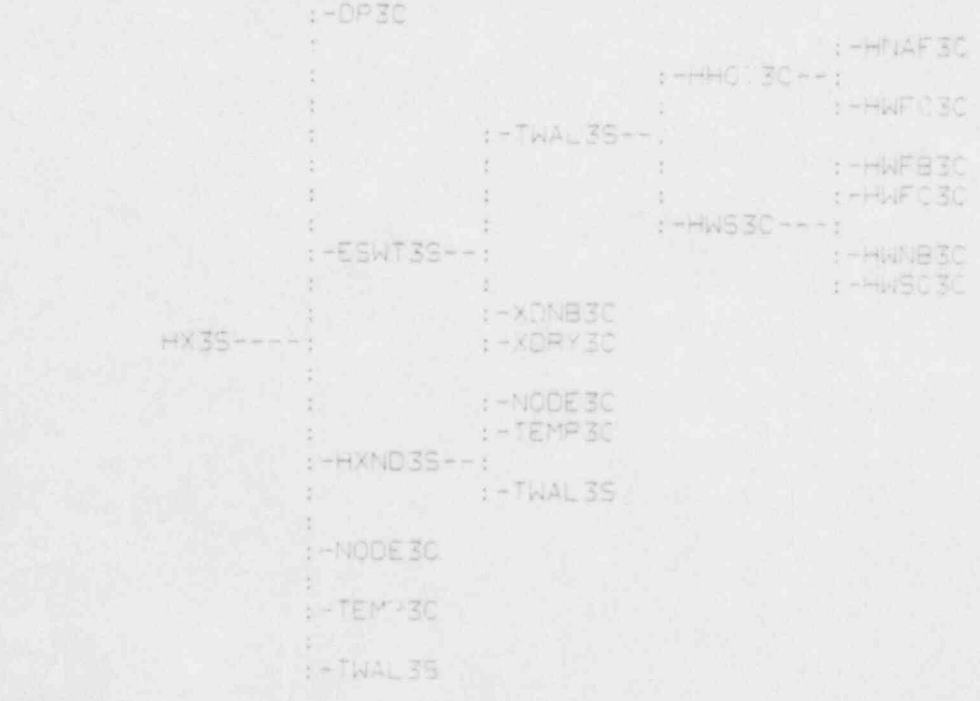

Figure 6-14 SG S-S Heat Exchanger Enthalpies

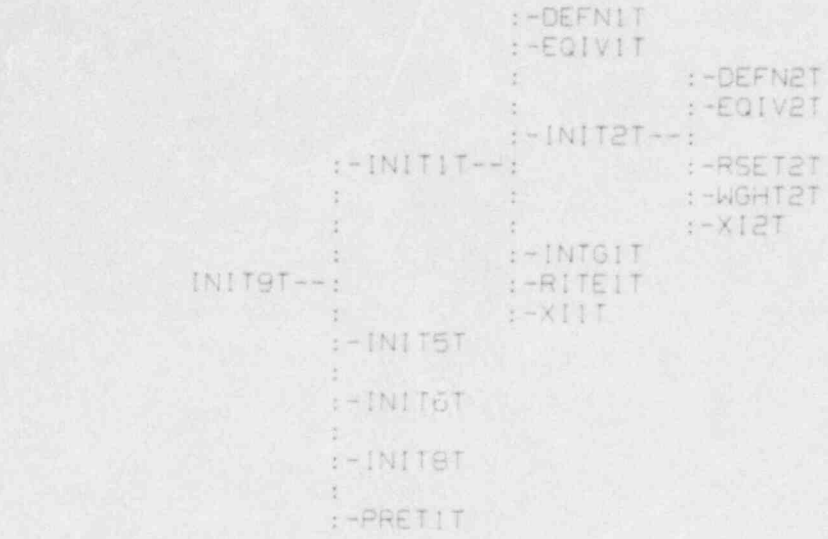

Figure 6-18 Pre-Transient Initialization

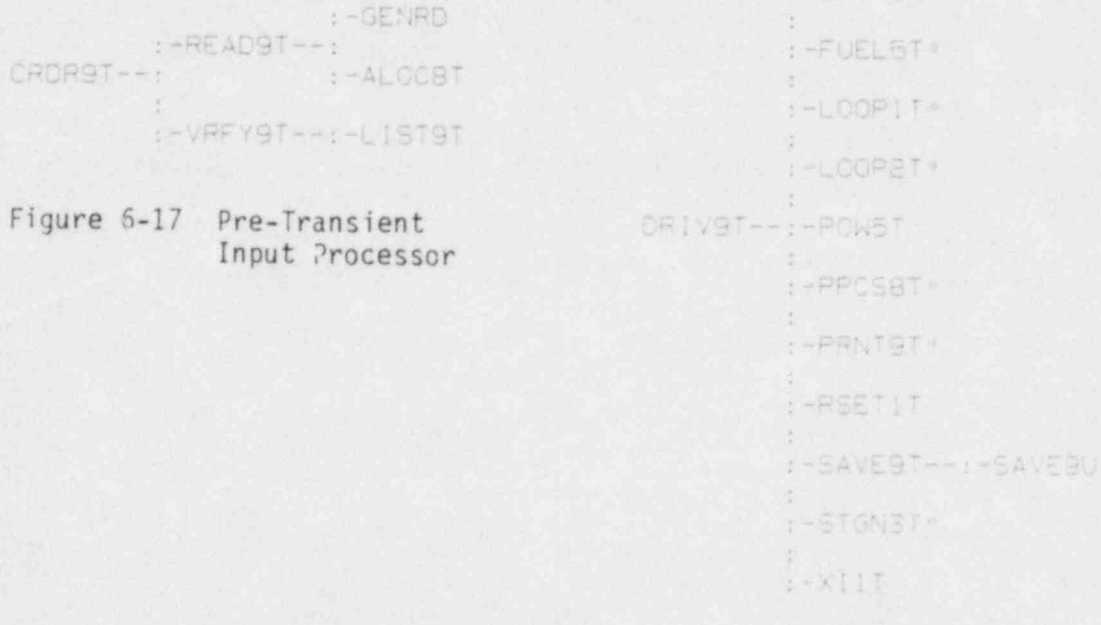

Figure 6-17 Pre-Transient Input Processor

Figure 6-19 Transient Integration Driver

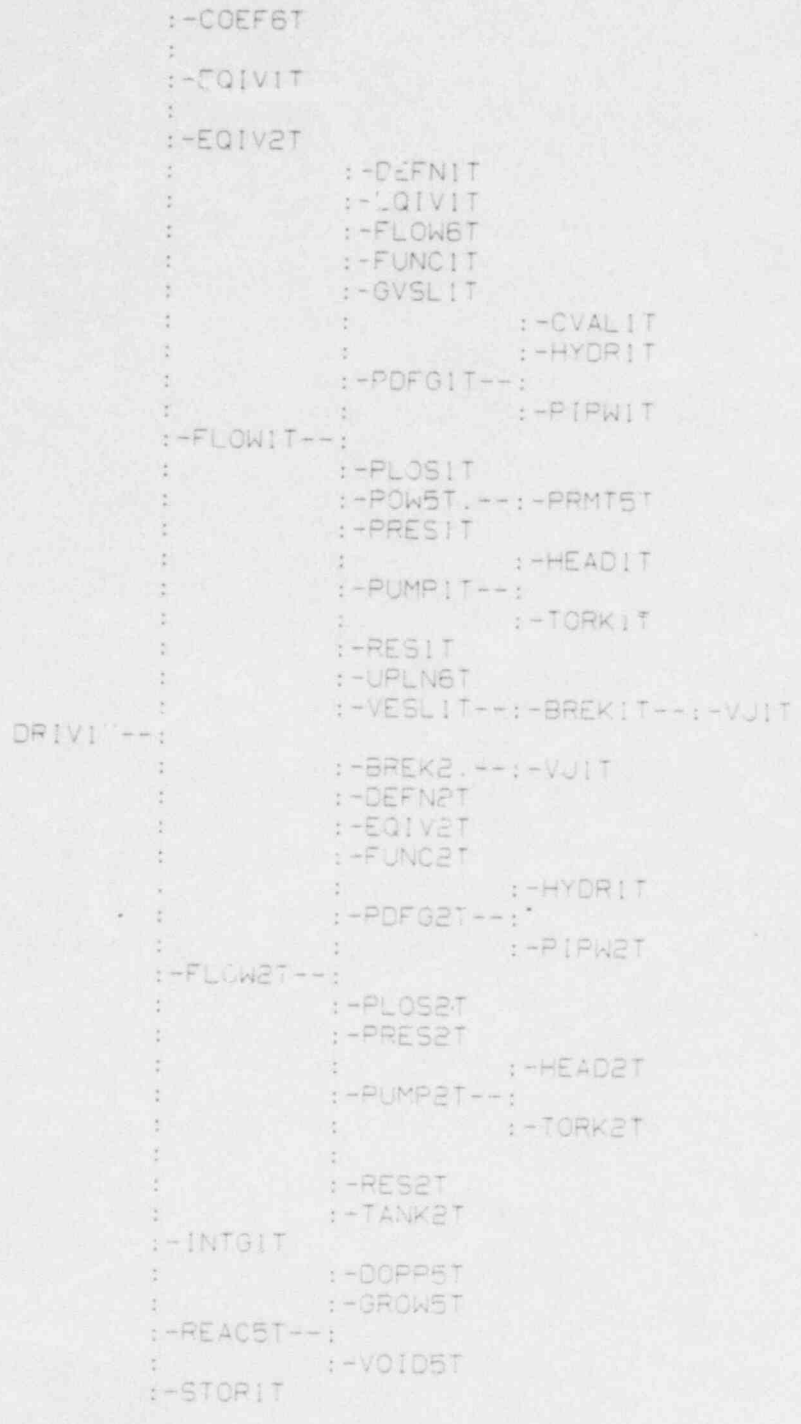

Figure 6-20 Driver for Hydraulics during Transient

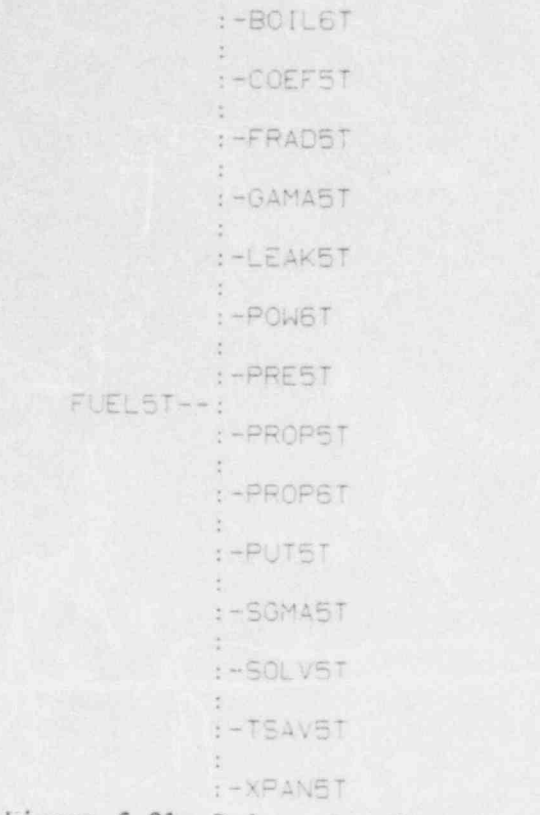

Figure 6-21 Driver for Transient Fuel Heat Conduction

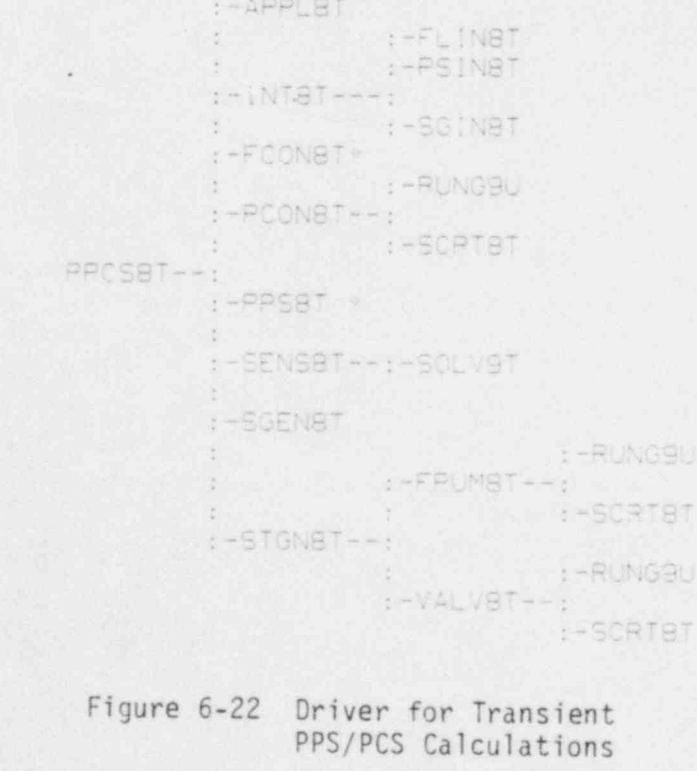

Figure 6-22 Driver for Transient PPS/PCS Calculations

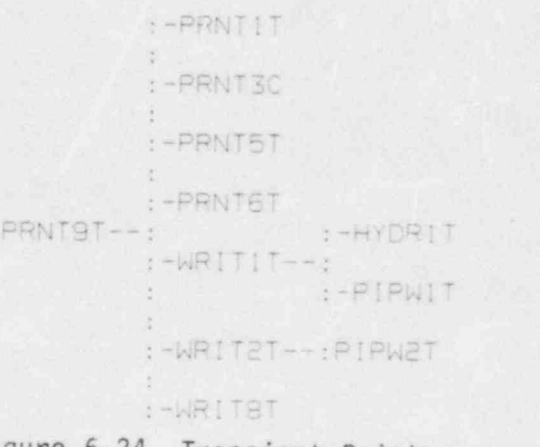

Figure 6-24 Transient Printer

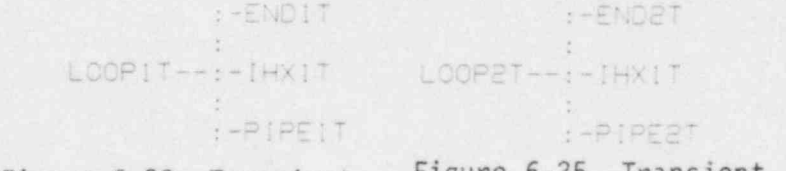

Figure 6-23 Transient Energy (1)

Figure 6-25 Transient Energy (2)

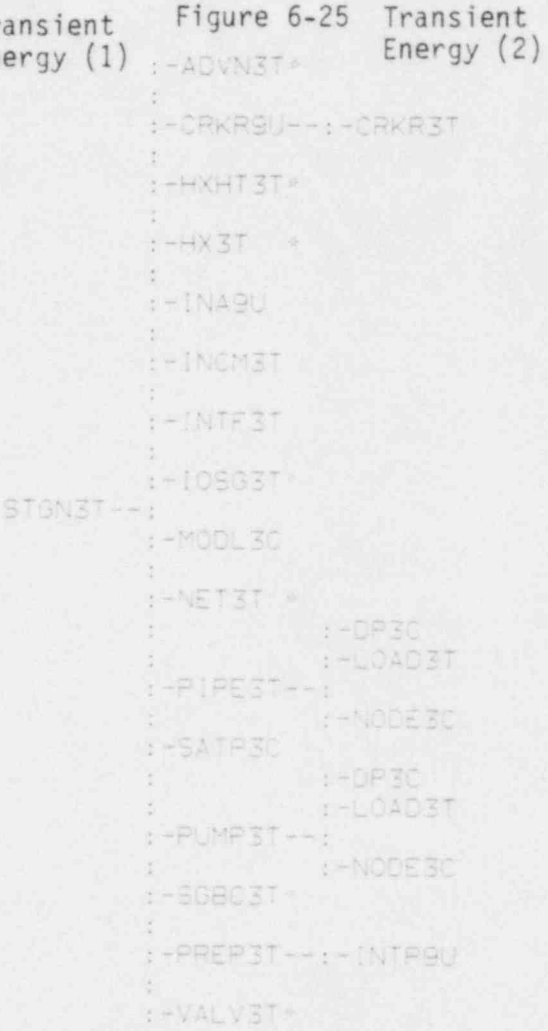

Figure 6-26 Transient SG Driver

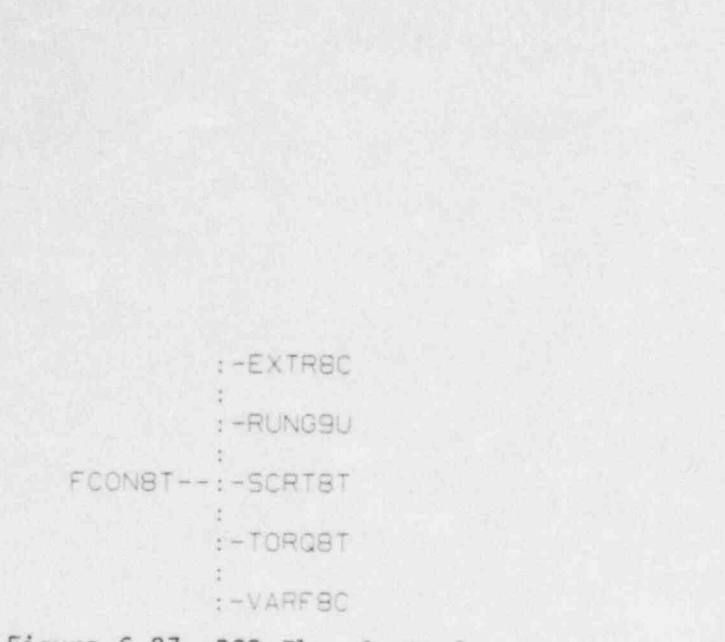

Figure 6-27 PCS Flow Control

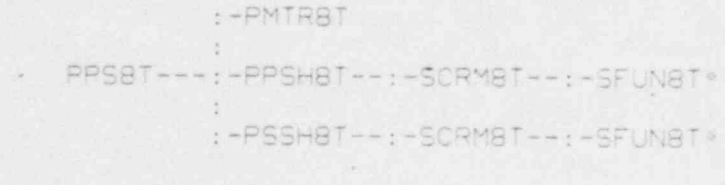

Figure 6-28 PPS Driver

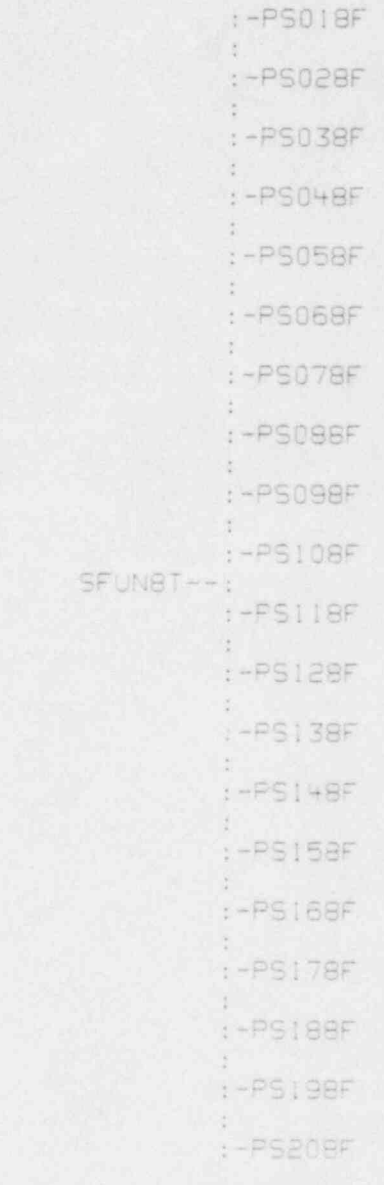

Figure 6-29 PPS Trip Functions

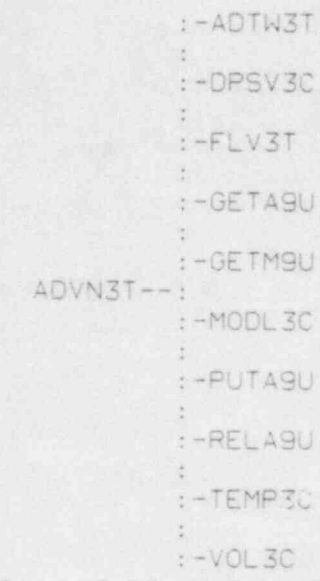

Figure 6-30 Update Transient SG Variables

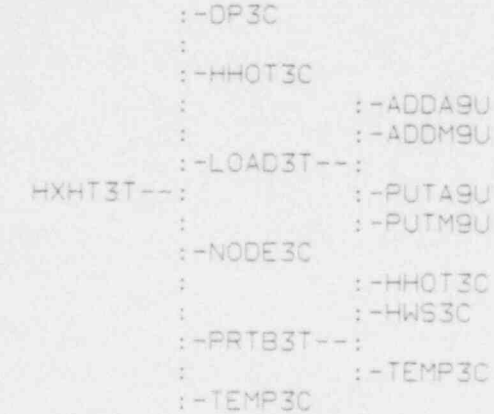

Figure 6-31 Transient SG Hot-Side Heat Exchanger Calculations

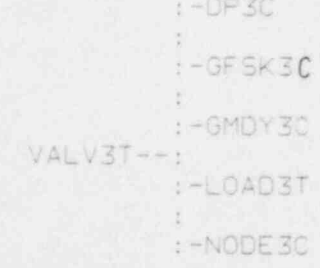

Figure 6-32 SG Transient Valve Conditions

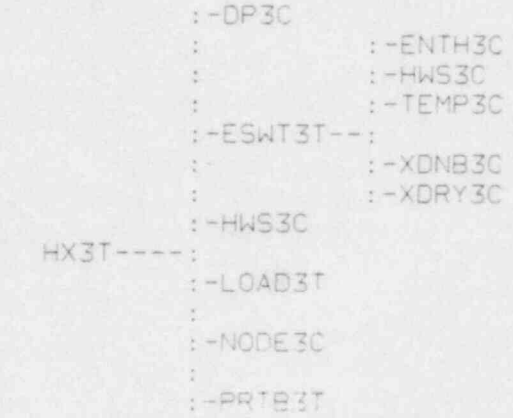

Figure 6-33 Transient SG Cold-Side Heat Exchanger Calculations

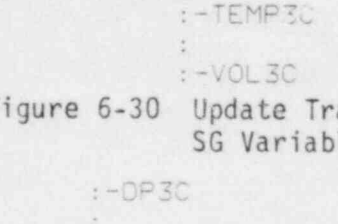

Figure 6-34 SG Matrix Calculations

Figure 6-35 Transient SG Mass and Energy Balance

Figure 6-36 Transient Boundary Conditions Into Segment Matrices

6.4 DATA DICTIONARY

Since SSC is a system simulation code, by its very nature it requires many variables and parameters to describe any given plant representation. To aid the user in understanding and interpreting SSC and its results, a data dictionary of all global variables has been constructed. A global variable is defined as any variable whose name adheres to the symbolic naming convention (see Section 6.2) and which resides in a labelled common block.

Contained in the alphabetically arranged data dictionary is the following information for each variable:

1. Type of variable (e.g., "A" designates array; "S" designates scalar).
2. Definition of the variable.
3. Units (in SI dimensions).
4. Labelled common block in which the variable resides (note - if reference is made to common block VD9V, this signifies that the variable is a dynamically allocated array).
5. Listing of each subroutine where the variable is referenced (i.e., where it appears on right hand side of an equal sign).
6. Lising of each subroutine where the variable is defined (i.e., where it appears on left hand side of an equal sign).
7. If the variable is an input quantity, the input file and data record it appears on. Abbreviations used are: V-VESSEL, N-NALOOP, S-STMGEN, O-OPDATA, M-MATDAT, T-TRNDAT.

Since the data dictionary encompasses approximately 200 pages, it is impractical to reproduce it here. However, a sample page is provided in Figure 6-37. A complete data dictionary is supplied to every user both on 48X magnification microfiche and on tape.

FORTRAN NAME	TYPE	DEFINITION	UNITS	LABELLED COMMON	REFERENCED	DEFINED
TIOUHX	A	TEMPERATURE OF COOLANT EXITING IHX PRIMARY SIDE	K	VD9V	HYDRIT PRNT9S PRNT1T PRET1T PSIN8T IHXIT PBAL9S END1S LOOP1S	IHX1S IHXIT END1T PBAL9S LOOP1S
TIOUTL	A	COOLANT TEMPERATURE AT OUTLET OF PRIMARY LOOP	K	VD9V	INTF9T FLIN8T PRNT1T LPLN6T	PRET1T LOOP1T
TIOUTP	A	COOLANT TEMPERATURE AT OUTLET OF PRIMARY PUMP	K	VD9V		INIT1T
TIOUT	A	COOLANT TEMPERATURE AT IHX PRIMARY OUTLET AT PREVIOUS TIME	K	VD9V	IHXIT	PRET1T IHX1T
TIPIN	S	COOLANT TEMPERATURE AT IHX INLET AT ADVANCED TIME	K	SCRH1V	IHXIT	IHXIT
TIPMP1	S	INITIAL VALUE OF TIPUMP	K	BNDS8R	LIST8R CALC8R	READ8R
TIPNAS	A	TEMPORARY ARRAY TO STORE ADVANCED TIME TEMPERATURES IN IHX SECONDARY SIDE	K	VD9V	IHXIT	IHXIT
TIPNA	A	COOLANT TEMPERATURE AT ADVANCED TIME	K	VD9V	IHXIT	IHXIT
TIPOUT	S	COOLANT TEMPERATURE AT IHX PRIMARY OUTLET AT ADVANCED TIME	K	SCRH1V		IHXIT
TIPSH	A	TEMPORARY ARRAY TO STORE IHX SHELL TEMPERATURE AT ADVANCED TIME	K	VD9V	IHXIT	IHXIT

Figure 6-37 Sample Page from Data Dictionary

7. INPUT/OUTPUT DESCRIPTION

7.1 GENERAL DESCRIPTION OF INPUT

In the design of SSC, great emphasis has been placed on flexibility and adaptability so as to make its capabilities applicable to any LMFBR design for a wide class of transients. This approach to modeling necessitates considerable interaction between the user and the code, especially during the initial stages of the calculation.

The structure of the SSC input is drawn on the same modular lines as that which dominates the calculational portion of the code. The basic component of the input is the input record or card-image record. These records are grouped on a modular basis to form subdivisions of the input, which in turn are referred to as data files (see Figure 7-1 and refer also to sample input provided in this section and Appendix B). Each data file has been assigned a file name to delimit as well as to identify the file partitioning. The entire sequence of input records constitutes the input file.

Input is processed by SSC in a three-fold operation (refer also to Figures 6-2, 6-5, 6-6 and 6-7). The interpreter, built around a version of the GENRD [7-1] processor makes the initial pass over the input. Verification follows, checking for consistency within the data set and against the criteria detailed in the data dictionary (Section 6.4 and accompanying micro-fiche). An inconsistency at this point causes the program to enter an error mode and generates a diagonistic message on the output file. The program is terminated at the end of this stage if any error has been detected. As a further check, all card-images are entered on the output file as they are interpreted, as are all decoded values assigned to all parameters.

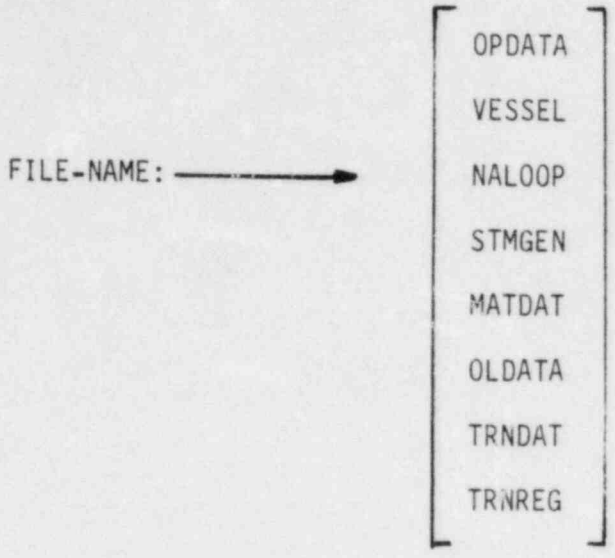

OPDATA - overall plant operating conditions

VESSEL - core and in-vessel components

NALOOP - primary and secondary heat transport systems

STMGEN - steam generator

MATDAT - material properties

OLDATA - user initiated program control

TRNDAT - conditions to initiate transient scenario

TRNREG - transient restart update

Figure 7-1 SSC Input Files

With the verification complete, the third processor proceeds to initialize a series of internal parameters on the basis of the defined input. The steady state calculations are then initiated.

The list of input required to initialize SSC consists of a series of free-format card-image records. These records contain control specifications and/or data in columns 1 through 72. The record format is 'free' in the sense that as long as the sequence of data conforms to the ordering detailed in this document, the physical placement of data fields as well as their degree of numerical accuracy is determined solely by the user.

A very rudamentary psuedo-grammar forms the basis on which the SSC input is constructed. The overall scheme in which this grammar operates is described in Figure 7-2. Its syntax is defined as follows:

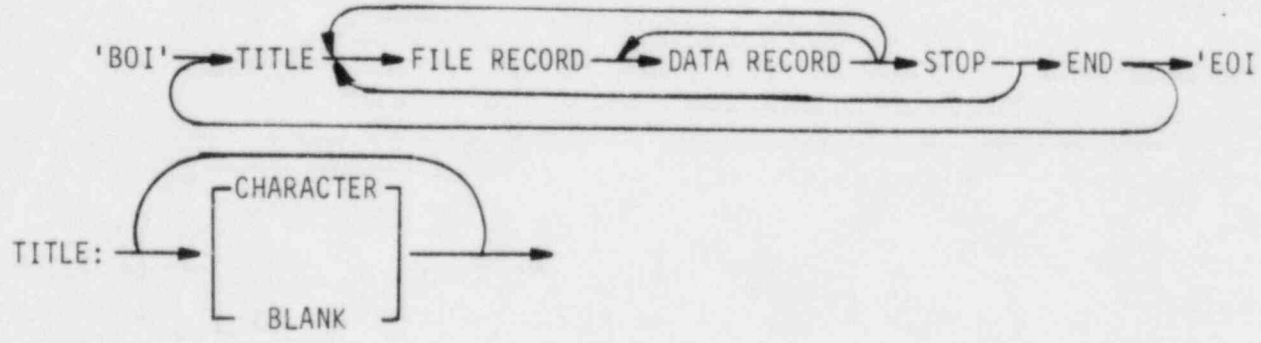

TITLE:

A title will appear as part of the banner heading on major pages of the output file. It is limited to one record's length but may extend beyond the seventy-two (72) character limit to eighty (80) characters. Although a required portion of the input, this record is provided solely as a means of associating an input with the resulting calculation. The user may choose any degree of functionality desired to assign to the titles, since it is not otherwise processed.

```
BEGIN
   GET NEXT-RECORD
   WHILE NEXT-RECORD IS NOT 'EOI'  DO
      PROCESS TITLE
      GET NEXT-RECORD
      WHILE NEXT-RECORD IS NOT 'END"  DO
         WHILE NEXT-RECORD IS NOT 'STOP"  DO
            IF NEXT-RECORD IS FILE-RECORD
            THEN
               CLOSE PREVIOUSLY OPENED DATA FILE (IF OPENED FILE EXISTS)
               OPEN NEW DATA FILE
               GET NEXT-RECORD
            ELSE
               IF NEXT-RECORD IS DATA-RECORD
               THEN
                  PROCESS DATA
                  GET NEXT-RECORD
               ELSE
                  ERROR CONDITION
                  GET NEXT-RECORD
         END
         INITIATE PROCESSING (TO EXTENT SPECIFIED)
         GET NEXT-RECORD
      END
   END
END-STOP
```

Figure 7-2 Psuedo-Grammar Format of SSC Input Files

FILE RECORD:

To open a data file, the following pseudo-grammar is appropriate:

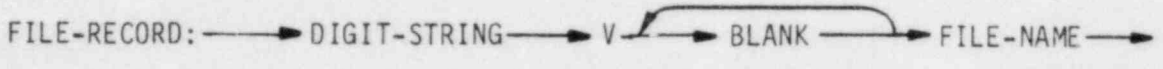

The numeric sequence accumulated in this field is used to identify differing versions (V) of similar input files. It is provided as a convenience and is subsequently ignored by the processor. The FILE-NAME provides an associative link between the data of the accompanying data file and a particular computational module(s). The current SSC FILE-NAMEs are shown in Figure 7-1.

DATA RECORD:

The pseudo-grammar for an individual DATA-RECORD is:

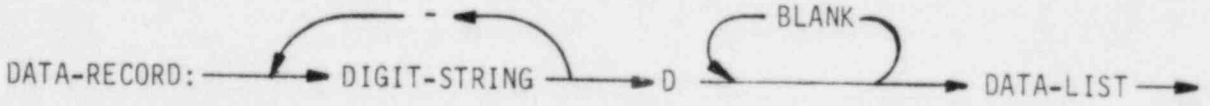

For a DATA-RECORD to be properly processed, its DIGIT-STRING (or strings) must be among the set of defined record numbers of the corresponding data file. A list of all valid record numbers can be found in the sections of this chapter dealing with the particulars of each data file.

The use of a hypenated digit string (e.g., 201-210D) indicates that the data which follows is to be assigned to a range of consecutive record numbers. This format is used exclusively with records whose record numbers possess an implied dependency (e.g., record 101D, file VESSEL).

A DATA-RECORD is completely processed before the next record is interpreted. A DATA-RECORD is implicitly defined to have a maximum length equal to one or more card-images (72 characters). It is terminated either by a slash (/) or by a column seventy-two (72) preceeding a DATA-RECORD, a FILE-RECORD or a STOP, as described below. Information following a slash (/) is not processed, nor is any information beyond column seventy-two (72). As a result, the user may find this to be a convenient place to annotate the data files. Within a given data partition, several options are available as described below:

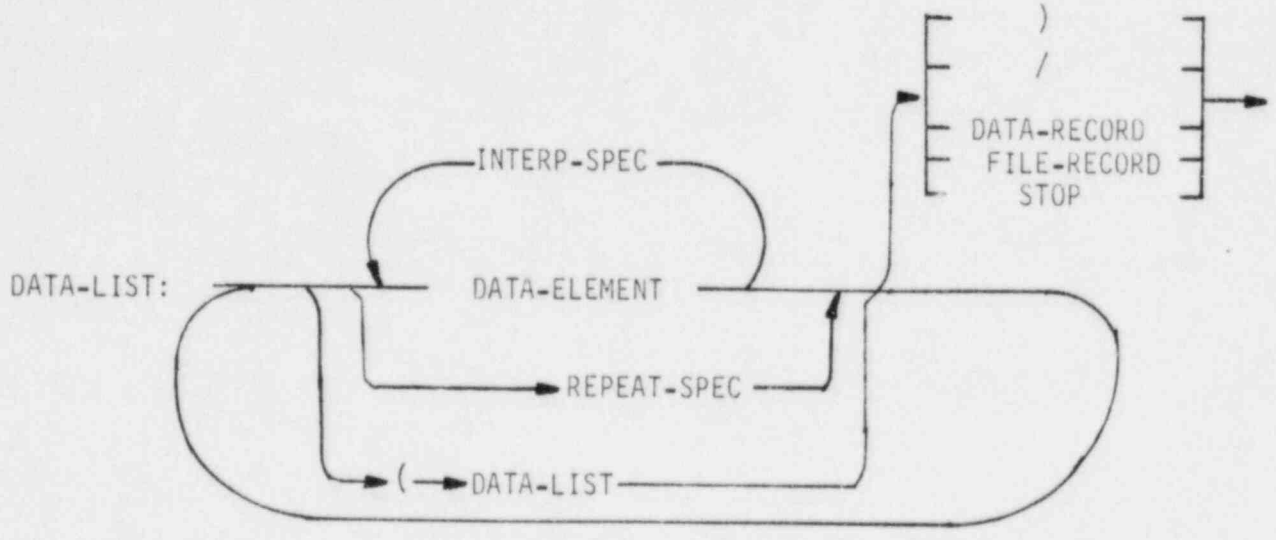

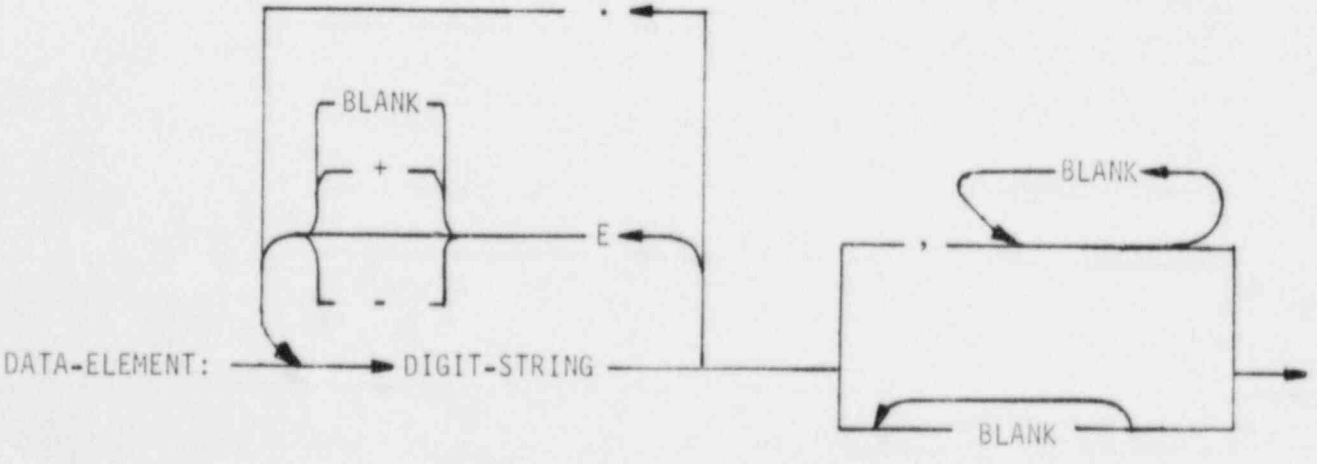

Two shorthand constructs are provided for the specification of input. The

INTERP-SPEC: ⟶ DIGIT-STRING ⟶ 'I'

and the

REPEAT-SPEC: ⟶ DIGIT-STRING ⟶ 'R'

Both are used to assign numeric data to consecutive memory locations. The REPEAT-SPEC stores a sequence of one or more constants. For example:

7.2, 3R

is equivalent to

7.2, 7.2, 7.2

and

(1.0, 15, 0.72), 4R

is equivalent to

1.0, 15, 0.72, 1.0, 15, 0.72, 1.0, 15, 0.72, 1.0, 15, 0.72

The 'I" specification provides a means of inserting one or more equally spaced values between two real (or two integer) end points. For example,

11, 7I, 19

is equivalent to

11, 12, 13, 14, 15, 16, 17, 18, 19

and

1.0, 3I, 2.0

is equivalent to

1.0, 1.25, 1.50, 1.75, 2.0

The integer preceding the 'I' specifies the number of equally spaced values to be inserted between the end points. The terminal points bound the sequence and are not strictly considered to be members of it, therefore, 1i, 7I, 19 and not 11, 9I, 19 and 1.0, 3I, 2.0 and 1.0, 5I, 2.0 in the preceding examples. A check is made to determine the data type (real or integer) of the end points. Both points must be of the same type. If an integer interpolation is indicated, the resulting increment must also be of integer type.

7.2 STRUCTURE OF THE INPUT FILE

The SSC input data files (refer to Figure 7-1) are of three basic types: component description, program control and transient delineation. The majority are of the first type. In this grouping are VESSEL, NALOOP, STMGEN, MATDAT and OPDATA. The third category is limited to TRNDAT and TRNREG (for an in-transient restart). OLDATA is the only file containing direct program control.

As might be expected, the entire system must be completely specified before the calculation can proceed. Under default program control, the processing of VESSEL, STMGEN, NALOOP and OPDATA fulfills this function. The file MATDAT is not required to make the plant specification, but it must be processed when the system is initialized if the user wishes to alter or add to the existing system defaulted material property parameters. OLDATA is also included at this point if other than default program control is required (for a definition of what constitutes default control, consult Section 7.9 of this document). The ordering of the files in this pre-calculational block is inconsequential, but a record containing only the character-string 'STOP' terminates it.

From a particular plant configuration, any number of valid transient scenarios may be initiated. The conditions and events which define a transient are specified in TRNDAT. This file is always followed by a 'STOP' record. The final record on the input file is the 'END' record which consists of the character-string 'END'.

7.3 IN-VESSEL DATA (VESSEL)

All geometric and hydraulic data required to specify the core and in-vessel components are described here. Subsequent pages of this section (Figure 7-3 and Table 7-1) show, on a record-by-record basis, how the specific information is supplied by the user.

These records may be input in any order, except that record 1 must be first, as it contains variable dimensioning data.

The core and in-vessel components are represented physically by a lower inlet plenum, core and upper outlet mixing plenum (see Figure 3.1-1). The core is composed of any number of parallel channels and a bypass (see Figure 3.1-3). For the input data, a distinction is made between number of channels simulated (denoted by N6CHAN and use of counter K) and number of rod types (denoted by N5RTYP and use of counter L). This is done, because any number of channels may be represented, but the physical makeup of many of these channels will probably be identical (i.e., N5RTYP less than N6CHAN).

The physical makeup of each rod type is assigned through records of the 101 series. Record numbers of this series possess implied rod type dependency. That is, the actual record number is formed by summing the value of the rod type identifier and 100 (i.e., record 101 = 100 + (the rod type identifier for rod type one (1))). Here, by allocating (or setting to zero) the required lengths, materials, etc., of the regions provided (i.e., lower fission gas plenum, lower blanket, fuel, upper blanket, upper fission gas plenum, also refer to Figure 3.1-4), any fuel, blanket or control rod description may be specified.

The rod type is assigned to the individual channels through record 2. Records 3 through 21 contain various other geometric and hydraulic data for the channels.

Record 23 contains data which is very useful for off-normal initial operating conditions. This data enables the user to correctly initialize the flow split to the various core channels under off-normal conditions and make use of known information obtained under normal (i.e., full power/flow) operation. Accurate data specifying the flow split to the core channels is usually available at design power and flow conditions. Thus, a steady-state case may be run at design conditions setting L60PT = 0 and specifying the known flow fractions through record 4. The result of this run will be the calculation of the F6LSA4(K) (refer also to Table 7-1, Record 23 and Section 3.1.2.5a, K_4). To then run at some off-normal condition where the individual flow fractions are not known, L60PT is set to 1 and the previously computed F6LSA4(K) values are used.

Records 31, 33 and 34 must be utilized together for each channel. These records contain data needed to specify frictional pressure drop information across the inlet orifice zone for each channel. Specifically, the following data are entered:

Record 31 - Effective hydraulic diameter (m).

Record 33 - Frictional pressure drop across orifice (N/m2).

Record 34 - Fraction of the total orifice zone length over which the frictional pressure drop is taken (value 0. to 1.0).

For each channel, two of these values must be non-zero, the other zero. If two or more values are zero, there is no frictional pressure drop across the assembly inlet orifice assigned to that channel.

In records 24, 28, 29 and 32, data for K-loss type pressure drop calculations are required. To allow the user some flexibility, these numbers may

be read in as either positive, negative or zero values. If the number is positive, it is assumed in each case to be the loss coefficient itself. If the value is less than zero, it is assumed to represent the actual K-loss pressure drop (N/m2). The value of the corresponding coefficient is then computed internally. If the value is zero, no K-loss pressure drop is assigned. It should be noted when running cases initiating from off-normal conditions (i.e., at some condition other than that at which the K-loss coefficient was computed), that the actual K-loss coefficient should be read in and not the pressure drop. This thus entails a two step procedure; first running a steady-state initialization case to obtain the K-loss coefficients at the nominal conditions at which the pressure drop is known, then running a subsequent case at the off-normal conditions where the previously calculated values for the K-loss coefficients are the known input.

The records of the 201, 301, 401 and 501 series contain various power profile and fission gas data for each channel. Record numbers of these series possess implied channel dependency.

```
0V VESSEL
1D 7,5,18,14,12,18,14,4,6R,1/
2D 4,1,5,2,5,2,3/
3D 2.667E-5, 7.206E-1, 4.175E-5, 1.710E-1, 2.790E-5, 1.034E-1, 2.060E-3/
4D 1.555E-5, 6.742E-1, 3.126E-5, 1.542E-1, 1.798E-5, 1.183E-1, 1.260E-2/
5D 1.162,1.76,1,126,15/
7D 1.704E-5,1.9979E-5, 3.497E-5,4.1883E-5, 3.497E-5,4.1883E-5,5.1438E-5/
8D 3.7261E-3,3.2537E-3,3.6242E-3,3.3985E-3,3.6242E-3,3.3985E-3,3.937E-3/
11D 0.0,7R/
12D 2.4575E-3,2R, 5.969E-3,4R, 5.8295E-3/ PSAR TABLE 4.3-1
13D 0.00254,2R, 0.0060450,4R, 0.0063755/
14D 0.002921,2R, 0.0064260,4R, 0.0076455/
15D 0.0,7R/
16D 2.413E-3,2R, 5.969E-3,4R, 5.8295E-3/ PSAR TABLE 4.3-1
17D 0.0,7R/
18D 2.413E-3,2R, 5.969E-3,4R, 5.8295E-3/
19D 1.E-5,1.0,1.E-5,1.0,1.E-5,1.0,1.0/
20D 1.0E+04,7R/
21D 3.5E+06,7R/
23D 0, 0.0,8R, 871497., 5222., 25, 25, 0.0001, 0.01, 5.0E5/
24D   86.2, 158533.2, 26205.3, .8, -39989./
25D   1, 300.0/
27D 0.,2R, 1.0773,6.5448,12.7495,7.7453,13.3153/
28D   16,.1.4,0.6,25.3,30.0,121.5,1.289,14.0,1400.0,
  560., 3.41,-15158.,.72.4,7126E7, 1.9517E7,12.8E7/
29D   20.15,1.25,2.585,0.1288, -300000.0 ,920000.0/
30D   0.316,0.25,-16.15,24.96,-8.55,0.3/
31D 0.0,7R/
32D 0.0,  14R/
33D 5.010E5, 4.85E5, 5.01E5, 4.86E5, 6.67E5, 6.84E5, 7.07E5/
34D  1.0 7R/
101D 0.0, 0.3556, 0.9144, 0.3556, 1.2192, 0, 2, 10, 2, 4,
     1.2509, 51.739, 60, 70, 40,.96, 0.96, 0.98, 50, 0.95, 0.96,
     0.98, 40,.96, 0.96, 0.98, 217, 0.0014, 0.1101, 0.00305 1.75/
102D 0.0, 0.0, 0.0, 1.6256, 1.159, 0,3R, 10, 4,
     1.072, 7.6923, 60, 70, 0, 0.0,3R, 0, 0.0,3R, 40, 0.96, 0.96, 0.98,
     61, 0.00084, 0.110, 0.00305  1.75 /
103D 0.36068, 0.0, 0.9144, 0.0, 0.57658, 2, 0, 8, 0, 2, 1.05, 21.179,
     60, 70, 0, 0.0,3R, 51, 1.0,3R, 0, 0.0,3R, 37, .000762, .10033,
     0.0011176  1.75 /
104D 0.0, 0.3556, 0.9144, 0.3556, 1.2192, 0, 2, 10, 2, 4,
     1.2509, 51.739, 60, 70, 40,.96, 0.96, 0.98, 50, 0.95, 0.96,
     0.98, 40,.96, 0.96, 0.98, 1, 0.0014, 0.1101, 0.00305 1.75/
105D 0.0, 0.0, 0.0, 1.6256, 1.159, 0,3R, 10, 4,
     1.072, 7.6923, 60, 70, 0, 0.0,3R, 0, 0.0,3R, 40, 0.96, 0.96, 0.98,
     1, 0.00084, 0.110, 0.00305  1.75 /
201-202D 0.03, 0.09, 0.750, 0.920, 1.090, 1.180, 1.210, 1.210, 1.130,
     1.010, 0.850, 0.660, 0.05, 0.02, 0.001,4R/
203-206D 0.3, 0.700, 1.300, 1.750, 1.900, 1.900, 1.700, 1.250,
     0.750, 0.3, 0.001,4R/
207D 0.001,2R, 1.0,8R, 0.001,2R/
301-306D 1.,4R/
307D  1./
401-407D 0.98, 0.01, 0.0/
501-507D 80, 0.95, 81, 0.03, 82, 0.02/
```

Figure 7-3 VESSEL Data File Sample Input for a Seven Channel Description (Typical of CRBRP)

***** FILE VESSEL

RECORD 1			
N6CHAN	INTEGER	-	NUMBER OF CHANNELS BEING SIMULATED
N5RTYP	INTEGER	-	NUMBER OF ROD TYPES
N5ASEC(L)	INTEGER	-	NUMBER OF AXIAL SECTIONS(SLICES) OF EACH ROD TYPE (L = 1,N5RTYP)
N5NFR(K)	INTEGER	-	NUMBER OF RADIAL FUEL NODES IN AN AXIAL SLICE OF EACH CHANNEL (K = 1,N6CHAN)
RECORD 2			
L6ATYP(K)	INTEGER	-	ROD TYPE ASSIGNED TO EACH CHANNEL. ALSO USED FOR FRICTION FACTOR CORRELATION. SEE EQ. 5.71 - 5.73 FOR ACCEPTABLE TYPE SELECTIONS. (K = 1,N6CHAN)
RECORD 3			
F6TPOW(K)	REAL	-	FRACTION OF TOTAL POWER IN EACH CHANNEL (K = 1,N6CHAN)
RECORD 4			
F6FLOW(K)	REAL	-	FRACTION OF TOTAL VESSEL FLOW IN EACH CHANNEL (K = 1,N6CHAN)
RECORD 5			
N5ASS(K)	INTEGER	-	NUMBER OF ASSEMBLIES REPRESENTED BY EACH CHANNEL (K = 1,N6CHAN)
RECORD 7			
A6ROD(K)	REAL	M2	SODIUM FLOW AREA PER ROD IN EACH CHANNEL (K = 1,N6CHAN)
RECORD 8			
Y6HYDR(K)	REAL	M	HYDRAULIC DIAMETER OF EACH COOLANT CHANNEL (K = 1,N6CHAN)
RECORD 11			
X5FIR(K)	REAL	M	FUEL INNER RADIUS OF EACH CHANNEL (K = 1,N6CHAN)
RECORD 12			
X5FOR(K)	REAL	M	FUEL OUTER RADIUS OF EACH CHANNEL (K = 1,N6CHAN)
RECORD 13			
X5CLIR(K)	REAL	M	CLADDING INNER RADIUS OF EACH CHANNEL (K = 1,N6CHAN)
RECORD 14			
X5CLOR(K)	REAL	M	CLADDING OUTER RADIUS OF EACH CHANNEL (K = 1,N6CHAN)
RECORD 15			
X5LBIR(K)	REAL	M	LOWER BLANKET INNER RADIUS OF EACH CHANNEL (K = 1,N6CHAN)
RECORD 16			
X5LBOR(K)	REAL	M	LOWER BLANKET OUTER RADIUS OF EACH CHANNEL (K = 1,N6CHAN)
RECORD 17			
X5UBIR(K)	REAL	M	UPPER BLANKET INNER RADIUS FOR EACH CHANNEL (K = 1,N6CHAN)

Table 7-1 Input Description for Data File VESSEL

RECORD 18				
XSUBOR(K)		REAL	M	UPPER BLANKET OUTER RADIUS FOR EACH CHANNEL (K = 1,NSCHAN)
RECORD 19				
FSASTR(K)		REAL	-	FRACTIONAL HEAT TRANSFER AREA OF STRUCTURE USED PER CHANNEL (K = 1,NSCHAN)
RECORD 20				
HSNDGP(K)		REAL	W/(K*M2)	HEAT TRANSFER COEF. FOR FUEL-CLAD CONTACT FOR EACH CHANNEL (K = 1,NSCHAN)
RECORD 21				
PSFGAS(K)		REAL	N/M2	FISSION GAS PRESSURE FOR EACH CHANNEL (K = 1,NSCHAN)
RECORD 23				
LSWOPT		INTEGER	-	FLOW FRACTION OPTION INDICATOR: 0-FRACTIONS KNOWN, 1-FRACTIONS UNKNOWN
FSLSAV(K)	*	REAL	-	TOTAL K-LOSS COEF. AT TOP OF EACH CHANNEL (K = 1,NSCHAN)
FSLSBP	*	REAL	-	BYPASS FLOW K-LOSS COEF.
PSDSGN		REAL	N/M2	WHEN LSWOPT=0, ACTUAL NOZZLE TO NOZZLE PRES DROP WHEN LSWOPT=1, CORE DESIGN DELTA-P (USED IN PSINIT GUESS)
WSDSGN	*	REAL	KG/S	DESIGN CORE FLOW RATE
NSPMAX	*	INTEGER	-	MAXIMUM ITERATION FOR PRESSURE CALULATION
NSFLMX	*	INTEGER	-	MAXIMUM ITERATIONS FOR FLOW CALCULATION
FSCONV	*	REAL	-	CONVERGENCE CRITERION (RELATIVE)
FSWSTP	*	REAL	-	MAXIMUM FLOW FRACTION CHANGE ALLOWED PER ITERATION
PSSTEP	*	REAL	N/M2	MAXIMUM PRESSURE CHANGE ALLOWED PER ITERATION
			* NOTE: NON-ZERO VALUE(S) NEED BE ASSIGNED ONLY WHEN LSWOPT=1	
RECORD 24				
VSLP		REAL	M3	VOLUME OF LOWER PLENUM
BSLPMC		REAL	J/K	MASS HEAT CAPACITY OF METAL IN LOWER PLENUM
HSLPUA		REAL	W/K	OVERALL HEAT TRANSFER COEFFICIENT IN LOWER PLENUM
ASLPLF		REAL	M2	X-SECTIONAL FLOW AREA OF LOWER PLENUM
FSPKLP		REAL	- OR (N/M2)	IF > 0, TOTAL K-LOSS COEFF. FROM INLET NOZ ELEV TO CORE BOTTOM IF < 0, TOTAL K-LOSS P-DROP FROM INLET NOZ ELEV TO CORE BOTTOM
RECORD 25				
LSMESH		INTEGER	-	FUEL RADIAL MESH INDICATOR: 0-EQUI-RADIUS, 1-EQUI-AREA
TSREF		REAL	K	TEMPERATURE AT WHICH THE ROD DIMENSIONS ARE REFERENCED

Table 7-1 (cont.)

RECORD 27			
Z6REF	REAL	M	REFERENCE ELEVATION OF REACTOR VESSEL
Z6INOZ	REAL	M	ELEVATION OF VESSEL INLET NOZZLE ABOVE Z6REF
Z6BCOR	REAL	M	ELEVATION OF BOTTOM OF CORE ABOVE Z6REF
Z6TCOR	REAL	M	ELEVATION OF TOP OF CORE ABOVE Z6REF
Z6UPLN	REAL	M	ELEVATION OF INITIAL UPPER PLENUM SODIUM LEVEL ABOVE Z6REF
Z6ONOZ	REAL	M	ELEVATION OF VESSEL OUTLET NOZZLE ABOVE Z6REF
Z6UPTL	REAL	M	ELEVATION OF TOP OF UPPER PLENUM (BOTTOM OF HEAD) ABOVE Z6REF
RECORD 28			
A6GL	REAL	M2	AREA BETWEEN GAS AND LIQUID IN VESSEL UPPER PLENUM (SAME AS FLOW X-SECTIONAL AREA)
A6GM1	REAL	M2	AREA BETWEEN GAS AND METAL 1 IN VESSEL UPPER PLENUM
A6GM2	REAL	M2	AREA BETWEEN GAS AND METAL 2 IN VESSEL UPPER PLENUM
A6GM3	REAL	M2	AREA BETWEEN GAS AND METAL 3 IN VESSEL UPPER PLENUM
A6LM1	REAL	M2	AREA BETWEEN LIQUID AND METAL 1 IN VESSEL UPPER PLENUM
A6LM2	REAL	M2	AREA BETWEEN LIQUID AND METAL 2 IN VESSEL UPPER PLENUM
A6JET	REAL	M2	AREA OF CORE JET FLOW
H6GAS	REAL	W/(K*M2)	HEAT TRANSFER COEF. FOR COVER GAS IN UPPER PLENUM
H6LNA	REAL	W/(K*M2)	HEAT TRANSFER COEF. BETWEEN SODIUM AND METAL IN UPPER PLENUM
H6INF	REAL	W/(K*M2)	HEAT TRANSFER COEF. AT INTERFACE OF TWO SODIUM ZONES IN UPPER PLENUM
Z6CHIM	REAL	M	LENGTH OF CHIMNEY ABOVE CORE OUTLET
F6PKUP	REAL	- OR (N/M2)	IF > 0, TOTAL K-LOSS COEFF. FROM CORE TOP TO OUTLET NOZ ELEV IF < 0, TOTAL K-LOSS P-DROP FROM CORE TOP TO OUTLET NOZ ELEV
F6LEAK	REAL	-	FRACTION OF BYPASS FLOW LEAKING DIRECTLY INTO UPPER PLENUM FROM LOWER BYPASS REGION
B6UMC1	REAL	J/K	MASS HEAT CAPACITY OF METAL 1 IN UPPER PLENUM
B6UMC2	REAL	J/K	MASS HEAT CAPACITY OF METAL 2 IN UPPER PLENUM
B6UMC3	REAL	J/K	MASS HEAT CAPACITY OF METAL 3 IN UPPER PLENUM

Table 7-1 (cont.)

RECORD 29			
A6LFBP	REAL	M2	FLOW AREA OF LOWER REGION OF BYPASS CHANNEL
A6UFBP	REAL	M2	FLOW AREA OF UPPER REGION OF BYPASS CHANNEL
Y6LRBP	REAL	M	HYDRAULIC DIAMETER OF LOWER BYPASS REGION CHANNEL
Y6URBP	REAL	M	HYDRAULIC DIAMETER OF UPPER BYPASS REGION CHANNEL
F6INBP	REAL	- OR (N/M2)	IF > 0, TOTAL K-LOSS COEFF. AT BYPASS INLET IF < 0, TOTAL K-LOSS P-DROP AT BYPASS INLET
H6ABP	REAL	W/K	OVERALL HEAT TRANSFER COEF. BETWEEN UPPER BYPASS REGION SODIUM AND LINER
RECORD 30			
F6FRC1	REAL	-	COEF. USED IN FRICTION FACTOR CORRELATION FOR ROD BUNDLES (EQ. 5-71)
F6FRC2	REAL	-	COEF. USED IN FRICTION FACTOR CORRELATION FOR ROD BUNDLES (EQ. 5-71)
F6NUC1	REAL	-	COEF. USED IN NU. NUMBER CORRELATION (FORCED CONVECTION - ROD BUNDLE) (EQ. 5-75)
F6NUC2	REAL	-	COEF. USED IN NU. NUMBER CORRELATION (FORCED CONVECTION - ROD BUNDLE) (EQ. 5-75)
F6NUC3	REAL	-	COEF. USED IN NU. NUMBER CORRELATION (FORCED CONVECTION - ROD BUNDLE) (EQ. 5-75)
F6NUC4	REAL	-	EXP. USED IN NU. NUMBER CORRELATION (FORCED CONVECTION - ROD BUNDLE) (EQ. 5-75)
RECORD 31			
Y6HYOZ(K) *	REAL	M	HYDRAULIC DIAMETER OF INLET ORIFICE ZONE OF EACH CHANNEL (K = 1,N6CHAN)

* NOTE: OF THE THREE PARAMETERS Y6HYOZ, P6FINZ, AND F6ZINZ TWO MUST BE NON-ZERO THE OTHER ZERO FOR EACH CHANNEL.

RECORD 32			
F6LSA(1,K) *	REAL	- OR (N/M2)	K-LOSS PRESSURE AT INLET ORIFICE ZONE FOR EACH CHANNEL (K = 1,N6CHAN)
F6LSA(2,K) *	REAL	- OR (N/M2)	K-LOSS PRESSURE AT ASSEMBLY OUTLET FOR EACH CHANNEL (K = 1,N6CHAN)

* NOTE: IF VALUE POSITIVE; THE ACTUAL K-LOSS FACTOR.
IF VALUE NEGATIVE; THE K-LOSS PRESSURE DROP (N/M2).

NOTE: DATA FOR THIS RECORD CONSISTS OF A SERIES OF PAIRED POINTS. THE INDEX (K) IS INCREMENTED OVER THE SET OF ALL DATA REQUIRED FOR THE RECORD. THAT IS: F6LSA(1,1),F6LSA(2,1),F6LSA(1,2),ETC.

RECORD 33			
P6FINZ(K) *	REAL	N/M2	PRESSURE DROP DUE TO FRICTION ACROSS THE INLET ORIFICE ZONE FOR EACH CHANNEL (K = 1,N6CHAN)

* NOTE: OF THE THREE PARAMETERS Y6HYOZ, P6FINZ, AND F6ZINZ TWO MUST BE NON-ZERO THE OTHER ZERO FOR EACH CHANNEL.

RECORD 34			
F6ZINZ(K) *	REAL	-	FRACTION OF ASSEMBLY INLET ORIFICE ZONE LENGTH (Z6INZ) ASSIGNED TO EACH CHANNEL (K = 1,N6CHAN)

* NOTE: OF THE THREE PARAMETERS Y6HYOZ, P6FINZ, AND F6ZINZ TWO MUST BE NON-ZERO THE OTHER ZERO FOR EACH CHANNEL.

Table 7-1 (cont.)

RECORD 101 - 199 (IMPLIED ROD TYPE DEPENDENCY, L = REC.NUM.-100)

Z6LFGP	REAL	M	AXIAL LENGTH OF LOWER FISSION GAS PLENUM REGION OF L-TH ROD TYPE
Z6LBLK	REAL	M	AXIAL LENGTH OF LOWER BLANKET REGION OF L-TH ROD TYPE
Z6AFUL	REAL	M	AXIAL LENGTH OF ACTIVE FUEL REGION OF L-TH ROD TYPE
Z6UBLK	REAL	M	AXIAL LENGTH OF UPPER BLANKET REGION OF L-TH ROD TYPE
Z6UFGP	REAL	M	AXIAL LENGTH OF UPPER FISSION GAS PLENUM REGION OF L-TH ROD TYPE
N6LFGP	INTEGER	-	NUMBER OF AXIAL COOLANT NODES IN LOWER FISSION GAS PLENUM REGION OF L-TH ROD TYPE
N6LBLK	INTEGER	-	NUMBER OF AXIAL COOLANT NODES IN LOWER BLANKET REGION OF L-TH ROD TYPE
N6AFUL	INTEGER	-	NUMBER OF AXIAL COOLANT NODES IN ACTIVE FUEL REGION OF L-TH ROD TYPE
N6UBLK	INTEGER	-	NUMBER OF AXIAL COOLANT NODES IN UPPER BLANKET REGION OF L-TH ROD TYPE
N6UFGP	INTEGER	-	NUMBER OF AXIAL COOLANT NODES IN UPPER FISSION GAS PLENUM REGION OF L-TH ROD TYPE
F6PD	REAL	-	PITCH TO DIAMETER RATIO OF L-TH ROD TYPE
F6PWD	REAL	-	PITCH TO DIAMETER RATIO FOR WIRE WRAP OF L-TH ROD TYPE
L5CLMT	INTEGER	-	INDEX OF CLADDING MATERIAL OF L-TH ROD TYPE
L5STMT	INTEGER	-	INDEX OF STRUCTURAL MATERIAL OF L-TH ROD TYPE
L5LBMT	INTEGER	-	INDEX OF LOWER BLANKET MATERIAL OF L-TH ROD TYPE
F5DLBU	REAL	-	FRACTIONAL UNRESTRUCTURED GRAIN DENSITY OF LOWER BLANKET OF L-TH ROD TYPE
F5DLBE	REAL	-	FRACTIONAL EQUIAXED GRAIN DENSITY OF LOWER BLANKET OF L-TH ROD TYPE
F5DLBC	REAL	-	FRACTIONAL COLUMNAR GRAIN DENSITY OF LOWER BLANKET OF L-TH ROD TYPE
L5AFMT	INTEGER	-	INDEX OF ACTIVE FUEL MATERIAL OF L-TH ROD TYPE
F5DAFU	REAL	-	FRACTIONAL UNRESTRUCTURED GRAIN DENSITY OF ACTIVE FUEL OF L-TH ROD TYPE
F5DAFE	REAL	-	FRACTIONAL EQUIXED GRAIN DENSITY OF ACTIVE FUEL FOR L-TH ROD TYPE
F5DAFC	REAL	-	FRACTIONAL COLUMNAR GRAIN DENSITY OF ACTIVE FUEL FOR L TH ROD TYPE
L5UBMT	INTEGER	-	INDEX OF UPPER BLANKET MATERIAL OF L-TH ROD TYPE
F5DUBU	REAL	-	FRACTIONAL UNRESTRUCTURED GRAIN DENSITY OF UPPER BLANKET OF L-TH ROD TYPE
F5DUBE	REAL	-	FRACTIONAL EQUIXIAXED GRAIN DENSITY OF UPPER BLANKET OF L-TH ROD TYPE
F5DUBC	REAL	-	FRACTIONAL COLUMNAR GRAIN DENSITY OF UPPER BLANKET OF L-TH ROD TYPE
N5AROD	INTEGER	-	NUMBER OF RODS PER ASSEMBLY OF L-TH ROD TYPE
Y5WIRE	REAL	M	WIRE WRAP DIAMETER OF L-TH ROD TYPE
Y5FLAT	REAL	M	HEX-CAN FLAT-TO-FLAT INNER DIAMETER OF L-TH ROD TYPE
X5HXCN	REAL	M	TOTAL HEX-CAN WALL THICKNESS OF L-TH ROD TYPE
Z6INZ	REAL	M	LENGTH OF THE INLET HYDRAULIC ORIFICE ZONE OF L-TH ROD TYPE

Table 7-1 (cont.)

RECORD 201 - 299	(IMPLIED CHANNEL DEPENDENCY, K = REC.NUM.-200)		
F5PAX(J)	REAL	-	AXIAL POWER FRACTION FOR EACH NODE IN THE K-TH CHANNEL. (J = N5ASEC(L5ATYP(K)))
RECORD 301 - 399	(IMPLIED CHANNEL DEPENDENCY, K = REC.NUM.-300)		
F5PRAD(I)	REAL	-	FUEL POWER FRACTION IN EACH RADIAL FUEL NODE IN THE K-TH CHANNEL (I = 1,N5NFR(K))
		NOTE: NO AXIAL DEPENDENCE	
RECORD 401 - 499	(IMPLIED CHANNEL DEPENDENCY, K = REC.NUM.-400)		
F5PWR5	REAL	-	FRACTION OF POWER GENERATED IN THE K-TH CHANNEL DEPOSITED DIRECTLY INTO THE FUEL
F5PWR6	REAL	-	FRACTION OF POWER GENERATED IN THE K-TH CHANNEL DEPOSITED DIRECTLY INTO THE CLAD
F5PWR1	REAL	-	FRACTION OF POWER GENERATED IN THE K-TH CHANNEL DEPOSITED DIRECTLY INTO THE COOLANT
RECORD 501 - 599	(IMPLIED CHANNEL DEPENDENCY, K = REC.NUM.-500)		
L5GAS(I)	INTEGER	-	INDEX OF EACH FISSION GAS TYPE IN THE K-TH CHANNEL
F5GAS(I)	REAL	-	MOLE FRACTION OF EACH FISSION GAS IN THE K-TH CHANNEL
		NOTE: DATA FOR THIS RECORD CONSISTS OF A MAXIMUM OF 3 PAIRED POINTS. THE INDEX 'I' IS INCREMENTED OVER THE SET OF ALL DATA REQUIRED FOR THE RECORD. THAT IS: L5GAS(1),F5GAS(1),L5GAS(2),F5GAS(2),ETC	

Table 7-1 (cont.)

7.4 SODIUM LOOP DATA (NALOOP)

All geometric and hydraulic data required to specify the primary and secondary loop piping, pumps and IHX is input using data file NALOOP. Sodium-side hydraulic information in the steam generator is input using data file STMGEN. The listing included on subsequent pages of this section (Figure 7-4 and Table 7-2) shows, on a record-by-record basis, how the specific information is supplied to NALOOP by the user. These records may be input in any order, except that record 1 must be read first, as it contains variable dimensioning data.

The present version of SSC assumes that all primary heat transport systems (HTSs) are geometrically identical and are operating initially at the same steady-state. The same assumption applies to all secondary HTSs.

The numbering sequence for pipes within an HTS is important. In the primary loop, the pipe numbers must start at 1 at the vessel outlet and proceed sequentially around to the vessel inlet. On the primary loop, the IHX primary side is considered a pipe and a number must be assigned to it (1100 + L1IHX).

On the secondary side, the pipe numbers must start at 1 at the IHX secondary outlet and proceed sequentially around to the IHX secondary inlet. Here, in the intermediate HTS, the IHX secondary side and the steam generator are not assigned pipe numbers.

Piping data are read in on records 1101-1199 for the primary HTS and on records 1201-1299 for the secondary HTS. The individual pipe number (K) is derived from

(a) K = Record Number - 1100 and

(b) K = Record Number - 1200

for the primary and secondary HTS, respectively. IHX data (geometry, noding, etc.) is read in on records 101-104, 1002 and 1003.

The positions of the pumps in both primary and secondary loops are specified via record 1001 by the pipe number preceeding the pump. Required data, e.g., rated head, speed, flow, torque, etc., must be provided on records 112 for the primary pump and 122 for the secondary pump. The coefficients in the polynomial equations describing head and torque characteristics are given default values which should be satisfactory for most situations.

The position of the check valve in the primary loop is specified on record 1001 by the pipe number preceeding the check valve. If the number specified is zero, then no check valve is assumed and the pressure drop across the valve is always zero. Check valve data is supplied on record 111.

Provisions have been included in SSC so that all plant loops which are operating identically can be grouped into one simulated loop for computational efficiency if desired. Specification of loop simulation is given in records 1 (the N1LOOP parameter) and 2 (F1LUMP (K), K = 1, N1LOOP). Note that the value of the summation of F1LUMP must equal the value of N9LOOP contained in record 1 of file OPDATA.

```
0V NALOOP
1D  1, 5, 19, 8, 40, 6, 16, 3, 31,  7, 19/
2D  3/
100D  2850, .019934, .02222, 1.9361, 7.5804, 14.5832,
  35607.0, 74.4153, 1.5, 0.0, 0.0, 70/
101D  -1,  0,  .314,  .273,  0,  .437,  0.0,  0.0,  .194/
102D  4.8585, 4.0234, 0.305, 4.572, 7.6172, 3.0582, 6.8527, 7.3624/
103D  39.5507, -32.0256, 0.0, 47.1703/
104D  13.259  0.8, -90./


111D  1, 1, 6894.76, 17.1,2R, 2.286E08/
112D  139.5984, 1116.0, 2.1261, 26981., 6.0, 3.066, 0.0/
122D  139.5984, 1116.0, 2.1261, 26981., 6.0, 3.0, 4.5, 12.0, 0.0/
1001D 1, 4, 3, 2, 2, 1/
1101D  0.4002, 36.1859, 0.889, 0.0127,
  10.2366, 46.1719, 2R, 20.7134, 6.9086, 9.44, 4R, 5.4087,
  0.0, -24.3443, -26.9663, -0.351, -32.2414, -46.88, -45.043, 0.0, 2R/
  $ PUMP TO IHX $
1102D  8.1600E-1, 26.2311, 0.5842, 0.0127,
  27.854, 34.2896, 0.0, 4R, -33.636, 0.0/
  $ IHX,  J = 3  $
1103D  132.54, 7.8639, 0.03686, 0.0127,
  -90.0, 40R/
1104D  3.7400E-1, 20.9702, 0.5842, 0.0127,
   16.53, 66.94, 2R, 22.487, 0.0, 0.0/
1105D  1.3883, 26.8225, 0.5842, 0.0127,
  -1.3593, -9.24, 4R, -9.08, 0.0, -31.9, -90 0, 6R, 0.0, 2R/
1002D  0.02825, 2250, 90024.9/
1201D  1.1, 150.015, 0.5842, 0.0127,
  -8.2564, 0.0, 4R, -30.77520, -27.19762, -0.6, 18R, -0.32844,
  0.00, 22.93075, 43.73177, 65.039, 0.0/
1202D  1.42, 34.864, 0.5842, 0.0127,
  45.1185, 3R, 28.418, 0.0, 3R/
1203D  1.2, 94.34, 0.5842, 0.0127,
  -69.85, 2R, -2.0746, 5.34, 10R, 2.1462, 0.0, 3R,  6.564,
  0.0/
1003D 73332.7, 0.0/
```

Figure 7-4 NALOOP Data File Sample Input for a One Loop Description (Typical of CRBRP)

***** FILE NALOOP

RECORD 1			MUST BE THE FIRST RECORD IN FILE NALOOP
NILOOP	INTEGER	-	NUMBER OF PRIMARY LOOPS SIMULATED
NIPIPE	INTEGER	-	NUMBER OF PIPES IN PRIMARY LOOP
NINODE(J)	INTEGER	-	NUMBER OF NODES IN EACH PIPE OF PRIMARY LOOP (J = 1,NIPIPE)
N2PIPE	INTEGER	-	NUMBER OF PIPES IN INTERMEDIATE LOOP
N2NODE(J)	INTEGER	-	NUMBER OF NODES IN EACH PIPE OF INTERMEDIATE LOOP (J = 1,N2PIPE)
			NOTE: THERE EXISTS AN IMPLIED MAXIMUM NUMBER OF DATA ELEMENTS FOR ANY RECORD. AT PRESENT THIS LIMIT IS 99. THIS MAY RESTRICT THE HEAT TRANSPORT SYSTEM NODALIZATION.
RECORD 2			
FILUMP(K)	REAL	-	NUMBER OF ACTUAL LOOPS IN EACH SIMULATED LOOP (K = 1,NILOOP)
RECORD 100			
NITUBE	INTEGER	-	NUMBER OF TUBES IN IHX
YITUB1	REAL	M	INNER DIAMETER OF IHX TUBES
YITUB2	REAL	M	OUTER DIAMETER OF IHX TUBES
AIIHX	REAL	M2	FLOW AREA ON PRIMARY SIDE OF IHX
V1BYP	REAL	M3	VOLUME OF SODIUM IN IHX PRIMARY BYPASS
V1IHX	REAL	M3	VOLUME OF SODIUM IN IHX PRIMARY HEAT EXCHANGE REGION
BISHEL	REAL	KG	MASS OF IHX SHELL
AISHEL	REAL	M2	HEAT TRANSFER AREA OF IHX SHELL
FIPOD	REAL	-	PITCH-TO-DIAMETER RATIO FOR IHX TUBE BUNDLE
HIFLP	REAL	(M2-K)/W	FOULING RESISTANCE ON OUTER(PRIMARY) SURFACE OF TUBES
HIFLS	REAL	(M2-K)/W	FOULING RESISTANCE ON INNER(SECONDARY) SURFACE OF TUBES
LISTRC	INTEGER	-	PRIMARY LOOP STRUCTURAL MATERIAL ID

Table 7-2 Input Description for Data File NALOOP

RECORD 101			
L1FDIR	INTEGER	-	IHX FLOW INDICATOR: 1 - PARALLEL FLOW IN IHX, -1 -COUNTER FLOW
L1KP	INTEGER	-	INPUT OPTION INDICATOR: 0 - P1PDHX SPECIFIED, 1 - F1LOSS(J1HX) SPECIFIED
F1IN	REAL	-	PRIMARY INLET LOSS COEFFICIENT FOR IHX
F1OUT	REAL	-	PRIMARY OUTLET LOSS COEFFICIENT FOR IHX
L1KS	INTEGER	-	INPUT OPTION INDICATOR: 0 - P2PDHX SPECIFIED, 1 - F2LOSX SPECIFIED
F2INHX	REAL	-	INLET LOSS COEFFICIENT TO IHX SECONDARY SIDE
F2EXPN	REAL	-	LOSS COEFFICIENT FOR EXPANSION FROM TUBES TO OUTLET REGION IN IHX
F2CONT	REAL	-	LOSS COEFFICIENT FOR CONTRACTION FROM INLET PLENUM TO TUBES IN IHX
F2OUHX	REAL	-	OUTLET LOSS COEFFICIENT FROM IHX SECONDARY SIDE
RECORD 102			
X1PLEN(1)	REAL	M	LENGTH OF IHX PRIMARY INLET PLENUM
X1PLEN(2)	REAL	M	LENGTH OF IHX PRIMARY OUTLET PLENUM
X2PLEN(1)	REAL	M	LENGTH OF IHX INTERMEDIATE INLET PLENUM
X2PLEN(2)	REAL	M	LENGTH OF IHX INTERMEDIATE OUTLET PLENUM
V1PLEN(1)	REAL	M3	SODIUM VOLUME OF IHX PRIMARY INLET PLENUM
V1PLEN(2)	REAL	M3	SODIUM VOLUME OF IHX PRIMARY OUTLET PLENUM
V2PLEN(1)	REAL	M3	SODIUM VOLUME OF IHX INTERMEDIATE INLET PLENUM
V2PLEN(2)	REAL	M3	SODIUM VOLUME OF IHX INTERMEDIATE OUTLET PLENUM
RECORD 103			
R1PLEN(1)	REAL	DEG	THE ANGLE OF FLOW IN IHX PRIMARY INLET PLENUM
R1PLEN(2)	REAL	DEG	THE ANGLE OF FLOW IN IHX PRIMARY OUTLET PLENUM
R2PLEN(1)	REAL	DEG	THE ANGLE OF FLOW IN IHX SECONDARY INLET PLENUM
R2PLEN(2)	REAL	DEG	THE ANGLE OF FLOW IN IHX SECONDARY OUTLET PLENUM
RECORD 104			
X2DOWN	REAL	M	LENGTH OF IHX CENTRAL DOWNCOMER REGION
Y2DOWN	REAL	M	INNER DIAMETER OF IHX CENTRAL DOWNCOMER
R2DOWN	REAL	D	THE ANGLE OF FLOW IN THE IHX CENTRAL DOWNCOMER
RECORD 105			
TICONV	REAL	K	CONVERGENCE CRITERION FOR TEMPERATURES IN IHX
F1EPS	REAL	M	ROUGHNESS OF PRIMARY LOOP PIPING
F2EPS	REAL	M	ROUGHNESS OF INTERMEDIATE LOOP PIPING

Table 7-2 (cont.)

RECORD 111			
I1FAIL	INTEGER	-	MODE OF PRIMARY CHECK VALVE: 0 - WORKING, 1 - FAILED
I1TYPE	INTEGER	-	TYPE OF PRIMARY CHECK VALVE
P1PCV	REAL	N/M2	BACKPRESSURE FOR CHECK VALVE TO CLOSE
F1CVAL(1)	REAL	M4	CHECK VALVE CHARACTISTIC COEF. FOR POSITIVE FLOW W/OPEN VALVE (EQ. 3.2-71)
F1CVAL(2)	REAL	M4	CHECK VALVE CHARACTISTIC COEF. FOR NEGATIVE FLOW W/OPEN VALVE (EQ. 3.2-71)
F1CVAL(3)	REAL	M4	CHECK VALVE CHARACTISTIC COEF. FOR NEGATIVE FLOW W/CLOSED VALVE (EQ. 3.2-71)
RECORD 112			
Z1HEDR	REAL	M	RATED HEAD OF PRIMARY PUMP
U1OMGR	REAL	RPM	RATED SPEED OF PRIMARY PUMP
Q1FLOR	REAL	M3/S	RATED VOLUMETRIC FLOW RATE OF PRIMARY PUMP
T1ORKR	REAL	N-M	RATED TORQUE OF PRIMARY PUMP
Z1RTOT	REAL	M	HEIGHT OF PRIMARY PUMP TANK
A1RES	REAL	M2	X-SECTIONAL AREA OF PRIMARY PUMP TANK
Q1PYTQ	REAL	N-M	PUMP TORQUE UNDER PONY MOTOR OPERATION
RECORD 122			
Z2HEDR	REAL	M	RATED HEAD OF INTERMEDIATE PUMP
U2OMGR	REAL	RPM	RATED SPEED OF INTERMEDIATE PUMP
Q2FLOR	REAL	M3/S	RATED VOLUMETRIC FLOW RATE OF INTERMEDIATE PUMP
T2ORKR	REAL	N-M	RATED TORQUE OF INTERMEDIATE PUMP
Z2RTOT	REAL	M	HEIGHT OF INTERMEDIATE PUMP TANK
A2RES	REAL	M2	X-SECTIONAL AREA OF INTERMEDIATE PUMP TANK
Z2TTOT	REAL	M	HEIGHT OF SURGE TANK
A2TANK	REAL	M2	X-SECTIONAL AREA OF SURGE TANK
Q2PYTQ	REAL	N-M	PUMP TORQUE UNDER PONY MOTOR OPERATION

Table 7-2 (cont.)

RECORD 1001				
	L1PUMP	INTEGER	-	PIPE NUMBER PRECEDING PUMP IN PRIMARY LOOP
	L1CV	INTEGER	-	PIPE NUMBER PRECEDING CHECK VALVE IN PRIMARY LOOP
	L1IHX	INTEGER	-	PIPE NUMBER OF IHX IN PRIMARY LOOP
	L2PUMP	INTEGER	-	PIPE NUMBER PRECEDING PUMP IN INTERMEDIATE LOOP
	L2TANK	INTEGER	-	PIPE NUMBER PRECEDING EXPANSION TANK IN INTERMEDIATE LOOP
	L2EV	INTEGER	-	PIPE NUMBER PRECEDING EVAPORATOR IN INTERMEDIATE LOOP
RECORD 1002				
	F1BETA	REAL	-	PRIMARY BYPASS FRACTION THROUGH IHX
	N1ACTV	INTEGER	-	NUMBER OF ACTIVE(UNPLUGGED) TUBES IN IHX OF LOOP
	P1PDHX	REAL	N/M2	PRESSURE DROP OVER IHX PRIMARY SIDE
RECORD 1003				
	P2PDHX	REAL	N/M2	PRESSURE DROP OVER SECONDARY SIDE OF IHX
	F2LOSX	REAL	-	LOSS COEFFICIENT FOR SECONDARY SIDE OF IHX
RECORD 1101 - 1199				(IMPLIED (PRIMARY LOOP) PIPE DEPENDENCY, J = REC.NUM.-1100)
	F1LOSS	REAL	-	LOSS COEFFICIENT FOR J-TH PIPE IN PRIMARY LOOP
	X1PIPE	REAL	M	LENGTH OF J-TH PIPE IN PRIMARY LOOP
	Y1PIPE *	REAL	M	INNER DIAMETER OF J-TH PIPE IN PRIMARY LOOP
	Y1THIK **	REAL	M	THICKNESS OF J-TH PIPE WALL IN PRIMARY LOOP
	R1SIN(I)	REAL	DEG	THE ANGLE OF PRIMARY FLOW AT EACH NODE IN J-TH PIPE OF LOOP (I = 1,N1NODE(N1PIPE(J)))
				* NOTE: FOR IHX, ENTER PRIMARY SIDE HYDRAULIC DIAMETER
				** NOTE: THIS VALUE IGNORED FOR IHX PRIMARY PIPE
RECORD 1201 - 1299				(IMPLIED (INTERMEDIATE LOOP) PIPE DEPENDENCY, J = REC.NUM.-1200)
	F2LOSS	REAL	-	LOSS COEFFICIENT FOR J-TH PIPE IN INTERMEDIATE LOOP
	X2PIPE	REAL	M	LENGTH OF J-TH PIPE IN INTERMEDIATE LOOP
	Y2PIPE	REAL	M	INNER DIAMETER OF J-TH PIPE IN INTERMEDIATE LOOP
	Y2THIK	REAL	M	THICKNESS OF J-TH PIPE WALL IN INTERMEDIATE LOOP
	R2SIN(I)	REAL	DEG	THE ANGLE OF INTERMEDIATE FLOW AT EACH NODE OF J-TH PIPE OF LOOP (I = 1,N2NODE(N2PIPE(J)))

Table 7-2 (cont.)

7.5 STEAM GENERATOR AND BALANCE OF PLANT DATA (STMGEN)

All data required to specify the steam generator system (including balance of plant) and its associated sodium-side interfaces are input to SSC through the data file STMGEN. A flexible approach to specifying overall plant geometry has been implemented. This results in an efficient user interface as well as the ability to handle a general class of plant configurations.

The abstract concepts of module and junction form a basis for the approach to specification of overall steam generator geometry. As such, they serve both to unify the implementation of the approach and to provide a convenient structure for the user to create an input file from plant specifications.

A module is defined to be an abstract entity which, for modeling purposes, represents a physical component (pipe, pump, heat exchanger, etc.) of the steam generating system and balance of plant. A set of basic module types is predefined within the scope of SSC, covering all major plant component types. Specific components are represented in the STMGEN input file by declaring appropriate module types and supplying each with a set of parameters determined from the original component. Each module declared in STMGEN is assigned a distinct MODID by which it may be referenced elsewhere in the file. Plant component interfaces are represented by module ports. Every module type has one or more ports associated with it. Distinct PORTIDs are assigned to each module port as part of the module declaration.

A junction is an abstract entity representing an interface between two plant components. Junctions are used for linking individual modules together to represent the overall plant structure. Each junction links two ports from different modules by referencing their MODIDs and PORTIDs. Additionally, junctions are used to specify the vertical elevation to the center of the two linked ports.

All STMGEN input records conform to the format defined in Sections 7.1. All records begin with a record number field which serves only to identify the record type. Following the record number field is a series of positional data fields containing the set of record data items. Data field definitions are fixed for each record type; there are no optional fields or alternate field definitions. A detailed listing of all valid record types and their data field definitions are given on subsequent pages of this section.

STMGEN records may be arranged in any order, although it is recommended that they be grouped for best readability.

There are four main categories of STMGEN input records:

(1) Module Specification

Module specification records are used to define a set of modules representing the set of real components of a particular steam generator plant. Each component is represented by a module of appropriate type, with a unique integer module identifier (MODID) assigned by the user. Additionally, each module has one or more ports (each assigned a PORTID), which need only be unique within the module. Ports within different modules may be assigned the same PORTID without conflict. A direction is assigned for each port, based on the direction of coolant flow during normal plant operation.

The number and direction of ports for most module types are predetermined by the type of component they represent. Pipes, for example, always have exactly one inlet and one outlet port. Some types, such as volumes, may be used to represent more than one component type and, therefore, require the number and direction of their ports be specified by the user.

There are three classes of module specification records:

- Module geometric records specify MODID, PORTID, and all geometric properties (dimensions, configuration, etc.)

- Module performance records specify properties of a parametric nature (operating characteristics, etc.)
- Module initialization records specify initial steady-state values for module-related variables (fluid levels, flow rates, valve positions, etc.).

All module types require a geometric specification record containing a unique MODID for each module declaration. Performance and initialization records, however, are required according to module type. Table 7-3 lists these requirements. Linkage between geometric, performance, and evaluation records for a specific module is accomplished by specifying the same MODID on each record.

(2) Interconnection Specification

Interconnection specification records are used to define the network of inter-module connections representing the structure of the real system being modeled. Each record defines a junction between a pair of ports belonging to two separate modules, by using their MODID and PORTID. The relative elevation to the center of the junction is also included in the record. A correct set of junction records must specify exactly one connection for each port in the system. Multiple connections and unconnected ports are treated as error conditions and a diagnostic message results.

(3) Key Module Declarations

Key module declaration records are used to specify the MODIDs of certain modules as required to recognize the network structure for processing purposes. For example, interfaces between STMGEN modules and specific intermediate loop numbers are specified by key module records.

Table 7-3 Required Data for Steam Generator Modules

MODULE	REQUIRED DATA
Pipe	Geometric Data
Volume	Geometric Data Initialization Data
Pump	Geometric Data Performance Data
Heat Exchanger	Geometric Data
Boundary	Geometric Data Initialization Data
Valve	Geometric Data Performance Data

(4) Global Specifications

Global specification records are used to define parameters relating to the STMGEN data set as a whole, as opposed to individual modules. These include control flags, convergence criteria, and system constants.

The following steps outline a recommended procedure for the construction of a STMGEN input file from a given set of plant specifications.

(1) Identify the set of plant components and the overall structure for the plant to be modeled.

(2) Make a schematic diagram representing the above in terms of a set of interconnected module types as defined by SSC. Assign all MODIDs, PORTIDs, flow directions, port elevations, and plant interfaces by labelling the diagram.

(3) Construct a set of module specification input data records for the above, supplying all required parameters from plant specifications.

(4) Construct a set of junction records to interconnect the modules according to the diagram.

(5) Construct a set of key module records from the diagram.

(6) Construct the remaining global specification records.

The STMGEN examples contained in the following pages and in Appendix B are derived from a simplified one loop and a two loop representation based on CRBR, respectively. Figure 7-5 is a schematic depicting the set of plant components to be represented by SSC modules. All major components are labelled, except for pipes. Figure 7-6 shows the same schematic with all module identifiers (MODIDs) and port identifiers (PORTIDs) assigned; labels from Fig. 7-6 have been omitted for clarity. The following pages (Figure 7-7 and Table 7-4) contain the completed STMGEN input file derived from the above.

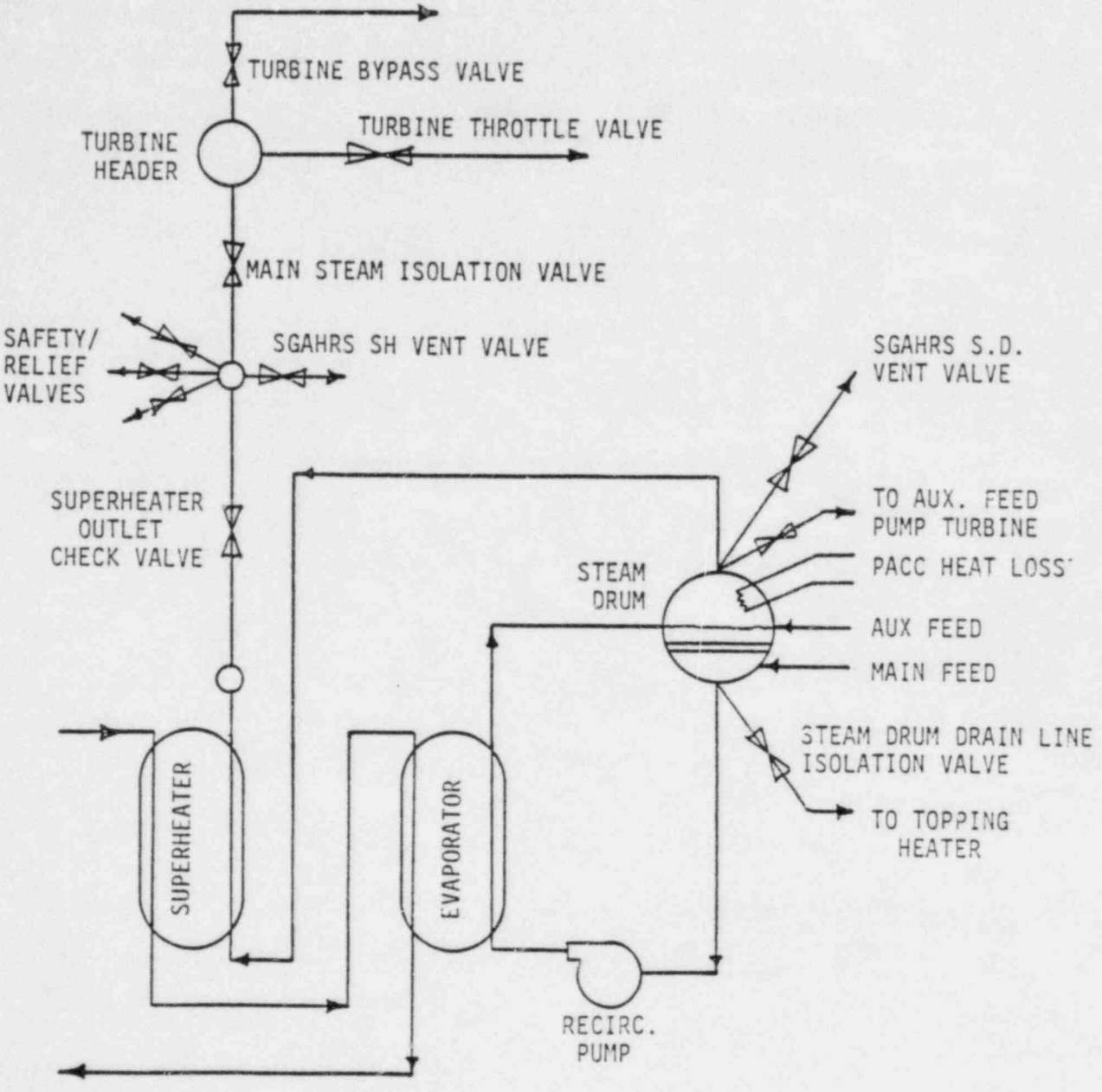

Figure 7-5 Schematic Depicting Steam Generator Components to be Represented (Typical of CRBRP)

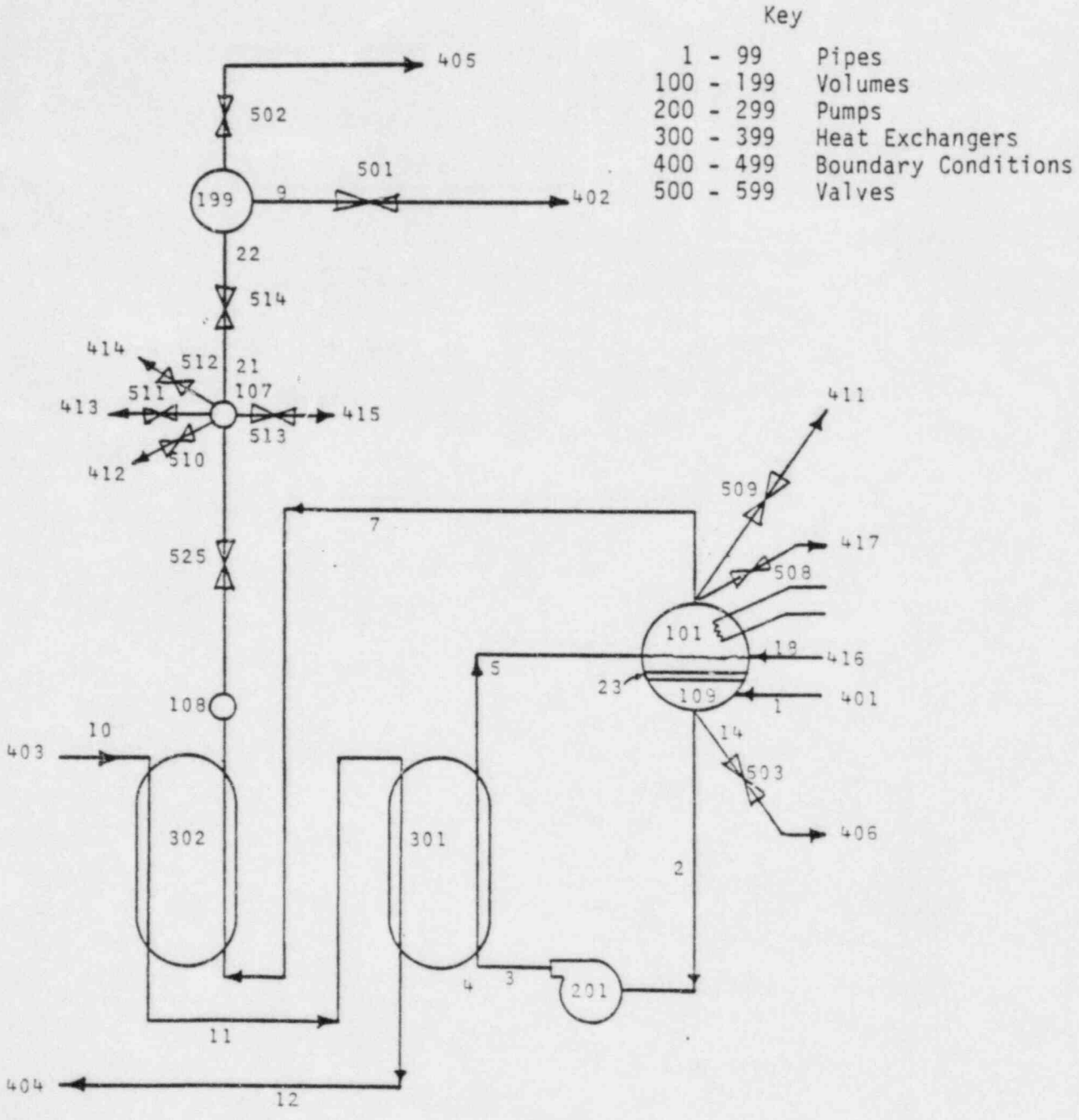

Figure 7-6 Schematic of Figure 7-5 with Module and Port Identifiers Assigned

```
0V STMGEN
1D 1,1,2,2.0,0.2540,3.0E-6,1,3/
1D 2,1,2,39.0,0.457,3.33E-6,2,3/
1D 3,1,2,7.9,0.3048,5.0E-6,1,3/
1D 4,1,2,30.0,0.254,6.0E-6,2,6/
1D 5,1,2,27.0,0.4064,3.75E-6,3,6/
1D 7,1,2,60.29,0.3048,5.0E-6,4,3/
1D 9,1,2,155.9,0.6096,3.75E-6,2,1/
1D 10,1,2,8.0,0.5842,3.0E-6,1,3/
1D 11,1,2,48.46,0.4318,3.0E-6,3,6/
1D 12,1,2,40.0,0.4318,3.0E-6,2,6/
1D 14,1,2,5.0,0.1524,3.0E-6,1,3/
1D 18,1,2,10.0,0.1524,3.0E-6,1,3/
1D 21,1,2,16.65,0.4064,3.33E-6,1,3/
1D 22,1,2,16.65,0.4064,3.33E-6,1,3/
1D 23,1,2,0.092,3.98,1.0E-6,1,3/
101D 101,2,20.325,1.83,0.2,1.0,255.12,3/
102D 101,1/
102D 101,2/
103D 101,3/
103D 101,4/
102D 101,5/
102D 101,6/
101D 107,1,0.1640,1.0,0.0,0.1,0.251.46,3/
102D 107,1/
102D 107,2/
103D 107,3/
102D 107,4/
102D 107,5/
102D 107,6/
101D 108,1,0.1640,1.0,0.0,0.1,0.249.94,3/
103D 108,1/
102D 108,2/
101D 109,2,2.23,1.83,0.0,0.15,255.12,3/
103D 109,1/
102D 109,2/
102D 109,3/
103D 109,4/
101D 199,1,38.5,0.46,0.0,1.0,257.56,1/
102D 199,1/
103D 199,2/
102D 199,3/
111D 101,2, 0.4028, -6.75E+6/
111D 107,1,-1.0,0.0/
111D 108,1,-1.0,0.0/
111D 109,1,-1.0,0.0/
111D 199,1,-1.0,0.0/
201D 201,1,2,0.1,0.3556,3.33E-6,3/
221D 201,111,24,0.40,279.253,10.0,99999.0,0.0/
301D 301,1,2,3,4,14.02,1.0339E-2,1.5874E-2,1 952,
     1.0E10,1.474E-4,757,15.71,1.0,6,0.0,1.0,-1.0,6/
301D 302,1,2,3,4,14.02,1.0339E-2,1.5874E-2,1.952,
     1.0E10,1.474E-4,757,6.71,1,0.6,0.0,1.0,-1.0,3/
402D 401,1/
401D 402,1/
402D 403,1/
401D 404,1/
401D 405,1/
401D 406,1/
401D 411,1/
401D 412,1/
401D 413,1/
401D 414,1/
401D 415,1/
402D 416,1/
401D 417,1/
411D 401, 444.0, 492.0 ,0.0,999/
411D 402,0.0,0.0,0.0,1.025E7,999/
411D 403,-1.0,0.0,0.0,0.0,1/
411D 404,0.0,0.0,0.0,0.0,1/
411D 405,0.0,0.0,0.0,1.013E5,999/
411D 406,0.0,0.0,0.0, 1.0E+7, 999/
411D 411,0.0,0.0,0.0,1.013E+05,999/
411D 412,0.0,0.0,0.0,1.013E+05,999/
411D 413,0.0,0.0,0.0,1.013E+05,999/
411D 414,0.0,0.0,0.0,1.013E+05,999/
411D 415,0.0,0.0,0.0,1.013E+05,999/
411D 416, 0.1, 297.0, 0.0, 999/
411D 417,0.0,0.0,0.0,1.1E+7,999/
501D 501,1,2,1.0,0.6096,3.75E-6,1,0.2919,0.5,1.0,1.0,0/
```

Figure 7-7 STMGEN Data File Sample Input for a One Loop Description (Typical of CRBRP)

```
501D 502,1,2,100.0,0.457,3.75E-6,1.0,0.042,0.5,1.0E-5,1.0,2/
501D 503,1,2,1.0,0.0964,3.0E-6,3.0,0.0073,0.5, 0.5 ,1.0,0/
501D 508,1,2,5.0,0.1016,1.0E-6,3.0,0.00811,0.5,1.0E-5,1.0,0/
501D 509,1,2,1.0,0.1524,3.0E-6,3.0,0.00581,0.5,1.0E-5,1.0,2/
501D 510,1,2,1.0,0.0586,3.0E-6,3.0,0.0027,0.5,1.0E-5,1.0,2/
501D 511,1,2,1.0,0.0586,3.0E-6,3.0,0.0027,0.5,1.0E-5,1.0,2/
501D 512,1,2,1.0,0.0586,3.0E-6,3.0,0.0027,0.5,1.0E-5,1.0,2/
501D 513,1,2,1.0,0.1524,3.0E-6,3.0,0.00581,0.5,1.0E-5,1.0,2/
501D 514,1,2,1.0,0.457,3.3E-6,3.0, 164,0.5,1.0,1.0,0/
501D 525,1,2,4.0,0.457,3.33E-6,3.0,0.1640,0.5,1.0,1.0,0/
521D 501,1.0E-6,-999,0.0,0.0,0.0,0.0,0.0/
521D 502,1.0E-6,199, 1.1E7, 1.0,6.0E6,1.0/
521D 503, 1.0E-6, -999,0.0,0.0,0.0,0.0,0.0/
521D 508, 1.0E-6,-999,0.0,0.0,0.0,0.0,0.0/
521D 509,1.0E-6,-999,0.0,0.0,0.0,0.0,0.0/
521D 510,1.0E-6,107,1.241E+07,1.0,1.240E+07,1.5/
521D 511,1.0E-6,107,1.275E+07,1.0,1.274E+07,1.5/
521D 512,1.0E-6,107,1.310E+07,1.0,1.309E+07,1.5/
521D 513,1.0E-6,-999,0.0,0.0,0.0,0.0,0.0/
521D 514,1.0E-6,-999,0.0,0.0,0.0,0.0,0.0/
521D 525,1.0E-5,0.0,0.01,1.0,-0.01,1.0/
621D 1,459.6,0.0/
621D 2, 839.15, 1.0/
621D 7,459.6,6.1/
621D 9,459.6,1.4/
621D 10, 4384.8, 0.029/
621D 502,0.1,1.0/
621D 18,0.0001,0.0/
621D 508,0.0001,0.0/
621D 14,41.67,1760.0/
621D 509,0.0001,0.0/
621D 510,0.001,0.0/
621D 511,0.001,0.0/
621D 512,0.001,0.0/
621D 513,0.001,0.0/
621D 21,414.5,0.0/
621D 525,414.5,0.0/
621D 23,459.6,0.1/
901D 251.16,401,1,1,1/
901D 254.4,1,2,109,1/
901D 254.205,109,3,2,1/
901D 234.36,2,2,201,1/
901D 234.74,201,2,3,1/
901D 234.74,3,2,4,1/
901D 235.92,4,2,301,1/
901D 249.94,301,2,5,1/
901D 254.571,101,1,23,1/
901D 254.48,23,2,109,4/
901D 256.0349,101,2,7,1/
901D 249.94,302,2,108,1/
901D 249.94,109,2,525,1/
901D 257.56,199,3,502,1/
901D 257.56,502,2,405,1/
901D 257.56,199,1,9,1/
901D 257.56,9,2,501,1/
901D 257.56,501,2,402,1/
901D 248.05,403,1,10,1/
901D 249.94,10,2,302,3/
901D 235.92,302,4,11,1/
901D 249.94,11,2,301,3/
901D 235.92,301,4,12,1/
901D 235.92,12,2,404,1/
901D 254.205,109,2,14,1/
901D 245.0,14,2,503,1/
901D 245.0,503,2,406,1/
901D 255.12,5,2,101,3/
901D 255.12,101,4,18,2/
901D 252.0,18,1,416,1/
901D 257.0,508,2,417,1/
901D 256.0349,101,5,508,1/
901D 256.0349,101,6,509,1/
901D 257.9,509,2,411,1/
901D 235.92,7,2,302,1/
901D 250.96,525,2,107,3/
901D 251.46,107,2,513,1/
901D 251.46,107,4,510,1/
901D 251.46,510,2,412,1/
901D 251.46,107,5,511,1/
901D 251.46,511,2,413,1/
901D 251.46,107,6,512,1/
```

Figure 7-7 (cont.)

```
901D 251.46,512,2,414,1/
901D 251.46,513,2,415,1/
901D 251.96,107,1,21,1/
901D 254.0,21,2,514,1/
901D 254.0,514,2,22,1/
901D 257.56,22,2,199,2/
1001D 1.0E-4,40,0,.99999 , 11.4E+6/
1002D 199.501,999,502/
1010D 1.999,101,302,999,301/
```

Figure 7-7 (cont.)

***** FILE STMGEN

* PIPE GEOMETRIC RECORD *

RECORD 1			
MODID	INTEGER	-	MODULE ID OF PIPE
PORTID	INTEGER	-	PIPE INLET PORT ID
PORTID	INTEGER	-	PIPE OUTLET PORT ID
X3PIPE	REAL	M	LENGTH OF PIPE
Y3ID	REAL	M	INNER DIAMETER OF PIPE
F3ZY	REAL	-	SURFACE ROUGHNESS TO DIAMETER RATIO
N3NODE	INTEGER	-	NUMBER OF CONTROL VOLUMES IN EACH MODULE
N3PATH	INTEGER	-	NUMBER OF PARRALLEL UNITS REPRESENTED BY MODULE

* VOLUME GEOMETRIC RECORD *

RECORD 101			
MODID	INTEGER	-	MODULE ID OF VOLUME
L3VSHP	INTEGER	-	VOLUME SHAPE INDICATOR; 1-BOX, 2-HORZONTAL CYLINDER
V3VOL	REAL	M3	VOLUME OF ACCUMULATOR (PER UNIT)
Y3VOL	REAL	M	VOLUME HEIGHT
F3VMIN	REAL	-	MINIMUM VOLUME BOUNDARY RELATIVE TO HEIGHT
F3VMAX	REAL	-	MAXIMUM VOLUME BOUNDARY RELATIVE TO HEIGHT
Z3VOL	REAL	M	ELEVATION OF VOLUME CENTERLINE
N3PATH	INTEGER	-	NUMBER OF PARRALLEL UNITS REPRESENTED BY MODULE

* VOLUME OUTLET GEOMETRIC RECORD *

RECORD 102			
MODID	INTEGER	-	MODULE ID OF VOLUME
PORTID	INTEGER	-	VOLUME OUTLET PORT ID

* VOLUME INLET GEOMETRIC RECORD *

RECORD 103			
MODID	INTEGER	-	MODULE ID OF VOLUME
PORTID	INTEGER	-	VOLUME INLET PORT ID

* VOLUME INITIALIZATION RECORD *

Table 7-4 Input Description for Data File STMGEN

RECORD 111			
MODID	INTEGER	-	MODULE ID OF VOLUME
L3PSEP	INTEGER	-	NUMBER OF REGIONS; 1-HOMOGENEOUS, 2-SEPARATED
F3LQLV	REAL	-	RELATIVE LIQUID LEVEL IN VOLUME
Q3VOL	REAL	J/S	HEAT INPUT INTO VOLUME
			* PUMP GEOMETRIC RECORD *
RECORD 201			
MODID	INTEGER	-	MODULE ID OF PUMP
PORTID	INTEGER	-	PUMP INLET PORT ID
PORTID	INTEGER	-	PUMP OUTLET PORT ID
X3PIPE	REAL	M	LENGTH OF MODULE
Y3ID	REAL	M	DIAMETER OF PIPE
F3ZY	REAL	-	SURFACE ROUGHNESS TO DIAMETER RATIO
N3PATH	INTEGER	-	NUMBER OF PARRALLEL UNITS REPRESENTED BY MODULE
			* PUMP PERFORMANCE RECORD *
RECORD 221			
MODID	INTEGER	-	MODULE ID OF PUMP
Z3PUMP	REAL	M	RATED HEAD OF PUMP
F3ZWP	REAL	J/S	COEFFICIENT OF PUMP HEAD VARIATION
W3REFF	REAL	KG/S	REFERENCE FLOW RATE FOR PUMP
S3PTAU *	REAL	S	PUMP COASTDOWN TIME CONSTANT
S3PSEZ *	REAL	S	PUMP SEIZURE TIME
R3PSEZ *	REAL	-	PUMP SEIZURE RELATIVE SPEED

* NOTE: OF THE THREE PARAMETERS S3PTAU, S3PSEZ, AND R3PSEZ TWO MUST BE NON-ZERO WHILE THE THIRD IS EQUAL TO ZERO.

* HEAT EXCHANGER GEOMETRIC RECORD *

Table 7-4 (cont.)

RECORD 301			
MODID	INTEGER	-	MODULE ID OF HEAT EXCHANGER
PORTID	INTEGER	-	WATER/STEAM SIDE INLET PORT ID
PORTID	INTEGER	-	WATER/STEAM SIDE OUTLET PORT ID
PORTID	INTEGER	-	SODIUM SIDE INLET PORT ID
PORTID	INTEGER	-	SODIUM SIDE OUTLET PORT ID
X3PIPE	REAL	M	LENGTH OF MODULE
Y3ID	REAL	M	INSIDE DIAMETER HX TUBE
Y3OD	REAL	M	TUBE OUTER DIAMETER FOR HX
F3TBPD	REAL	-	PITCH TO OUTER DIAMETER RATIO FOR TUBE BUNDLE IN HX
H3FOUL	REAL	-	WATER SIDE FOULING HEAT TRANSFER COEFFICIENT FOR HX
F3?Y	REAL	-	SURFACE ROUGHNESS TO DIAMETER RATIO
N3TUBE	INTEGER	-	NUMBER OF TUBES IN EACH HEAT EXCHANGER
N3NODE	INTEGER	-	NUMBER OF NODES TO BE USED IN REPRESENTING IN EACH MODULE
M3TYPE	INTEGER	-	ID NUMBER OF HEAT TRANSFER TUBE MATERIAL
I3LVTP	INTEGER	-	TYPE OF LEVEL CALCULATION NEEDED, 1-DNB,2-DRYOUT,3-X=0.7
I3HSID	INTEGER	-	INDICATES HOT SIDE POSITION WITH RESPECT TO TUBES; 0-OUTSIDE, 1-INSIDE
I3GRID	INTEGER	-	NUMBER OF TUBES EQUI-DISTANT FROM REFERENCE TUBE; 1-CO-AX; 4-SQUARE; 6-HEX
D3COIL	REAL	M	HELICAL COIL DIAMETER (0 IF STRAIGHT TUBE)
F3ITOO	REAL	-	RATIO OF INNER LENGTH TO OUTER LENGTH (1 IF STRAIGHT TUBE)
F3CCFL	REAL	-	CO-AND COUNTER-FLOW MULTIPLIER (-1 IF COUNTER-CURRENT HX, +1 IF CO-CURRENT HX)
N3PATH	INTEGER	-	NUMBER OF PARRALLEL UNITS REPRESENTED BY MODULE
* OUTLET BOUNDARY GEOMETRIC RECORD *			
RECORD 401			
MODID	INTEGER	-	MODULE ID OF OUTLET BOUNDARY
PORTID	INTEGER	-	BOUNDARY PORT ID
* INLET BOUNDARY GEOMETRIC RECORD *			
RECORD 402			
MODID	INTEGER	-	MODULE ID OF INLET BOUNDARY
PORTID	INTEGER	-	BOUNDARY PORT ID
* BOUNDARY INITIALIZATION CONDITION RECORD *			

Table 7-4 (cont.)

RECORD 411			
MODID	INTEGER	-	MODULE ID OF BOUNDARY
W3BC	REAL	KG/S	FLOW AT BOUNDARY MODULE
E3BC	REAL	J/KG	ENTHALPY AT BOUNDARY
P3BC	REAL	N/M2	PRESSURE AT BOUNDARY MODULE ,
K3LOOP	INTEGER	-	POINTS TO CONNECTING LOOP ORDINATE IF HOT SIDE=999 (GROUND) ON COLD SIDE
			* VALVE GEOMETRIC RECORD *
RECORD 501			
MODID	INTEGER	-	MODULE ID OF VALVE
PORTID	INTEGER	-	VALVE INLET PORT ID
PORTID	INTEGER	-	VALVE OUTLET PORT ID
X3PIPE	REAL	M	LENGTH OF MODULE
Y3ID	REAL	M	INNER DIAMETER OF PIPE
F3ZY	REAL	-	SURFACE ROUGHNESS TO DIAMETER RATIO
N3PATH	INTEGER	-	NUMBER OF PARRALLEL UNITS REPRESENTED BY MODULE
A3VMAX	REAL	M2	VALVE FLOW AREA WHEN FULL OPEN
F3VALV	REAL	-	VALVE LOSS COEFFICIENT
S3VPOS	REAL	S	VALVE POSITION
F3STOA	REAL	-	VALVE AREA=(S3VPOS**F3STOA)*A3VMAX
I3CHOK	INTEGER	-	CHOKE FLOW OPTION 0-BYPASS CHOKE POSSIBILITY, 1-FAUSKE, 2-MOODY
			* VALVE PERFORMANCE RECORD *
RECORD 521			
MODID	INTEGER	-	MODULE ID OF PIPE
S3VMIN	REAL	S	MINIMUM VALVE STEM POSITION (GREATER THAN ZERO)
J3VPRS	INTEGER	-	VOLUME ID WHERE PRESSURE IS MONITORED
P3VOPN	REAL	N/M2	FOR SAFETY VALVES, PRESSURE SETPOINT FOR OPENING
S3VOPN	REAL	S	FOR SAFETY VALVES, OPENING TIME CONSTANT
P3VCLO	REAL	N/M2	FOR SAFETY VALVES, PRESSURE SETPOINT FOR CLOSING
S3VCLO	REAL	S	FOR SAFETY VALVES, CLOSING TIME CONSTANT
			* FLOW SEGMENT PERFORMANCE RECORD *

Table 7-4 (cont.)

RECORD 621			
MOD1D	INTEGER	-	MODULE ID OF FIRST MODULE IN FLOW SEGMENT
W3BAR	REAL	KG/S	AVERAGE FLOW RATE IN FLOW SEGMENT
F3K	REAL	-	SEGMENT FORM LOSS COEFFICIENT
		* JUNCTION GEOMETRIC RECORD *	
RECORD 901			
Z3JCTN	REAL	M	JUNCTION ELEVATION
MOD1D1	INTEGER	-	MODULE ID OF FIRST MODULE
PORT1D1	INTEGER	-	PORT ID OF FIRST MODULE
MOD1D2	INTEGER	-	MODULE ID OF SECOND MODULE
PORT1D2	INTEGER	-	PORT ID OF SECOND MODULE
		* RUN OPTION RECORD *	
RECORD 1001			
R3CONV	REAL	-	RELATIVE CONVERGENCE CRITERIA
N3ITER	INTEGER	-	MAX NUMBER OF ALLOWED ITERATIONS FOR ANY ITERATIVE CALCULATION
I3HTYP	INTEGER	-	HOT SIDE FLUID TYPE; 0-SODIUM, 1-WATER
L3PRON	INTEGER	-	STEP NUMBER FROM WHICH S.G. WILL PRINT AT EACH STEP
P3GUES	REAL	N/M2	INITIAL PRESSURE GUESS FOR WATER/STEAM SIDE
		* KEY MODULE DEFINITION RECORD *	
RECORD 1002			
HDR ID	INTEGER	-	MODULE ID OF STEAM HEADER
TVLV ID	INTEGER	-	MODULE ID OF TURBINE VALVE
TBVLV ID	INTEGER	-	MODULE ID OF TURBINE BYPASS VALVE
RVLV ID	INTEGER	-	MODULE ID OF RELIEF VLAVE

Table 7-4 (cont.)

* INTERMEDIATE LOOP DEFINITION RECORD *

RECORD 1010			
LOOP NUM	INTEGER	-	LOOP NUMBER
FWVLV ID	INTEGER	-	MODULE ID OF FEEDWATER VALVE
STDRM ID	INTEGER	-	MODULE ID OF STEAM DRUM
SPHTR ID	INTEGER	-	MODULE ID OF SUPERHEATER
FWPMP ID	INTEGER	-	MODULE ID OF FEEDWATER PUMP
EVAP ID	INTEGER	-	MODULE ID OF EVAPORATOR

Table 7-4 (cont.)

7.6 OPERATING DATA (OPDATA)

Data pertaining to the initial overall plant operating conditions, plus specification of the plant balance initialization logic are input to SSC through the data file OPDATA. The listing included on subsequent pages (Figure 7-8 and Table 7-5) shows, on a record-by-record basis, how the specific information is suppied by the user. The records for this data file may be entered in any order.

Record 2 is used to determine the particular plant balance initialization logic the user desires (refer also to Section 4.1.2). Of the three values contained on record 2, two must be specified as known (denoted by entering values greater than zero) while the other one is assumed unknown (denoted by entering a value less than zero) and will be calculated by SSC. The unknown value to be entered need not be too precise; it can be an approximate initial guess (but it must be entered as a negative value).

The accuracy of the initial guesses entered on record 3 are more important. The value of the parameter assigned as positive is used internally in SSC to start the iterative logic for the intermediate loop and steam generator balance. Thus, the more accurate the guess, the quicker the converged solution is obtained.

```
0V OPDATA
1D    974.8E06. 3 /
2D   -817.59.  671.04. 1742.55/
3D    0.0. 0.0. 1610.25/
4D    1.04E 05.  8.6E 05.  4.0.  0.0.  0.0/
5D    1.3.1.1/
```

Figure 7-8 Data File OPDATA Sample Input (Typical of CRBRP)

***** FILE OPDATA

RECORD 1				
P90P		REAL	W	REACTOR POWER
N9LOOP		INTEGER	-	NUMBER OF OPERATING LOOPS PRESENT IN PLANT
RECORD 2 *				
T60UTL	*	REAL	K	VESSEL SODIUM OUTLET TEMPERATURE
T61NLT	*	REAL	K	VESSEL COOLANT INLET TEMPERATURE
W1LOOP	*	REAL	KG/S	SODIUM FLOW RATE IN PRIMARY LOOP
				* NOTE: OF THE THREE PARAMETERS IN THIS RECORD, TWO MUST BE GREATER THAN ZERO AND ONE MUST BE LESS THAN ZERO
RECORD 3 *				
T21HXI	*	REAL	K	IHX INTERMEDIATE SODIUM INLET TEMPERATURE
T21HXO	*	REAL	K	IHX INTERMEDIATE SODIUM OUTLET TEMPERATURE
W2LOOP	*	REAL	KG/S	SODIUM FLOW RATE IN SECONDARY LOOP
				* NOTE: OF THE THREE PARAMETERS IN THIS RECORD, ONE MUST BE GREATER THAN ZERO AND TWO MUST BE LESS THAN ZERO
RECORD 4				
P1GAS1		REAL	N/M2	INITIAL COVER GAS PRESSURE IN EACH PRIMARY PUMP TANK
P2GAS1		REAL	N/M2	INITIAL COVER GAS PRESSURE IN EACH INTERMEDIATE LOOP
Z2TANK		REAL	M	HEIGHT OF COOLANT IN SURGE (EXPANSION) TANK
T1PUMP		REAL	K	TEMPERATURE RISE ACROSS PRIMARY PUMP
T2PUMP		REAL	K	TEMPERATURE RISE ACROSS INTERMEDIATE PUMP
RECORD 5				
L1EPRT		INTEGER	-	PRIMARY AND SECONDARY LOOP DETAILED PRINT OPTION; 1 - REPORT, 0 - NO REPORT
L3PRNT		INTEGER	-	SG DETAILED PRINT OPTION; 1-4 - LOW TO HIGH DETAIL REPORT, 0 - NO REPORT
L5PRNT		INTEGER	-	DETAILED IN-VESSEL TEMP. DISTRIBUTION PRINT OPTION; 1 - REPORT, 0 - NO REPORT
L6PRNT		INTEGER	-	IN-VESSEL FLUID DYNAMICS DETAILED PRINT OPTION; 1 - REPORT, 0 - NO REPORT

Table 7-5 Input Description for Data File OPDATA

7.7 MATERIAL PROPERTIES DATA (MATDAT)

A set of material properties data is built into the code. These are described in Section 5. Any of these properties may be altered by the user. The data required to alter the default values of the material properties provided within SSC, or to create new material properties, are input to the code through data file MATDAT. The listing included on subsequent pages (Figure 7-9 and Table 7-6) shows, on a record-by-record basis, how this specific information must be supplied by the user. The records within this file may be entered in any order.

The numbering scheme for the various records follows the global naming convention for material property constants (see Table 6-2). For example, the 50-series records (50-59) are used to provide data for the fuel material types (global material property number 5). Computer storage within SSC can be allocated to accommodate only one heat transport system coolant (sodium), but up to 10 types of blanket material, 10 types of fuel material, 10 types of cladding material, 10 types of structural material and 10 kinds of fission gasses.

Default values are presently provided in SSC for material property numbers 10, 40, 50, 60, 70, 81, 82 and 83. Refer to Section 5 for further specific information on these particular materials.

```
0V MATDAT
10D   109.7, -6.4499E-02, 1.1728E-05, 1630.22, -0.83354, 4.62838E-04,
      1011.597, -0.220510, -1.92243E-05, 5.63769E-09, 370.9, 1644.2,
      -6.7511E+04, 1630.22, -0.41674, 1.54279E-04, 11.35977, -5567.0,
      -0.5, 11.68672, -5544.97, -0.61344, 1144.2, -2.4892, 220.65,
      -0.4925, 0.001, 1.0E-05, 750.0, -12130.0, 10.5/
51D    334.130      21.6178       5.381E-02       0.0
         2.2          0.0          1741.79  2.34856E-04
         0.0          0.0            0.0         0.0
      -46634.7       9999.0        9999.0    2.25E-06
       2.5E-09         0.0          295.4      9999.0
        9999.0       2381.0           0.0        0.55
       2.5E-04        400.0         9999.0          3R   /
71D   4.9341695E+01 -1.71228E-02 0.0 0.0 460.59 0.0 0.0 0.0 0.0 0.0 0.0
      0.0 7833.35 /
```

Figure 7-9 Data File MATDAT Sample Input

***** FILE MATDAT

RECORD ID			
C1K0	REAL	W/(M*K)	ADDITIVE CONSTANT FOR LIQUID SODIUM THERMAL CONDUCTIVITY FUNCTION (5-29)
C1K1	REAL	W/(M*K2)	FIRST ORDER COEF. FOR LIQUID SODIUM THERMAL CONDUCTIVITY FUNCTION (5-29)
C1K2	REAL	W/(M*K3)	SECOND ORDER COEF. FOR LIQUID SODIUM THERMAL CONDUCTIVITY FUNCTION (5-29)
C1C0	REAL	J/(KG*K)	ADDITIVE CONSTANT FOR LIQUID SODIUM SPEC. HEAT CAP. FUNCTION (5-30)
C1C1	REAL	J/(KG*K2)	FIRST ORDER COEF. FOR LIQUID SODIUM SPEC. HEAT CAP. FUNCTION (5-30)
C1C2	REAL	J/(KG*K3)	SECOND ORDER COEF. FOR LIQUID SODIUM SPEC. HEAT CAP. FUNCTION (5-30)
C1D0	REAL	KG/(M3)	ADDITIVE CONSTANT FOR SATURATED LIQUID SODIUM DENSITY FUNCTION (5-38)
C1D1	REAL	KG/(M3*K)	FIRST ORDER COEF. FOR SATURATED LIQUID SODIUM DENSITY FUNCTION (5-38)
C1D2	REAL	KG/(M3*K2)	SECOND ORDER COEF. FOR SATURATED LIQUID SODIUM DENSITY FUNCTION (5-38)
C1D3	REAL	KG/(M3*K3)	THIRD ORDER COEF. FOR SATURATED LIQUID SODIUM DENSITY FUNCTION (5-38)
C1DT1	REAL	K	LOWER SATURATED LIQUID SODIUM TEMPERATURE BOUND FOR EQUATION (5-38)
C1DT2	REAL	K	UPPER SATURATED LIQUID SODIUM TEMPERATURE BOUND FOR EQUATION (5-38)
C1H0	REAL	J/KG	ADDITIVE CONSTANT FOR SATURATED LIQUID SODIUM ENTHALPY FUNCTION (5-31)
C1H1	REAL	J/(KG*K)	FIRST ORDER COEF. FOR SATURATED LIQUID SODIUM ENTHALPY FUNCTION (5-31)
C1H2	REAL	J/(KG*K2)	SECOND ORDER COEF. FOR SATURATED LIQUID SODIUM ENTHALPY FUNCTION (5-31)
C1H3	REAL	J/(KG*K3)	THIRD ORDER COEF. FOR SATURATED LIQUID SODIUM ENTHALPY FUNCTION (5-31)
C1P1	REAL	LN(N/M2)	ADDITIVE CONSTANT FOR SODIUM SATURATED VAPOR PRESSURE FUNCTION (5-35)
C1P2	REAL	LN(N/M2)*K	FIRST ORDER COEF. FOR SODIUM SATURATED VAPOR PRESSURE FUNCTION (5-35)
C1P3	REAL	LN(N/(M2*K))	FIRST ORDER COEF. FOR SODIUM SATURATED VAPOR PRESSURE FUNCTION (5-35)
C1P4	REAL	LN(N/M2)	ADDITIVE CONSTANT FOR SODIUM SATURATED VAPOR PRESSURE FUNCTION (5-36)
C1P5	REAL	LN(N/M2)*K	FIRST ORDER COEF. FOR SODIUM SATURATED VAPOR PRESSURE FUNCTION (5-36)
C1P6	REAL	LN(N/(M2*K))	FIRST ORDER COEF. FOR SODIUM SATURATED VAPOR PRESSURE FUNCTION (5-36)
C1PT1	REAL	K	SATURATED SODIUM VAPOR PRESSURE TEMPERATURE CRITERION (EQS. 5-35, 5-36)
C1N1	REAL	LN(N*S/M2)	ADDITIVE CONSTANT FOR LIQUID SODIUM DYNAMIC VISCOSITY FUNCTION (5-41)
C1N2	REAL	LN(N*S/M2)*K	FIRST ORDER COEF. FOR LIQUID SODIUM DYNAMIC VISCOSITY FUNCTION (5-41)
C1N3	REAL	LN(N*S/(M2*K))	FIRST ORDER COEF. FOR LIQUID SODIUM DYNAMIC VISCOSITY FUNCTION (5-41)
C1T1	REAL	-	FRACTION OF INITIAL TEMPERATURE GUESS TO INCREMENT FOR SECOND PASS IN SATURATED SODIUM TEMPERATURE ITERATION
C1T2	REAL	-	RELATIVE CONVERGENCE CRITERION FOR SATURATED SODIUM TEMPERATURE CALCULATION
C1T3	REAL	K	INITIAL GUESS FOR SATURATED SODIUM TEMPERATURE CALCULATION
C1TS0	REAL	K*LN(N/M2)	CONSTANT USED IN CALCULATING SODIUM SATURATION TEMPERATURE (EQ. 5-37)
C1TS1	REAL	LN(N/M2)	CONSTANT USED IN CALCULATING SODIUM SATURATED TEMPERATURE (EQ. 5-37)

Table 7-6 Input Description for Data File MATDAT

RECORD 40 - 49			
C4K0(I)	REAL	W/(M*K)	COEF. K0 FOR BLANKET MATERIAL THERMAL CONDUCTIVITY (EQ. 5-1)
C4K1(I)	REAL	-	COEF. K1 FOR BLANKET MATERIAL THERMAL CONDUCTIVITY (EQ. 5-1)
C4K2(I)	REAL	1/K	COEF. K2 FOR BLANKET MATERIAL THERMAL CONDUCTIVITY (EQ. 5-1)
C4K3(I)	REAL	1/K3	COEF. K3 FOR BLANKET MATERIAL THERMAL CONDUCTIVITY (EQ. 5-1)
C4K4(I)	REAL	-	COEF. K4 FOR BLANKET MATERIAL THERMAL CONDUCTIVITY (EQ. 5-1)
C4K5(I)	REAL	-	COEF. K5 FOR BLANKET MATERIAL THERMAL CONDUCTIVITY (EQ. 5-1)
C4C0(I)	REAL	J/(KG*K)	ADDITIVE CONSTANT FOR BLANKET MATERIAL SPEC. HEAT CAP. FUNCTION (5-2)
C4C1(I)	REAL	1/K	FIRST ORDER COEF. FOR BLANKET MATERIAL SPEC. HEAT CAP. FUNCTION (5-2)
C4C2(I)	REAL	1/K2	SECOND ORDER COEF. FOR BLANKET MATERIAL SPEC. HEAT CAP. FUNCTION (5-2)
C4C3(I)	REAL	1/K3	THIRD ORDER COEF. FOR BLANKET MATERIAL SPEC. HEAT CAP. FUNCTION (5-2)
C4C4(I)	REAL	J/(KG*K)	ADDITIVE CONSTANT FOR BLANKET MATERIAL SPEC. HEAT CAP. FUNCTION (5-4)
C4C5(I)	REAL	J/(KG*K2)	FIRTH ORDER COEF. FOR BLANKET MATERIAL SPEC. HEAT CAP. FUNCTION (5-4)
C4C6(I)	REAL	K2	INVERSE SECOND ORDER COEF. FOR BLANKET MATERIAL SPEC. HEAT CAP. FUNCTION (5-2)
C4CT1(I)	REAL	K	LOWER BLANKET MATERIAL TEMPERATURE BOUND FOR EQUATIONS (5-2), (5-3) AND (5-4)
C4CT2(I)	REAL	K	UPPER BLANKET MATERIAL TEMPERATURE BOUND FOR EQUATIONS (5-2), (5-3) AND (5-4)
C4A0(I)	REAL	M/(M*K)	ADDITIVE CONSTANT FOR BLANKET MATERIAL COEF. OF THERMAL EXPANSION FUNCTION (5-7)
C4A1(I)	REAL	M/(M*K2)	FIRST ORDER COEF. FOR BLANKET MATERIAL COEF. OF THERMAL EXPANSION FUNCTION (5-7)
C4A2(I)	REAL	M/(M*K)	ADDITIVE CONSTANT FOR BLANKET MATERIAL COEF. OF THERMAL EXPANSION FUNCTION (5-8)
C4AT0(I)	REAL	K	REFERENCE TEMPERATURE FOR C4A0
C4AT1(I)	REAL	K	BLANKET MATERIAL TEMPERATURE BOUND FOR EQUATION (5-7)
C4AT2(I)	REAL	K	BLANKET MATERIAL TEMPERATURE BOUND FOR EQUATION (5-8)
C4D0(I)	REAL	KG/M3	FIRST ORDER COEF. FOR BLANKET MATERIAL DENSITY FUNCTION (5-15)
C4D1(I)	REAL	KG/M3	ADDITIVE CONSTANT FOR BLANKET MATERIAL DENSITY FUNCTION (5-16)
C4E0(I)	REAL	-	ADDITIVE CONSTANT FOR BLANKET MATERIAL EMISSIVITY FUNCTION (5-17)
C4E1(I)	REAL	1/K	FIRST ORDER COEF. FOR BLANKET MATERIAL EMISSIVITY FUNCTION (5-18)
C4ET0(I)	REAL	K	BLANKET MATERIAL TEMPERATURE CRITERION FOR EQUATIONS (5-17) AND (5-18)
C4TMLT(I)	REAL	K	BLANKET MATERIAL MELTING TEMPERATURE
C4TEGG(I)	REAL	K	TEMPERATURE AT ONSET OF COLUMNAR GRAIN GROWTH FOR BLANKET MATERIALS
C4TCGG(I)	REAL	K	TEMPERATURE AT ONSET OF COLUMNAR GRAIN GROWTH FOR BLANKET MATERIALS

Table 7-6 (cont.)

RECORD 50 - 59			
C5K0(I)	REAL	W/(M*K)	COEF. K0 FOR FUEL MATERIAL THERMAL CONDUCTIVITY (EQ. 5
C5K1(I)	REAL	-	COEF. K1 FOR FUEL MATERIAL THERMAL CONDUCTIVITY (EQ. 5-1)
C5K2(I)	REAL	1/K	COEF. K2 FOR FUEL MATERIAL THERMAL CONDUCTIVITY (EQ. 5-1)
C5K3(I)	REAL	1/K3	COEF. K3 FOR FUEL MATERIAL THERMAL CONDUCTIVITY (EQ. 5-1)
C5K4(I)	REAL	-	COEF. K4 FOR FUEL MATERIAL THERMAL CONDUCTIVITY (EQ. 5-1)
C5K5(I)	REAL	-	COEF. K5 FOR FUEL MATERIAL THERMAL CONDUCTIVITY (EQ. 5-1)
C5C0(I)	REAL	J/(KG*K)	ADDITIVE CONSTANT FOR FUEL MATERIAL SPEC. HEAT CAP. FUNCTION (5-2)
C5C1(I)	REAL	1/K	FIRST ORDER COEF. FOR FUEL MATERIAL SPEC. HEAT CAP. FUNCTION (5-2)
C5C2(I)	REAL	1/K2	SECOND ORDER COEF. FOR FUEL MATERIAL SPEC. HEAT CAP. FUNCTION (5-2)
C5C3(I)	REAL	1/K3	THIRD ORDER COEF. FOR FUEL MATERIAL SPEC. HEAT CAP. FUNCTION (5-2)
C5C4(I)	REAL	J/(KG*K)	ADDITIVE CONSTANT FOR FUEL MATERIAL SPEC. HEAT CAP. FUNCTION (5-4)
C5C5(I)	REAL	J/(KG*K2)	FIRTH ORDER COEF. FOR FUEL MATERIAL SPEC. HEAT CAP. FUNCTION (5-4)
C5C6(I)	REAL		INVERSE SECOND ORDER COEF. FOR FUEL MATERIAL SPEC. HEAT CAP. FUNCTION (5-2)
C5CT1(I)	REAL		LOWER FUEL MATERIAL TEMPERATURE BOUND FOR EQUATIONS (5-2), (5-3) AND (5-4)
C5CT2(I)	REAL	K	UPPER FUEL MATERIAL TEMPERATURE BOUND FOR EQUATIONS (5-2), (5-3) AND (5-4)
C5A0(I)	REAL	M/(M*K)	ADDITIVE CONSTANT FOR FUEL MATERIAL COEF. OF THERMAL EXPANSION (5-7)
C5A1(I)	REAL	M/(M*K2)	FIRST ORDER COEF. FOR FUEL MATERIAL COEF. OF THERMAL EXPANSION (5-7)
C5A2(I)	REAL	M/(M*K)	ADDITIVE CONSTANT FOR FUEL MATERIAL COEF. OF THERMAL EXPANSION (5-8)
C5AT0(I)	REAL	K	REFERENCE TEMPERATURE FOR C5A0
C5AT1(I)	REAL	K	LOWER FUEL MATERIAL TEMPERATURE BOUND FOR EQUATION (5-7)
C5AT2(I)	REAL	K	UPPER FUEL MATERIAL TEMPERATURE BOUND FOR EQUATION (5-8)
C5D0(I)	REAL	KG/M3	FIRST ORDER COEF. FOR FUEL MATERIAL DENSITY FUNCTION (5-15)
C5D1(I)	REAL	KG/M3	ADDITIVE CONSTANT FOR FUEL MATERIAL DENSITY FUNCTION (5-16)
C5E0(I)	REAL	-	ADDITIVE CONSTANT FOR FUEL MATERIAL EMISSIVITY FUNCTION (5-17)
C5E1(I)	REAL	1/K	FIRST ORDER COEF. FOR FUEL MATERIAL EMISSIVITY FUNCTION (5-18)
C5ET0(I)	REAL	K	FUEL MATERIAL TEMPERATURE CRITERION FOR EQUATIONS (5-17) AND (5-18)
C5TMLT(I)	REAL	K	FUEL MATERIAL MELTING TEMPERATURE
C5TEQ(I)	REAL	K	TEMPERATURE AT ONSET OF EQUIAXED GRAIN GROWTH FOR FUEL MATERIALS
C5TCGG(I)	REAL	K	TEMPERATURE AT ONSET OF COLMNAR GRAIN GROWTH FOR FUEL MATERIALS

Table 7-6 (cont.)

RECORD 60 - 69			
C6K0(I)	REAL	W/(M*K)	ADDITIVE CONSTANT FOR CLADDING MATERIAL THERMAL CONDUCTIVITY FUNCTION (5-19)
C6K1(I)	REAL	W/(M*K2)	FIRST ORDER COEF. FOR CLADDING MATERIAL THERMAL CONDUCTIVITY FUNCTION (5-19)
C6K2(I)	REAL	W/(M*K3)	SECOND ORDER COEF. FOR CLADDING MATERIAL THERMAL CONDUCTIVITY FUNCTION (5-19)
C6K3(I)	REAL	W/(M*K4)	THIRD ORDER COEF. FOR CLADDING MATERIAL THERMAL CONDUCTIVITY FUNCTION (5-19)
C6C0(I)	REAL	J/(KG*K)	ADDITIVE CONSTANT FOR CLADDING MATERIAL SPEC. HEAT CAP. FUNCTION (5-20)
C6C1(I)	REAL	J/(KG*K2)	FIRST ORDER COEF. FOR CLADDING MATERIAL SPEC. HEAT CAP. FUNCTION (5-20)
C6C2(I)	REAL	J/(KG*K3)	SECOND ORDER COEF. FOR CLADDING MATERIAL SPEC. HEAT CAP. FUNCTION (5-20)
C6C3(I)	REAL	J/(KG*K4)	THIRD ORDER COEF. FOR CLADDING MATERIAL SPEC. HEAT CAP. FUNCTION (5-20)
C6A0(I)	REAL	M/(M*K)	ADDITIVE CONSTANT FOR CLADDING MATERIAL COEF. OF THERMAL EXPANSION FUNCTION (5-21)
C6A1(I)	REAL	M/(M*K2)	FIRST ORDER COEF. FOR CLADDING MATERIAL COEF. OF THERMAL EXPANSION FUNCTION (5-21)
C6A2(I)	REAL	M/(M*K3)	SECOND ORDER COEF. FOR CLADDING MATERIAL COEF. OF THERMAL EXPANSION FUNCTION (5-21)
C6AT0(I)	REAL	K	REFERENCE TEMPERATURE FOR C6A0
C6AT1(I)	REAL	K	MAXIMUM TEMPERATURE RANGE FOR CLADDING COEF. OF EXPANSION
C6D0(I)	REAL	KG/M3	REFERENCE DENSITY FOR CLADDING MATERIAL DENSITY FUNCTION (5-22)
C6E0(I)	REAL	-	ADDITIVE CONSTANT FOR CLADDING MATERIAL EMISSIVITY FUNCTION (5-23) AND (5-24)
C6E1(I)	REAL	1/K	FIRST ORDER COEF. FOR CLADDING MATERIAL EMISSIVITY FUNCTION (5-24)
C6ET0(I)	REAL	K	REFERENCE TEMPERATURE FOR C6E0
C6TMLT(I)	REAL	K	CLADDING MATERIAL MELTING TEMPERATURE

Table 7-6 (cont.)

RECORD 70 - 79			
C7K0(I)	REAL	W/(M*K)	ADDITIVE CONSTANT FOR STRUCTURAL MATERIAL THERMAL CONDUCTIVITY FUNCTION (5-19)
C7K1(I)	REAL	W/(M*K2)	FIRST ORDER COEF. FOR STRUCTURAL MATERIAL THERMAL CONDUCTIVITY FUNCTION (5-19)
C7K2(I)	REAL	W/(M*K3)	SECOND ORDER COEF. FOR STRUCTURAL MATERIAL THERMAL CONDUCTIVITY FUNCTION (5-19)
C7K3(I)	REAL	W/(M*K4)	THIRD ORDER COEF. FOR STRUCTURAL MATERIAL THERMAL CONDUCTIVITY FUNCTION (5-19)
C7C0(I)	REAL	J/(KG*K)	ADDITIVE CONSTANT FOR STRUCTURAL MATERIAL SPEC. HEAT CAP. FUNCTION (5-20)
C7C1(I)	REAL	J/(KG*K2)	FIRST ORDER COEF. FOR STRUCTURAL MATERIAL SPEC. HEAT CAP. FUNCTION (5-20)
C7C2(I)	REAL	J/(KG*K3)	SECOND ORDER COEF. FOR STRUCTURAL MATERIAL SPEC. HEAT CAP. FUNCTION (5-20)
C7C3(I)	REAL	J/(KG*K4)	THIRD ORDER COEF. FOR STRUCTURAL MATERIAL SPEC. HEAT CAP. FUNCTION (5-20)
C7A0(I)	REAL	M/(M*K)	ADDITIVE STRUCTURAL MATERIAL COEF. FOR THERMAL EXPANSION FUNCTION (5-21)
C7A1(I)	REAL	M/(M*K2)	FIRST ORDER STRUCTURAL MATERIAL COEF. FOR THERMAL EXPANSION FUNCTION (5-21)
C7A2(I)	REAL	M/(M*K3)	SECOND ORDER STRUCTURAL MATERIAL COEF. FOR THERMAL EXPANSION FUNCTION (5-21)
C7DT0(I)	REAL	K	TEMPERATURE AT WHICH REFERENCE DENSITY IS SPECIFIED (5-22)
C7D0(I)	REAL	KG/M3	REFERENCE DENSITY FOR STRUCTURAL MATERIAL DENSITY FUNCTION (5-22)
RECORD 80 - 89			
C8K1(I)	REAL	W/(M*K)	ADDITIVE TERM FOR COVER GAS THERMAL CONDUCTIVITY FUNCTION (FORM SIMILAR TO (5-29) AND USED IN (3.1-14))
C8K2(I)	REAL	W/(M*K2)	FIRST ORDER COEF. FOR COVER GAS THERMAL CONDUCTIVITY FUNCTION (FORM SIMILAR TO (5-29) AND USED IN (3.1-14))
C8K3(I)	REAL	W/(M*K3)	SECOND ORDER COEF. FOR COVER GAS THERMAL CONDUCTIVITY FUNCTION (FORM SIMILAR TO (5-29) AND USED IN (3.1-14))

Table 7-6 (cont.)

7.8 TRANSIENT DATA (TRNDAT)

All data required to specify a particular transient scenario are input to SSC through the data file TRNDAT. The record-by-record listing is given on the following pages in Figure 7-10 and Table 7-7..

It should be noted that certain records are not required for all transients. In particular, if the check valve status is not to be changed from that set in steady-state, record 1004 would not be entered. Similarly, if no pipe break is to be imulated, the 1100-series and 1200-series records would be omitted.

The frequency with which results are printed/stored during the transient is dictated by the S9PINT(J) array on record 9001. The selection of the print intervals is very important because it can have the secondary effect of disturbing the synchronization of the master clock timestep with the subordinate timesteps of the major computational segments (see Chapter 4). Thus, although there is quite a bit of latitude in the setting of the print intervals, they must be carefully chosen, as detailed below. Otherwise, a verification diagnostic will result which will terminate the run.

Regarding the S9PINT(J) array, the following holds:

- S9PINT(J) is the master clock interval after which results will be printed/stored.
- S9PINT(J+1) is the master clock time after which the previous S9PINT is no longer valid.
- Thus, the index "J" is incremented over the set of paired points. There may be as many pairs (intervals) as the user finds necessary.
- S9PINT(1) is imposed from time 0.0 to S9PINT(2). S9PINT(3) is then used from the master clock time S9PINT(2) to S9PINT(4), similarly,

S9PINT(5) is used from S9PINT(4) to S9PINT(6), and so on. It should be apparent that S9PINT(4) must be strictly greater than S9PINT(2), and S9PINT(6) must be strictly greater than S9PINT(4), and so on.

- S9PINT(1) is used to define the initial transient timestep (S9DELZ), such that:

$$S9DELZ = 2^{n} * S9PINT(1)$$

where n is an integer less than or equal to one (1).

- Since the master clock timestep is only allowed to increase and/or decrease by factors of 2, all acceptable succeeding print intervals must be functionally related to S9DELZ and thus to S9PINT(1). Specifically:

$$S9PINT(2*J+1) = 2^{m} * S9DELZ = 2^{m+n} * S9PINT(1)$$

where m is some integer greater than or equal to zero (0).

An example of an acceptable S9PINT(J) array is as follows:

0.25,2.0, 0.50,5.0, 1.0,16., 4.0,100., 2.0,200.

since S9PINT(3), (5), (7) and (9) are all integer powers of two (2) of S9PINT(1).

An example of an unacceptable S9PINT(J) array is as follows:

0.1, 1.0 0.2,5.0 0.5,10., 1.0,100.

since S9PINT(5) and (7) are not an exact power of two (2) of S9PINT(1).

Record 9004 has been included in the present version of the code on an experimental basis. It is strongly suggested that at least four of the six options (i.e., L1ECAL, L1WCALL, L5CALL and L6CALL) be engaged (i.e., set equal to one (1)) on a regular basis.

```
OV TRNDAT
1001D 0. 0.1. 1182./
1002D 0. 0.1. 1182./
1003D 0. 21.946. 10.912. 0.0. 0.2002. 0.0. 0.0.10R. 76.45/
3101D 401. 3. 1/
3101D 402.3.2/
3101D 405.2.2/
3101D 406.3.2/
3101D 411.2.2/
3101D 412.2.2/
3101D 413.2.2/
3101D 414.2.2/
3101D 415.2.2/
3101D 416. 13. 1/
3101D 417.4.1/
3111D 401.0.0. 492.0. 444.0.
        3.0. 492.0.   0.0001.
      99999.0. 492.0.   0.0001/
3111D 402.0.0.3.373987E+6.1.025E+7.
        5.0.3.373987E+6.5.0E+6.
      99999.0.3.373987E+6.5.0E+6/
3111D 405.0.0.3.373987E+6.1.013E+5/
      99999.0.3.373987E+6.1.013E+5/
3111D 406.0.0. 1.25E+6.1.0E+07.
        1.0. 1.25E+6.1.0E+07.
      99999.0. 1.25E+6.1.0E+07/
3111D 411.0.0.2.6E+6.1.013E+5.
        99999.0.2.6E+6.1.013E+5/
3111D 412.0.0.3.33E+6.1.013E+5.
      99999.0.3.33E+6.1.013E+5/
3111D 413.0.0.3.33E+6.1.013E+5.
      99999.0.3.33E+6.1.013E+5/
3111D 414.0.0.3.33E+6.1.013E+5.
      99999.0.3.33E+6.1.013E+5/
3111D 415.0.0.3.33E+6.1.013E+5.
      99999.0.3.33E+6.1.013E+5/
3111D 416.0.0. 297.0.  0.1.
        41.3. 297.0.  0.1.
        47.8. 297.0.104.78.
        52.9. 297.0.104.78.
        67.6. 297.0. 65.37.
        91.5. 297.0. 31.22.
       109.3. 297.0. 22.44.
       167.3. 297.0. 13.17.
       239.0. 297.0. 15.80.
       290.9. 297.0. 12.49.
       378.7. 297.0. 14.63.
       600.0. 297.0. 18.54.
      99999.0. 297.0. 18.54/ AUX FEED
3111D 417.0.0.2.7E+6.0.01.
        2.0.2.7E+6.0.01.
       30.0.2.7E+6.12.6.
      99999.0.2.70E+6.12.6/ LINE TO TURBINE FOR AFW PUMP,TAB 5.6-1
3201D 101.8/
3201D 107.2/
3201D 108.2/
3201D 109.2/
3201D 199.2/
```

Figure 7-10 Data File TRNDAT Sample Input for a One Loop Description (Typical of CRBRP)

```
3211D 101,0.0,-6.75E+6,
        64.6,-8.29E+6,
        77.2,-7.42E+6,
       165.5,-7.77E+6,
       241.2,-9.95E+6,
       289.0,-1.31E+7,
       600.0,-1.32E+7,
     99999.0,-1.32E+7/  PACC
3211D 107,0.0,0.0,
      99999.0,0.0/
3211D 108,0.0,0.0,
     99999.0,0.0/
3211D 109,0.0,0.0,
     99999.0,0.0/
3211D 199,0.0,0.0,
      99999.0,0.0/
3301D 501,3,0/
3301D 502,0,0/
3301D 503,4,0/
3301D 508,4,0/
3301D 509,9,0/
3301D 510,0,0/
3301D 511,0,0/
3301D 512,0,0/
3301D 513,11,0/
3301D 514,4,0/
3301D 525,0,0/
3311D 501,0.0,1.0,
        1.0,0.0001,
     99999.0,0.0001/  TURBINE THROTTLE VALVE
3311D 503,0.0, 0.5,
        2.0, 0.5,
        5.0, 0.0001,
     99999.0, 0.0001/ SD ISO VALVE TO TOPPING HEATER
3311D 508,0.0,1.0E-05,
        2.0,1.0E-05,
       30.0,1.0,
     99999.0,1.0/ LINE TO TURBINE FOR AFW PUMP
3311D 509,0.0,1.0E-5,
        1.0,1.0,
       16.1,1.0,
       18.2,0.7,
       22.3,0.45,
       42.0,0.14,
       52.2,1.0E-5,
      600.0,1.0E-5,
     99999.0,1.0E-5/  SGAHRS SD VENT VALVE
3311D 513,0.0,1.0E-5,
        1.0,1.0,
       16.1,1.0,
       25.7,0.86,
       46.6,0.75,
       75.7,1.0E-5,
      287.6,1.0E-5,
      294.0,0.03,
      317.5,0.05,
      600.0,0.05,
     99999.0,0.05/  SGAHRS SH VENT VALVE
```

Figure 7-10 (cont.)

```
3311D 514,0.0,1.0,
        2.0,1.0,
        5.0,0.0001,
      99999.0,0.0001/ SH ISO VALVE CLOSES 2-5(S)
3401D 201.3, 0.01, 0/   RECIRC PUMP TRIP
3411D 201,0.0,1.0,
        4.0,0.0,
      99999.0,0.0/
/
5001D 0, 6, 6.0E-07/
5002D .92754,2R,.91485,2R,.91897,2R,.99464,.92384/
5003D 8.145E-05, 7.554E-04, 6.438E-04, 1.287E-03, 5.583E-04,
   1.732E-04 /
5004D 0.0129, 0.0308, 0.132, 0.335, 1.34, 3.27/
5005D 1.0, 0.0, 0.5, 200.0, 0.25, 400.0, 0.25, 9999.0 /
5101-5102D 1.,0., .9476,1., .8859,2.031, .8178,4.125,
   .7447,8.377, .7245,10., .6468,20.31, .5662,41.25, .5065,70.17,
  .4683,100., .4331,142.5, .4017,203.1, .349,412.5, .3119,701.7
  .2864,1000., .2335,2031., .1848,4125.
   /
5103-5104D 1.,0., .9423,1., .8753,2.031, .8053,4.125,
   .7341,8.377, .7163,10., .6439,20.31, .5724,41.25, .5207,70.17,
   .488,100., .4575,142.5, .4302,203.1, .382,412.5, .3459,701.7,
   .3197,1000., .2628,2031., .209,4125.   /
5105-5106D 1.,0., .9473,1., .8858,2.031, .8212,4.125,
   .7549,8.377, .7383,10., .6703,20.31, .6027,41.25, .5533,70.17,
   .5218,100., .4924,142.5, .4655,203.1, .417,412.5, .3792,701.7,
   .3515,1000., .2898,2031., .2311,4125.   /
5107D 1.,0.,.99988,1.E3,.9988,1.E4,.9881,1.E5,.88718,1.E6/
5201-5202D 0.0,18R/
5203-5206D 0.0,14R/
5207D      0.0,12R/
5301-5302D 0.0,18R/
5303-5306D 0.0,14R/
5307D      0.0,12R/
5401-5402D 0.0,18R/
5403-5406D 0.0,14R/
5407D      0.0,12R/
5501-5502D 0.0,18R/
5503-5506D 0.0,14R/
5507D      0.0,12R/
6001D 2, 1, 0.0/
6002D 2, 0., 0./
9001D 180.0, 1.0, 0.00001, 1., 0.25,5.0, 1.0,10.0, 2.0,9999.
9002D .001, .001, .02, .02 /
9003D .01, .01/
9004D 1, 1, 1, 1, 1, 0/
9005D  1, 1, 3, 1, 1, 0/
9101D 101,201,301,501,601,901/
8001D 3,3/
8002D 1,5R/
8003D 999.0,5R/    *** TIME DELAY AFTER AUTO PUMP TRIP
8004D  0.01,5R/    *** TIME OF MANUAL PUMP TRIP
8020D 1, 999.0,    0.6/    *** PRIMARY SCRAM
8021D 1, 999.0,    0.6/    *** SECONDARY SCRAM
8006D 8.41, -24.54, 0.94, 8.41, 2.75, 2.1/ ***REACTIVITY
8007D 1.00457,-0.32893,-3.36569,4.83219,
     -2.48130, 0.44254, 0.0,0.99814,-.01961,
     -7.2467 ,16.21624,-17.71316,
     10.13424,-2.36038 ,2.0,0.30/
8008D 0.93602,-.3620,
     -1.50373,1.84077,-.79071,.11714,0.0,2.0/
```

Figure 7-10 (cont.)

```
8005D 1.,1.0,0.0,0.0/ LOAD DEMAND FORCING FUNCTION CONSTANTS
8009D 0.0, 0.0, 0.0, 0.0/
8010D (1.0, 0.01),4R/F8VMAX,F8TRMA
8011D (0.0, -0.01),4R/F8VMIN,F8TRMN
8012D 1.0,4R/G8OPEN
8013D 1.0,4R/S8CLOS
8014D 0.150,.50,.20,2R,.5,3R,.2/ PPS SENSOR TIME CONSTANTS
8015D 1121.94, 1113.0, 1746.36, 1613.64, 822.52, 673.30,
      787.21,  4.0E+2, 9.5696E+5, 10892506.0, 137895.14, 139.68,
      139.68/
8016D 1,2,3,4,5,6,7,8,9,10,20/
8017D 11,12,13,14,15,16,17,18,19/
8018D 1,2,3,4,5,6,7,8,9,10,20/
8019D 11,12,13,14,15,16,17,18,19/
8101D 1.15/ HIGH FLUX SET POINT
8102D .03607,.036,-.99,.1706,.0364,1.01,.03607,.036,.1969,.0416/ FLUX-DE
8103D 1.318,-1.0,.0425/ C1-C3 (FLUX-SQRT(PR))
8104D .147,-1.0,1.0,-1.0,.0075,.0595/ D1-D6 (P/I SPEED RATIO)
8105D -999999./
8106D 6.0/  REACTOR VESSEL LEVEL*
8107D 42.0/ E1 ( STEAM-FEED WATER RATIO)
8108D 716.0/ SETPOINT FOR IHX PRIMARY OUTLET TEMP
8109D -999999./
8110D .147,-1.0,1.0,-1.0,.0075,.05/G1-G6(PRIMARY TO INT FLOW RATIO)
8111D 1.120,.71/MAX AND MIN STEAM DRUM LEVEL SETPOINTS
8112D 672.0/SETPOINT FOR HIGH EVA OUTLET SODIUM TEMP
8113D 850.0/SETPOINT FOR REACTOR OUTLET NOZZLE SODIUM TEMP
8114D 0.20/LOW PRIMARY LOOP SODIUM FLOW SET POINT
8115D 0.2/LOW INT LOOP SODIUM FLOW RATE
8116-8120D -999999./
8200D 1.0,.01/ F8HFXL,F8CRDZ
8201D 010, 0.5,  0.94, 0.94, 0., 0.94, -3.81E-3, 3.81E-3, 2.60/CBNK1
8201D 020, 0.94, 0.94, 0.94, 0., 0.94, -3.81E-3, 3.81E-3, 9.35/CBNK2
8201D 030, 0.94, 0.94, 0.94, 0., 0.94, -3.81E-3, 3.81E-3, 5.48/CBNK3
8301D.101, 0.3,60.0,1.085,1.11685,.065,5.34,5.34,1.,30.0,.2067725,1200./
8301D 201, 0.3,60.0,1.085,1.0397,.065,5.34,5.34,1.0,30.0,.2067725,1200./
8400D 3,3,1,3,1,1,1/
8401D 111, 0,1.0,0.05,0.0,10.0,-10.0,0.01,1.0,0.2,0.88,0.12,0.0/ P,C1,L1
8401D 121, 0,0.375,0.8,0.0,10.0,-10.0,0.01,1.0,0.5,0.0,1.0,0.0 / P,C2,L1
8401D 131, 0,1.0,0.02,0.0,10.0,-10.0,0.01,1.0,0.02,0.0,1.0,0.0 / P,C3,L1
8401D 211, 0,1.0,0.02,0.0,10.0,-10.0,0.01,1.0,0.15,1.0,0.0,0.0/  I,C1,L1
8401D 221, 0,1.752E-5,.02,.0,10.,-10.,.01,1.0,0.5,0.0,1.0,0.0/  I,C2,L1
8401D 231, 0,1.0,0.02,0.0,10.0,-10.0,0.01,1.0,0.02,0.0,1.0,0.0/  I,C3,L1
8401D 311, 0,1.0,0.0,0.0,10.0,-10.0,0.01,1.0,0.02,1.0,0.0,0.0/  FP,C1,L1
8401D 411, 0,1.0,0.0,0.0,10.0,-10.0,0.01,1.0,0.5,1.0,0.0,0.0/  FV,C1,L1
8401D 421, 0,-1.0,0.0,0.0,10.0,-10.0,0.0,1.0,0.5,0.0,0.0,0.0/  FV,C2,L1
8401D 431, 0,1.0,0.0,0.0,10.0,-10.0,0.01,1.0,0.5,0.0,0.0,0.0/  FV,C3,L1
8401D 510, 0,1.0,0.0,0.0,10.0,-10.0,0.01,1.0,0.15,1.0,0.0,0.0/  TV,C1
8401D 610, 0,1.0,0.0,0.0,10.0,-10.0,0.01,1.0,0.15,1.01,0.0,0.0/ BV,C1
8401D 710, 0,1.0,0.0,0.0,10.0,-10.0,0.01,1.0,0.15,1.02,0.0,0.0/ RV,C1
8401D 810, 0.2,0.0,0.0,0.0,10.0,-10.0,0.01,1.0,0.2,0.93,0.17,-0.1/ P,CS1
8401D 820, 0.2,0.0,0.0,0.0,10.0,-10.0,0.01,1.0,0.2,0.89,0.11,0.0/  P,CS2
8401D 830, 0.1,0.1,0.0,0.0,10.0,-10.0,0.01,1.0,0.05,0.0,1.00,0.0/  P,CS3
```

Figure 7-10 (cont.)

***** FILE TRNDAT

RECORD 1001			
L1PONY(K)	INTEGER	-	PRIMARY LOOP PONY MOTOR STATUS; 1 - MOTOR IS ON, 0 - MOTOR IS OFF (K = 1,N1LOOP)
F1PONY	REAL	-	PRIMARY PONY MOTOR SPEED FRACTION OF RATED SPEED
Q1NRTA	REAL	KG*M2	PRIMARY PUMP INERTIA
RECORD 1002			
L2PONY(K)	INTEGER	-	SECONDARY LOOP PONY MOTOR STATUS; 1 - MOTOR IS ON, 0 - MOTOR IS OFF (K = 1,N1LOOP)
F2PONY	REAL	-	SECONDARY PONY MOTOR SPEED FRACTION OF RATED SPEED
Q2NRTA	REAL	KG*M2	SECONDARY PUMP INERTIA
RECORD 1003			
L1GV(K)	INTEGER	-	GUARD VESSEL OPTION; 0 - NO GUARD VESSEL, 1 - REACTOR VESSEL OUTLET, 2 - RV INLET, 3 - PUMP INLET, 4 - PUMP OUTLET, 5 - IHX INLET, 6 - IHX OUTLET (K = 1,N1LOOP)
V1MINR	REAL	M3	R.V. GUARD VESSEL VOLUME AT LEVEL WITH BREAK
Z1MAXR	REAL	M	R.V. GUARD VESSEL MAXIMUM LEVEL THAT CAN BE REACHED BY COOLANT
F1GVR(1)	REAL	-	R.V. GUARD VESSEL VOLUME TO LEVEL COEF.
F1GVR(2)	REAL	-	R.V. GUARD VESSEL VOLUME TO LEVEL COEF.
F1GVR(3)	REAL	-	R.V. GUARD VESSEL VOLUME TO LEVEL COEF.
V1MINP	REAL	M3	PUMP GUARD VESSEL VOLUME AT LEVEL WITH PIPE BREAK
Z1MAXP	REAL	M	PUMP GUARD VESSEL MAXIMUM LEVEL THAT CAN BE REACHED BY COOLANT
F1GVP(1)	REAL	-	PUMP GUARD VESSEL VOLUME TO LEVEL COEF.
F1GVP(2)	REAL	-	PUMP GUARD VESSEL VOLUME TO LEVEL COEF.
F1GVP(3)	REAL	-	PUMP GUARD VESSEL VOLUME TO LEVEL COEF.
V1MINX	REAL	M3	IHX GUARD VESSEL VOLUME AT LEVEL WITH PIPE BREAK
Z1MAXX	REAL	M	IHX GUARD VESSEL MAXIMUM LEVEL THAT CAN REACHED BY COOLANT
F1GVX(1)	REAL	-	IHX GUARD VESSEL VOLUME TO LEVEL COEF.
F1GVX(2)	REAL	-	IHX GUARD VESSEL VOLUME TO LEVEL COEF.
F1GVX(3)	REAL	-	IHX GUARD VESSEL VOLUME TO LEVEL COEF.
V1MAX	REAL	M3	MAXIMUM VOLUME THAT CAN BE FILLED IN GUARD VESSEL IN ANY LOCATION
RECORD 1004			
I1FAIL(K)	INTEGER	-	PRIMARY CHECK VALVE STATUS; 0 - WORKING, 1 - FAILED (K = 1,N1LOOP)

Table 7-7 Input Description for Data File TRNDAT

RECORD 1101 - 1199 (IMPLIED PRIMARY LOOP DEPENDENCY, J = REC.NUM.-1100)

J1BREK	INTEGER	-	PRIMARY LOOP PIPE NUMBER CONTAINING BREAK
N1NBRK	INTEGER	-	NUMBER OF NODES IN BROKEN PRIMARY PIPE UPSTREAM OF BREAK
X1BREK	REAL	M	LENGTH OF PRIMARY PIPE UPSTREAM OF BREAK
F1LSBK	REAL	-	LOSS COEFFICIENT AT PRIMARY BREAK
A1BREK	REAL	M2	BREAK AREA IN PRIMARY PIPE
A1GAP	REAL	M2	X-SECTIONAL AREA BETWEEN BROKEN PRIMARY PIPE AND GUARD VESSEL
S1BREK	REAL	S	TIME OF PRIMARY PIPE BREAK

NOTE: THIS RECORD SERIES IS SPECIFIED ONLY FOR LOOP(S) CONTAINING BREAK(S).

RECORD 1201 - 1299 (IMPLIED SECONDARY LOOP DEPENDENCY, J = REC.NUM.-1200)

J2BREK	INTEGER	-	SECONDARY LOOP PIPE NUMBER CONTAINING BREAK
N2NBRK	INTEGER	-	NUMBER OF NODES IN BROKEN SECONDARY PIPE UPSTREAM OF BREAK
X2BREK	REAL	M	LENGTH OF PRIMARY PIPE UPSTREAM OF BREAK
F2LSBK	REAL	-	LOSS COEFFICIENT AT SECONDARY BREAK
A2BREK	REAL	M2	BREAK AREA IN SECONDARY PIPE
A2GAP	REAL	M2	X-SECTIONAL AREA BETWEEN BROKEN SECONDARY PIPE AND GUARD PIPE
S2BREK	REAL	S	TIME OF SECONDARY PIPE BREAK

NOTE: THIS RECORD SERIES IS SPECIFIED ONLY FOR LOOP(S) CONTAINING BREAK(S).

RECORD 3101

MODID	INTEGER	-	MODULE ID OF BOUNDARY
N3TAB	INTEGER	-	NUMBER OF TABLE ENTRIES ON CORRESPONDING 3111 RECORD
I3BCTP	INTEGER	-	BOUNARY CONDITION TYPE 1 - FLOW; 2 - PRESSURE

RECORD 3111

MODID		INTEGER	-	MODULE ID OF BOUNDARY
S3TAB(I)	*	REAL	S	TIME FOR TABLE ENTRY
E3TAB(I)	*	REAL	J/KG OR K	ENTHALPY(J/KG) OR TEMPERATURE(K) FOR TABLE ENTRY
P3WTAB(I)	*	REAL	PA OR KG/S	PRESSURE(PA) OR FLOW(KG/S) FOR TABLE ENTRY

* NOTE: DATA IS ENTERED AS A USER DEFINED SERIES OF PAIRED POINTS.

Table 7-7 (cont.)

RECORD 3201				
MODID		INTEGER	-	MODULE ID OF VOLUME(ACCUMULATOR)
N3VOLT		INTEGER	-	NUMBER OF TABLE ENTRIES ON CORRESPONDING 3211 RECORD
RECORD 3211				
MODID		INTEGER	-	MODULE ID OF VOLUME
S3VOLT(I)	*	REAL	S	TIME FOR TABLE ENTRY
Q3VOLT(I)	*	REAL	J/S	HEAT INPUT TO ALL PARALLEL VOLUMES

* NOTE: DATA IS ENTERED AS A USER DEFINED SERIES OF PAIRED POINTS.

RECORD 3301				
MODID		INTEGER	-	MODULE ID OF VALVE
N3VALT(I)		INTEGER	-	NUMBER OF TABLE ENTRIES ON CORRESPONDING 3311 RECORD
N3VCAS	*	INTEGER	-	PPS/PCS OPTION 0-IGNORE PPS/PCS; 1-ACCEPT PPS/PCS SIGNAL

* NOTE: AT PRESENT, N3VCAS MUST BE SET EQUAL TO ZERO(0).

RECORD 3311				
MODID		INTEGER	-	MODULE ID OF VALVE
S3VALT(I)	*	REAL	S	TIME FOR TABLE ENTRY
S3VPST(I)	*	REAL	-	VALVE STEM POSITION 0-FULL CLOSED; 1-FULL OPEN

* NOTE: DATA IS ENTERED AS A USER DEFINED SERIES OF PAIRED POINTS.

RECORD 3401				
MODID		INTEGER	-	MODULE ID OF PUMP
N3PUMT(I)		INTEGER	-	NUMBER OF TABLE ENTRIES ON CORRESPONDING 3411 RECORD
S3PTRP		REAL	S	PUMP TRIP TIME
N3PCAS	*	INTEGER	-	PPS/PCS OPTION 0-IGNORE PPS/PCS; 1-ACCEPT PPS/PCS SIGNAL

* NOTE: AT PRESENT, N3PCAS MUST BE SET EQUAL TO ZERO(0).

RECORD 3411				
MODID		INTEGER	-	MODULE ID OF PUMP
S3PUMT(I)	*	REAL	S	TIME FOR TABLE ENTRY
R3PUMT(I)	*	REAL	-	RELATIVE PUMP SPEED 0-FULL STOPPED; 1-FULL SPEED

* NOTE: DATA IS ENTERED AS A USER DEFINED SERIES OF PAIRED POINTS.

Table 7-7 (cont.)

RECORD 5001				
L5POPT	INTEGER	-		TRANSIENT POWER FLAG; 0 - PROMT JUMP APPROXIMATION, 1 - EXACT
N5DNGP	INTEGER	-		NUMBER OF DELAYED NEUTRON GROUPS (MAXIMUM OF 6)
C5LN	REAL	S		PROMT NEUTRON GENERATION TIME
RECORD 5002				
F5PFIS(K)	REAL	-		FRACTIONAL POWER IN EACH CHANNEL AND BYPASS DUE TO FISSION HEATING (K = 1,N6CHAN+1)
RECORD 5003				
F5BETA(N)	REAL	-		FRACTION OF N-TH EFFECTIVE DELAYED NEUTRON GROUP (0<N<7)
RECORD 5004				
C5LMDA(N)	REAL	S-1		DECAY CONSTANT OF N-TH DELAYED NEUTRON GROUP (0<N<7)
RECORD 5005				
F5PBPD(I) *	REAL	-		FRACTIONAL TRANSIENT DECAY POWER IN BYPASS
S5PBPD(I) *	REAL	S		TRANSIENT POSTSCRAM TIME FOR DECAY POWER IN BYPASS
			* NOTE: DATA IS ASSIGNED AS A USER DEFINED SERIES OF PAIRED POINTS OF UP TO 25 PAIRS.	
RECORD 5101 - 5199			(IMPLIED CHANNEL DEPENDENCY, K = REC.NUM.-5100)	
F5PD(I) *	REAL	-		FRACTIONAL TRANSIENT DECAY POWER IN K-TH CHANNEL
S5PD(I) *	REAL	S		TRANSIENT POSTSCRAM TIME FOR DECAY POWER IN K-TH CHANNEL
			* NOTE: DATA IS ASSIGNED AS A USER DEFINED SERIES OF PAIRED POINTS OF UP TO 25 PAIRS.	
RECORD 5201 - 5299			(IMPLIED CHANNEL DEPENDENCY, K = REC.NUM.-5200)	
F5BDOP(J)	REAL	R		MESH WEIGHTED DOPPLER REACT.COEF. WITH SODIUM PRESENT FOR K-TH CHANNEL (J = 1,N5SLIC(K))
RECORD 5301 - 5399			(IMPLIED CHANNEL DEPENDENCY, K = REC.NUM.-5300)	
F5GDOP(J)	REAL	R		MESH WEIGHTED DOPPLER RLACT.COEF. W/O SODIUM PRESENT FOR K-TH CHANNEL (J = 1,N5SLIC(K))
RECORD 5401 - 5499			(IMPLIED CHANNEL DEPENDENCY, K = REC.NUM.-5400)	
F5VWGT(J)	REAL	R/KG		MESH WEIGHTED SODIUM VOID REACT.COEF. FOR K-TH CHANNEL (J = 1,N5SLIC(K))
RECORD 5501 - 5599			(IMPLIED CHANNEL DEPENDENCY, K = REC.NUM.-5500)	
F5AWGT(J)	REAL	R/KG		MESH WEIGHTED FUEL AXIAL EXPANSION REACT.COEF. FOR K-TH CHANNEL (J = 1,N5SLIC(K))
RECORD 6001				
L6MIX	INTEGER	-		MIXING TYPE OPTION; 1 - ONE ZONE MIXING, 2 - TWO ZONE MIXING
L6FLOW	INTEGER			FLOW REDISTRIBUTION OPTION; 0 - NO FLOW REDISTRIBUTION, 1 - FLOW REDISTRIBUTION
T6SUPH	REAL	K		SUPER HEAT TEMPERATURE IF SET .LT. 0.0 THEN THERMAL EXPANSION MODEL WILL BE USED IN BOILING CALCULATIONS. IF SET .GE. 0.0 THEN SINGLE MASS FLOW RATE WILL BE USED IN BOILING CALCULATIONS.

Table 7-7 (cont.)

RECORD 6002			
L6CGAS	INTEGER	-	COVER GAS PRESSURE OPTION; 1 - CONSTANT MASS, 2 - CONSTANT PRESSURE, 3 - CONSTANT FEED/BLEED RATE
Q6CGFB	REAL	KG/S	COVER GAS FEED/BLEED RATE
P6CGFB	REAL	N/M2	COVER GAS PRESSURE CHANGE REQUIRED TO ACTUATE FEED/BLEED VALVE
RECORD 8001			
N8PCSD	INTEGER	-	NUMBER OF FEEDBACK CASCADES IN THE REACTOR POWER CONTROLLER
N8CBNK	INTEGER	-	NUMBER OF PRIMARY CONTROL ROD BANKS
RECORD 8002			
L8PUMP(J) *	INTEGER	-	MANUAL/AUTO PUMP TRIP FLAG; 1 - MANUAL, 0 - AUTO (J = 1,(4*NILOOP+1))

NOTE: PARAMETERS ARE ASSIGNED ON A SUBSYSTEM/COMPONENT BASIS. THAT IS, DATA ASSIGNMENTS ARE MADE FOR THE PUMP IN PRIMARY LOOP 1, THE PUMP IN PRIMARY LOOP 2 (IF NEEDED), AND SO SO ON, UP TO THE PUMP IN PRIMARY LOOP "NILOOP". THE DATA FOR ALL "NILOOP" PRIMARY LOOP PUMPS IS FOLLOWED BY CORRESPONDING SERIES FOR THE SECONDARY LOOP(S) AND EACH OF TWO DUMMY STEAM GENERATOR PUMPS. DATA FOR THE LAST PUMP IS ASSIGNED TO THE TURBINE. PUMP TRIPS FOR THE STEAM GENERATOR AND TURBINE MUST BE SET THROUGH RECORD 3401.

RECORD 8003			
S8TDLY(J) *	REAL	S	PUMP TRIP TIME DELAY AFTER AN AUTOMATIC PPS SIGNAL (J = 1,(4*NILOOP+1))

NOTE: PARAMETERS ARE ASSIGNED ON A SUBSYSTEM/COMPONENT BASIS. THAT IS, DATA ASSIGNMENTS ARE MADE FOR THE PUMP IN PRIMARY LOOP 1, THE PUMP IN PRIMARY LOOP 2 (IF NEEDED), AND SO SO ON, UP TO THE PUMP IN PRIMARY LOOP "NILOOP". THE DATA FOR ALL "N.LOOP" PRIMARY LOOP PUMPS IS FOLLOWED BY CORRESPONDING SERIES FOR THE SECONDARY LOOP(S) AND EACH OF TWO DUMMY STEAM GENERATOR PUMPS. DATA FOR THE LAST PUMP IS ASSIGNED TO THE TURBINE. PUMP TRIPS FOR THE STEAM GENERATOR AND TURBINE MUST BE SET THROUGH RECORD 3401.

RECORD 8004			
S8MANP(J) *	REAL	S	TIME AT WHICH PUMPS ARE TO BE TRIPPED MANUALLY (J = 1,(4*NILOOP+1))

NOTE: PARAMETERS ARE ASSIGNED ON A SUBSYSTEM/COMPONENT BASIS. THAT IS, DATA ASSIGNMENTS ARE MADE FOR THE PUMP IN PRIMARY LOOP 1, THE PUMP IN PRIMARY LOOP 2 (IF NEEDED), AND SO SO ON, UP TO THE PUMP IN PRIMARY LOOP "NILOOP". THE DATA FOR ALL "NILOOP" PRIMARY LOOP PUMPS IS FOLLOWED BY CORRESPONDING SERIES FOR THE SECONDARY LOOP(S) AND EACH OF TWO DUMMY STEAM GENERATOR PUMPS. DATA FOR THE LAST PUMP IS ASSIGNED TO THE TURBINE. PUMP TRIPS FOR THE STEAM GENERATOR AND TURBINE MUST BE SET THROUGH RECORD 3401.

RECORD 8005			
F8PD1	REAL	-	FRACTIONAL POWER DEMAND AT TIME = S8DT1
F8PD2	REAL	-	FRACTIONAL POWER DEMAND AT TIME = S8DT2
S8DT1	REAL	S	TIME AT WHICH THE LOAD DEMAND STARTS CHANGING
S8DT2	REAL	S	TIME AT WHICH THE LOAD DEMAND REACHES A CONSTANT LEVEL

Table 7-7 (cont.)

RECORD 8006				
	FBRSCR	REAL	$	REACTIVITY WORTH DUE THE SECONDARY CONTROL RODS (EQ 3.4-33)
	FBRSDM	REAL	$	COLD SHUTDOWN MARGIN OF REACTIVITY (CONSTANT) (EQ. 3.4-30)
	ZBSRMX	REAL	M	MAXIMUM INSERTION LIMIT OF THE SECONDARY CONTROL RODS CORRESPONDING TO FBSRMX (EQ. 3.4-31)
	FBSRMX	REAL	$	MAXIMUM REACTIVITY WORTH OF THE SECONDRY CONTROL RODS (EQ. 3.4-31)
	FBRSTP	REAL	$	REACTIVITY WORTH OF THE PRIMARY SYSTEM STUCK ROD (EQ. 3.4-38A)
	FBRSTS	REAL	$	REACTIVITY WORTH OF THE SECONDARD SYSTEM STUCK ROD (EQ. 3.4-38B)
RECORD 8007				
	CBA0 *	REAL	-	COEFFICIENTS FOR A 6TH DEGREE POLYNIMIAL (EQ. 3.4-37)
	CBA1 *	REAL	-	COEFFICIENTS FOR A 6TH DEGREE POLYNIMIAL (EQ. 3.4-37)
	CBA2 *	REAL	-	COEFFICIENTS FOR A 6TH DEGREE POLYNIMIAL (EQ. 3.4-37)
	CBA3 *	REAL	-	COEFFICIENTS FOR A 6TH DEGREE POLYNIMIAL (EQ. 3.4-37)
	CBA4 *	REAL	-	COEFFICIENTS FOR A 6TH DEGREE POLYNIMIAL (EQ. 3.4-37)
	CBA5 *	REAL	-	COEFFICIENTS FOR A 6TH DEGREE POLYNIMIAL (EQ. 3.4-37)
	CBA6 *	REAL	-	COEFFICIENTS FOR A 6TH DEGREE POLYNIMIAL (EQ. 3.4-37)
	CBB0 **	REAL	-	COEFFICIENTS FOR A 6TH DEGREE POLYNIMIAL (EQ. 3.4-37)
	CBB1 **	REAL	-	COEFFICIENTS FOR A 6TH DEGREE POLYNIMIAL (EQ. 3.4-37)
	CBB2 **	REAL	-	COEFFICIENTS FOR A 6TH DEGREE POLYNIMIAL (EQ. 3.4-37)
	CBB3 **	REAL	-	COEFFICIENTS FOR A 6TH DEGREE POLYNIMIAL (EQ. 3.4-37)
	CBB4 **	REAL	-	COEFFICIENTS FOR A 6TH DEGREE POLYNIMIAL (EQ. 3.4-37)
	CBB5 **	REAL	-	COEFFICIENTS FOR A 6TH DEGREE POLYNIMIAL (EQ. 3.4-37)
	CBB6 **	REAL	-	COEFFICIENTS FOR A 6TH DEGREE POLYNIMIAL (EQ. 3.4-37)
	SBDSPT	REAL	S	MAXIMUM TIME RANGE OF VALIDITY OF POLYNOMIALS FOR THE PRIMARY RODS
	FBZSPT	REAL	-	FRACTIONAL PORTION OF THE SCRAM RODS AT WHICH WE SHIFT TO SECOND POLYNOMIAL FIT

* NOTE: THIS POLYNOMIAL DESCRIBES THE PRIMARY ROD POSITION AS A FUNCTION OF TIME AFTER SCRAM WITH THE RODS FULLY OUT.

** NOTE: THIS POLYNOMIAL DESCRIBES THE PRIMARY ROD POSITION AS A FUNCTION OF TIME AFTER SCRAM WITH THE RODS PARTIALLY INSERTED.

Table 7-7 (cont.)

RECORD 8008				
C8C0	*	REAL	-	COEFFICIENTS FOR A 6TH DEGREE POLYNIMIAL (EQ. 3.4-37)
C8C1	*	REAL	-	COEFFICIENTS FOR A 6TH DEGREE POLYNIMIAL (EQ. 3.4-37)
C8C2	*	REAL	-	COEFFICIENTS FOR A 6TH DEGREE POLYNIMIAL (EQ. 3.4-37)
C8C3	*	REAL	-	COEFFICIENTS FOR A 6TH DEGREE POLYNIMIAL (EQ. 3.4-37)
C8C4	*	REAL	-	COEFFICIENTS FOR A 6TH DEGREE POLYNIMIAL (EQ. 3.4-37)
C8C5	*	REAL	-	COEFFICIENTS FOR A 6TH DEGREE POLYNIMIAL (EQ. 3.4-37)
C8C6	*	REAL	-	COEFFICIENTS FOR A 6TH DEGREE POLYNIMIAL (EQ. 3.4-37)
S8DSST		REAL	S	MAXIMUM TIME RANGE OF VALIDITY OF POLYNOMIALS FOR THE SECONDARY RODS

* NOTE: THIS POLYNOMIAL DESCRIBES THE SECONDARY ROD POSITION AS A FUNCTION OF TIME AFTER SCRAM. SINCE THE SECONDARY RODS ARE ASSUMED TO BE FULLY OUT, ONLY ONE POLYNOMIAL IS USED.

RECORD 8009				
S8RI1		REAL	S	TIME AT WHICH THE REACTIVITY INSERTION STARTS.
S8RI2		REAL	S	TIME AT WHICH THE REACTIVITY INSERTION ENDS.
F8RI1		REAL	$	REACTIVITY AT THE START OF THE INSERTION (CORRESPONDING TO S8RI1)
F8RI2		REAL	$	REACTIVITY AT THE END OF THE INSERTION (CORRESPONDING TO S8RI2)

RECORD 8010				
F8VMAX(I)	*	REAL	-	MAXIMUM FRACTIONAL VALVE OPENING (I = 1,(NILOOP+3)) (EQ. 3.4-57)
F8TRMA(I)	*	REAL	-	MAXIMUM VALVE TRIM (I = 1,(NILOOP+3)) (EQ. 3.4-57)

* NOTE: DATA IS ENTERED AS A SERIES OF PAIRED POINTS. THE INDEX "I" IS INCREMENTED OVER THE SET OF ALL REQUIRED DATA. THE REQUIRED VALVE SEQUENCING IS:
- MAIN FEED WATER CONTROL VALVE (ONE ENTRY PER LOOP),
- THROTTLE VALVE,
- BYPASS VALVE,
- MOTOR OPERATED RELIEF VALVE

RECORD 8011				
F8VMIN(I)	*	REAL	-	MINIMUM FRACTIONAL VALVE OPENING (I = 1,(NILOOP+3)) (EQ. 3.4-57)
F8TRMN(I)	*	REAL	-	MINIMUM VALVE TRIM (I = 1,(NILOOP+3)) (EQ. 3.4-57)

* NOTE: DATA IS ENTERED AS A SERIES OF PAIRED POINTS. THE INDEX "I" IS INCREMENTED OVER THE SET OF ALL REQUIRED DATA. THE REQUIRED VALVE SEQUENCING IS:
- MAIN FEED WATER CONTROL VALVE (ONE ENTRY PER LOOP),
- THROTTLE VALVE,
- BYPASS VALVE,
- MOTOR OPERATED RELIEF VALVE

Table 7-7 (cont.)

RECORD 8012 SBOPEN(I)	REAL	S	VALVE OPENING TIME (I = 1,(N1LOOP+3)) (EQ.3.4-57) * NOTE: THE REQUIRED VALVE SEQUENCING IS: - MAIN FEED WATER CONTROL VALVE (ONE ENTRY PER LOOP), - THROTTLE VALVE, - BYPASS VALVE, - MOTOR OPERATED RELIEF VALVE
RECORD 8013 SBCLOS(I)	REAL	S	VALVE CLOSING TIME (I = 1,(N1LOOP+3)) (EQ.3.4-57) * NOTE: THE REQUIRED VALVE SEQUENCING IS: - MAIN FEED WATER CONTROL VALVE (ONE ENTRY PER LOOP), - THROTTLE VALVE, - BYPASS VALVE, - MOTOR OPERATED RELIEF VALVE
RECORD 8014 CBTIME(I)	REAL	S	TIME CONSTANTS USED IN COMPUTING SENSOR MEASUREMENT TIME LAGS. (I = 1,3+5*N1LOOP) (EQ. 3.4-1) NOTE: THESE CONSTANTS CORRESPOND TO THE FOLLOWING SENSORS: - REFERENCE PRESSURE - SODIUM LEVEL - IHX OUTLET TEMPERATURE (ONE ENTRY PER LOOP) - EVAPORATOR INLET TEMPERATURE (ONE ENTRY PER LOOP) - FEED WATER FLOW RATE (ONE ENTRY PER LOOP) - STEAM FLOW RATE (ONE ENTRY PER LOOP) - STEAM DRUM LEVEL (ONE ENTRY PER LOOP) - REACTOR OUTLET NOZZLE TEMPERATURE
RECORD 8015 UB1REF	REAL	RPM	REFERENCE 100 PERCENT POWER, PRIMARY LOOP PUMP SPEED
UB2REF	REAL	RPM	REFERENCE 100 PERCENT POWER, INTERMEDIATE LOOP PUMP SPEED
WB1REF	REAL	KG/S	REFERENCE 100 PERCENT POWER, PRIMARY LOOP SODIUM MASS FLOW RATE
WB2REF	REAL	KG/S	REFERENCE 100 PERCENT POWER, INTERMEDIATE LOOP SODIUM MASS FLOW RATE
TBRREF	REAL	K	REFERENCE 100 PERCENT POWER, CORE MIXED MEAN OUTLET TEMPERATURE
TB1REF	REAL	K	REFERENCE 100 PERCENT POWER, REACTOR VESSEL SODIUM INLET TEMPERATURE
TBTREF	REAL	K	REFERENCE 100% POWER, STEAM TEMPERATURE AT THE TURBINE INLET
TB5REF	REAL	K	REFERENCE 100 PERCENT POWER, COLD SHUT DOWN TEMPERATURE
PB6REF	REAL	N/M**2	REFERENCE 100 PERCENT POWER, REACTOR INLET PLENUM PRESSURE
PBTREF	REAL	N/M**2	REFERENCE 100 PERCENT POWER, TURBINE INLET PRESSURE
PBDPRF	REAL	N/M**2	REFERENCE 100 PERCENT POWER, PRESSURE DROP ACROSS FEEDWATER VALVE
WBFWRF	REAL	KG/S	REFERENCE 100 PERCENT POWER, FEED WATER FLOW RATE
WBSTRF	REAL	KG/S	REFERENCE 100 PERCENT POWER, STEAM FLOW RATE

Table 7-7 (cont.)

RECORD 8016			
LBAVLP(I)	INTEGER	-	PROTECTIVE FUNCTIONS EXAMINED BY THE PRIM. SHUTDOWN SYSTEM (I = 1,J: 0<J<21)
RECORD 8017			
LBAVLS(I)	INTEGER	-	PROTECTIVE FUNCTIONS EXAMINED BY THE SEC. SHUTDOWN SYSTEM (I = 1,J: 0<J<21)
RECORD 8018			
LBFUNP(I)	INTEGER	-	PROTECTIVE FUNCTIONS OPERATIVE FOR PRIMARY SHUT DOWN SYSTEM (I = 1,J: 0<J<21)
			* NOTE: AT LEAST ONE MUST BE OPERATIVE.
RECORD 8019			
LBFUNS(I)	INTEGER	-	PROTECTIVE FUNCTIONS OPERATIVE FOR SECONDARY SHUT DOWN SYSTEM (I = 1,J: 0<J<21)
			* NOTE: AT LEAST ONE MUST BE OPERATIVE.
RECORD 8020			
LBPMAN	INTEGER	-	MANUAL/AUTO SCRAM FLAG FOR THE PRIMARY SHUTDOWN SYSTEM; 1 - MANUAL, 0 - AUTO
SBPDLY	REAL	S	PRIMARY SHUTDOWN SYSTEM SCRAM TIME DELAY AFTER AN AUTOMATIC PPS SIGNAL
SBPMAN	REAL	S	TIME AT WHICH PRIMARY SHUTDOWN SYSTEM IS TO BE MANUALLY TRIPPED
			NOTE: SELECTION OF MANUAL SCRAM DOES NOT PREVENT AN AUTOMATIC SCRAM. TO PREVENT AN AUTOMATIC SCRAM FROM THE PRIMARY SHUTDOWN SYSTEM, SBPDLY SHOULD BE SET TO A LONG TIME.
RECORD 8021			
LBSMAN	INTEGER	-	MANUAL /AUTO SCRAM FLAG FOR THE SECONDARY SHUTDOWN SYSTEM; 1 - MANUAL, 0 - AUTO
SBSDLY	REAL	S	SECONDARY SHUTDOWN SYSTEM SCRAM TIME DELAY AFTER AN AUTOMATIC PPS SIGNAL
SBSMAN	REAL	S	TIME AT WHICH SECONDARY SHUTDOWN SYSTEM IS TO BE MANUALLY TRIPPED
			NOTE: SELECTION OF MANUAL SCRAM DOES NOT PREVENT AN AUTOMATIC SCRAM. TO PREVENT AN AUTOMATIC SCRAM FROM THE SECONDARY SHUTDOWN SYSTEM, SBSDLY SHOULD BE SET TO A LONG TIME.
RECORD 8101			
FBBSFX	REAL	-	FRACTIONAL HIGH NEUTRON FLUX (PPS SETTING) (EQ. 3.4-2)

Table 7-7 (cont.)

RECORD 8106			
Z86SNA	REAL	-	REACTOR VESSEL SODIUM LEVEL PPS SETTING (EQ. 3.4-10)
RECORD 8107			
C8PE1	REAL	-	SETPOINT CONSTANT FOR STEAM TO FEED WATER RATIO FUNCTION(PPS FUNCTION 7) (EQ. 3.4-11)
RECORD 8108			
T82SHX	REAL	K	IHX OUTLET TEMPERATURE % SETTING (EQ. 3.4-12)
RECORD 8110			
C8PG1	REAL	-	CONSTANT USED IN DETERMINING THE SETPOINT FOR THE PRIMARY TO INTERMEDIATE FLOW RATIO (PPS FUNCTION 10) (EQ. 3.4-14)
C8PG2	REAL	-	CONSTANT USED IN DETERMINING THE SETPOINT FOR THE PRIMARY TO INTERMEDIATE FLOW RATIO (PPS FUNCTION 10) (EQ. 3.4-14)
C8PG3	REAL	-	CONSTANT USED IN DETERMINING THE SETPOINT FOR THE PRIMARY TO INTERMEDIATE FLOW RATIO (PPS FUNCTION 10) (EQ. 3.4-14)
C8PG4	REAL	-	CONSTANT USED IN DETERMINING THE SETPOINT FOR THE PRIMARY TO INTERMEDIATE FLOW RATIO (PPS FUNCTION 10) (EQ. 3.4-14)
C8PG5	REAL	-	CONSTANT USED IN DETERMINING THE SETPOINT FOR THE PRIMARY TO INTERMEDIATE FLOW RATIO (PPS FUNCTION 10) (EQ. 3.4-14)
C8PG6	REAL	-	CONSTANT USED IN DETERMINING THE SETPOINT FOR THE PRIMARY TO INTERMEDIATE FLOW RATIO (PPS FUNCTION 10) (EQ. 3.4-14)
RECORD 8111			
Z83SMX	REAL	M	SETPOINT STEAM DRUM MAXIMUM WATER LEVEL PPS SETTING (EQ. 3.4-15)
Z83SMN	REAL	-	SETPOINT STEAM DRUM WATER LEVEL PPS SETTING (EQ. 3.4-15)
RECORD 8112			
T83SEV	REAL	K	PPS SETTING EVAPORATOR EXIT SODIUM TEMPERATURE (EQ. 3.4-16)
RECORD 8113			
T86SNZ	REAL	K	PPS SETTING REACTOR OUTLET NOZZLE TEMPERATURE (EQ. 3.4-17)
RECORD 8114			
F81SFL	REAL	-	PRIMARY PUMP PPS SETTING (EQ. 3.4-18)
RECORD 8115			
F82SFL	REAL	-	INTERMEDIATE PUMP SPEED PPS SETTING (EQ. 3.4-18)
RECORD 8200			
F8HFXL	REAL	-	HIGH FLUX LIMITER(FRACTION OF 1)
F8CRDZ	REAL	-	CONTROL ROD DEAD ZONE (FRACTION OF 1)

Table 7.7 (cont.)

RECORD 8102			
C8PA1	REAL	-	CONSTANTS USED IN DETERMINING THE SETPOINT FOR FLUX DELAYED FLUX FUNCTION WHEN RHO IS GREATER THAN 0(PPS FUNCTION 2) (EQ. 3.4-3)
C8PA2	REAL	-	CONSTANTS USED IN DETERMINING THE SETPOINT FOR FLUX DELAYED FLUX FUNCTION WHEN RHO IS GREATER THAN 0(PPS FUNCTION 2) (EQ. 3.4-3)
C8PA3	REAL	-	CONSTANTS USED IN DETERMINING THE SETPOINT FOR FLUX DELAYED FLUX FUNCTION WHEN RHO IS GREATER THAN 0(PPS FUNCTION 2) (EQ. 3.4-3)
C8PA4	REAL	-	CONSTANTS USED IN DETERMINING THE SETPOINT FOR FLUX DELAYED FLUX FUNCTION WHEN RHO IS GREATER THAN 0(PPS FUNCTION 2) (EQ. 3.4-3)
C8PA5	REAL	-	CONSTANTS USED IN DETERMINING THE SETPOINT FOR FLUX DELAYED FLUX FUNCTION WHEN RHO IS GREATER THAN 0(PPS FUNCTION 2) (EQ. 3.4-3)
C8PB1	REAL	-	CONSTANTS USED IN DETERMINING THE SETPOINT FOR FLUX DELAYED FLUX FUNCTION WHEN RHO IS LESS THAN 0(PPS FUNCTION 2) (EQ. 3.4-3)
C8PB2	REAL	-	CONSTANTS USED IN DETERMINING THE SETPOINT FOR FLUX DELAYED FLUX FUNCTION WHEN RHO IS LESS THAN 0(PPS FUNCTION 2) (EQ. 3.4-3)
C8PB3	REAL	-	CONSTANTS USED IN DETERMINING THE SETPOINT FOR FLUX DELAYED FLUX FUNCTION WHEN RHO IS LESS THAN 0(PPS FUNCTION 2) (EQ. 3.4-3)
C8PB4	REAL	-	CONSTANTS USED IN DETERMINING THE SETPOINT FOR FLUX DELAYED FLUX FUNCTION WHEN RHO IS LESS THAN 0(PPS FUNCTION 2) (EQ. 3.4-3)
C8PB5	REAL	-	CONSTANTS USED IN DETERMINING THE SETPOINT FOR FLUX DELAYED FLUX FUNCTION WHEN RHO IS LESS THAN 0(PPS FUNCTION 2) (EQ. 3.4-3)
RECORD 8103			
C8PC1	REAL	-	CONSTANT USED IN DETERMINING THE SETPOINT FOR FLUX-SQRT(PRESSURE) FUNCTION(PPS FUNCTION 3) (EQ. 3.4-8)
C8PC2	REAL	-	CONSTANT USED IN DETERMINING THE SETPOINT FOR FLUX-SQRT(PRESSURE) FUNCTION(PPS FUNCTION 3) (EQ. 3.4-8)
C8PC3	REAL	-	CONSTANT USED IN DETERMINING THE SETPOINT FOR FLUX-SQRT(PRESSURE) FUNCTION(PPS FUNCTION 3) (EQ. 3.4-8)
RECORD 8104			
C8PD1	REAL	-	CONSTANT USED TO DETERMINE THE SETPOINT FOR PRIMARY TO INTERMEDIATE SPEED RATIO FUNCTION (PPS FUNCTION 4) (EQ. 3.4-9)
C8PD2	REAL	-	CONSTANT USED TO DETERMINE THE SETPOINT FOR PRIMARY TO INTERMEDIATE SPEED RATIO FUNCTION (PPS FUNCTION 4) (EQ. 3.4-9)
C8PD3	REAL	-	CONSTANT USED TO DETERMINE THE SETPOINT FOR PRIMARY TO INTERMEDIATE SPEED RATIO FUNCTION (PPS FUNCTION 4) (EQ. 3.4-9)
C8PD4	REAL	-	CONSTANT USED TO DETERMINE THE SETPOINT FOR PRIMARY TO INTERMEDIATE SPEED RATIO FUNCTION (PPS FUNCTION 4) (EQ. 3.4-9)
C8PD5	REAL	-	CONSTANT USED TO DETERMINE THE SETPOINT FOR PRIMARY TO INTERMEDIATE SPEED RATIO FUNCTION (PPS FUNCTION 4) (EQ. 3.4-9)
C8PD6	REAL	-	CONSTANT USED TO DETERMINE THE SETPOINT FOR PRIMARY TO INTERMEDIATE SPEED RATIO FUNCTION (PPS FUNCTION 4) (EQ. 3.4-9)

Table 7-7 (cont.)

RECORD 8201			
MODID *	INTEGER	-	PPS/PCS MODULE IDENTIFIER
Z8CRIN	REAL	M	INITIAL POSITION OF THE PRIMARY CONTROL RODS, MAY VARY FROM 0.0(FULLY INSERTED) TO THE VALUE ASSIGNED Z8CRMX (FULLY WITHDRAWN) (EQ. 3.4-34)
Z8CRMX	REAL	M	MAXIMUM INSERTION LIMIT OF THE PRIMARY CONTROL RODS (EQ. 3.4-34)
Z8SAT	REAL	M	PRIMARY CONTROL ROD SATURATION POSITION
Z8LOCR	REAL	M	LOWER POSITION OF THE ROD BANK BEFORE THE NEXT BANK MOVEMENT BEGINS
Z8CRUP	REAL	M	UPPER POSITION OF THE ROD BANK BEFORE THE NEXT BANK MOVEMENT BEGINS
U8CRDN	REAL	M/S	PRIMARY CONTROL ROD DOWNWARD VELOCITY(NEGATIVE VALUE) (EQ. 3.4-36)
U8CRUP	REAL	M/S	PRIMARY CONTROL ROD UPWARD VELOCITY (POSITIVE VALUE) (EQ. 3.4-36)
F8ROMX	REAL	$	MAXIMUM REACTIVITY OF THE PRIMARY CONTROL ROD BANKS (EQ. 3.4-34)

* NOTE: A MODID IS A THREE(3) DIGIT CODE DESIGNED TO UNIQUELY IDENTIFY A PCS CONTROLLER. SINCE A CONTROL ROD BANK IS DEFINED WITH NEITHER SUB-SYSTEM NOR LOOP DEPENDENCIES, DIGITS ONE(1) AND THREE(3) ARE BY CONVENTION ALWAYS ASSIGNED A VALUE OF ZERO(0). THE REMAINING DIGIT (2) DESIGNATES THE BANK TO WHICH THE DATA IS ASSOCIATED. IT'S VALUE WILL RANGE FROM ONE(1) TO THE USER DEFINED MAXIMUM NUMBER OF CONTROL ROD BANKS (N8CBNK) WHICH IS FOUND ON RECORD 8001.

RECORD 8301			
MODID *	INTEGER	-	PPS/PCS MODULE IDENTIFIER
M8MOTR	INTEGER	-	MOTOR TYPE FLAG (0/1 , SQUIRREL CAGE / WOUND ROTOR)
N8POLE	INTEGER	-	NUMBER OF PAIRS OF POLES FOR SQUIRREL CAGE TYPE MOTOR (EQ. 3.4-43)
Q8FREF	REAL	HERTZ	100 PERCENT REFERENCE FREQUENCY OF THE MOTOR-GENERATOR SET
C8PCS	REAL	-	CONSTANTS ASSOCIATED WITH THE PUMP DRIVE SYSTEM (EQ. 3.4-40)
C8ACT	REAL	-	ACTUATOR CONSTANTS (EQ. 3.4-44)
F8HSPL	REAL	-	PUMP HIGH SPEED LIMIT
R8MAX	REAL	OHMS	MAXIMUM RESISTANCE OF THE LIQUID RHEOSTAT ACTUATOR (EQ. 3.4-51)
R8ROT	REAL	OHMS	MOTOR RESISTANCE (EQ. 3.4-50)
U8SRPM	REAL	RPM	SYNCHRONOUS SPEED OF THE SODIUM PUMPS (EQ. 3.4-53)

* NOTE: A MODID IS A THREE(3) DIGIT CODE DESIGNED TO UNIQUELY IDENTIFY A PCS CONTROLLER. SINCE THERE IS ONLY ONE DRIVER PER PUMP AND ONE PUMP PER LOOP, THE SECOND DIGIT OF THE PUMP CONTROLLER MODID IS SUPERFLUOUS AND IS BY CONVENTION ALWAYS ASSIGNED A VALUE OF ZERO(0). THE FIRST DIGIT OF THE MODID CODE IS ASSIGNED ON A SUBSYSTEM BASIS. A PUMP DRIVER IN A PRIMARY HEAT TRANSPORT SYSTEM IS ASSIGNED A VALUE OF ONE(1) WHILE THE SECONDARY SYSTEM COUNTERPART IS ASSIGNED A VALUE OF TWO(2). THE PLANT LOOP IS IDENTIFIED BY THE MODID'S LAST DIGIT. IT'S RANGE OF VALID VALUES IS ONE(1) THROUGH THE MAXIMUM NUMBER OF LOOPS SIMULATED (N1LOOP).

Table 7-7 (cont.)

RECORD 8400			
NBCYCD(I)	INTEGER	-	NUMBER OF FLOW CONTROLLER CASCADES ASSOCIATED WITH EACH SUBSYSTEM/COMPONENT (I = 1,(4*NILOOP+3))

* NOTE: THE FOLLOWING CASCADE SEQUENCING IS ASSUMED;
- PRIMARY HEAT TRANSPORT SYSTEM (ONE ENTRY FOR EACH LOOP),
- SECONDARY HEAT TRANSPORT SYSTEM (ONE ENTRY FOR EACH LOOP),
- FEEDWATER WATER PUMP (ONE ENTRY FOR EACH LOOP),
- FEEDWATER VALVE (ONE ENTRY FOR EACH LOOP),
- THROTTLE VALVE,
- BYPASS VALVE,
- RELIEF VALVE

RECORD 8401			
MODID *	INTEGER	-	PPS/PCS MODULE IDENTIFIER
MBFLAG	INTEGER	-	CONTROLLER MODE FLAG(0/1 ,AUTOMATIC/MANUAL) (FIGURE 3.4-3)
FBGAIN	REAL	-	CONTROLLER GAIN (EQ. 3.4-22)
FBREPT	REAL	1/S	INTEGRAL CONTROLLER REPETITION RATE
CBTIME	REAL	S	TIME CONSTANTS (EQ. 3.4-22)
FBROLU	REAL	-	INTEGRAL LIMITER(UPPER LIMIT)
FBROLD	REAL	-	INTEGRAL LIMITER(LOWER LIMIT)
FBDBND	REAL	-	DEAD BAND (FRACTION OF 1)
XBPM	REAL	-	MANUAL ADJUSTIBLE SETPOINTS FOR CONTROLLERS
CBTIME	REAL	S	TIME CONSTANTS
CBFP	REAL	-	FLOW CONTROLLER PART-LOAD PROFILE COEFFICIENTS FOR LOAD DEPENDENT SET POINTS

* NOTE: A MODID IS A THREE(3) DIGIT CODE DESIGNED TO UNIQUELY IDENTIFY A PCS CONTROLLER. THE FIRST DIGIT DENOTES THE SUBSYSTEM/COMPONENT. IT MAY ASSUME VALUES OF ONE(1) THROUGH EIGHT(8) IN ACCORDANCE WITH THE FOLLOWING DEFINITION:
1 - PRIMARY HEAT TRANSPORT SYSTEM
2 - SECONDARY HEAT TRANSPORT SYSTEM
3 - FEEDWATER PUMP
4 - FEEDWATER VALVE
5 - THROTTLE VALVE
F - BYPASS VALVE
7 - RELIEF VALVE
8 - POWER CONTROLLER
DIGIT TWO(2) IDENTIFIES A CASCADE WITHIN A SUBSYSTEM. IT IS ASSIGNED A VALUE OF ONE(1) TO A USER DEFINED MAXIMUM. FOR SUBSYSTEMS 1 THROUGH 7 THIS MAXIMUM IS DEFINED BY A CORRESPONDING ENTRY ON THE 8400 RECORD. THE MAXIMUM NUMBER OF POWER CONTROLLERS (SUBSYSTEM 8) IS DEFINED ON RECORD 8001. THE PLANT LOOP IS IDENTIFIED BY THE LAST DIGIT OF THE MODID. IT'S RANGE IS ZERO(0) THROUGH THE MAXIMUM NUMBER OF LOOPS SIMULATED (NILOOP). A VALVE OF ZERO(0) IN THE THIRD DIGIT INDICATES NO LOOP DEPENDENCY. BY CONVENTION A ZERO(0) IS ALWAYS ASSIGNED TO THE THIRD DIGIT OF POWER CONTROLLER MODID.

Table 7-7 (cont.)

RECORD 9001			
S9LAST	REAL	S	TOTAL PROBLEM SIMULATION TIME
S9MAXA	REAL	S	MAXIMUM TIMESTEP ALLOWED
S9MINA	REAL	S	MINIMUM TIMESTEP ALLOWED
S9SINT	REAL	S	MASTER CLOCK INTERVAL AT WHICH A RESTART DUMP WILL OCCUR
S9PINT(J) *	REAL	S	MASTER CLOCK INTERVAL AT WHICH A SYSTEM REPORT WILL BE GENERATED
S9PINT(J+1)*	REAL	S	MASTER CLOCK TIME AFTER WHICH THE CORRESPONDING S9PINT IS NO LONGER VALID

* NOTE: THE INDEX "J" IS INCREMENTED OVER THE SET OF PAIRED POINTS.
THERE MAY BE AS MANY PAIRS (INTERVALS) AS THE USERS FINDS NECESSARY.

S9PINT(1) IS IMPOSED FROM TIME 0 TO S9PINT(2). S9PINT(3) IS THEN USED FROM THE MASTER CLOCK TIME S9PINT(2 TO S9PINT(4), SIMILARILY, S9PINT(5) IS USED FROM S9PINT(4) TO S9PINT(6), AND SO ON.
IT SHOULD BE APPARENT THAT S9PINT(4) MUST BE STRICTLY GREATER THAN S9PINT(2), AND S9PINT(6) MUST BE STRICTLY GREATER THAN S9PINT(4), AND SO ON.

THERE IS QUITE A BIT OF LATITUDE PERMITTED IN THE SELECTION OF PRINT INTERVALS BUT THEY MUST BE CAREFULLY CHOSEN (SEE SECTION 7.8)

RECORD 9002			
F1EMXA	REAL	-	RELATIVE ACCURACY ACCEPTANCE LIMIT FOR LOOP THERMAL CALCULATIONS
F1WMXA	REAL	-	RELATIVE ACCURACY ACCEPTANCE LIMIT FOR LOOP HYDRAULIC CALCULATIONS
F5MAXA	REAL	-	RELATIVE ACCURACY ACCEPTANCE LIMIT FOR FUEL CALCULATIONS
F6MAXA	REAL	-	RELATIVE ACCURACY ACCEPTANCE LIMIT FOR IN-VESSEL COOLANT CALCULATIONS
RECORD 9003			
F1ICDA	REAL	-	RELATIVE INTERFACE CONDITION ACCEPTANCE LIMIT FOR LOOP HYDRAULIC CALCULATIONS
F61CDA	REAL	-	RELATIVE INTERFACE CONDITION ACCEPTANE LIMIT FOR IN-VESSEL COOLANT CALCULATIONS
RECORD 9004			
L1ECAL	INTEGER	-	LOOP THERMAL OPTION; 1 - MODULE IS CALLED, 0 - MODULE IS NOT CALLED
L1WCAL	INTEGER	-	LOOP HYDRAULIC OPTION; 1 - MODULE IS CALLED, 0 - MODULE IS NOT CALLED
L3CALL	INTEGER	-	STEAM GENERATOR OPTION; 1 - MODULE IS CALLED, 0 - MODULE IS NOT CALLED
L5CALL	INTEGER	-	FUEL OPTION; 1 - MODULE IS CALLED, 0 - MODULE IS NOT CALLED
L6CALL	INTEGER	-	IN-VESSEL COOLANT OPTION, 1 - MODULE IS CALLED, 0 - MODULE IS NOT CALLED
L8CALL	INTEGER	-	PCS OPTION; 1 - MODULE IS CALLED, 0 - MODULE IS NOT CALLED

Table 7-7 (cont.)

RECORD 9005			
L1EPRT	INTEGER	-	LOOP THERMAL REPORT OPTION; 0 - NO REPORT, 1 - REPORT IS GENERATED
L1HPRT	INTEGER	-	LOOP HYDRAULIC REPORT OPTION; 0 - NO REPORT, 1 - REPORT IS GENERATED
L3PRNT	INTEGER	-	STEAM GENERATOR REPORT OPTION; 0 - NO REPORT, 1-4 - REPORT IS GENERATED WITH CORRESPONDINGLY GREATER DETAIL
L5PRNT	INTEGER	-	FUEL REPORT OPTION; 0 - NO REPORT, 1 - REPORT IS GENERATED
L6PRNT	INTEGER	-	IN-VESSEL COLLANT REPORT OPTION; 0 - NO REPORT, 1 - REPORT IS GENERATED
L8PRNT	INTEGER	-	PPS/PCS REPORT OPTION; 0 - NO REPORT, 1 - REPORT IS GENERATED
RECORD 9008 *			
L9DMPZ	INTEGER	-	DUMP LABELLED COMMON BEFORE INITIALIZATION; 1 - YES, 0 - NO
L9DMPI	INTEGER	-	DUMP LABELLED COMMON AFTER INITIALIZATION; 1 - YES, 0 - NO
L9DMPL	INTEGER	-	DUMP LABELLED COMMON AFTER LAST TIME STEP; 1 - YES, 0 - NO
L9TBLD	INTEGER	-	DUMP CONTAINER ARRAY TABLE INFORMATION; 1 - YES, 0 - NO

* NOTE: THIS RECORD IS CURRENTLY VALID ONLY ON CDC INSTALLATIONS.

Table 7-7 (cont.)

7.9 PROGRAM CONTROL FILE (OLDATA)

The input data file OLDATA allows the exercise of other than default program control. Its principle function is in the generation and subsequent use of restart data files. There may be up to three records in this file, one corresponding to each of the code's three control points. In the absence of a control record, the associated control point default values are assumed.

The syntax of all the records in this file is:

n D m, IN, OUT/

The record number, 'n', identifies the control point. It may be assigned the values 1, 2 or 3 corresponding to the pre-steady-state initialization, the steady-state or the transient control points, respectively. The function parameter, 'm', indicates the control option to be exercised. Its value is assigned from the following table:

Function Parameter	Function
0	No-op
1	Read
2	Write (only)
3	Read and Write
4 (or greater)	Default

The fact that OLDATA is not a member of the set of required input files should not belie its usefulness. While it is true that the file's utility

should not be unduly exaggerated, the file serves a function which, if not essential to the smooth operation of the code, adds sufficiently to it.

In the absence of OLDATA, the system maintains default control. What constitutes default control is particular to the individual control points. In both the pre-steady-state and steady-state modules, processing proceeds from beginning to end, neither reading nor writing a restart. Under default control, the transient is initiated at time zero with the current data image. A restart is subsequently stored at the interval (S9SINT) specified on TRNDAT record 9001. By assigning this parameter a sufficiently large value, the saving of a restart can be effectively subverted.

By employing other than default control, the user can not only initialize to a previous state, but can also dictate which computational modules will be processed. Access is barred to either the steady-state or transient module by specifying a No-op (0) on the corresponding control record. Since OLDATA is itself processed by the pre-steady-state module, a No-op is ignored on record one (1). The steady-state calculations could be bypassed if, for example, the transient was to be initialized from a previously determined steady-state or resumed at a simulation time greater than zero. Often, parametric studies requiring only the steady-state portion of the code are desired. For these computations, a No-op would be assigned on the transient control record. It should be noted, that if the transient were to be resumed at a simulation time greater than zero, the function parameter on record three (3) must be assigned a negative value.

The "IN" and "OUT" control record parameters correspond to the available I/O devices from which a restart will be read and/or written. The program contains default values for these terms. The default values are retained if the user terminated the control record after the function declaration (e.g., 2D 2/). The default values for the "IN" and "OUT" parameters are:

Record	In	Out
1D	10	20
2D	30	40
3D	50	60

It should be noted that the last digit in each of these terms is zero. This indicates that there is to be no file position before a read/write operation. This, once again, is the default mode of operation. If file positioning is required, up to 99 files may be skipped before a given I/O operation is initiated. This type of control may be exercised by specifying the number of files to be skipped as part of the I/O device assignment. For example,

```
3D    1,    52,    40/
```

would read the third file (skip 2) from unit 50.
Similarly,

```
3D    1,    347,    60/
```

would skip the first 47 files on unit 30 before initializing the transient. What should be evident is that a given I/O device assignment is comprised of two fields; the device field and the file positioning field. The first field contains only one digit (the first). By convention, user interaction is per-

mitted only with a device whose unit number is an integer multiple of ten (10-90). The value found in the device field when multiplied by ten yields the I/O device. The remaining one or two digits make up the file positioning field and according to its value the device will be positioned to retrieve a particular file.

An I/O device is rewound before it is either read or written. The rewind before a write may be suppressed by signing the "OUT" parameter negatively (e.g., 3D 1, 50, -60). This will result in a series of consecutive restarts generated at intervals of S9SINT seconds through the course of the transient. A particular file may be accessed on a subsequent restart by entering the appropriate file positioning control as discussed above.

```
0V OLDATA
1D 99/
2D 99/
3D 99/
```

Figure 7-11 Data File OLDATA Sample Input (Default Values)

7.10 RESTART TRANSIENT DATA (TRNREG)

The data file TRNREG may be used to alter a transient proceeding from a restart at simulation time greater than zero. The two records in this file, 101 and 105, correspond to TRNDAT records 9001 and 9005, respectively.

This file is not required and either or both records may be omitted. If not re-initialized, the parameters previously set would be maintained.

***** FILE TRNREG

RECORD 101			
S9LAST	REAL	S	TOTAL PROBLEM SIMULATION TIME
S9MAXA	REAL	S	MAXIMUM TIMESTEP ALLOWED
S9MINA	REAL	S	MINIMUM TIMESTEP ALLOWED
S9SINT	REAL	S	MASTER CLOCK INTERVAL AT WHICH A RESTART DUMP WILL OCCUR
S9PINT(J) *	REAL	S	MASTER CLOCK INTERVAL AT WHICH A SYSTEM REPORT WILL BE GENERATED
S9PINT(J+1)*	REAL	S	MASTER CLOCK TIME AFTER WHICH THE CORRESPONDING S9PINT IS NO LONGER VALID

* NOTE: THE INDEX "J" IS INCREMENTED OVER THE SET OF PAIRED POINTS.
THERE MAY BE AS MANY PAIRS (INTERVALS) AS THE USERS FINDS NECESSARY.

S9PINT(1) IS IMPOSED FROM TIME 0.0 TO S9PINT(2). S9PINT(3) IS THEN USED FROM THE MASTER CLOCK TIME S9PINT(2) TO S9PINT(4), SIMILARILY, S9PINT(5) IS USED FROM S9PINT(4) TO S9PINT(6), AND SO ON.
IT SHOULD BE APPARENT THAT S9PINT(4) MUST BE STRICTLY GREATER THAN S9PINT(2), AND S9PINT(6) MUST BE STRICTLY GREATER THAN S9PINT(4), AND SO ON.

THERE IS QUITE A BIT OF LATITUDE PERMITTED IN THE SELECTION OF PRINT INTERVALS BUT THEY MUST BE CAREFULLY CHOSEN (SEE SECTION 7.8)

RECORD 105			
L1EPRT	INTEGER	-	LOOP THERMAL REPORT OPTION; 0 - NO REPORT, 1 - REPORT IS GENERATED
L1HPRT	INTEGER	-	LOOP HYDRAULIC REPORT OPTION; 0 - NO REPORT, 1 - REPORT IS GENERATED
L3PRNT	INTEGER	-	STEAM GENERATOR REPORT OPTION; 0 - NO REPORT, 1-4 - REPORT IS GENERATED WITH CORRESPONDINGLY GREATER DETAIL
L5PRNT	INTEGER	-	FUEL REPORT OPTION; 0 - NO REPORT, 1 - REPORT IS GENERATED
L6PRNT	INTEGER	-	IN-VESSEL COLLANT REPORT OPTION; 0 - NO REPORT, 1 - REPORT IS GENERATED
L8PRNT	INTEGER	-	PPS/PCS REPORT OPTION; 0 - NO REPORT, 1 - REPORT IS GENERATED

Table 7-8 Input Description for Data File TRNREG

APPENDIX A

Alphabetical Listing of Subroutines in SSC-L

ADDA9U

This steady-state utility module adds a floating point data value to an array entry.

ADDM9U

This transient utility module adds a floating point data value to an array entry.

ADTW3T

This transient module advances heat exchanger tube wall temperatures at the end of the time step. Heat transfer ratio in the "level" nodes are adjusted to match implicitly advanced nodal average heat transfer rates.

ADVN3T

This transient module advances almost all steam generator variables at the end of a time step. It uses segment response matrices and changes in accumulator pressures and enthalpies to calculate advanced enthalpies and mass flow rates.

ALFA5S

This steady-state module calculates the coefficient of thermal expansion for each node in the fuel slice.

ALOC3R

This reader module allocates global container storage for steam generator variables.

ALOC8T

This transient module allocates container space for the PCS/PPS variably dimensioned global variables.

APPL8T

This transient module calculates the scram reactivity worth of the primary and/or secondary control rods utilizing the user supplied polynomial coefficients for rod position as a function of time after reactor scram.

BOIL6T

This transient module calculates liquid and bubble temperatures in upper and lower slugs under boiling conditions.

BREK1T

This transient module computes pressures at any primary loop break location.

BREK2T

This transient module computes pressures at any intermediate loop break location.

CALC1R

This reader module manipulates certain primary and secondary loop input data and initializes subsequent loop structures where the user has chosen to default these values to those entered for the primary loop.

CALC3R

This reader module loads the steam generator input data into the data arrays, using the component order information generated by VRFY3R.

CALC7R

This reader module sets fuel/rod slice-type dependent arrays and determines normalized axial and radial power distributions.

CALC8R

This reader module interprets the coded iterative scheme designated by the user for establishing the initial plant balance.

CHEX9R

This reader module calls the verification routines.

COEF5T

This transient module calculates appropriate coefficients for the transient temperature calculations in the fuel/rod.

COEF6T

This transient module calculates coefficients for the various pressure loss terms used in FLOW6T.

COOL6S

This steady-state module is the driver routine for in-vessel coolant energy calculations.

COOL6T

This transient module is the driver for the transient coolant calculations. It provides initial conditions; determines step size; and then employs several sub-modules to calculate temperature, pressure, enthalpy, and mass flow rate of the coolant in all axial nodes of all channels. It then stores values for fuel calculations.

CORE6S

This steady-state module is the core coolant driver. It calculates axial temperatures, enthalpy gradients, friction factors, heat transfer coefficients and pressures at each node in each channel.

CRDR9R

This reader module is the primary controller for the processing of initialization data. It calls the free-format reader routines.

CRDR9T

This transient module is the driver for the transient input processor.

CRKR3T

This transient module solves the segment matrix equation for the segment response matrix. It uses a close-packed form of Gaussian elimination.

CRKR9U

This utility module solves a system of linear equations.

CVAL1S

This steady-state module computes the steady-state pressure drop across the check valve.

CVAL1T

This transient module computes the pressure drop across the check valve.

DEFN1T

This transient module defines pipe flow rates, as well as input and output pump flow rates for the primary loop(s).

DEFN2T

This transient module defines pipe flow rates, as well as input and output pump flow rates for the intermediate loop(s).

DMOD3R

This reader module decodes the steam generator input data.

DOPP5T

This transient module calculates the reactivity feedback due to the Doppler effect.

DPSV3C

This material property module calculates the pressure difference between junction and volume average.

DP3C

This correlation module calculates steam generator nodal pressure losses.

DRIV1T

This transient module is the driver for heat transport system transient hydraulics.

DRIV9T

This transient module is the driver routine for the time integration during the transient calculations. It also handles the overall timestep control.

DT9S

This steady-state module solves the log mean temperature difference equation.

END1S

This steady-state module calculates the temperature boundary conditions for the sub-pipe in the primary loop and, in doing so, accounts for the temperature rise across the pump, as well as the IHX plena temperatures at the proper locations.

END1T

This transient module sets transient thermal boundary conditions from one pipe to the next in the primary loop(s).

END2S

This steady-state module sets the inlet temperature and mass flow rate boundary conditions for pipe (J+1) in the intermediate coolant loop(s). Additionally, it accounts for temperature rise across the pump and mass flow rate division due to branch lines for coolant flow at the steam generator.

END2T

This transient module sets the transient thermal boundary conditions from one pipe to the next in the intermediate loop(s).

END9U

This utility module performs the case wrap-up.

ENET3S

This steady-state module performs global energy balance calculations for current mass flow rates and pressures. Principal variables calculated include volume enthalpies, segment inlet and outlet enthalpies, segment heat transfer rates, subsystem heat transfer rates and heat exchanger heat transfer rates.

ENTH3C

This fluid property module calculates steam generator enthalpies corresponding to temperature or quality and pressure.

EQIV1T

This transient module equivalences the names of primary loop variables and their time derivatives in terms of names used in the integrating subroutine.

EQIV2T

This transient module equivalences the names of intermediate loop variables and their time derivatives in terms of names used in the integrating subroutine.

ERR9R

This reader module is the input processor abort routine.

ESWT3S

This steady-state module calculates water/steam side enthalpy at the end of the current heat transfer regime. For subcooled convection this enthalpy corresponds to a tube wall temperature equal to the fluid saturation temperature. The saturated liquid enthalpy terminates the subcooled nucleate boiling region. For the forced convection vaporization region, the enthalpy required for critical heat flux is calculated. The film boiling region ends at the saturated vapor enthalpy.

ESWT3T

This transient module determines the switch enthalpy for heat transfer mode in transient. It requires the current heat transfer mode as an input.

ETST3R

This reader module tests the steam generator input data for errors.

EVLV3S

This steady-state module calculates the accumulator average enthalpy from level, saturation conditions, and accumulator shape.

EXIT9U

This utility module is the SSC abnormal termination subroutine.

EXTR8C

This correlation module calculates the initial steady-state external rheostat electrode position.

FCON8T

This transient module simulates the sodium flow-speed control and the pump drive mechanism.

FLIN8T

This transient module is called by INT8T for the primary and intermediate flow control systems.

FLOW1T

This transient module sets the proper calling sequence to primary loop hydraulic computational submodules.

FLOW2T

This transient module sets the proper calling sequence to intermediate loop hydraulic computational submodules.

FLOW6T

This transient module simulates the flow redistribution model. It calculates the mass flow rate time derivative in each channel and bypass channel.

FLV3T

This transient module advances the liquid level in accumulator modules, given advanced enthalpy and pressure. If the accumulator is a horizontal cylinder, an iterative process is required.

FPUM8T

This transient module simulates the steam generator feedwater pump flow-speed control and the pump drive mechanism.

FRAD5S

This steady-state module calculates the average power generation for all radial nodes in any rod slice.

FRAD5T

This transient module calculates the average power for all radial nodes in any rod slice. It also calculates the power generation multiplier to be used later in calculating the transient volumetric power generation.

FUEL5S

This steady-state module is the driver for fuel heat conduction calculations. It treats a fuel slice as the basic computational element, calls all major fuel computational modules, and controls convergence.

FUEL5T

This transient module is the driver for the fuel rod and structure calculations. By calling series of modules in succession, it calculates quantities such as temperature and radii of the fuel, cladding, and structure nodes.

FUNC1T

This transient module calculates the time derivatives of differential equations (other than pump and reservoir) for the primary loop hydraulics.

FUNC2T

This transient module calculates the time derivatives of differential equations (other than pump and reservoir) for the intermediate loop hydraulics.

GAMA5S

This steady-state module calculates the thermal conductivity for fuel and clad nodes for the slice and heat transfer coefficients for the interfaces.

GAMA5T

This transient module calculates the thermal conductivity and emissivity for fuel and clad nodes and also computes the heat transfer coefficient for gaseous mixtures in the gap.

GENRD

This is a general purpose reader routine as developed by the Los Alamos National Laboratory and modified for usage in SSC.

GETA9U

This steady-state utility module gets a data entry value from an array.

GETM9U

This transient utility module gets a data entry value from an array.

GFSK3C

This correlation module calculates the Fauske choke flow rate.

GMDY3C

This correlation module calculates a Moody choke flow rate.

GROW5T

This transient module calculates the reactivity feedback due to axial expansion.

GRO5S

This steady-state module sets pointers for restructuring in the rod slice.

GVSL1T

This transient module computes the coolant level in the guard vessel, pressure external to a break and the time derivative for any accumulated volume of coolant in the guard vessel.

HBAL3S

This steady-state module takes intermediate loop temperatures, mass flow rates, and pressures and loads information into appropriate boundary module arrays for enthalpy, mass flow rate, and pressure. It also calculates total energy being transferred to the intermediate side of the system.

HEAD1T

This transient module computes the head(s) of the primary pump(s) and defines its operational region.

HEAD2T

This transient module computes the head(s) of the intermediate pump(s) and defines its operational region.

HHOT3C

This correlation module calculates the heat transfer coefficient from the hot side to the (cold side) tube wall.

HNAF3C

This correlation module calculates the sodium heat transfer coefficient using the Graber-Reiger correlation.

HWFB3C

This correlation module calculates the film boiling heat transfer coefficient using the Bishop correlation.

HWFC3C

This correlation module calculates the forced convection heat transfer coefficient using the Dittus-Boelter correlation.

HWNB3C

This correlation module calculates the nucleate boiling heat transfer coefficient using the Chen correlation.

HWSC3C

This correlation module calculates the heat transfer coefficient to superheated steam using the Heineman correlation.

HWS3C

This correlation module determines which heat transfer correlation is appropriate for the present water/steam conditions.

HXHT3S

This steady-state module marches through the heat exchanger nodes on the intermediate side. Because the enthalpy distribution is determined while the water/steam side was being calculated in HX3S, only pressure drops are calculated in HXHT3S.

HXHT3T

This transient module calculates the heat transfer rates and derivatives of heat transfer rates on the hot side of the heat exchangers during transient calculations. It loops over all nodes, calculating parameters needed to load the segment matrix equations.

HXND3S

This steady-state module performs the nodal energy balance for a heat exchanger node. If the node being analyzed (in HX3S) contains two heat transfer regimes, HXND3S will be called twice to analyze each part separately.

HX3S

This steady-state module marches through the heat exchanger nodes, advancing enthalpies on hot and water/steam sides of the heat exchanger. It iterates on the area correction factor, so as to find an area multiplier that leads to the correct integral heat transfer rate. It calls DP3C for each (converged) node and sums the nodal pressure losses.

HX3T

This transient module calculates heat transfer rates and derivatives of heat transfer rates on the water/steam side of the heat exchangers during transient calculations. It loops over all nodes calculating parameters needed to load the segment matrix equations.

HYDR1S

This steady-state module solves the steady-state hydraulics momentum equations for both primary and secondary sides of the IHX.

HYDR1T

This transient module computes transient hydraulics in the IHX(s).

IHX1S

This steady-state module solves the steady-state energy equations for the IHX. IHX1S and HYDR1S are the only interface between the primary and intermediate loop modules.

IHX1T

This transient module solves the transient energy equations in the IHX(s).

INA9U

This utility module initializes the array data abstraction.

INCM3T

This transient module converts incoming information from the intermediate loop(s) to the steam generator data arrays. It also interfaces information from the plant protection and control systems.

INIT1T

This transient module sets variables needed for the first call to the primary loop hydraulic integration scheme.

INIT2T

This transient module sets variables needed for the first call to the secondary loop hydraulic integrating routine.

INIT3R

This reader module initializes certain steam generator constants.

INIT3S

This steady-state module loads initial guesses for system pressures, mass flow rates, enthalpies and heat transfer rates. Values for pressure and mass are user-input. Initial enthalpies and heat transfer rates are zeroed, as ENET3S is called soon after INIT3S.

INIT5T

This transient module initializes variables used in the fuel and reactivity calculations.

INIT6T

This transient module initiates variables used by the in-vessel coolant hydraulics modules.

INIT8T

This transient module initializes values used in the PPS/PCS subroutines.

INIT9R

This reader module calls a series of intermediate data management routines.

INIT9T

This transient module is the driver for the transient initialization routines.

INIT9U

This utility module reads the title card.

INRD3R

This reader module initializes the steam generator input data reader.

INSG3S

This steady-state module sets segment inlet enthalpy and flow rate in nodal arrays using values in segment arrays.

INTF3T

This transient module converts outgoing information from the steam generator data arrays to the intermediate loop. It also interfaces information to the plant protection and control systems.

INTG1T

This transient module advances the hydraulic equations using a predictor-corrector method of the Adams type.

INTP9U

This utility module is an interpolation subroutine.

INT8T

This transient module interfaces the PPS/PCS modules to the rest of SSC by fetching the actual values of the desired process variables for cascade selection for reactor power control and normalizing them against their respective 100% steady-state values. It also calls other subroutines to do similar calculations for PPS, flow controllers and the steam generator controllers.

IOSG3T

This transient module initiates and concludes the process of loading the segment matrix equation. It loads the equations for the enthalpy of the flow entering the segment (from either end) and some of the segment momentum equations (or choke limit).

LEAK5T

This transient module tests for cladding rupture due to fission gas pressure for each axial fuel slice in the current channel. Cladding rupture conditions exist if the difference between fission gas pressure and coolant pressure exceeds a critical value defined by cladding dimensions and material yield point for the calculated cladding temperature.

LEQ9U

This utility module solves a set of linear equations.

LINK3R

This reader module generates geometric links for the steam generator data modules.

LIST1R - LIST9R

These reader modules list the data processed by the corresponding READ routines.

LIST9T

This transient module lists the data processed by READ9T.

LOAD3T

This transient module loads the nodal mass and energy equations into the segment matrix equations. It also loads a contribution to the momentum equation for each node.

LOOP1R

This reader module verifies that the net summation of input heights around each loop is zero.

LOOP1S

This steady-state module drives the primary loop steady-state calculation. In particular, it interprets the logical variables in order to select the proper calling sequence to the various subroutines. This routine also copies the results of the computations for loop i into the arrays for the rest of the loops.

LOOP1T

This transient module is the main driver for transient thermal computations in the primary loop(s).

LOOP2S

This steady-state module drives the intermediate loop steady-state computations. The rest of the description is the same as for LOOP1S.

LOOP2T

This transient module is the main driver for transient thermal computations in the intermediate loop(s).

LPLN6S

This steady-state module calculates the coolant temperatures in the lower plenum module. It initializes values of temperature, enthalpy and pressure for the first axial nodal interface of each channel. It calculates pressures at the bottom of the core.

LPLN6T

This transient module performs the transient lower plenum calculations. It extrapolates boundary conditions. It terminates its procedure by calculating coolant and metal temperatures and pressures at the bottom of the core.

MAIN9R

This reader module is the main driver for the input-initialization segment. It calls the three input processor submodules (CRDR9R, CHEX9R and INIT9R).

MAIN9S

This steady-state module is the main driver for the steady-state calculations.

MAIN9T

This transient module is the overall driver routine for the transient calculations.

MODL3C

This subroutine transfers data from global arrays into local scratch arrays and performs limited computations of module geometric parameters.

NET3T

This transient module performs the accumulator mass and energy balance to determine advanced time enthalpies and pressures. It references the segment response matrices.

NEWA9U

This utility module constructs a new update of the two dimensional array data abstraction.

NODE3C

This material property module drives the calculations of nodal specific volume, quality, temperature, viscosity and their derivatives.

OPTN6S

This steady-state module computes either the steady-state channel flow rate distribution or pressure loss coefficients, depending on the user specified option.

ORDR3R

This reader module generates a list defining the sequential module order for steam generator geometric modules.

PBAL9S

This steady-state module performs the global thermal balance for the whole plant.

PCHK9R

This reader module checks for valid material property identifications.

PCON8T

This transient module simulates the reactor power control and the control rod drive mechanisms. It also calculates the reactivity worth of the reactor control rods.

PDFG1T

This transient module sets the logic to compute pressure losses across different elements of the primary loop(s).

PDFG2T

This transient module sets the logic to compute pressure losses across different elements of the intermediate loop(s).

PINT1S

This steady-state module interfaces the in-vessel and primary loop pressures.

PIPE1S

This steady-state module solves the steady-state energy and momentum equations for pipe J in the primary coolant loop. It is assumed that the pipe diameter is constant, and the pipe wall is in thermal equilibrium with the coolant.

PIPE1T

This transient module solves the transient energy equations in the primary loop piping.

PIPE2S

This steady-state module solves the steady-state energy and momentum equations for pipe J in the intermediate coolant loop.

PIPE2T

This transient module solves the transient energy equations in the intermediate loop piping.

PIPE3S

This steady-state module marches through all pipe nodes, setting enthalpies and mass flow rates at nodal outlets to the values at the nodal inlets. It calls DP3C for each node and sums the nodal pressure losses.

PIPE3T

This transient module loops over all nodes, calculating parameters needed to load the segment matrix equations.

PIPW1T

This transient module computes the pressure losses in the pipe sections in the primary loop(s).

PIPW2T

This transient module computes the pressure losses in the pipe sections in the intermediate loop(s).

PLOS1T

This transient module computes the pressure losses in appropriate sections of the primary loop(s) from the losses in individual components.

PLOS2T

This transient module computes the pressure losses in appropriate sections of the intermediate loop(s) from the losses in individual components.

PMTR8T

This transient module regulates the shutdown of all coolant pumps (primary, secondary, recirculation and feedwater pumps) and the turbine trip.

POW5T

This transient module serves as the driver for the rod transient fission power generation calculations.

POW6T

This transient module calculates the power deposited in the reactor coolant for use in COOL6T.

PPCS8T

This transient module is the main driver for the PPS/PCS transient calculations.

PPSH8T

This transient module is the subdriver for the primary shutdown system.

PPS8T

This transient module is the subdriver routine for the plant protection system.

PREP3T

This transient module prepares the steam generator calculations for another time step. It uses the minimum time constant calculated during the last step to set a new one. It interpolates tables for any time dependent user-input parameters, e.g., boundary conditions.

PRES1S

This steady-state module determines the pressures at pipe endpoints around the primary loop.

PRES1T

This transient module sets inlet and outlet pressures of uniform mass flow rate sections in the primary loop(s).

PRES2S

This steady-state module determines the pressures at pipe endpoints around the intermediate loop.

PRES2T

This transient module sets inlet and outlet pressures of uniform mass flow rate sections in the intermediate loop(s).

PRES6S

This steady-state module determines the nodal pressures in each reactor coolant channel.

PRET1T

This transient module initializes the primary and secondary loop variables for the thermal calculations.

PREX5S

This steady-state module initializes nodal distances for either equal radius increments or equal area increments of the rod slice.

PRE5S

This steady-state module performs the initialization for FUEL5S by obtaining data computed by other modules. Among others, it sets the proper rod nodal temperature to T6COOL(J,K), places the heat transfer coefficient for the slice in a local variable HCOOL, initializes tags for restructuring and calls PREX5S to initialize nodal distances at temperature T5REF.

PRE5T

This transient module transfers the temperature from storage arrays into local scratch arrays for the particular rod slice in question at the start of each timestep.

PRFL3S

This steady-state module performs global pressure and mass flow rate balance calculations for current enthalpies and heat transfer rates. Principal variables calculated include segment mass flow rates, inlet and outlet pressures, volume pressures and boundary module pressures and mass flows (if not user specified).

PRMT5T

This transient module handles the advancement in time of the fission power generation.

PRNT1T

This transient module prints out primary loop temperature variables.

PRNT3C

This module prints out steam generator network variables (steady-state or transient).

PRNT5S

This steady-state module prints steady-state results for the fuel (rod) calculations.

PRNT5T

This transient module prints out transient results for fuel (rod) variables.

PRNT6T

This transient module prints out transient in-vessel coolant variables.

PRNT9S

This steady-state module prints a plant-wide steady-state summary of results.

PRNT9T

This transient module is the main printing routine for the transient.

PROP5T

This transient module calculates all properties for the fuel (rod) heat conduction calculations.

PROP6T

This transient module calculates all properties used in the in-vessel coolant energy and fluid dynamics subroutines.

PRTB3T

This transient module evaluates derivatives of heat transfer rate with respect to enthalpy and mass flow rate. A perturbation technique is used.

PSIN8T

This transient module is called by INT8T for PPS variables.

PSSH8T

This transient module is the subdriver for the secondary shutdown system.

PS018F

This function is the PPS High Flux subsystem.

PS028F

This function is the PPS Flux-to-Delayed-Flux subsystem.

PS038F

This function is the PPS Flux-to- $\sqrt{\text{Pressure}}$ subsystem.

PS048F

This function is the PPS Primary-to-Intermediate Speed Ratio subsystem.

PS058F

This function is the PPS Pump Electrics subsystem.

PS068F

This function is the PPS Low Reactor Vessel Level subsystem.

PS078F

This function is the PPS Steam-to-Feedwater Flow Ratio subsystem.

PS088F

This function is the PPS High IHX Primary Sodium Outlet Temperature subsystem.

PS098F

This function is the PPS Power-to-Flow Ratio subsystem.

PS108F

This function is the PPS Primary-to-Intermediate Flow Ratio subsystem.

PS118F

This function is the PPS Steam Drum Level subsystem.

PS128F

This function is the PPS High Evaporator Outlet Sodium Temperature subsystem.

PS138F

This function is the PPS High Reactor Outlet Nozzzle Sodium Temperature subsystem.

PS148F

This function is the PPS Low Primary Loop Sodium Flow Rate subsystem.

PS158F

This function is the PPS Low Intermediate Loop Sodium Flow Rate subsystem.

PPS168F

Spare PPS function.

PPS178F

Spare PPS function.

PPS188F

Spare PPS function.

PPS198F

Spare PPS function.

PPS208

Spare PPS function

PUMP1S

This steady-state module determines the pump pressure rise by mathcing it with the overall load in the primary circuit. It then sets up the polynomial equation for pump head and calls ROOT1U to calculate the pump operating speed.

PUMP1T

This transient module computes primary pump variables and time derivative for pump speed(s).

PUMP2S

This steady-state module determines the pump pressure rise by matching it with overall load in the intermediate circuit. It then sets up the polynomial equation for pump head and calls ROOT1U to calculate the pump operating speed.

PUMP2T

This transient module computes intermediate pump variables and time derivative for pump speed(s).

PUMP3S

This steady-state module initializes the steam generator pump at full speed and calculates the head delivered under current conditions. It neglects enthalpy rise, setting enthalpy and mass flow rate at the outlet to the corresponding inlet values.

PUMP3T

This transient module calculates the advanced time pump speed(s) and head(s). It calculates other parameters needed to load the segment matrix equations.

PUTA9U

This steady-state utility module puts a data entry into an array.

PUTM9U

This transient utility module puts a data entry into an array.

PUT5S

This steady-state module moves the calculated steady-state values for the rod slice into storage locations.

PUT5T

At the time this transient module is invoked, all formal calculations of the fuel and clad and structure have been completed for that timestep and for the given axial node. This module then moves all temperatures and radii so far calculated from local scratch variables into global storage arrays for subsequent timesteps.

REAC5T

This transient module initiates calls to other modules to obtain the various applied and feedback reactivity contributions.

READ1R

This reader module processes free-format card-image input for the initialization of the primary and secondary loop modules.

READ3R

This reader module processes free-format card-image input for the initialization of the steam generator modules.

READ7R

This reader module processes free-format card-image input for the initialization of the in-vessel modules.

READ8R

This reader module processes free-format card-image input for the initialization of the plant balance routine.

READ9R

This reader module processes free-format card-image input for the initialization of the material property parameters.

READ9T

This transient module reads free-format card-image input for the initialization of transient parameters.

RELA9U

This utility module releases storage assigned to the array data abstraction.

REPT9R

This reader module loads fuel (rod) slice-type dependent parameters.

REST9R

This reader module reads a program generated file for the reinitialization of labeled common blocks in the event of a restart.

REST9T

This transient module reads a transient restart file.

REST9U

This utility module calls the global retrieval subroutines.

RES1S

This steady-state module computes the height of coolant in the primary pump tank and the mass of cover gas above the coolant level.

RES1T

This transient module computes variables and time derivatives for level in the primary pump reservoir(s).

RES2S

This steady-state module computes the height of coolant in the intermediate pump tank(s) and the mass of cover gas above the coolant level(s).

RES2T

This transient module computes variables and time derivatives for level in the intermediate pump reservoir(s)

RITE1S

This steady-state module prints out the primary loop steady-state solution.

RITE1T

Dummy subroutine.

RITE2S

This steady-state module prints out the secondary loop steady-state solution.

RSET1T

This transient module resets all logical variables and data for components and piping if a break is present in a primary loop.

RSET2T

This transient module resets all logical variables and data for components and piping if a break is present in a secondary loop.

RUNG9U

This utility module uses a fourth order Runge-Kutta algorithm to integrate a system of ordinary differential equations.

SATP3C

This fluid property module loads saturation properties calculated at the segment reference pressure.

SAVE9R

This reader module generates an ordered file for a re-initialization restart.

SAVE9S

This steady-state module creates an ordered file containing information necessary to re-initialize all common blocks to computed steady-state values.

SAVE9T

This transient module creates an ordered file containing information necessary to re-initialize all common blocks to a given transient solution.

SAVE9U

This utility module calls the global storage routines.

SCRM8T

This transient module, common to both primary and secondary shutdown systems, is the subdriver which calls the routines for the PPS trip equations to check for possible scram signals.

SCRT8T

This transient module allocates all scratch arrays used in the PPS/PCS calculations.

SENS8T

This transient module takes the actual sensed values from the controller cascades and compensates them for the inherent time lags imposed by the measuring devices.

SFUN8T

This transient module is the subdriver for the PPS trip equations.

SGBC3T

This transient module factors the advanced time boundary conditions into the segment response matrices. For a flow boundary condition, the pressure column is factored into the columns for enthalpy and pressure at the opposite end, plus the constant column.

SGEN8T

This transient module calculates the load-dependent setpoints as governed by the supervisory controller, using the user specified second-order polynomial coefficients.

SGIN8T

This transient module, called by INT8T, acts as the sensor and transmitter by compensating the actual values of the process variables for the inherent time lags to calculate their measured values.

SGMA5T

This transient module calculates the volumetric heat source for the fuel (rod) nodes, clad, coolant and structure in an axial slice.

SOLV5T

This transient module solves the fuel (rod) matrix equation using Gaussian elimination with full pivoting.

SOLV8T

This transient module uses the fourth-order Runge-Kutta algorithm to integrate Equation (3.4-1). It assures numerical stability by cutting the timestep by half in order to achieve timesteps less than or equal to the time constant of the first order system. It also sets the measured value to the actual value in case of a zero time constant (instartaneous response).

SSC

Overall main driver for entire program.

STEM5S

This steady-state module calculates the temperature of the fuel (rod), structure and fission gas plenum for steady-state.

STGN3S

This steady-state module is the driver for steam generator system calculations. Its principal function is to call other subroutines, but some high level (system-wide or segment) calculations are performed within.

STGN3T

This transient module is the driver for steam generator system calculations. Its principal function is to call other subroutines, but some high level (system-wide or segment) calculations are performed within.

STGN8T

This transient module is the subdriver for steam generator controller routines.

STOR1T

This transient module stores the previous and updated values of flow rate(s) for subsequent interface boundary condition generation.

SUBS3S

This steady-state module partitions systems into subsystems, each of which must transfer a given amount of heat to remain in equilibrium. The fraction of flow through each segment and accumulator contributing to each subsystem's energy balance is determined.

TANK2S

This steady-state module computes the pressure in the loop at the location of the surge tank, and further, calculates the mass of gas in the surge tank.

TANK2T

This transient module computes pressures and time derivative for level in the surge tank(s).

TEMP3C

This fluid property module computes fluid temperature given pressure, enthalpy and fluid type.

TEMP5S

This steady-state module calculates the steady-state radial temperature distribution in the rod and cladding for any slice.

TORK1T

This transient module computes hydraulic and frictional torques for the primary pump(s).

TORK2T

This transient module computes hydraulic and frictional torques for the intermediate pump(s).

TORQ8T

This transient module calculates the sodium pump drive motor torque for both squirrel cage and wound rotor induction motors.

TRAN9R

This reader module transfers arrays which are read via input into storage.

TSAV5S

This steady-state module determines the average temperature in each rod slice (except fission gas plenum slices).

TSAV5T

This transient module calculates certain fuel (rod) slice dependent quantities required in GROW5T, DOPP5T, and VOID5T.

TWAL3S

Given the temperatures on the hot and cold sides of the tube, this steady-state module solves iteratively for the tube wall temperatures and the heat transfer coefficients on either side of the wall. An accelerated iterative scheme is tried first, with a more reliable (though slower) bisection scheme used if the first scheme fails to converge.

TYPE5R

This reader module loads channel-dependent parameters for use in the slice-type dependent in-vessel modules.

UPLN6S

This upper plenum coolant steady-state module calculates the upper plenum temperatures, the exit enthalpy, outlet, and top of core pressures and finds pressure loss factors for each channel.

UPLN6T

This transient module updates the time derivatives for: sodium level; temperature of sodium in two mixing zones; temperature of cover gas; and temperatures of the inner structure, thermal liner, and the vessel closure head. It terminates by calculating the pressure at the vessel outlet.

VALV3S

This steady-state module initializes valve positions at user input quantities. It neglects enthalpy rise, setting enthalpy and mass flow rate at the outlet to the corresponding inlet valves.

VALV3T

This transient module calculates advanced time valve position(s) and corresponding form loss(es). It calculates other parameters needed to load the segment matrix equations.

VALV8T

This transient module simulates the steam generator valve flow, level and pressure control and the valve drive mechanism.

VARF8C

This correlation module calculates the initial steady-state frequency of the power to the pump drive system.

VESL1T

This transient module calculates certain algebraic relationships at the vessel-loop(s) interface(s) and within the vessel which are used in the hydraulic computations.

VJ1T

This transient module determines the velocity of the fluid jet out of a pipe break.

VOID5T

This transient module calculates the reactivity feedback due to sodium voiding.

VOL3C

This material property module calculates volume temperature, density and density derivatives.

VRFY1R - VRFY9R

These reader modules validate the data processed by the corresponding READ routines against established criteria.

VRFY9T

This transient module validates the data processed by the READ9T routine against established criteria.

WGHT2T

This transient module computes the appropriate multiplication (weighting) factors for parallel piping and components.

WRIT1T

This transient module prints out primary loop coolant hydraulic results.

WRIT2T

This transient module prints out secondary loop coolant hydraulic results.

WRIT8T

This transient module prints out PPS/PCS results.

XDNB3C

This correlation module computes the quality at DNB using a correlation developed at Atomics International.

XDRY3C

This correlation module calculates the critical heat flux using the MacBeth correlation.

XI1T

This transient module initializes the inertance in each primary loop flow segment.

XI2T

This transient module initializes the inertance in each secondary loop flow segment.

XPAN5S

This steady-state module adjusts radii due to thermal expansion for each node in the fuel (rod) slice.

XPAN5T

This transient module recalculates the radii of the fuel (rod) and cladding, necessary because of the thermal expansion of the radial nodes. Two methods are employed in calculating radii; equal area increment or equal radii increment.

NRC FORM 335 (6 83) U.S. NUCLEAR REGULATORY COMMISSION

BIBLIOGRAPHIC DATA SHEET

1 REPORT NUMBER (Assigned by TIDC add Vol No if any)
NUREG/CR 3169
BNL-NUREG-51650

2 Leave blank

3 TITLE AND SUBTITLE
Super System Code (SSC, Rev. 0) An Advanced Thermo-hydraulic Simulation Code for Transients in LMFBRs

4 RECIPIENT'S ACCESSION NUMBER

5 DATE REPORT COMPLETED
MONTH: April YEAR: 1983

6 AUTHOR(S)
J.G. Guppy et al.

7 DATE REPORT ISSUED
MONTH: April YEAR: 1983

8 PERFORMING ORGANIZATION NAME AND MAILING ADDRESS (Include Zip Code)
Department of Nuclear Energy
Brookhaven National Laboratory
Upton, Long Island, New York 11973

9 PROJECT TASK WORK UNIT NUMBER

10 FIN NUMBER
A-3015

11 SPONSORING ORGANIZATION NAME AND MAILING ADDRESS (Include Zip Code)
Division of Accident Evaluation
Office of Nuclear Regulatory Research
U.S. Nuclear Regulatory Commission
Washington, D.C. 20555

12a TYPE OF REPORT
Technical Report

12b PERIOD COVERED (Inclusive dates)

13 SUPPLEMENTARY NOTES

14 ABSTRACT (200 words or less)

The Super System Code (SSC) calculates the response of nuclear reactor systems during operational, incidental and accidental transients, especially natural circulation events. Modules simulated and parameters calculated include: core flow rates and temperatures, loop flow rates and temperatures, pump performance, and heat exchanger operation. Additionally, all plant protection systems and plant control systems are accounted for. All calculations are done in SI units.

SSC is a general system transient code. It is highly flexible, with complete variable dimensioning, allowing any number of user specified loops, pipes and nodes. Single phase and two phase thermal hydraulics are used in a multi-channel core representation. Inter-assembly flow redistribution is accounted for; a detailed fuel pin model is used. The heat transport system geometry is user specified. The code has both transient and steady state options. Restart capability is provided.

SSC is available in either a CDC UPDATE format or as FORTRAN source. The customary transmittal package also includes the input files for the three standard benchmark problems, as well as 48x microfiche which contain the SSC support documentation and sample output for each of the benchmark problems. SSC is currently available as a draft release from Brookhaven National Laboratory with NRC consent.

15a KEY WORDS AND DOCUMENT ANALYSIS

15b DESCRIPTORS

1. Transient Analysis
2. Fast Reactor
3. System Simulation
4. Thermal-Hydraulic Analysis
5. Generic

16 AVAILABILITY STATEMENT
UNLIMITED

17 SECURITY CLASSIFICATION (This report) UNCLASSIFIED

18 SECURITY CLASSIFICATION (This page) UNCLASSIFIED

19 NUMBER OF PAGES

20 PRICE
$